

STRUCTURAL, STRATIGRAPHIC, AND GEOCHRONOLOGIC ANALYSIS OF
THE ALEXANDER - TAKU TERRANE BOUNDARY AND THE OVERLAPPING
UPPER JURASSIC TO LOWER CRETACEOUS GRAVINA SEQUENCE,
SOUTHEAST ALASKA

Thesis by
Charles Martin Rubin

In Partial Fulfillment of the Requirements
for the degree of
Doctor of Philosophy

California Institute of Technology
Pasadena, California

1991

(Submitted July 9, 1990)

ACKNOWLEDGEMENTS

This study was conducted under the supervision of Jason B. Saleeby of the California Institute of Technology who provided both financial support and encouragement throughout my Ph.D. program at Caltech. His enthusiasm, assistance, and friendship have been invaluable.

Field work in southeast Alaska has been supported by the National Science Foundation, the U.S. Geological Survey, U.S. Forest Service, research grants from the Geological Society of America, Sigma-Xi, and a F. Beach Leighton Fellowship in Geology. Ken Eichner and Bill Gale of Tempsco Helicopters generously provided helicopter support for the work on central Revillagigedo and Gravina Islands. I thank Jeff Marshall, Mark Fahnestock, Meghan Miller, and Jon Nourse for their assistance in the field during the summers of 1987 and 1988.

U-Pb geochronology was conducted at the California Institute of Technology under the direction of, and in collaboration with, Jason B. Saleeby. Jason Saleeby and Lee Silver taught me the theory and lab procedures of U-Pb geochronology. Mike Orchard (Canadian Geological Survey) analyzed conodonts collected during this study. Fred Barker (U.S. Geological Survey) and David Marrett (University of California, Riverside) provided geochemical analyses. Discussions with Darrel Cowan, Meghan Miller, Bill McClelland, Jim Monger, Margi Rusmore, Lee Silver, and Jim Wright are appreciated. Finally, I would like to thank my colleagues at Caltech for their support and enthusiasm during my studies in Pasadena.

ABSTRACT

An imbricate thrust belt that extends along strike for over 2000 km overprints the tectonic boundary between two of the largest allochthonous crustal fragments (Intermontane and Insular superterrane) in the North American Cordillera and affects rocks west of the Coast Plutonic Complex in southeast Alaska, western British Columbia and northern Washington. Deformation was broadly coeval with mid-Cretaceous magmatism and involved the emplacement of west-directed thrust nappes over a structurally intact and relatively unmetamorphosed basement. The Paleozoic and lower Mesozoic Alexander terrane forms structural basement for much of the thrust belt, along a moderately northeast-dipping ramp.

The western metamorphic belt of the Coast Plutonic Complex consists of the Alexander and Taku terranes, and the Upper Jurassic and Lower Cretaceous Gravina sequence. The Alexander terrane consists of lower Paleozoic metavolcanic and metasedimentary rocks (Descon Formation) and dioritic plutons that are unconformably overlain by Lower Devonian clastic strata (Karheen Formation). These rocks are overlain locally by Upper Triassic basalt, rhyolite and marine clastic strata (Hyd Group). The Taku terrane consists of polydeformed and metamorphosed strata that are divided into an upper Paleozoic and lower Mesozoic assemblage (Alava sequence) and a lower Paleozoic assemblage (Kah Shakes sequence). The lower Paleozoic Kah Shakes sequence consists of Devonian orthogneiss, quartz-rich metasedimentary rocks, metabasalt, meta-silicic tuff, marble, calc-silicate, and quartzite. The quartz-rich metasedimentary rocks may be correlative with the lower Paleozoic and mid-Paleozoic Yukon-Tanana terrane, which represents an east-Pacific fringing arc complex built on continental slope and rise deposits. The upper Paleozoic and lower Mesozoic Alava sequence consists of crinoidal and argillaceous marble, carbonaceous phyllite, argillite, mafic flows, pillow breccia, pyroclastic tuff, and minor quartz-rich metasedimentary rocks. The upper Paleozoic part of the Alava sequence is probably correlative with the mid- to late Paleozoic portion of the Yukon-Tanana terrane. The Middle and Upper Triassic portion of the Alava sequence may represent a metamorphic vestige of the Stuhini Group, now exposed on the western flank of the Coast Batholithic belt.

Upper Jurassic and Lower Cretaceous metavolcanic and metasedimentary strata of the Gravina sequence unconformably overlie both the Alexander and Taku terranes. These rocks form two distinct lithotectonic units in southern southeast Alaska. The lower unit consists of coarse marine pyroclastic and volcanoclastic strata, mafic flows, breccia, and fine-grained tuff which are locally intruded by hypabyssal bodies of diorite and quartz diorite. Fine- to coarse-grained turbidites and related channel-fill deposits comprise the epiclastic part of the Gravina sequence. Conglomerate units contain mostly volcanic and plutonic lithic clasts that suggest they were derived from a composite igneous source. Clasts from the channel-fill deposits yield Pb-U zircon ages of 154 to 158 Ma. The pyroclastic and volcanoclastic rocks represent remnants of a Late Jurassic oceanic arc system that was constructed on a composite basement consisting of the Alexander and Taku terranes; the Taku terrane is inferred to represent the westernmost extent of the Stikine and Yukon-Tanana terranes. These data suggest that the Intermontane (Stikine and Yukon-Tanana terranes) and Insular (Alexander terrane) superterrane were juxtaposed prior deposition of the Upper Jurassic and Lower Cretaceous Gravina sequence.

The lower Paleozoic to Early Cretaceous rocks were deformed in the mid-Cretaceous and tectonism was broadly coeval with arc magmatism. Deformation involved the emplacement of west-directed thrust nappes over a structurally intact and relatively unmetamorphosed basement. Mid-Cretaceous tonalite, granodiorite, and quartz diorite intrude rocks of the thrust belt and were locally affected by the deformation. Mid-Cretaceous deformation occurred during two episodes that were contemporaneous with the emplacement of sill-like plutonic bodies. Older structures record ductile southwest-vergent folding and faulting, regional metamorphism and contain a well-developed axial-planar foliation. The second generation structures developed during the later stages of southwest-directed reverse faulting that juxtaposes rocks of contrasting metamorphic pressures and temperatures. The presence of syntectonic kyanite-staurolite-garnet-biotite assemblages in the more eastern high-strain zones indicates that at least some of the reverse faults were generated at depths in excess of 20 km during the later stages of thrust faulting and associated uplift.

Paleocene and younger (?) deformation has also affected rocks on the western margin of the Coast Plutonic Complex. Younger fabrics are dominated by low to moderate west-dipping foliation surfaces that are axial planar to asymmetric east-vergent folds. The east-verging fabrics have transposed earlier mid-Cretaceous fabrics. Late Paleocene pegmatite dikes are highly deformed and are affected by the west-dipping structures. Exposure of mid-crustal level rocks might be related to a reversal in vergence during Paleocene time, in which deep levels of the mid-Cretaceous thrust system were transported upward along east-vergent structures. A swarm of hornblende-bearing diabase dikes cross-cut all structures and fabrics. These dikes trend northeast and mark a regional change in the overall regional strain patterns during Miocene time.

Structural, stratigraphic and geochronologic data suggest that regional-scale deformation in southeast Alaska occurred between 113 Ma and 89 Ma. Rocks in the thrust belt were regionally uplifted by 70 Ma, at an average minimum rate of ≈ 0.9 mm/yr. Mid-Cretaceous deformation involved the collapse of marginal basin(s) and a magmatic arc, overprinting the older tectonic boundary between the Insular superterrane and the late Mesozoic western margin of North America (i.e., the Intermontane superterrane). Contractional deformation along the length of the thrust belt was broadly coeval with arc magmatism, and thus records intra-arc tectonism. Late Paleocene to Early Eocene deformation and uplift may mark the transition from contractional to extensional tectonism, and perhaps records the collapse of tectonically thickened crust.

ACKNOWLEDGEMENTS	ii
ABSTRACT	iii
TABLE OF CONTENTS	vi
LIST OF FIGURES	viii
LIST OF TABLES	xii
LIST OF PLATES	xiii
CHAPTER 1: INTRODUCTION	1-1
REFERENCES	1-10
CHAPTER 2: THE GRAVINA SEQUENCE - REMNANTS OF A MID-MESOZOIC OCEANIC ARC IN SOUTHERN SOUTHEAST ALASKA	2-1
ABSTRACT	2-1
INTRODUCTION	2-2
GEOLOGIC SETTING	2-10
GRAVINA SEQUENCE	2-11
DISCUSSION	2-44
CONCLUSIONS	2-48
REFERENCES	2-49
ACKNOWLEDGEMENTS	2-53
CHAPTER 3: THE GEOLOGIC AND STRUCTURAL HISTORY OF THE WESTERN METAMOPHICROCKS OF THE COAST PLUTONIC COMPLEX, SOUTHERN SOUTHEAST ALASKA	3-1
ABSTRACT	3-1
INTRODUCTION	3-2
GEOLOGIC SETTING	3-5
GEOLOGIC FRAMEWORK	3-10
STRUCTURAL GEOLOGY AND METAMORPHISM	3-25
DISCUSSION AND TECTONIC HISTORY	3-49
ACKNOWLEDGEMENTS	3-52
REFERENCES	3-53
CHAPTER 4: TECTONIC FRAMEWORK OF THE UPPER PALEOZOIC AND LOWER MESOZOIC ALAVA SEQUENCE: A REVISED VIEW OF THE POLYGENETIC TAKU TERRANE IN SOUTHERN SOUTHEAST ALASKA	4-1
ABSTRACT	4-1
INTRODUCTION	4-1
GEOLOGIC SETTING	4-4
ALAVA SEQUENCE	4-8
REGIONAL TECTONIC IMPLICATIONS	4-31
ACKNOWLEDGEMENTS	4-33
REFERENCES	4-33
CHAPTER 5: THRUST TECTONICS AND CRETACEOUS INTRACONTINENTAL SHORTENING IN SOUTHEAST ALASKA	5-1

ABSTRACT	5-1
TECTONIC FRAMEWORK	5-5
GEOLOGIC AND STRATIGRAPHIC SETTING	5-5
IMPLICATIONS FOR BASEMENT TECTONICS AND CONVERGENT MARGIN TECTONICS	5-22
ACKNOWLEDGEMENTS	5-25
REFERENCES	5-25
 CHAPTER 6: DEVELOPMENT OF A MID-CRETACEOUS WEST-VERGENT THRUST SYSTEM IN THE NORTHWESTERN CORDILLERA: IMPLICATIONS FOR CONVERGENT-MARGIN TECTONISM	
ABSTRACT	6-1
INTRODUCTION	6-1
TECTONIC FRAMEWORK	6-4
DISCUSSION	6-11
CONCLUSIONS	6-14
REFERENCES	6-19
ACKNOWLEDGEMENTS	6-19
 APPENDIX 1: U-PB GEOCHRONOLOGIC METHODS	A-1
LABORATORY METHODS	A-1
REFERENCES	A-10
 APPENDIX 2: FIELD ABBREVIATIONS	B-1

LIST OF FIGURES

CHAPTER 1

Figure 1-1. Generalized distribution of lithotectonic elements in the northern Cordillera (modified from Monger et al., 1982; Monger and Berg, 1987; Wheeler et al., 1988; Miller, 1987). Also shown are some large strike-slip faults. Initial Sr 0.706 isopleth from Kistler and Peterman (1973), Farmer and DePaolo (1983), and Armstrong (1988). Wr = Wrangellia, At = Alexander terrane, St = Stikine terrane, Q = Quesnel terrane, Cc = Cache Creek terrane, Ytt = Yukon-Tanana terrane.

1-3

Figure 1-2. Petrotectonic and structural histories of the Intermontane and Insular superterrane of British Columbia and southern Alaska (modified from Saleeby, 1983; Gardner et al., 1989; Anderson, 1989). Time scale after Harland and others (1982).

1-6

CHAPTER 2

Figure 2-1. Location map of the Gravina sequence in the northwestern Cordillera, showing regions and features referred to in text. Adapted from Beikman, 1980; Monger and Berg, 1985.

2-4

Figure 2-2. Geologic map showing distribution of geologic units, major structures, and sample locations in southern southeastern Alaska. Adapted from C.M. Rubin (Unpublished mapping, 1985, 1986, 1987) (Cleveland Peninsula and adjacent islands); C.M. Rubin and J.B. Saleeby (Unpublished mapping, 1986, 1987, 1988) (Revillagigedo and adjacent islands); Berg (1972, 1973) (Annette and Gravina Islands).

2-8

Figure 2-3. Generalized stratigraphic section of the Gravina sequence on Gravina Island (Figure 2). The base of the section is in fault contact with the underlying Alexander terrane and the top of the section is not seen in this area. On northwestern Annette and northern Gravina Islands, similar strata unconformably overlie the Alexander terrane.

2-13

Figure 2-4. Deformed basal conglomerate of the lower member of the Gravina sequence on northwestern Annette Island (Fig. 2), with clasts from the underlying Triassic Hyd Group of the Alexander terrane.

2-16

Figure 2-5. Trace-element discrimination diagrams showing data from Gravina sequence metabasalts. A) Ti/Zr discrimination diagram of Pearce and Cann (1973); B) Cr/Y discrimination diagram of Pearce (1982); Zr/TiO₂ vs Nb/Y discrimination diagram of Winchester and Floyd (1977).

2-22

Figure 2-6. Normalized incompatible-element patterns for the Gravina sequence metabasalts. A) Chondrite-normalized plot after Thompson (1982), B) MORB-normalized plot after Pearce (1983), C) Chondrite-normalized REE plot. All data normalized after Nakamura (1974). Multi-element plots generated by program after Wheatley and Rock (1988).

2-24

Figure 2-7. Measured lithostratigraphic section of part of the upper member of the Gravina sequence on Back Island.

2-31

Figure 2-8. Highly deformed channel-fill conglomerate of the upper member of the Gravina sequence on Betton Island. Plutonic clasts in the conglomerate yield Pb-U zircon ages of 154 Ma to 158 Ma. The largest clast in the photograph is approximately 45 cm in diameter;

- clasts at Gnat Cove and Back Island are locally over 60 cm in diameter. 2-33
- Figure 2-9. Composition of pebble and cobble populations from conglomerate within the upper member of the Gravina sequence, Lsu, lithic sedimentary undifferentiated; Liv, lithic volcanic and plutonic; Li, lithic plutonic; Lv, lithic volcanic, lq, lithic quartzite and vein quartz. 2-35
- Figure 2-10. Stacked segments of concordia and data points for clasts within the upper member of the Gravina sequence. Concordia diagram after Tera and Wasserburg (1971). Linear regression and errors in lower and upper intercepts are adapted from York (1969). Bars at ends of concordia segments show uncertainty in $^{207}\text{Pb}/^{206}\text{Pb}$ values of concordia from uncertainties in ^{238}U and ^{235}U decay constants after Jaffey and others (1971). 2-41
- ### CHAPTER 3
- Figure 3-1. Regional geologic map of study area, with study area highlighted. Zone of mid-Cretaceous and younger deformation stippled. 3-4
- Figure 3-2. Generalized geologic map of the Ketchikan area. 3-9
- Figure 3-3. Geologic cross-sections: (A) northern Cleveland Peninsula, (B) southern Cleveland Peninsula, (C) Carol Inlet. 3-12
- Figure 3-4. Amphibolite facies rocks of quartzite and marble in the Kah Shakes sequence, exposed north of Rudyerd Inlet on the east-side of Behm Canal. 3-21
- Figure 3-5. Geologic sketch map of the contact between the Alexander terrane and the Gravina sequence, exposed in an unnamed cove, northeast of Caamano Point, southern Cleveland Peninsula. Regional location shown in inset. (Ketchikan C-6 quadrangle) 3-28
- Figure 3-6. Lower-hemisphere, equal-area plot showing (A) poles to foliation surfaces on northwest Cleveland Peninsula, (B) poles to foliation surfaces on southern Cleveland Peninsula, (C) trend and plunge of small-scale folds and poles to foliation surfaces in higher level thrust nappes on northern Cleveland Peninsula, and (D) poles to foliation surfaces and trend and plunge of elongation lineation in higher level thrust nappes. 3-30
- Figure 3-7. Asymmetric folds truncated by moderately-dipping thrust faults in the Permian part of the Alava sequence, exposed on Revillagigedo Island. This fault zone places Permian marble and metabasalt over Triassic carbonaceous pelitic schist. 3-32
- Figure 3-8. Geologic cross-section across the Black Mountain fault zone, exposed on southwestern Revillagigedo Island. 3-36
- Figure 3-9. Weakly deformed tonalitic clasts in a mylonitic matrix. These fabrics developed within the Black Mountain Fault zone on southern Revillagigedo Island. 3-38
- Figure 3-10. Geologic sketch of transposed foliation (S1) and associated isoclinal folds in banded kyanite schist along the Northern Revillagigedo fault zone. Elongation lineation dips moderately to the southeast. 3-42

Figure 3-11. Lower hemisphere equal-area plot showing (A) poles to foliation surfaces, small-scale folds, and lineations along the southern Revillagigedo fault zone, (B) poles to foliation surfaces and small-scale folds of D₁ and D₂ fabrics,

(C) Contour of poles to dike orientation. C.I. = confidence interval, after Kamb (1959). • = S₁ foliation; □ = S₂ foliation; ★ = trend and plunge of small scale folds; O = trend and plunge of lineation. 3-44

Figure 3-12. Aeromagnetic and gravity profiles and geologic cross-section across the western wall rocks of the Coast Plutonic Complex showing the major mid-Cretaceous structural domains. AT = Alexander terrane; GS = Gravina sequence; AS = Alava sequence; KSS = Kah Shakes sequence. 3-47

CHAPTER 4

Figure 4-1. Location map of the Taku terrane in the northwestern Cordillera, showing regions and features referred to in text. K = Ketchikan, P = Petersburg, J = Juneau. Inset shows location of Figure 2. Adapted from Beikman (1980); Monger and Berg (1987); Wheeler and McFeely (1987); Wheeler et al. (1988). 4-3

Figure 4-2. Geologic sketch map showing distribution of geologic units, major structures, and sample locations in the Ketchikan area. AB = Alava Bay, CI = Carol Inlet, GI = George Inlet, and POW = Prince of Wales Island. Adapted from Berg (1972, 1973; parts of Annette and Gravina Islands), Gehrels and Saleeby (1987a,b; Prince of Wales Island, parts of Annette, Duke, and Gravina islands), C.M. Rubin (unpublished mapping, 1985, 1986, 1987; Cleveland Peninsula and adjacent islands); C.M. Rubin and J.B. Saleeby (unpublished mapping, 1986, 1987, 1988; Revillagigedo and adjacent Islands). 4-6

Figure 4-3. Geologic sketch map of central Revillagigedo Island from C.M. Rubin (unpublished mapping) and Berg et al. (1988). 4-10

Figure 4-4. Schematic structural-stratigraphic section of the Alava sequence in George Inlet. 4-13

Figure 4-5. Early Late Permian crinoidal marble of the Alava sequence on Carol Inlet, Revillagigedo Island. 4-15

Figure 4-6. Schematic structural-stratigraphic section showing geologic relations between the Upper Jurassic to Early Cretaceous Gravina sequence and the Alava sequence on Carol Inlet, Revillagigedo Island. 4-18

Figure 4-7 Late Middle Triassic crinoidal limestone containing well-preserved *Pentacrinites* on George Inlet, Revillagigedo Island. 4-20

Figure 4-8. Trace element discrimination diagrams showing data from fresh pillowed metabasalts of the Alava sequence. MORB = mid-ocean-ridge basalt field. WPB = within-plate basalt field. IAT = island-arc tholeiite field. (A) Cr-Y discrimination diagram of Pearce (1982). (B) Ti-Zr discrimination diagram of Pearce and Cann (1973). (C) Zr/Y-Zr discrimination diagram of Pearce (1980). 4-25

Figure 4-9. Correlation chart for mid-Paleozoic and lower Mesozoic volcanic and basinal assemblages in the Pacific northwest Cordillera. References used in constructing this chart include Anderson (1989), Berg and Cruz (1982), Gehrels and Saleeby (1987), Lowe et al. (1982), Monger (1977), Mortensen and Jilson (1985), Richter (1976), Richter and Dutro (1975), Silberling et al. (1982), Weber et al. (1978), and Werner (1977, 1978). 4-28

CHAPTER 5

- Figure 5-1. Map showing the major lithotectonic elements and the region of mid-Cretaceous and younger deformation in southeast Alaska. Inset shows superterrane and intervening Coast Plutonic Complex (CPC). SJ/Cs = San Juan Islands - northern Cascades. 5-4
- Figure 5-2. Generalized distribution of the Intermontane and Insular superterrane and the miogeocline of the northern Cordillera (modified after Monger et al. 1982; Monger & Berg 1987; Wheeler et al., 1988.; Miller 1987). Also shown are some large-strike-slip faults. Initial Sr 0.706 isopleth from Kistler & Peterman (1973), Farmer & DePaolo (1983) and Armstrong (1988). 5-7
- Figure 5-3. Petrotectonic and structural histories of the Intermontane and Insular superterrane of British Columbia and southern Alaska (modified from Saleeby 1982; Gardner et al. 1986; Miller 1987; Anderson 1989). 5-9
- Figure 5-4. Geologic cross-section, aeromagnetic, and gravity profiles across the western metamorphic belt of the Coast Plutonic Complex showing the mid-Cretaceous structural domains. Late Paleocene-Eocene fabrics do not strongly overprint this area. AT = Alexander terrane; GS = Gravina sequence; AS = Alava sequence; KSS = Kah Shakes sequence. 5-13
- Figure 5-5. Lower-hemisphere, equal-area plot showing poles to foliation surfaces domain I, (A) northwest Cleveland Peninsula, (B) Annette Island, (C) Gravina Island. 5-16
- Figure 5-6. Lower-hemisphere, equal-area plot showing, (A) poles to foliation and cleavage in domain II, (B) poles to foliation and trend and plunge of small-scale folds in domain II, and (C) poles to foliation and trend and plunge of elongation lineation in domain III. 5-19
- ## CHAPTER 6
- Figure 6-1. Distribution of mid-Cretaceous thrust system in northwestern Cordillera after Brandon et al., (1988); Brandon (1989); Crawford et al., (1987); Rubin and Saleeby (1987a, and 1987b). Terranes I and II of Monger et al., (1982). 6-3
- Figure 6-2. Structural transects across the mid-Cretaceous thrust system. PZ = Paleozoic, P = Permian, MZ = Mesozoic, TR = Triassic, J = Jurassic, K = Cretaceous, UK = Upper Cretaceous. A: After Rubin and Saleeby (1987a, 1987b) and unpublished mapping by Rubin and Saleeby. B: After work of Crawford et al., (1987). C: After Brandon et al., (1988) and Brandon (1989). Locations of cross sections are shown in Figure 1. 6-6
- Figure 6-3. Tectonic models for origin of mid-Cretaceous deformation within Coast Plutonic Complex. I = Intermontane superterrane; II = Insular superterrane. Model 1 adapted from Goodwin (1975) and Monger et al., (1982). Model 2 adapted from Berg et al., (1972), Monger and others (1972), Armstrong (1988), and Van der Heyden and Woodsworth (1988). 6-13

LIST OF TABLES

CHAPTER 2

TABLE 2-1. Major and minor element chemical analyses of Gravina sequence metabasalts from the Ketchikan area.	2-19
---	------

TABLE 2-2. Trace element chemical analyses of Gravina sequence metabasalts from the Ketchikan area.	2-20
---	------

TABLE 2-3. Pebble counts, upper member of the Gravina sequence.	2-36
---	------

TABLE 2-4. Pb-U zircon isotopic data.	2-38
---------------------------------------	------

TABLE 2-5. Pb-U geochronologic sample information	2-39
---	------

CHAPTER 3

TABLE 3-1. Pb-U geochronologic sample information	3-6
---	-----

TABLE 3-2. Pb-U zircon isotopic data	3-14
--------------------------------------	------

CHAPTER 4

TABLE 4-1. Trace element chemical analyses of Alava sequence metabasalts from the Ketchikan area.	4-23
---	------

APPENDIX 1

TABLE A-1: Isotopic composition of lead in NBS 983 standard, measured by the VG mass spectrometer and other mass spectrometers at CIT, the University of California at Santa Barbara, and VG and Finnegan MAT factories. Internal precisions for all runs given as 1σ . Uncertainties for actual samples are probably higher, due to minor variations in sample purity.	A-5
--	-----

TABLE A-2: Isotopic composition of lead in NBS 981 standard, measured by the VG mass spectrometer and other mass spectrometers at CIT, the University of California at Santa Barbara, the Max Planck-Institut für Chemie (Mainz), and VG and Finnegan MAT factories. Internal precisions for all runs given as 1σ . Uncertainties for actual samples are probably higher, due to minor variations in sample purity.	A-7
--	-----

TABLE A-3: Isotopic composition of Uranium in NBS 500 standard measured by the VG mass spectrometer at Caltech. Internal precisions for all runs given as 1σ . Uncertainties for actual samples are probably higher, due to minor variations in sample purity.	A-9
---	-----

APPENDIX 2

TABLE B-1: Field abbreviations for Ketchikan and adjacent geologic 15° sheets	B-1
---	-----

LIST OF PLATES

- Plate 1: Geologic map of Cleveland Peninsula, Revillagigedo and adjacent Islands, southern southeast Alaska, 1:125,000 scale. in pocket A
- Plate 2: Geologic map and U-Pb zircon samples locations - Cleveland Peninsula, Revillagigedo and adjacent Islands, southern southeast Alaska, 1:125,000 scale. in pocket A
- Plate 3: Geologic cross-sections across Cleveland Peninsula and Revillagigedo Island. in pocket A
- Plate 4: Location map and geologic field sheets of the Ketchikan and adjacent quadrangles, scale 1:63,360. in pocket B

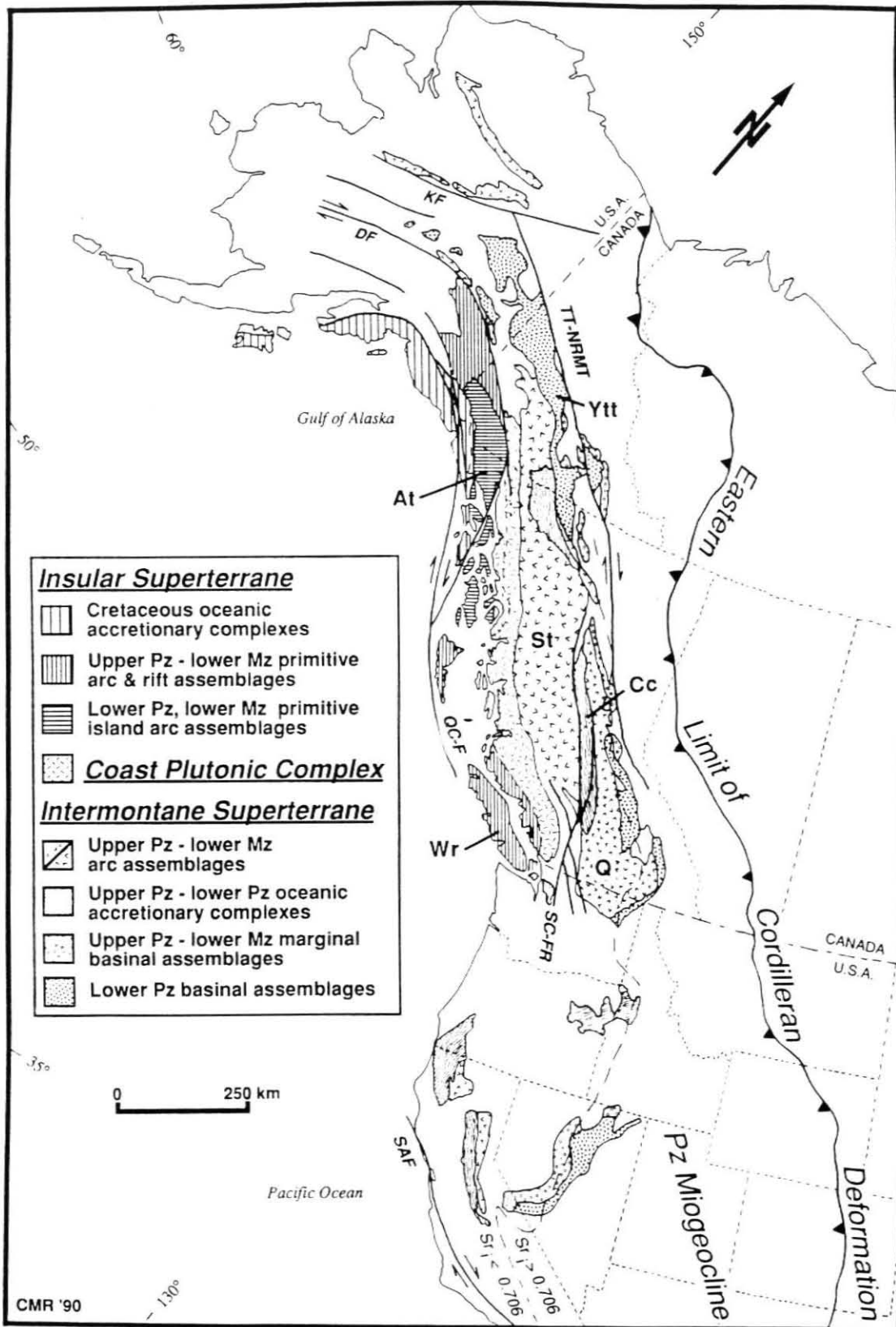
CHAPTER 1

Introduction

Many mountain belts in the world are formed by crustal shortening and concurrent metamorphism. Along convergent plate margins, deformation is generally accompanied by widespread magmatism which is one of the primary mechanisms for the development of new continental crust. The accretion of oceanic material along active plate margins is another important mechanism in continental growth, yet the interplay between magmatism, deformation, and accretion of crustal fragments is controversial. Some workers consider almost all Mesozoic high-grade metamorphism and deformation in the North American Cordillera to be the result of accretionary processes (e.g., Coney et al., 1980), with magmatism playing only a secondary role. In contrast, other workers have emphasized that deformation, associated metamorphism and coeval magmatism can be explained by convergent-margin processes and that the collision of exotic components is not the primary geodynamic control of Cordilleran orogenic belts (e.g., Burchfiel and Davis, 1972).

The relationship between accretion of crustal fragments, deformation, and magmatism is well displayed in the northwestern Cordillera. The Cordillera is characterized by a collage of discrete crustal fragments or terranes (Monger and Berg, 1987), high-grade metamorphic belts, and a large-scale arc-related batholithic belt (Coast Plutonic Complex). The Canadian segment of the Cordillera, between latitudes 40° and 60°N, can be grouped into two major crustal elements based on wallrock geology, the Intermontane and Insular superterrane (Figure 1). The boundary between the two superterrane is a major structural feature and can be traced for over 2000 km along the eastern edge of the Insular superterrane, from southwest British Columbia to southeast Alaska (Figure 1). The boundary divides ensimatic crust from the western margin of Jurassic North America. The Coast batholithic belt was emplaced along the superterrane boundary.

Figure 1-1. Generalized distribution of lithotectonic elements of the northern Cordillera (modified from Monger et al., 1982; Monger and Berg, 1987; Wheeler et al., 1988; Miller, 1987; Miller et al., in press). Also shown are some large strike-slip faults. Initial Sr 0.706 isopleth from Kistler and Peterman (1973), Farmer and DePaolo (1983), and Armstrong (1988). Wr = Wrangellia, At = Alexander terrane, St = Stikine terrane, Q = Quesnel terrane, Cc = Cache Creek terrane, Ytt = Yukon-Tanana terrane.



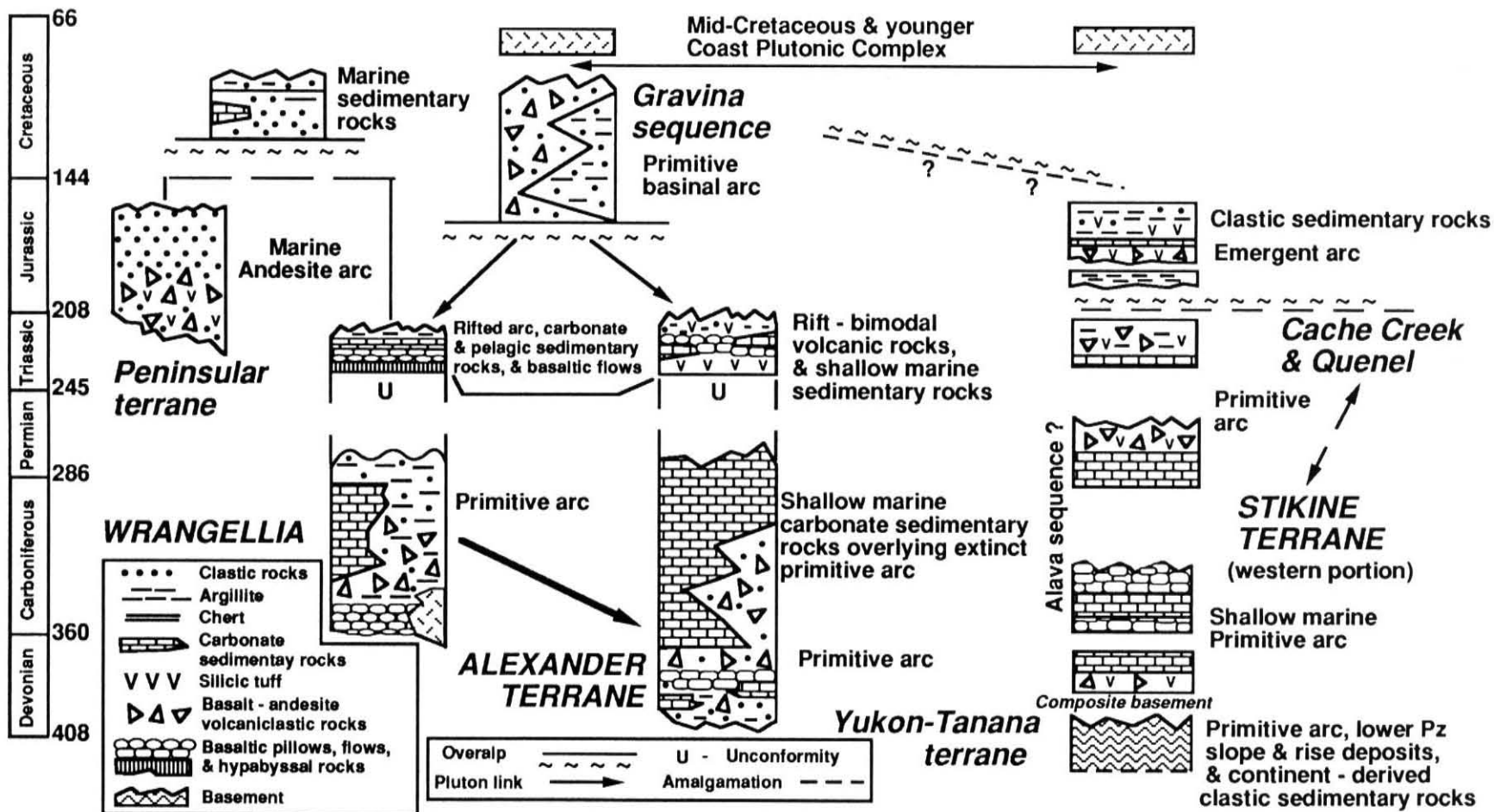
The Intermontane superterrane consists of Stikine, Cache Creek, and Quesnel terranes (Figure 2) and was accreted to North America in the Middle Jurassic time (Monger et al., 1982), thus forming the western margin to the continent during the Cretaceous. The Stikine, Quesnel, and correlative terranes to south (Figure 1) rest unconformably on older oceanic arc rocks and rocks of continental affinity (slope and rise deposits and attenuated or rifted continental crust) (Figure 2), and lie outboard of contemporaneous shelf and platform strata. Volcanic and basinal strata of the Intermontane superterrane have depositional and structural ties with western North America and, combined with recent geochemical and isotopic studies and geologic mapping, the superterrane represents a long-lived east-Pacific fringing arc system that was adjacent to North America for much of its history (Rubin et al., 1990). The Insular superterrane, consisting of the Alexander, Peninsula, and Wrangellia terranes (Figure 2), lies parallel to and west of the Intermontane superterrane. Isotopic studies indicate that the Alexander terrane consists of Phanerozoic depleted mantle-derived crustal material (Samson et al., 1990), in contrast to parts of the Intermontane superterrane which shows recycling of Proterozoic sialic material. The Insular superterrane, extending for over 2000 km along strike, has no apparent paleogeographic tie to North America until Cretaceous time (Monger et al., 1982; Saleeby, 1983) and consists of a lower Paleozoic oceanic arc sequence overlain by an Upper Triassic rift assemblage (Figure 2; Gehrels and Saleeby, 1987). The striking geologic contrasts between the two superterranes were first recognized by Wilson (1968) and Jones et al. (1972), and later emphasized by Coney et al. (1980). The contact between the Insular and Intermontane superterranes is generally masked by younger batholithic rocks of the Coast Plutonic Complex, covered by inland marine waterways or structurally disrupted by Cenozoic strike-slip faults, except in southeast Alaska where the Alexander terrane and its Upper Triassic and Upper Jurassic to Lower Cretaceous cover are in contact with the Taku terrane. The Taku terrane represents a highly metamorphosed vestige of portions of the Yukon-Tanana and Stikine terranes (Figure 2; e.g., Intermontane superterrane).

Late Mesozoic deformation and associated metamorphism along the eastern boundary of the Insular superterrane have been thought to be the result of the collision between the Insular

Figure 1-2. Petrotectonic and structural histories of the Intermontane and Insular superterrane of British Columbia and southern Alaska (modified from Saleeby, 1983; Gardner et al., 1989; Anderson, 1989; Rubin et al., 1990). Time scale after Harland and others (1982).

Insular Superterrane

Intermontane Superterrane



superterrane and North America during Cretaceous time (Crawford et al., 1987; Monger et al., 1982). Structural, stratigraphic and geochronologic data suggest that regional-scale deformation in southeast Alaska occurred between 113 Ma and 89 Ma and is characterized by widespread Cretaceous crustal shortening, metamorphism, and deep erosion (Crawford et al., 1987; Rubin et al., 1990). Deformation was broadly coeval with mid-Cretaceous magmatism and involved the emplacement of west-directed thrust nappes over a structurally-intact and relatively unmetamorphosed basement. Thrust sheets in the belt show extensive basement involvement, including both juvenile, ensimatic elements of the Alexander terrane and continent-derived North American slope and rise deposits. Progress in U-Pb geochronology, geologic mapping and thermobarometry in the late 1980's along the eastern edge of the Insular superterrane has provided an initial framework for understanding the nature and character of the boundary between allochthonous ensimatic crustal fragments and the western margin of late Mesozoic North America. Late Mesozoic tectonism along the western margin of the Canadian Cordillera can now be re-interpreted in light of new data presented here.

The primary objective of my work in southeast Alaska has been to characterize the boundary between the Insular-Intermontane superterrane and to construct a stratigraphic and structural chronology in highly metamorphosed sequences of the western metamorphic framework rocks of the Coast Plutonic Complex in southeast Alaska. Geologic mapping along the western flank of the Coast Plutonic Complex, on Cleveland and Portland Peninsulas and Revillagigedo and adjacent islands (Figure 1), has formed the basis for these tectonic studies. The investigation is based on detailed U-Pb geochronologic studies, combined with field, petrologic and geochemical studies. Field studies have also characterized the depositional setting of a poorly-understood Mesozoic arc sequence which overlaps both superterrane, and have provided new constraints on the paleogeography and paleotectonic setting of Mesozoic western North America. By comparing the geology of southern southeast Alaska to age-equivalent sequences throughout the Cordillera, structural styles, stratigraphic and age relations, and magmatic episodes can be

interpreted in a Circum-Pacific tectonic framework. These geologic studies have formed the framework for U-Pb geochronologic studies (in collaboration with Jason Saleeby, Caltech), geochemical analyses (by the U.S. Geological Survey under the supervision of Fred Barker), identification of conodonts (by Mike Orchard, Geological Survey of Canada), and regional oxygen isotope variations in highly metamorphosed terranes (in collaboration with Hugh Taylor, Jr., Caltech).

This thesis has been organized into six chapters including this introduction; the other chapters were written as separate manuscripts, with one appendix. Chapter 2 describes the depositional setting and geologic evolution of the Upper Jurassic and Lower Cretaceous Gravina sequence, and presents U-Pb geochronologic and geochemical data. Chapter 3 provides a description of the basement constituents along the western flank of the Coast Plutonic Complex, on Cleveland Peninsula, Revillagigedo and adjacent islands, and presents U-Pb geochronologic and structural data from these areas. Laboratory methods used in these geochronologic studies are described in the Appendix. Chapter 4 provides a new interpretation of the upper Paleozoic and lower Mesozoic portion of the Taku terrane, a polygenetic assemblage that forms much of the western metamorphic belt of the Coast Plutonic Complex, and presents U-Pb geochronologic, geochemical data and conodont ages. Chapter 5 discusses the zonation of the thrust belt, inferred cooling and uplift rates, and foredeep basin development. A qualitative model for the geodynamic setting of the thrust belt is presented. Chapter 6 presents a synthesis of the mid-Cretaceous structural evolution of the northwest Cordillera and points out the remarkable similarities in structural styles and timing of deformation along the length of the orogen.

The fundamental conclusions of my research are: (1) that a previously unrecognized thrust belt occurs discontinuously for over 2000 km along strike, between latitudes 49° and 56°N, (2) the western framework rocks of the Coast Plutonic Complex consist of metamorphic equivalents of the Alexander, Stikine, Yukon-Tanana terranes and the Gravina sequence, (3) that much of the deformation along the Coast Plutonic

Complex and the eastern edge of the Alexander terrane was broadly coeval with arc magmatism, and thus records intra-arc tectonism. In this view, the collision of exotic tectonic elements is not required to explain the stratigraphic, structural, and metamorphic relations seen in southeast Alaska and western British Columbia. Geologic, stratigraphic, structural and, in part, paleobiogeographic relations support the hypothesis that the the Insular superterrane was juxtaposed against North America during Middle Jurassic time.

REFERENCES

- Armstrong, R.L., 1988, Mesozoic and early Cenozoic magmatic evolution of the Canadian Cordillera, in Clark, S.P., Burchfiel, B.C., and Suppe, J., eds., Processes in continental lithospheric deformation: Geological Society of America Special Paper 218, p. 55-91.
- Anderson, R.G., 1989, A stratigraphic, plutonic, and structural framework for the Iskut River map area, northwestern British Columbia, in Current research, Part E: Geological Survey of Canada Paper 89-1E, p. 145-154.
- Burchfiel, B.C., and Davis, G.A., 1972, Structural framework and evolution of the southern part of the Cordilleran orogen, western United States: American Journal of Science, v. 272, p. 97-118.
- Coney, P.J., Jones, D.L., and Monger, J.W.H., 1980, Cordilleran suspect terranes: Nature, v. 228, p. 329-333.
- Crawford, M.L., Hollister, L.S., and Woodsworth, G.J., 1987, Crustal deformation and regional metamorphism across a terrane boundary, Coast Plutonic Complex, British Columbia: Tectonics, v. 6, p. 343-361.
- Farmer, G.L. and DePaolo, D.J., 1983, Origin of Mesozoic and Tertiary granite in the western United States and implications for pre-Mesozoic crustal structure - 1. Nd and Sr isotopic studies in the geocline of the Northern Great Basin: Journal of Geophysical Research, v. 88, p. 3379-3401.
- Gardner, M.C., Bergman, S.C., Cushing, G.W., Mackevett, E.M. Jr., Plafker, G., Campbell, R.B., Dodds, C.J., McClelland, W.C., and Mueller, P.A., 1988, Pennsylvanian pluton stitching of Wrangellia and the Alexander terrane, Wrangell Mountains, Alaska: Geology, v. 16, p. 967-971.
- Gehrels, G.E., and Saleeby, J.B., 1987, Geology of Prince of Wales Island, southeastern Alaska: Geological Society of America Bulletin: v. 98, p. 123-137.
- Harland, W.B., Cox, A.V., Lewellyn, P.G., Pickton, C.A.G., Smith, A.G. and Walters, R., 1982, A Geologic time scale: Cambridge, England, Cambridge University Press, 131 p.
- Jones, D.L., Irwin, W.P., and Ovenshine, A.T., 1972, Southeastern Alaska - a displaced continental fragment: U.S. Geological Survey Professional Paper 880B, p. B211-217.
- Kistler, R.W. and Peterman, Z.E., 1973, Variations in Sr, Rb, K, Na and initial $^{87}\text{Rb}/^{86}\text{Sr}$ in Mesozoic granitic rocks and intruded wall rocks in central California: Geological Society of America Bulletin, v. 84, p. 3489-3512.
- Miller, E.L., Miller, M.M., Stevens, C.H., Wright, J.E., and Madrid, R., in press, Late Paleozoic paleogeography and tectonic evolution of the western U.S. Cordillera, in B.C., Burchfiel, M.L. Zoback, and P. Lipman, eds., Tectonic development of the conterminous western United States Cordillera: Decade of North American Geology, Geological Society of America, Boulder, Colorado.
- Miller, M.M., 1987, Dispersed remnants of a northeast Pacific fringing arc -- Upper Paleozoic island arc terrane of Permian McCloud faunal affinity, western U.S.: Tectonics, v. 6, p. 807-830.
- Monger, J.W.H., and Berg, H., 1987, Lithotectonic terrane map of western Canada and southeastern Alaska: U.S. Geological Survey Miscellaneous Field Studies Map MF 1874B, scale 1: 2,500,000.

- Monger, J.W.H., Price, R.A. and Tempelman-Kluit, J.D., 1982, Tectonic accretion and the origin of the two major metamorphic and plutonic belts in the Canadian Cordillera: *Geology*, v. 10, p. 70-75.
- Rubin C.M., Saleeby, J.B., Cowan, D.S., McGroder M.F. and Brandon, M.T., 1990, Late Mesozoic compressional tectonism: Development of a west-vergent thrust system in the northwestern Cordillera: *Geology*, v. 18, p. 276-280.
- Rubin, C.M., Miller, M.M., and Smith, G.M., 1990, Tectonic development of Cordilleran mid-Paleozoic volcano-plutonic complexes, *in* Harwood, D.S., and Miller, M.M., eds., *The paleogeography of the Klamath Mountains, Sierra Nevada, and adjacent areas*: Geological Society of America Special Paper 255.
- Saleeby, J.B., 1983, Accretionary tectonics of the North American Cordillera: *Annual. Reviews in Earth and Planetary Sciences*, v. 15, p. 45-73.
- Samson, S.D., McClelland, W.C., Patchett, P.J. and Gehrels, G.E., 1989, Nd isotopes and Phanerozoic crustal genesis in the Canadian Cordillera: *Nature*, v. 337, p. 705-709.
- Wilson, J.T., 1968, Static mobile earth, the current scientific revolution: *Proceeding of the American Philosophical Society*, v. 112, p. 309-320.
- Wheeler, J.O., Brookfield, A.J., Gabrielse, H., Monger, J.W.H., Tipper, H.W. and Woodsworth, G.J., 1988, Terrane map of the Canadian Cordillera: Canadian Geological Survey Open-File Report 1894, scale 1:2,000,000

CHAPTER 2

THE GRAVINA SEQUENCE - REMNANTS OF A MID-MESOZOIC OCEANIC ARC IN SOUTHERN SOUTHEAST ALASKA

Charles M. Rubin and Jason B. Saleeby *California Institute of Technology, Pasadena, California.*

submitted to Journal of Geophysical Research

ABSTRACT. Fragments of Upper Jurassic to Lower Cretaceous volcanic and basinal strata constitute the Gravina belt in southeast Alaska. In the Ketchikan area, Gravina belt form two lithotectonic units. The lower unit consists of coarse marine pyroclastic and volcanoclastic strata, mafic flows, breccia, and fine-grained tuff which are locally intruded by hypabyssal bodies of diorite and quartz diorite. The volcanic rocks are characterized by tholeiitic arc basalts, lack felsic volcanic strata, and overlie Upper Triassic and older strata of the Alexander terrane. Augite - hornblende - bearing porphyritic rocks are common and locally intrude the Alexander terrane basement, where they are thought to represent the intrusive equivalents of lavas recognized in the section. Age constraints for the volcanic unit come from structural and stratigraphic relations with adjacent units and are interpreted as late Middle to Late Jurassic in age. The Gravina belt epiclastic unit consists of fine- to coarse-grained turbidites and related channel-fill deposits. In the Ketchikan area, the basinal rocks unconformably overlie Permian rocks of the Taku terrane and remnants of the lower volcanic part of the Gravina sequence which overlie the Alexander terrane. The conglomerate units contain mostly volcanic and plutonic lithic clasts that suggests that they were derived from a composite volcano-plutonic setting. Clasts in the channel-fill deposits yield Pb-U zircon ages of 154-158 Ma.

The predominance of pyroclastic deposits interbedded with massive flows, tuff, breccia, and argillaceous turbidites and the lithologic and chemical composition of the volcanic rocks indicate a submarine volcanic arc setting for the Gravina sequence. The basinal pyroclastic rocks are inferred to have been shed from submarine strato-volcanos during the Late Jurassic. Epiclastic rocks were deposited in a submarine fan setting. Volcanic and plutonic provenance for coarse epiclastic units indicate uplift and

erosion of an arc edifice. The presence of fine-grained tuffaceous turbidites imply ongoing, but distal volcanism.

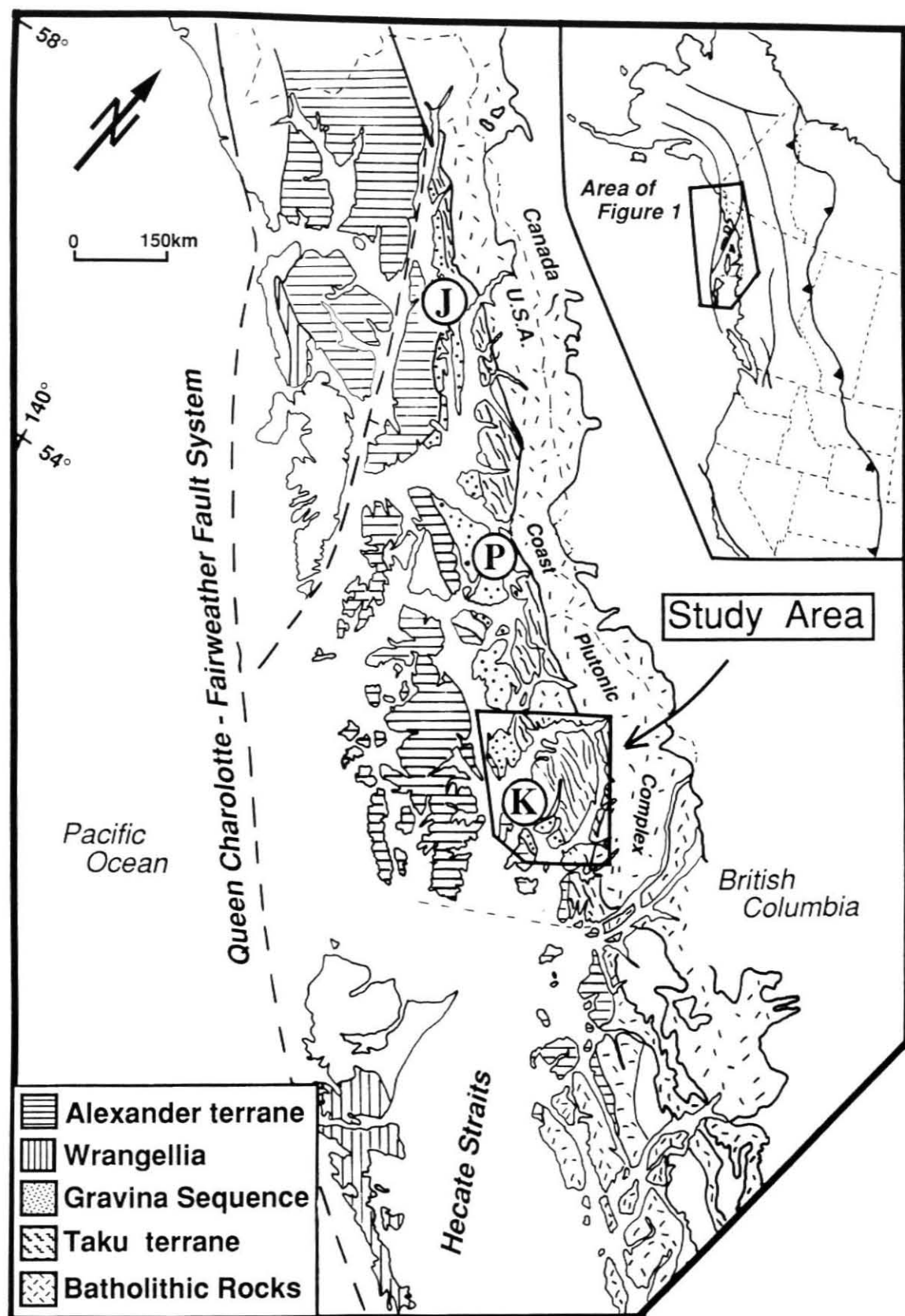
The pyroclastic and volcanoclastic rocks represent remnants of a Late Jurassic oceanic arc system that was constructed on a composite basement consisting of the Alexander and Taku terranes. The strata accumulated in an intra-arc basin on the eastern edge of the Alexander terrane. Arc volcanism continued into Early Cretaceous time. The volcanic and basinal rocks were deformed during a major intra-arc contractional event during mid-Cretaceous time, in conjunction with the emplacement of a distinctly younger, arc-related plutonic suite.

INTRODUCTION

Variably deformed and metamorphosed Upper Jurassic to Lower Cretaceous metavolcanic and metasedimentary strata form a discontinuous belt in northwestern British Columbia and southeastern Alaska, between lat. 54° and 59°N (Figure 1). These rocks are called the Gravina-Nutzotin belt [Berg et al., 1972], with protoliths consisting of interbedded marine basaltic breccia, flows, tuff, and turbidites. The Gravina-Nutzotin belt is best exposed from the eastern Alaska Range to southeastern Alaska and northwestern British Columbia over a distance of 750 km. Mesozoic volcanic rocks overlie both the Alexander terrane and Wrangellia [Berg et al., 1972], which collectively form the Insular superterrane [terrane II of Monger et al. 1982]. Rocks that lie to the east of the Insular superterrane belong to the Intermontane superterrane [terrane I of Monger et al. 1982] and probably formed the western margin of middle Mesozoic North America. Regional geologic relations within the Gravina belt and between adjacent terranes, however, are poorly understood. These geologic uncertainties stem from a lack of age constraints on most protoliths of the Gravina sequence, meager geochemical data on the volcanic rocks, and the need for detailed stratigraphic and provenance studies on the belt. If the Gravina volcanic rocks represent a Late Jurassic to Early Cretaceous oceanic volcanic arc system as originally suggested by Berg et al [1972], its correlation with coeval strata in the Cordillera may provide new insights into the stratigraphic and tectonic evolution of volcanic arcs, and its subsequent accretion to the continent. Recent tectonic syntheses of Mesozoic paleogeography have been limited by the stratigraphic and structural complexity of Gravina belt [e.g., Monger et al., 1982; Pavlis,

Figure 2-1. Location map of the Gravina sequence in the northwestern Cordillera, showing regions and features referred to in text. (Adapted from Beikman, 1980; Monger and Berg, 1985).

K = Ketchikan, P = Petersburg, and J = Juneau.



1982; Plafker et al., 1989]. The initial stratigraphic and tectonic relations between the Insular superterrane and North America are obscured by mid-Cretaceous polyphase deformation and metamorphism, thus the initial tectonic boundary is highly modified. For example, the timing and style of accretion of the Insular superterrane (Alexander terrane and Wrangellia) to the western North American continental margin remains enigmatic. Gravina belt rocks play a critical role in addressing these tectonic questions, due to their unique stratigraphic and paleogeographic position along the eastern margin of the Insular superterrane. If Gravina belt strata overlap both the Insular superterrane and inboard terranes that were adjacent to the North America continent, then a pre-Late Jurassic tie between the Insular superterrane and the western margin of North America is implied. The accurate characterization the Gravina belt may provide a critical tie between the Insular superterrane and western North America, and help resolve paleogeographic reconstructions of late Mesozoic east-Pacific fringing arc systems.

The relationship between Gravina belt strata and coeval volcanic and basinal strata elsewhere in the western North American Cordillera is not well understood. Partly age correlative Upper Jurassic to Lower Cretaceous volcanic arc and epiclastic basinal strata extend from northern Mexico to southern Oregon. In northern California and southern Oregon, these strata include the Upper Jurassic Galice and Mariposa Formations and broadly coeval volcanic strata of the Rogue Formation, which formed in an arc-related setting adjacent to a convergent-margin accretionary complex. The lower part of the Great Valley sequence is also age-correlative to parts of the Gravina belt, and consists of siliciclastic turbidites strata that formed in a fore-arc setting.

Recent paleogeographic reconstructions suggest that Upper Jurassic to Lower Cretaceous Gravina volcanic strata in the northwestern Cordillera represent a magmatic arc that is allochthonous with respect to North America prior to mid Cretaceous time [Howell et al., 1985]. In this view, the Gravina arc was built upon a composite basement of Wrangellia, the Alexander terrane and fragments of the Peninsular terrane. Alternatively, its development may have been analogous to the Jurassic arc rocks in California. Upper Jurassic arc strata in northern California were deposited on the western margin of North America which consisted of structurally imbricated, older accreted terranes [Harper and Wright, 1984]. By analogy, Late Jurassic arc magmatism of the Gravina sequence may have been superimposed across not only across a

composite basement of the Alexander terrane and Wrangellia, but across parts of the Intermontane superterrane. This paper presents evidence in support of this view. In southern southeast Alaska, arc magmatism was active over a relatively short period of time in the mid-Late Jurassic and can be compared with other ancient arc systems in the western Cordillera.

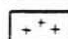

This paper presents new stratigraphic, structural, geochronologic and geochemical data on the Gravina belt in southern southeast Alaska. Although rocks of the Gravina sequence have been metamorphosed to greenschist and lower amphibolite facies, locally original bedding features are preserved. This study is based upon detailed geologic mapping along the shorelines of Annette, Gravina and Revillagigedo Islands, adjacent smaller islands, and Cleveland Peninsula (Figure 2). This paper characterizes the depositional setting of the Gravina sequence, provides a reference section for comparison to age-correlative volcanic sequences elsewhere in the Cordillera, and provides new constraints on mid-Mesozoic paleogeography and paleotectonic setting of the northwestern Cordillera.

Previous Work


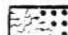
Rocks of the Gravina belt in southeast Alaska were originally described by Buddington and Chapin [1929]. Studies by Gabrielse and Wheeler [1961] and Brew et al., [1966] have characterized the regional geologic relations and provided some of the first tectonic syntheses of this region. It was not until the early 1970's, that workers recognized the continuation of these Upper Jurassic to Lower Cretaceous volcanic and sedimentary rocks across the Chatham Strait fault into the Yukon Territory and the eastern Alaska Range. In their pioneering study, Berg et al., [1972] defined the Gravina-Nutzotin belt, described the sedimentary and volcanic rocks along strike and provided a coherent geologic framework to interpret the belt using plate-tectonic models. Recently, the contact relations between the Gravina-Nutzotin belt and adjacent terranes were reexamined by Brew and Karl [1987]. In southern southeastern Alaska, near the Ketchikan area, sedimentary and volcanic rocks assigned to the Gravina-Nutzotin belt were described by Brooks, [1902], Wright and Wright [1908], Smith [1915], Chapin [1918], Berg [1973] and Berg et al., [1978].

Figure 2-2. Geologic map and zircon sample locations on Cleveland Peninsula, Revillagigedo and adjacent islands, BI = Bell Island Pluton, BP = Bushy Point Pluton, MB = Moth Bay Pluton, EP = Eaton Point Pluton, AB = Alava Bay, CI = Carol Inlet, GI = George Inlet, and POW = Prince of Wales Island, SB = Spacious Bay. BMT = Black Mountain Thrust, NRSZ = northern Revillagigedo Island fault zone, SRSZ = southern Revillagigedo Island fault zone. Adapted from Berg (1972, 1973; parts of Annette and Gravina Islands), Gehrels and Saleeby (1987b, parts of Annette, Duke, and Gravina islands), C.M. Rubin (unpublished mapping, 1985, 1986, 1987; Cleveland Peninsula and adjacent islands); C.M. Rubin and J.B. Saleeby (unpublished mapping, 1986, 1987, 1988; Revillagigedo and adjacent Islands).

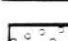
PALEOCENE AND YOUNGER (?) INTRUSIVE ROCKS

-  Tonalite, quartz diorite, & granodiorite
-  Pegmatite dike swarm

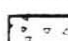
MIDDLE CRETACEOUS INTRUSIVE ROCKS

-  Tonalite, granodiorite, diorite, & gabbro
-  Zoned ultramafic complexes


U. JURASSIC & L. CRETACEOUS GRAVINA SEQUENCE

-  Metamorphosed tuff, greywacke, argillite, conglomerate, basalt-andesite tuff, breccia & pillow flows, & hypabyssal intrusive rocks


U. PALEOZOIC & L. MESOZOIC ALAVA SEQUENCE

-  Metamorphosed mafic pillow flows, tuff & breccia, argillite, marble, & quartzite


PALEOZOIC & L. MESOZOIC ALEXANDER TERRANE

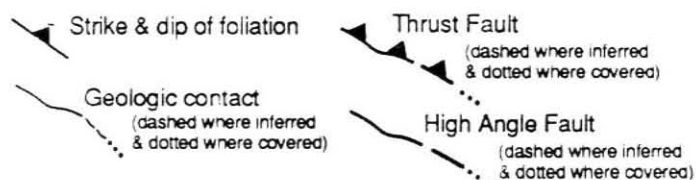
-  Triassic conglomerate, siltstone, limestone, basalt, & rhyolite \ Gabbro
-  Devonian conglomerate, sandstone, siltstone, & marble
-  Ordovician-Silurian basaltic andesite tuff, breccia, pillowed flows, & hypabyssal rocks
-  Silurian trondhjemite & local diorite
-  Ordovician-Silurian tonalite, diorite, & gabbro
-  Cambrian & older (?) meta-igneous rocks

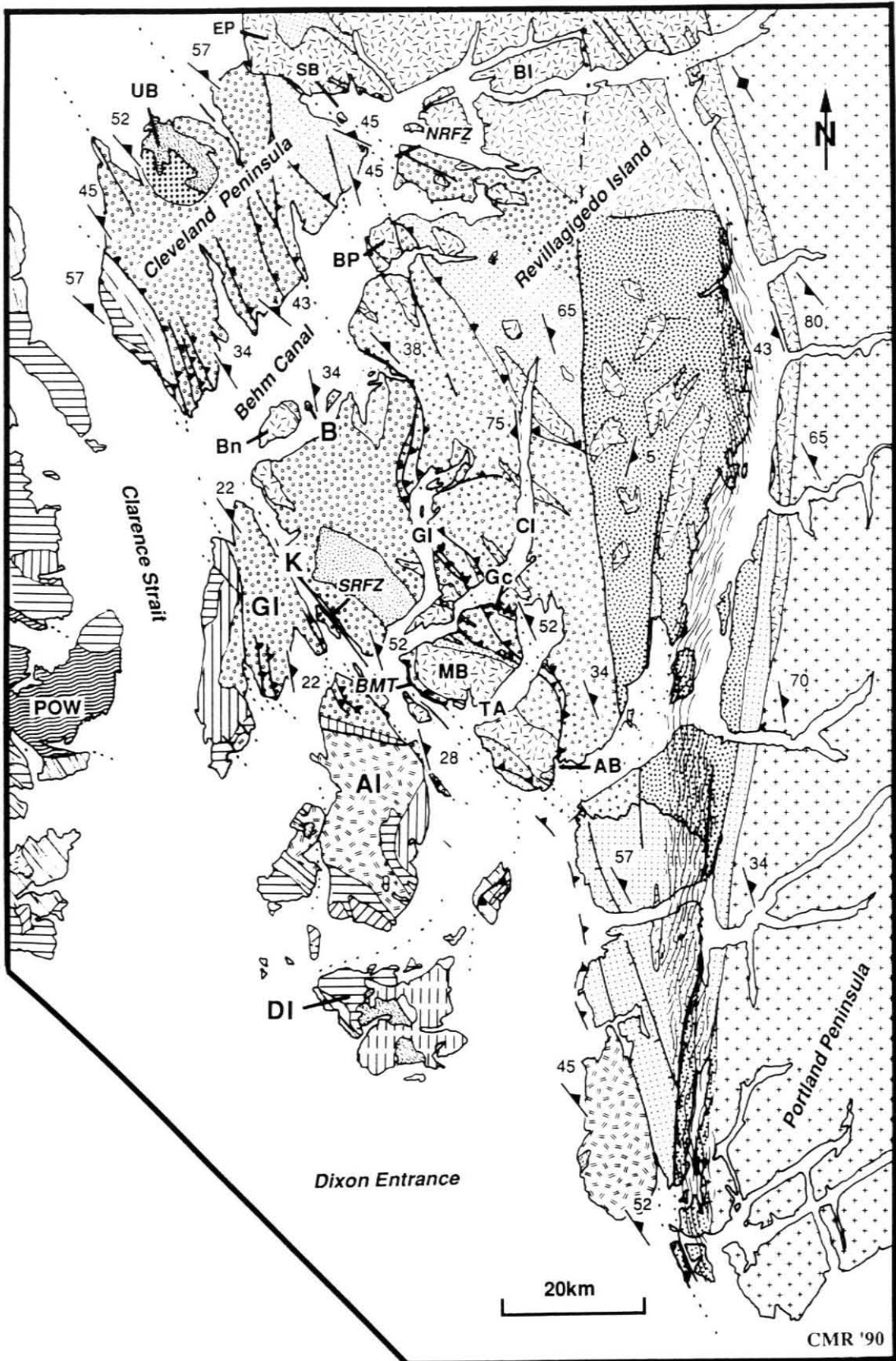
PALEOZOIC KAH SHAKES SEQUENCE

-  Devonian orthogneiss, lower Paleozoic quartz-bearing psammitic rocks, silicic metavolcanic rocks, amphibolite, metapelite, quartzite & marble

EAST BEHM CANAL GNEISS COMPLEX

-  Lower Paleozoic, tonalite gneiss, diorite gneiss, amphibolite, & psammitic gneiss





GEOLOGIC SETTING

The Gravina belt consists of distinctive lithotectonic assemblage extending from the eastern Alaska Range to southernmost Alaska and forms a narrow belt which in general separate the Alexander and Taku terranes [Berg et al., 1972; Monger and Berg, 1985]. Gravina strata appear to depositionally overlie the Alexander terrane on Gravina Island [Berg, 1973; Rubin, unpublished mapping], Annette Island [Rubin, unpublished mapping], and on Kupreanoff Island [McClelland and Gehrels, 1987]; however, the contact is never exposed at any of these localities. To the east, Gravina strata unconformably overlie metamorphosed and deformed rocks of the Permian and Triassic parts of the Taku terrane [Rubin and Saleeby, 1988]. To the north on the Chilkat Peninsula, Gravina strata unconformably overlie the Cilkat sequence that is interpreted as a displaced fragment of Wrangellia [Plafker et al., 1989]. Gravina belt strata have not been identified within or east of the Coast Plutonic Complex.

In southern southeast Alaska, the Alexander terrane forms structural basement for most of the rocks that lie west of the Coast Plutonic Complex, including rocks of the Gravina sequence (Figure 2). The Alexander terrane consists of a structurally intact lower Paleozoic ensimatic arc sequence overlain by middle Paleozoic clastic and carbonate strata and a Upper Triassic rift-related assemblage [Gehrels and Saleeby, 1987a]. In most areas, rocks of the Alexander terrane are only slightly deformed and are not highly metamorphosed [Gehrels and Saleeby, 1987a, b], except near the eastern edge of the terrane where they are overprinted by late Mesozoic deformation [Rubin and Saleeby, 1987a; Saleeby, 1987]. East of and apparently depositionally overlying the Alexander terrane lies the mid-Upper Jurassic to Lower Cretaceous Gravina belt.

Structurally overlying the Alexander terrane and Gravina belt is the Taku terrane. In the Ketchikan area, the Taku terrane has two major lithologic components : 1) the upper Paleozoic and middle Mesozoic Alava sequence and 2) the mid-Paleozoic and older Kah Shakes sequence. The Alava sequence contains Pennsylvanian, Lower Permian and middle Triassic shallow water limestone interbedded with and overlain by mafic aphyric flows, pillow breccia, pyroclastic strata, and quartzite [Silberling et al., 1981; Rubin and Saleeby, 1988; Rubin and Saleeby, in review]. Based on the similarities in lithologies and fossil ages, the Alava sequence may represent a highly metamorphosed and structurally fragmented part of the Yukon-Tanana

and Stikine terranes [Rubin and Saleeby, 1988, Rubin and Saleeby, in review]. Locally, channel-fill deposits of the Gravina sequence unconformably overlie the Alava sequence and thus form an overlap between the Alexander terrane and the Alava sequence. The Kah Shakes sequence locally occupies higher structural levels and consists of Devonian orthogneiss, silicic metavolcanic rocks, quartz-rich metasediments, metabasalt, marble, calc-silicate, and quartzite. The quartz-rich metasedimentary rocks may be correlative with the lower Paleozoic portion of the Yukon-Tanana terrane [Gehrels et al., 1990; Saleeby and Rubin, 1989, 1990] and record deposition on a slope and continental margin setting. Primary relations between the Kah Shakes and Alava sequences are uncertain; however, the presence of Alava crinoidal marble interlayered Kah Shakes affinity quartzite suggest an early depositional tie. Thus, the Gravina sequence may overlap both the Alexander terrane, Alava, and Kah Shakes sequences.

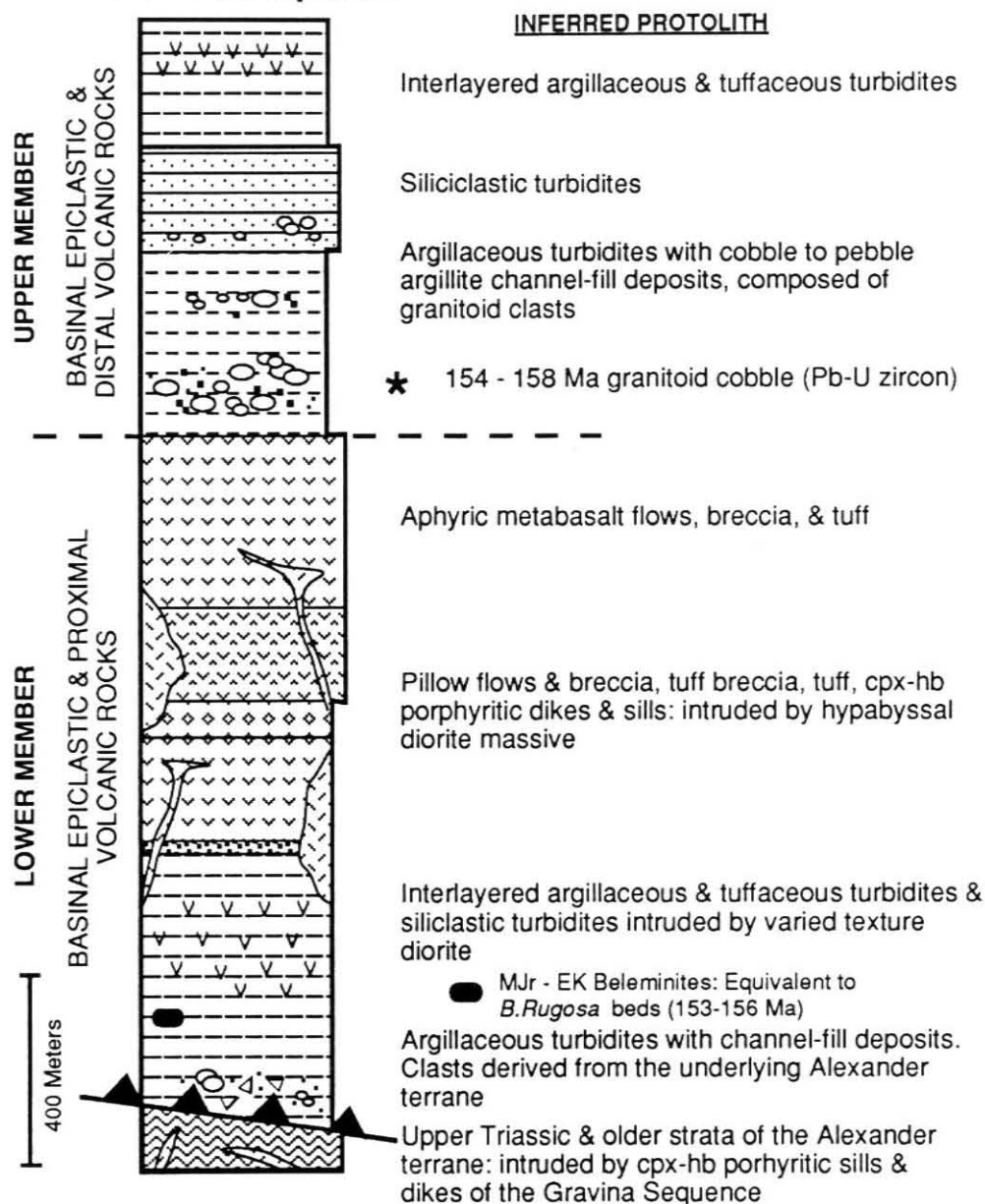
GRAVINA SEQUENCE

A revised stratigraphy is presented here for the southernmost part of the belt, where it is exposed on Annette, Gravina, and Revillagigedo Islands and Cleveland Peninsula (Figure 2). Our data suggest that the ages and lithologies of the assemblage exposed in the Ketchikan area are atypical of the Gravina belt exposed to the north in the Juneau area and in the eastern Alaska Range. Because of these differences, we informally use the Gravina sequence to include all the Upper Jurassic to Lower Cretaceous rocks in the Ketchikan-Prince Rupert region. The revised stratigraphy includes the least deformed and metamorphosed rocks of the Gravina Formation and rocks that until now were thought to constitute part the Taku terrane [Berg et al., 1988].

The Gravina sequence consists of marine pyroclastic and volcanoclastic strata, argillite, greywacke, and conglomerate [Berg et al., 1978] and is intruded by plutons that range in composition from diorite to granodiorite. Locally, Alaska-type zoned ultramafic bodies intrude epiclastic rocks of the Gravina sequence. Approximately 70 km north of the Ketchikan area, the youngest fossils obtained from the Gravina sequence are Albian in age [Berg et al., 1972]. Near Ketchikan, the Gravina sequence consists of two distinctive members that can be recognized throughout the study area (Figure 3). The lower member consists of coarse marine pyroclastic strata, mafic flows, breccia, and fine-grained tuff which are locally intruded by hypabyssal bodies of diorite and quartz diorite. Fine- to coarse-grained turbidites and related channel-fill deposits

Figure 2-3. Generalized stratigraphic section of the Gravina sequence on Gravina Island (Figure 2). The base of the section is in fault contact with the underlying Alexander terrane and the top of the section is not seen in this area. On northwestern Annette and northern Gravina Islands, similar strata unconformably overlie the Alexander terrane.

Gravina Sequence



compose the upper member of the Gravina sequence, which appears to locally lie unconformably upon the Alava sequence and locally on the lower volcanic member of the Gravina sequence. The stratigraphic thickness of the Gravina sequence remains uncertain due to deformation and thrust faulting.

LOWER MEMBER

Stratigraphy

The lower member of the Gravina sequence is characterized by massive, cliff-forming basaltic breccia, flows, and tuff on Cleveland Peninsula and Gravina Island. This member extends from the south on Annette Island to Gravina Island and Cleveland Peninsula in the north (Figure 2). The lower contact of this member is not exposed and at most localities the base of the Gravina sequence is in fault contact with the Alexander terrane [Brew and Karl, 1987]. On northwestern Annette Island and northern Gravina Island, clasts that are lithologically and petrographically identical to the underlying Triassic Hyd Group of the Alexander terrane are incorporated in Gravina argillite (Figure 4). The contact between the Gravina sequence and the Alexander terrane on these Islands is interpreted as a faulted unconformity, based on the presence of these coarse detritus in the Gravina sequence. The top of the lower member is designated at the base of the overlying tuffaceous and argillaceous turbidites and conglomerate. This stratigraphic contact is exposed on Gravina and Revillagigedo Islands and on Cleveland Peninsula.

The lower member has a structural thickness of ≈ 1300 meters and is easily distinguished from similar lithologies in the Alexander terrane by the predominance of relatively fresh hornblende and augite phenocrysts, and the lack of near pervasive Fe-carbonate alteration in the flows, breccia, and tuffs. Lithologic units within the lower member are divided into four groups: (1) mudstone, calcareous argillite, conglomerate and carbonate, (2) water-laid coarse pyroclastic deposits and tuff, (3) lava flows, and (4) intrusive rocks.

A distinctive silicic- and carbonate-clast conglomerate is present at the base of the lower member. The conglomerate consists of matrix and locally grain-supported pebble- to cobble-sized, angular to sub-angular clasts of meta-rhyolite, metabasalt, limestone and dolomite, that were derived from the underlying Alexander terrane. Conglomerate beds are lenticular in shape and are interbedded with planar laminated

Figure 2-4. Deformed basal conglomerate of the lower member of the Gravina sequence on northwestern Annette Island (Fig. 2), with clasts from the underlying Triassic Hyd Group of the Alexander terrane.



argillite and siltstone. The conglomerate is succeeded by thinly laminated, black to grey argillite, siltstone and shale. Siliciclastic rocks display cm-sized fining-upwards sequences of siltstone-mudstone couplets.

Pyroclastic deposits and lava flows dominate the lower member (Figure 3). Pyroclastic deposits overlie argillite and occur in units generally less than 20 m in structural thickness, but vary up to 500 m. The coarse-grained pyroclastic flow breccias contain clasts as coarse as 40 cm that are angular to sub-angular in shape. These deposits are generally monolithologic, with large hornblende and augite phenocrysts present in both the matrix and clasts; phenocrysts are up to 3 cm in diameter. Lithic fragments within the pyroclastic deposits consist of hornblende-augite phyric angular to sub-angular clasts in a phyric or aphyric tuffaceous matrix. Subordinate pyroclastic deposits with aphyric matrix and clasts are also present. The proportion of matrix is generally 50% and clast-supported fabrics are rarely observed. Bedding is characteristically massive; however, tectonic deformation probably obscures original bedding features. A second category of volcanic deposits include crystal-rich tuff and tuffaceous argillite. These rocks consist of euhedral amphibole and augite, and rare feldspar phenocrysts in a pale green tuffaceous matrix containing augite, hornblende, epidote-clinozoisite, albite, quartz and white mica. Typically the phenocrysts make up 10-15% of the rock. Locally, crystals occur in discrete layers or horizons. In places, dikes of hornblende-augite porphyry cross-cut the interlayered argillite.

Pillowed and massive mafic to silicic flows make up the remaining part of the lower member and are best exposed on southern Cleveland Peninsula. Typically, the mafic phyric flows are massive and are locally interlayered with black argillite. Hornblende-augite-bearing porphyries intrude parts of the lower member argillite and tuffaceous argillite. The phenocrysts and matrix of these dikes are compositionally similar to the phyric flows and tuff which are common within the lower member. On the northwest shore of Annette Island, massive augite porphyry intrudes banded carbonaceous limestone, laminated felsic tuff, and limestone of the Alexander terrane.

Structurally concordant tabular bodies of hypabyssal diorite intrude lower member Gravina rocks. The diorite is texturally diverse and displays relict porphyritic, ophitic and granular textures. The contact between the diorite and enclosing volcanic rocks are compositionally and texturally gradational, and lacks

well-defined contact aureole. Attempts to extract zircon (for U-Pb isotopic analyses) from varied textured diorite were unsuccessful.

Age

The age of the lower member is poorly constrained and is based upon fossil ages reported by Chapin, [1918], Berg et al., [1972], and Berg [1973]. Poorly preserved *Buchia rugosa* is present in argillite on southern Gravina Island, indicating a Late Jurassic age (Kimmeridgian) (Figure 3). Abundant belemnites (*Cylindroteuthis*) which range in age from Middle to Late Jurassic [Berg, 1973] are present from Blank Inlet on southern Gravina Island. Large pelecypods, up to 20 cm in diameter (*Entolium*) are also present from Blank Inlet and Blank Island, which range in age from Middle Triassic to Early Cretaceous [Berg, 1973]. The age is limited to post-Upper Triassic, the age of the youngest fossils in the underlying Alexander terrane. In summary, available fossil age data indicate a Late Jurassic age for at least part of the lower member of the Gravina sequence [Berg, 1973; Berg et al., 1988].

Geochemistry

A critical question concerning the Gravina sequence volcanics is the identification of their paleotectonic environment. For mafic volcanic rocks which have undergone low grade metamorphism, two useful methods classify and discriminate magmas erupted in different tectonic settings: (1) examination of the concentration of trace elements such as Ti, Zr, Y, Cr, Nb and (2) rare-earth elements (REE) in the lavas and dikes [Pearce and Cann, 1973; Winchester and Floyd, 1973; Garcia, 1978; Gill, 1981; Pearce, 1982, 1983; Pearce et al., 1984; Thompson, 1982]. The criteria used to distinguish tectonic affinities of magmas are derived from empirically determined values from a variety of modern plate tectonic settings [Pearce, 1982, 1983; Pearce and Norry, 1979]. Trace elements that are relatively immobile during seafloor alteration and greenschist facies metamorphism are used [Cann, 1970; Humphris and Thompson, 1978]. Rare earth, major, and trace element analyses of lavas and dikes from the Gravina sequence are given in Table 1 and 2, and the data are plotted on both trace element discrimination diagrams (Figure 5) and on a trace-element

Table 1 Gravina Sequence volcanics; major and minor element analyses

Sample #	84JRa	84JRb	85CR104a	85CR206	85CR220a	85CR221	85CR227	87CR31	87CR38
SiO ₂ ^a	49.40	52.10	47.90	46.90	48.70	48.44	49.40	47.90	47.60
Al ₂ O ₃	16.90	17.70	16.50	18.20	10.60	18.50	18.50	12.50	13.20
Fe ₂ O ₃	8.85	8.59	11.10	11.80	9.73	10.60	9.41	14.10	11.20
MgO	6.39	5.88	6.55	5.92	12.10	4.85	5.08	8.91	10.30
CaO	9.49	9.03	12.90	3.86	11.40	10.50	12.00	11.00	9.81
K ₂ O	0.66	0.91	0.83	0.51	0.61	0.86	1.20	0.24	0.15
Na ₂ O	3.19	3.40	1.73	4.80	2.91	2.91	2.00	1.29	3.12
TiO ₂	0.53	0.50	0.69	1.15	0.65	0.56	0.60	1.00	0.15
P ₂ O ₅	0.09	0.09	0.11	0.49	0.21	0.12	0.12	0.28	0.83
MnO	0.19	0.19	0.21	0.19	0.15	0.19	0.15	0.19	0.28

Determined by ED-XRF; analysts: J. Taggart, A. Bartel, and D. Siems.

Table 2. Gravina Sequence mafic volcanic rocks; trace element analyses

Sample #	84JRa	84JRb	85CR104a	85CR206	85CR220a	85CR221	85CR227	87CR31	87CR38
Ba ^b	214	255	314	316	201	208	234	58.1	39.8
Rb ^a	10	16.5	13	16.3	7.6	15.9	11.6	7.9	2.6
Th	0.8	0.771	0.57	3.7	1.0	1.0	0.9	1.4	1.8
K	5478	7554.0	6891.0	4234	5064	7143	9962	-	-
Nb ^a	<10	<10	<10	<10	<10	<10	<10	<10	<10
Ta	0.2	0.2	0.1	0.5	0.2	0.1	0.1	0.2	0.2
La	4.9	4.9	4.6	20.9	8.5	6.2	5.1	10.1	10.9
Lu	0.23	0.3	0.2	0.3	0.2	0.3	0.2	0.2	0.2
Ce	10.4	10.6	10.1	46.6	20.0	12.5	9.9	24.1	24.3
Eu	0.7	0.8	0.8	1.8	1.0	0.7	0.6	1.2	1.1
Sr ^a	500	480	370	620	300	490	350	741	494
Nd	6.5	7.2	6.8	26.7	12.7	7.9	7.5	13.5	13.7
Sm	1.9	2.	2.2	6.5	3.2	2.1	1.9	3.6	3.4
Ni	50	47.5	28.1	31.5	116	26	20	38.5	70.6
Cr	209	124	50.8	30.1	622	14.7	14	253	42.6
P	393.	393	480	2138	916	524	524	370	629
Hf	1.1	1.1	0.8	2.5	1.1	1.2	1.0	1.2	1.5
Ti	3177	2998	4136	6894	3897	3357	3597	5999	4975
U	0.3	0.4	0.3	1.5	0.4	0.6	0.3	0.7	0.8
Y ^a	12.	12	10	20	12	12	10	9.0	11
Yb	1.8	1.8	1.6	2.1	1.1	1.7	1.5	1.4	1.3
Zr ^a	55	55	40	110	55	60	45	54	21.9
Ba/La	43	52	68	15	24	34	46	5.8	3.5
Ba/Ta	1065	4256	3655	640	1233	1486	1857	331	173.8
Ce/Yb	5.9	5.9	6.2	21.8	17.4	7.3	6.7	17	18
Hf/Lu	4.0	4.0	3.6	8.0	6.0	4.5	4.3	5.9	7.6
Hf/Ta	5.4	4.5	9.3	5.1	7.0	8.3	7.6	6.8	6.9
La/Sm	2.5	2.4	2.1	3.2	2.7	2.9	2.6	2.8	3.2
La/Ta	24	24	54	43	52	44	40	57	47.6

Minor elements and REE's in PPM

^aDetermined by ED-XRF; other minor elements by INAA. Analysis: D. Fey, J. Budahn, T. Frost (trace elements) and S. Mac Pherson (wet chemistry).

Figure 2-5. Trace-element discrimination diagrams showing data from Gravina sequence metabasalts. A) Ti/Zr discrimination diagram of Pearce and Cann (1973); B) Cr/Y discrimination diagram of Pearce (1982); Zr/TiO₂ vs Nb/Y discrimination diagram of Winchester and Floyd (1977).

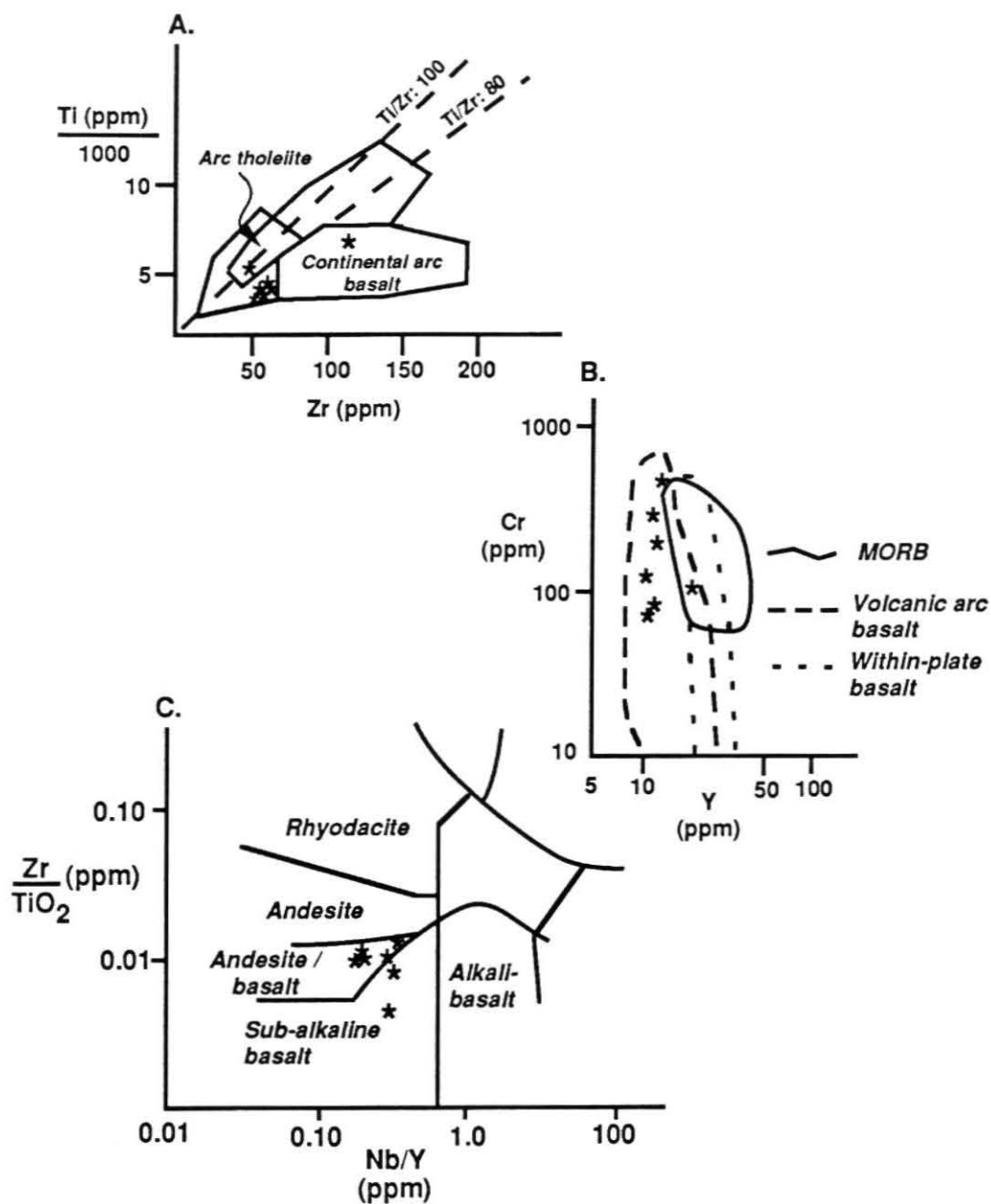
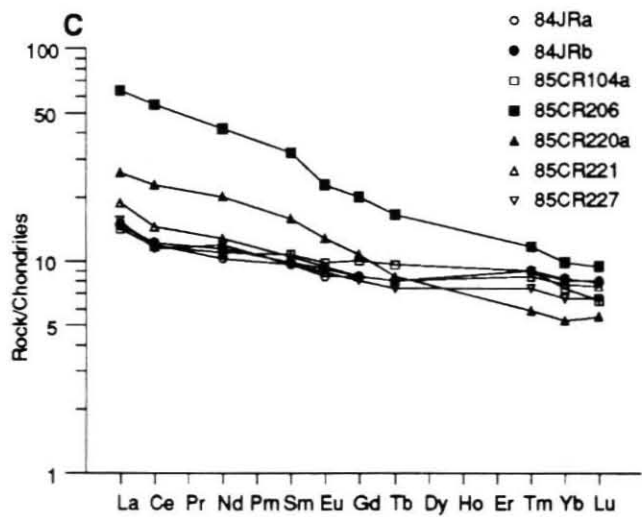
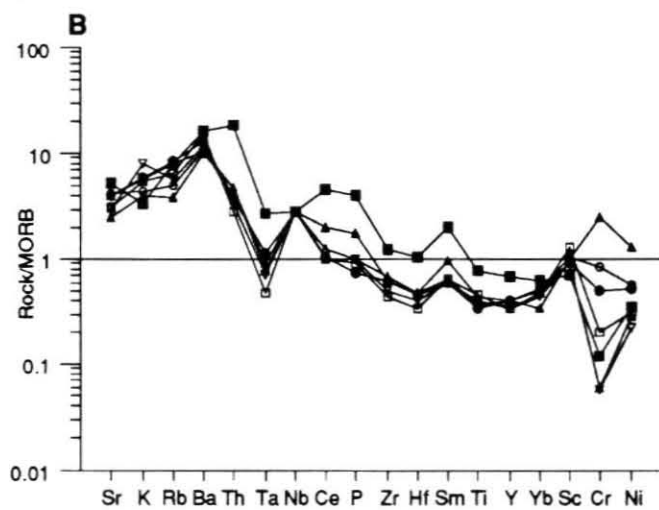
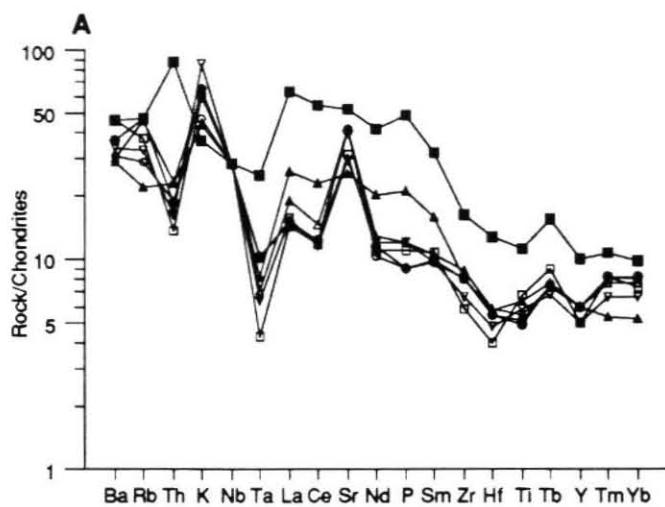


Figure 2-6. Normalized incompatible-element patterns for the Gravina sequence metabasalts. A) Chondrite-normalized plot after Thompson (1982), B) MORB-normalized plot after Pearce (1983), C) Chondrite-normalized REE plot. All data normalized after Nakamura (1974). Multi-element plots generated by program after Wheatley and Rock (1988).



discrimination diagrams (Figure 6) according to the conventions suggested by Thompson, [1982], and Pearce [1982].

These discrimination diagrams suggest that most of the Gravina sequence lavas and dikes closely resemble modern-island arc tholeiites (Figure 5 a,b). Ti/Zr ratios of the Gravina volcanics fall within the arc tholeiite field, with the only exception of sample 85 CR 206, which falls in the continental arc basalt field. On a Cr/Y plot (Figure 5 b), the data plot either in the low Y part of the arc tholeiite field or in the high Y part of the MORB field. Ti/Zr ratios are low and plot within the IAT and continental-arc basalt field or arc tholeiite-MORB overlap fields; however, these low TiO₂ and Zr values are not typically seen in MORB [Pearce and Cann, 1973]. When Nb/Y is plotted against Zr/TiO₂, all of the values fall within the andesite/basalt and overlap with the sub-alkaline basalt fields. Typically, these samples have low Nb/Y and Zr/TiO₂ ratios. REE and incompatible trace-element data show typical patterns for basalts erupted in a oceanic island arc setting (Figure 6). These analyses indicated that they are generally similar to the average island arc tholeiite basalt [Pearce, 1980, 1982; Thompson, 1982] and are products of subduction-related magmatism. The Gravina volcanics have low REE abundances and minor LREE (light rare earth elements) enrichment (Figure 6c), which is characteristic of modern arc tholeiite suites [Gill, 1981]. Low TiO₂ and Cr contents are consistent with this interpretation.

Trace elements also provide information on both the source and subsequent differentiation history of magmas. There is a characteristic trace element signature for volcanic rocks erupted at convergent plate margins, in particular, source regions are typically enriched relative to REE in both K-group and Th-group trace elements and depleted in Ti-group trace elements [Gill, 1981]. Ratios of highly incompatible trace elements reflect source composition because they do not change during melting or fractionation. The Gravina sequence mafic lavas are enriched, relative to MORB in Ba, Sr, K, Rb, and Th (Figure 6); these patterns may be attributed to a subducted sedimentary component [e.g., Kay, 1980], however, this enrichment can also record local variations of arc basement [Moorbath and Hildreth, 1988]. Alternately, seafloor and subsequent regional metamorphism may have affected these values. A subducted-slab source for this enrichment is unlikely, because of the absence of negative Eu and Ce anomalies. The lack of Eu and Ce anomalies is thought to reflect the relative absence of a sedimentary contribution to the magma source

[McLennan and Taylor, 1981; White and Dupré, 1986]. The mafic rocks are enriched in LIL (large ion lithophile) elements relative to MORB and have high Ba/Ta ratios (>24 , except 87CR206) which indicate excess LIL to LRE elements relative to MORB. High Ba/Ta ratios are common in volcanic arcs and are representative of low-K island arc tholeiite magmas [Gill, 1981]. High Ba/La and Ba/Ta ratios, moderate La/Ta ratios, and moderate LIL elements contents (relative to high field strength and LRE elements) are also characteristic of the Gravina sequence mafic rocks (Table 2). These values suggest that the Gravina basaltic magmas were controlled by the underlying mantle wedge and locally influenced by its ensimatic arc basement.

In summary, based upon trace-element abundances for Cr, Zr, Ti, multi-element and REE patterns, combined with the presence of significant amounts of pyroclastic volcanic rocks and interbedded turbidites, we interpret the lower member Gravina sequence volcanics as products of a oceanic volcanic arc complex. These compositions and geochemical variations are similar to immature island arcs of the western Pacific [Gill, 1981]. Mafic rocks from the island-arc tholeiite suite are distinguished by low abundances of Ti, Cr, Zr, and \[for example see Gill, 1981 and Ewart, 1982], which also characterize the Gravina volcanics. These features, along with flat REE patterns with minor LREE enrichment indicate an island-arc tholeiitic paleotectonic setting [e.g., Garcia, 1978; Gill, 1981; Thorpe, 1982 and many others] for the lower member Gravina volcanic strata.

Depositional setting

The base of the lower member of the Gravina sequence contains pebble to cobble conglomerate which are thought to have been derived from the underlying Triassic Hyd Group. Based upon the presence of laterally continuous, planar-laminated, normally graded sequences of argillite, calcareous argillite, and siltstone, and the lenticular beds of the predominantly matrix-supported conglomerate, the lowermost part of the Gravina sequence is interpreted as submarine turbidite deposits. Lenses of coarse-grained conglomerate represent associated channel-fill deposits. Proximity to the Alexander terrane is suggested by two lines of evidence. (1) The coarse-grained detritus in the turbidites was derived from the underlying Alexander terrane. (2) Lower member hornblende-augite porphyry intrudes Upper Triassic rocks of the Alexander terrane on

Annette Island. Hornblende-augite porphyry dikes represent the subvolcanic feeder to the overlying volcanic rocks.

Large volumes of mafic to intermediate volcanic debris overlie the argillaceous turbidites. These volcanic rocks contain mostly coarse-grained pyroclastic deposits, phryic tuff and massive flows. Monolithologic blocks in tuff breccia and blocky flows indicate little or no mixing of volcanogenic debris. The compositionally uniform crystal-rich mafic tuff matrix suggests that the deposits are a direct result of explosive eruptions. Locally, pillowed and massive flows overlie and are intercalated with argillaceous turbidites. Deeper structural levels are represented by the texturally varied diorite. The diorite is compositionally and texturally similar to the volcanic rocks, displays the same structural and metamorphic features, and lacks a well-defined contact aureole, substantiating that the diorite and metavolcanic rocks are co-genetic as suggested by Berg [1972]. The intrusion of hypabyssal diorite into the pyroclastic aprons probably caused sediment failure that resulted in volcanic slides, similar to geologic relations observed in volcanoclastic sedimentary rocks on Cedros Island [Busby-Spera, 1988a].

Sedimentary and igneous structures of the pyroclastic deposits and mafic lava flows indicate both distal and proximal volcanic facies are present. Proximal lava flows are pillowed and unbroken, whereas in distal positions are dominated by pillow breccia. The proximal pyroclastic deposits contain large, juvenile monolithologic blocks; accidental fragments are uncommon. Fine-grained crystal-rich tuff, lapilli-sized lithic tuff, and tuffaceous turbidites are more common in distal areas. A northern and western source area for the volcanoclastic aprons are supported by stratigraphic and sedimentologic data. The thickness and overall grain size of mafic pyroclastic deposits decrease to the south and east. There are no known coarse-grained pyroclastic rocks on the eastern and southern portions of the Gravina basin in the Ketchikan area. Vent plugs, represented by varied-texture hypabyssal diorite, are present on the northern and western margin, which supports the idea of a northern and western source for the volcanoclastic sedimentary rocks. The widespread occurrence of mafic flows indicate fissures must have been present throughout the basin.

In summary, a simple progradational depositional sequence emerges from facies relations within the lower member. The basal unit was deposited as turbiditic flows with channel-fill sequences containing clasts derived from the underlying Alexander terrane. The turbidites are overlain by thick, submarine pyroclastic

debris and lava flows. The predominance of pyroclastic deposits interbedded with massive flows, tuff and argillaceous turbidites together with the presence of co-genetic intrusives and trace element geochemistry indicate a basinal volcanic arc setting for the lower part of the Gravina sequence. These basinal pyroclastic deposits were shed from the flanks of submarine strato-volcanos during Late Jurassic time and represent the initial stage of arc activity. Hypabyssal intrusive rocks represent the intrusive equivalents of the lavas recognized within the section.

UPPER MEMBER

Stratigraphy

The upper member consists of poorly exposed siltstone, argillite, tuff, slate and conglomerate. In the study area, this member extends from the south on Annette Island to Cleveland Peninsula in the north (Figure 2). The best exposures are on southern Cleveland Peninsula, southwestern Revillagigedo and adjacent smaller islands. The lower contact of this member is not exposed; however, locally it is inferred to unconformably overlie both the lower volcanic member of the Gravina sequence and the Permian and Triassic Alava sequence (Figure 4). Basal conglomerate unconformably overlies Alava strata; no evidence for faulting is present. The top of the section is not exposed and the highest observed levels are in fault contact with adjacent terranes.

The upper member has an approximate structural thickness of 900 meters. The member is readily distinguished from similar rock types in both the lower member of the Gravina sequence and the Alava sequence by the predominance of argillaceous turbidites, the presence of interbedded pebble to cobble conglomerate interstratified with the turbidite deposits, and by the lack of interlayered, thick units of marble and mafic metavolcanic rocks. Sedimentary structures are generally better preserved here than in the lower member.

Lithologic units in the upper member can be divided into two groups or facies: (1) argillaceous and tuffaceous turbidites, and (2) pebble to cobble conglomerate. The argillaceous strata are characterized very fine- to fine-grained clastic beds which contain mostly dark grey, argillaceous siltstone, mudstone, and minor feldspathic sandstone and silty limestone. Sparse granules and pebbles are present within the argillaceous

layers and are composed of very-fine grained felsic igneous clasts. Bedding is generally medium to thick (20-80 cm); however, locally massive beds are up to 2 meters thick. Argillite rip-up clasts are common within the sandy layers. Graded bedding, plane laminated sandy layers, and amalgamated beds are together present locally (Figure 7). Other bedform structures are not recognized. The tuffaceous strata consist of very fine- to fine-grained, light gray to tan beds with very small crystals of feldspar and mafic minerals in a white mica-epidote-feldspar matrix

Pebble and cobble conglomerate is interbedded with the argillaceous turbidites (Figure 8). Conglomerate beds occur in a distinctive mappable horizon that is exposed between southeastern Revillagigedo Island and southern Cleveland Peninsula and consists of beds 0.5 to 2 m thick. Beds are commonly lenticular on an outcrop scale. The conglomerate overlies finely laminated argillite and siltstone and grades stratigraphically upwards into grey argillite that contains fewer coarse clasts (Figure 7). The conglomerate bearing horizon also contains thin layers of grey phyllite and siltstone with sparse granules of leucocratic fragments and argillite rip-up clasts. Clasts are matrix-supported and are usually less than 18 cm in diameter, and average 3-8 cm in an argillaceous matrix. On Revillagigedo and adjacent islands, boulders up to 40 cm in diameter occur. Few sedimentary structures are present due to polyphase deformation. The clasts are spheroidal to ellipsoidal as the result of younger deformation (Figure 8), and consist of fine- to coarse-grained granodiorite, quartz diorite and leucocratic diorite, volcanic porphyry, argillite, minor marble and vein quartz material. The matrix is fine-grained argillite containing quartz, albite, biotite, epidote, calcite and white mica.

Provenance and U-Pb isotopic data

The rock types of clasts in the pebble to cobble conglomerates were counted in the field (Table 3) and are plotted according to major constituents on ternary diagrams (Figure 9). The conglomerate units contain mostly volcanic and plutonic lithic clasts, with relatively few sedimentary lithic clasts. Mixing of these two rock types within the conglomerate suggests that they were derived from a composite volcano-plutonic source. The presence of plutonic and lesser volcanic clasts suggest deposition near an uplifted region comprised of both its volcanic cover and plutonic substrate.

Figure 2-7. Measured lithostratigraphic section of part of the upper member of the Gravina sequence on Back Island.

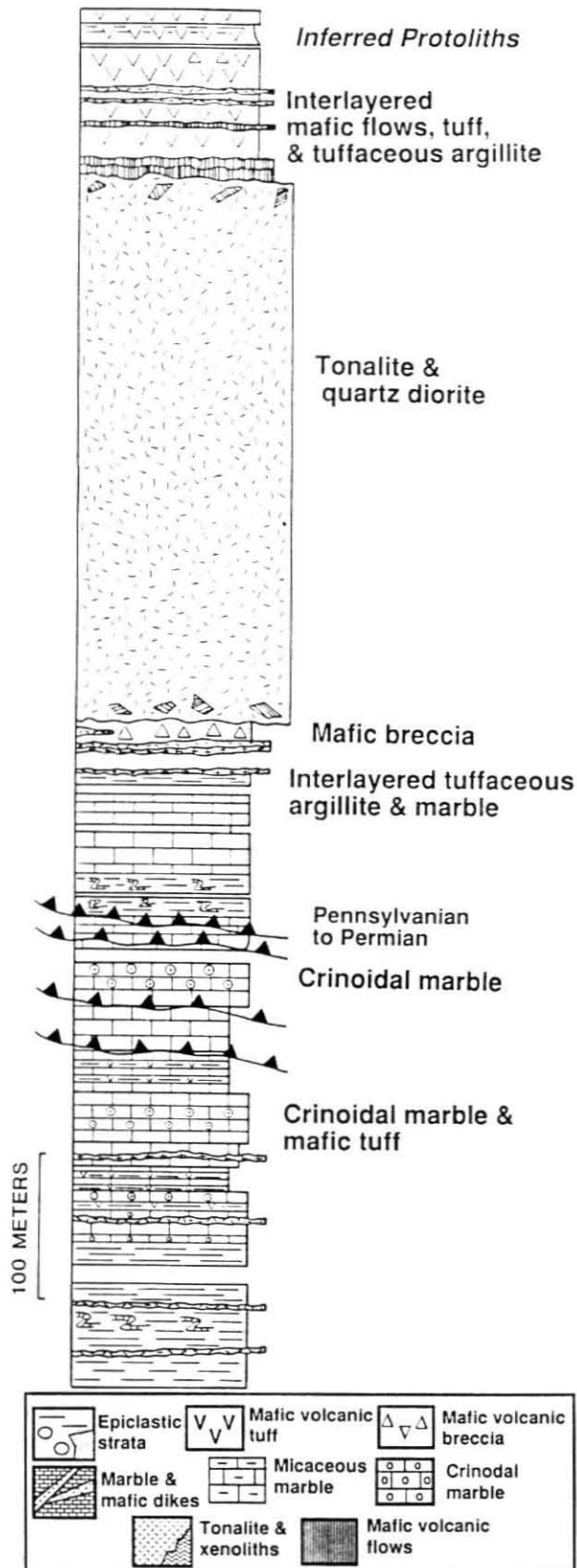


Figure 2-8. Highly deformed channel-fill conglomerate of the upper member of the Gravina sequence on Betton Island. Plutonic clasts in the conglomerate yield Pb-U zircon ages of 154 Ma to 158 Ma. The largest clast in the photograph is approximately 45 cm in diameter; clasts at Gnat Cove and Back Island are locally over 60 cm in diameter.



Figure 2-9. Composition of pebble and cobble populations from conglomerate within the upper member of the Gravina sequence, Lsu, lithic sedimentary undifferentiated; Liv, lithic volcanic and plutonic; Li, lithic plutonic; Lv, lithic volcanic, lq, lithic quartzite and vein quartz.

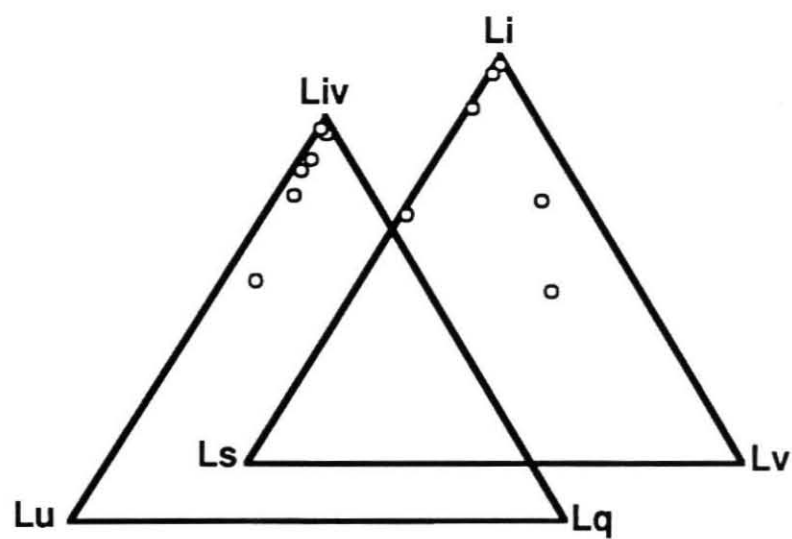


Table 3. Pebble and cobble counts, upper member of the Gravina sequence, southern southeastern Alaska

Samples	N	Occurrence (% of clasts randomly encountered)					
		Li Intrusive	Lv volcanic	Lvi	Ls argillite, marble	Lq quartz vein	Lsu
Gnat Cove	102	98	-	98	2	-	2
South Hume Island	102	96	-	96	2	2	2
Betton Island	269	63	27	90	7.3	2	7.3
Back Island	102	47	34	81	16	3	16
Gin Point	105	87	-	87	11	2	11
Guckers Cabin	109	60	-	60	34	6	34

Ages of granodiorite and quartz diorite clasts within the pebble to cobble conglomerate have been determined using Pb-U zircon methods (Tables 4 and 5). Zircon separates were prepared by standard mineral separation techniques. Isotopic data were determined on a 35 cm VG 90° extended geometry sector multicollector and on a 30.48 cm, 60° Lunatic IV mass spectrometers at Caltech. Lead was loaded with H₃PO₄ acid-silica gel [Cameron et al., 1969] and uranium was loaded with H₃PO₄ acid and graphite. Uranium and lead concentrations were determined on solution aliquots from each sample by isotope dilution using a mixed ²⁰⁵Pb-²³⁰Th-²³⁵U spike.

Seven fractions from four granodiorite and quartz diorite clasts from Gnat Cove and Back Island were analyzed (Tables 4 and 5). The zircon isotopic systematics of the Gnat Cove samples (84JR28 C-1 and C-3; Table 5) are relatively simple and are interpreted as crystallization ages. These samples yield concordant ages of 154 Ma and 158 Ma (Figure 10). The zircon isotopic data for clast C-3 are slightly discordant. The igneous age interpretation for this sample is highly dependent on the discordance mechanism chosen to explain the data. The limited zircon yield from the clast prohibit an in-depth analysis of this question. Broad age bounds are assigned as 172 to 154 Ma (Figure 10) based on possible minor disturbance at a level which would permit the >62μm fraction to retain its internal concordance, or alternatively minor inheritance which would disperse the >62μm fraction off of concordia from the internally concordant fraction. Thus, we interpret the age as 154 Ma. The igneous clast from Back Island (Figure 2) yields an internally concordant age of 157 Ma (Figure 10). The close agreement between the U-Pb ages of all four samples indicate that they represent Late Jurassic crystallization ages for the clasts and suggest a homogeneous or localized source terrane. Clasts from localities that occur over 35 km along strike have common lithologic and U-Pb zircon systematics.

Several possible origins for the coarse-grained plutonic detritus exist. The clasts were previously thought to have been derived from early Paleozoic plutons that are part of the Alexander terrane [Berg et al., 1988]; this possibility is ruled out by geochronologic data presented above. A likely possibility is that the coarse-grained detritus was derived from an uplifted and dissected part of the Gravina arc and its underlying basement complex. The ages of the clasts are similar to those of Late Jurassic fossils found in the lower member of the Gravina sequence [Harland et al., 1982], however, intrusive bodies of similar age have yet to

Table 4. ZIRCON ISOTOPIIC AGE DATA

Sample	Fraction† (μm)	Amount Analyzed (mg)@	Concentrations (ppm)			Atomic Ratios			Isotopic ages (Ma) §		
			²³⁸ U	²⁰⁶ Pb*	²⁰⁶ Pb/ ²⁰⁴ Pb	²⁰⁶ Pb*/ ²³⁸ U	²⁰⁷ Pb*/ ²³⁵ U	²⁰⁷ Pb*/ ²⁰⁶ Pb*	²⁰⁶ Pb*/ ²³⁸ U	²⁰⁷ Pb*/ ²³⁵ U	²⁰⁷ Pb*/ ²⁰⁶ Pb*
84JR28 C-1	<45μ	6.4	944	19.7	4125	0.02407(19)	0.1634	.04925(14)	153.4	153.7	159 ± 5
	45-80μ	1.2	917	19.5	2604	0.02431(21)	0.1645	.04910(44)	154.9	154.7	152 ± 5
84JR28 C-2	60-80μ	1.5	590	12.8	2062	0.02487(14)	0.1685	.04915(07)	158.4	158.1	155 ± 4
	80-100	3.7	448	9.0	6090	0.02344(40)	0.1611	.04989(26)	149.4	151.8	189 ± 12
84JR28 C-3	<62μ	0.4	66	1.4	954	0.02478(14)	0.1691	.04953(10)	157.8	158.7	172 ± 5
	>62μ	2.1	954	20.1	1205	0.02474(16)	0.0673	.04908(06)	154.7	154.5	152 ± 3
84JR12 C3	45-80	3.6	135	3.0	1227	0.24740(12)	0.1673	.04908(44)			
157.6	157.1	151 ± 21									

* Radiogenic; nonradiogenic correction based upon 40 picogram blank Pb (1:18.78;15.61;38.50) and initial Pb approximations: 206/204=48.6; 207/204=15.6; 208/204=38.2.

† Fractions separated by grain size and magnetic properties. Magnetic properties are given as non-magnetic split at side/front slopes for 1.7 amps on Franz Isodynamic Separator. Samples hand-picked to 99.9% purity prior to dissolution. Dissolution and chemical extraction technique modified from Krogh (1973).

§ Decay constants used in age calculation: $\lambda^{238}\text{U} = 1.55125 \times 10^{-10}$, $\text{U}^{235}\text{U} = 9.98465 \times 10^{-10}$ (Jaffey and others, 1971); $^{238}\text{U}/^{235}\text{U}$ atom=137.88. Uncertainties (±) in radiogenic ratios calculated by quadratic sum of total derivatives of ^{238}U and $^{206}\text{Pb}^*$ concentration and $^{207}\text{Pb}^*/^{206}\text{Pb}^*$ equations with error differentials defined as follows: (1) Isotope ratio determinations from standard errors (8/n) of mass spectrometer runs plus uncertainties in fractionation corrections based on multiple runs of NBS 981, 983, and U500 standards; (2) Spike concentrations from range of deviations in multiple calibrations with normal solutions; (3) Spike compositions from external precisions of multiple isotope ratio determinations; (4) Uncertainty in natural $^{238}\text{U}/^{235}\text{U}$ from Chen and Wasserburg (1981); and (5) Nonradiogenic Pb isotopic compositions from uncertainties in isotope ratio determinations of blank Pb and uncertainties in composition of initial Pb from estimates of regional variations based on references given above and consideration of rock type.

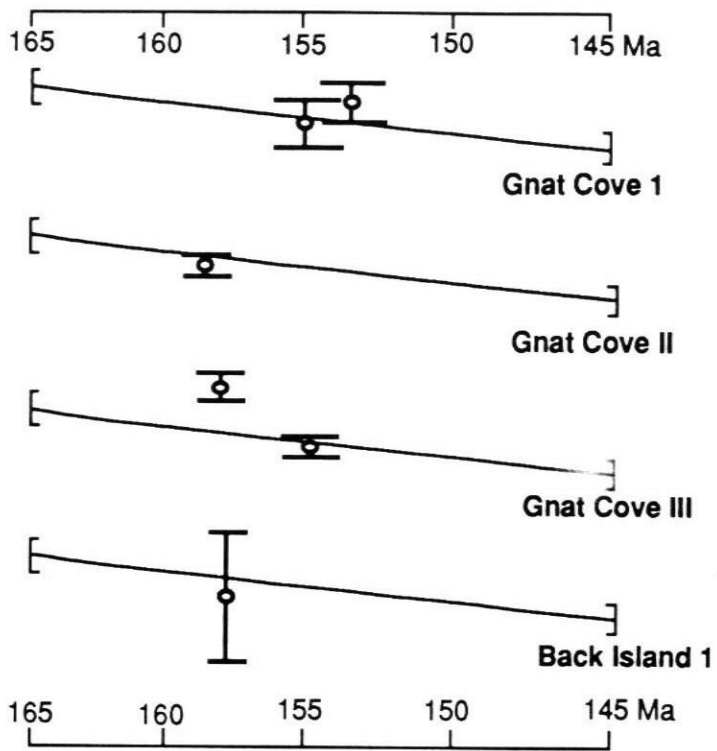
@ Due to uncertainties in weight of sample, U-Pb concentration may be in error, use of mixed ^{205}Pb - ^{235}Th - ^{235}U spike insures age of sample is correct.

Table 5. Pb-U geochronologic sample locations from the Ketchikan area and descriptions of clasts from the epiclastic member of the Gravina sequence.

Sample #	Latitude	Longitude	Lithology	Zircon properties
88JR28				
C-1	N55° 22'50"	131° 19' 24"	Slightly altered, non-foliated fine-grained granodiorite	2:1 to 3:1; Sub=An>Eu; irregular shapes; colorless, grey-tint; colorless, grey-tint; inclusions common.
C-2	N55° 22'50"	131° 19' 24"	Slightly altered, non-foliated medium-grained biotite granodiorite	2:1 to 3:1; Sub>Eu>An; irregular shapes; colorless, grey-tint; inclusions common
C-3	N55° 22'50"	131° 19' 24"	Slightly altered, non-foliated fine-grained leucogranodiorite	3:1; Sub=Eu>An; irregular shapes; colorless, grey-tint; inclusions common in all grains
88JR12				
C-3	N55° 32'9"	131° 45'15"	Slightly altered, non-foliated fine-grained granodiorite	2:1, Sub>Eu>An; colorless, grey-tint inclusions common in all grains

notes: Eu, euhedral; Sb, subhedral; An, anhedral. 2:1, length:width ratios of zircon grains. color determined under reflected light. C-1, clast number.

Figure 2-10. Stacked segments of concordia and data points for clasts within the upper member of the Gravina sequence. Concordia diagram after Tera and Wasserburg (1971). Linear regression and errors in lower and upper intercepts are adapted from York (1969). Bars at ends of concordia segments show uncertainty in $^{207}\text{Pb}/^{206}\text{Pb}$ values of concordia from uncertainties in ^{238}U and ^{235}U decay constants after Jaffey and others (1971).



be found in the lower member or its substrate. Despite the lack of dated intrusive rocks in the lower member, the lower member does contain compositionally similar rock types to some of the plutonic clasts that have been interpreted as cogenetic with the volcanic section, as discussed above. Furthermore, since Gravina overlap strata and its basement were structurally imbricated during mid-Cretaceous time, much of the arc may be concealed beneath thrust sheets.

Another possibility is that the granitic debris may have been derived from a displaced arc terrane that has been removed by strike-slip faulting. It has long been recognized that major strike-slip faulting has affected northwestern Cordillera [Gabrielse, 1985; Oldow et al., 1989]. Both southern and northern possible source terranes exist which may have provided detritus for the upper member conglomerates. To the south, in northwestern British Columbia, Late Jurassic igneous activity has been recently recognized within the Coast Plutonic Complex [Armstrong, 1988; Van der Heyden, 1987]. Although many of these plutons display internal discordance, zircon from quartz diorite and granodiorite plutons yield crystallization ages from 154 Ma to 158 Ma [Van der Heyden, 1988]. This Late Jurassic plutonic suite may have provided the clastic detritus to the upper member of the Gravina sequence, requiring 150 km of post-Late Jurassic sinistral strike-slip displacement along inferred faults within the western boundary of the Gravina sequence. Strike-slip faults and associated fabrics of this age in southeastern Alaska and western British Columbia are lacking and this hypothesis is difficult to test since critical contacts might lie underwater beneath Dixon Entrance or within the younger Coast Plutonic Complex on the mainland. Late Jurassic to Early Cretaceous sinistral strike-slip motion in southeastern Alaska has been suggested by Plafker et al. [1989]; however, and may provide indirect support for strike-slip displacement of the plutonic source terrane.

Alternatively, Late Jurassic metaplutonic rocks in the eastern Chugach and St. Elias Mountains, exposed to the north, may represent the source terrane for the upper member igneous clasts. These metaplutonic rocks extend south-eastward toward Chichagof Island in southeastern Alaska and are part of the Tonsina-Chichagof belt of Hudson [1983] and the Muir-Chichagof belt of Brew and Morrell [1983]. The belt consists of foliated hornblende quartz diorite, tonalite and granodiorite. Age relations are poorly known; however, hornblende K/Ar cooling ages for these plutons range between 143 Ma and 170 Ma which suggest a regionally extensive Late Jurassic magmatic belt in southwestern Yukon and southeastern Alaska [Dodds

and Campbell, 1978; Grantz et al., 1966; Loney et al., 1975; Karl et al., 1987]. If these plutons are the source for the upper member clasts, approximately 250 km of sinistral strike-slip offset is required along inferred faults located within or east of the Gravina arc strata. However, no such faults or associated fabrics in post-Jurassic strata have been recognized in the region.

In summary, the three possible source terranes for the coarse-grained plutonic detritus include: (1) uplifted and dissected parts of the Gravina arc, (2) Late Jurassic plutonic rocks exposed to the south in northwestern British Columbia, and (3) Late Jurassic plutonic rocks exposed to the north in the eastern Chugach and St. Elias Mountains. We prefer the *in situ* model for the origin of the coarse detritus since no direct evidence exists for Late Jurassic to Early Cretaceous strike-slip faulting in southern southeast Alaska.

Age

No fossils have been found within the upper member of the Gravina sequence in southern southeastern Alaska, thus, its depositional age is poorly constrained. The Late Jurassic provenance ages for granitic clasts provide a maximum age for deposition. Locally, the upper member depositionally overlies the Upper Jurassic and Lower Cretaceous arc strata of the lower member, which suggest a post-Early Cretaceous age; however, no primary fossil ages have been obtained from this part of the Gravina sequence.

North of the study area (Figure 1), on Etolin Island, ammonites (*Archoplites belli* and *grantziceras* sp.) of early Albian age are present in interbedded argillite, tuff, and volcanic breccia [Berg et al., 1972]. Based on similarities in lithology and stratigraphic position, the lower Albian strata on Etolin Island probably correlate with the upper member of the Gravina sequence. Similar ammonites also occur in lower Albian strata of the Wrangell Mountains to the north [Imley, 1960; Jones, 1967]. Based on geologic relations and sparse fossil data, an Early Albian age is inferred for the upper member clastic and tuffaceous strata.

Depositional setting

The upper member of the Gravina sequence contains epiclastic and tuffaceous turbidites which were deposited in a submarine fan setting. The turbidites were deposited on a composite basement, consisting of

the Alava sequence, the Alexander terrane, and the lower volcanic member of the Gravina sequence. Large volumes of epiclastic debris were shed off the flanks of dissected volcanic centers in Early Cretaceous time. Fine-grained tuffaceous turbidites and lapilli commonly form in the distal portions of pyroclastic aprons. Distal turbiditic strata locally interfinger with tuffaceous deposits suggesting ongoing volcanism. Although volumetrically much less abundant, conglomerates are present. Clasts in the conglomerate are commonly well-rounded indicating that detritus must have been reworked in a fluvial or beach environment prior to deposition by turbidity flows. The well-rounded cobbles in the channel-fill deposits suggest that parts of the arc was subaerially exposed and subject to erosion. Epiclastic debris was derived from the intermediate to shallow levels of a dissected magmatic arc complex. The Late Jurassic Gravina arc may have been the source terrane for the epiclastic debris and this interpretation is consistent with the presence of Upper Jurassic volcanic arc strata in the lower member.

DISCUSSION

The Gravina sequence represents remnants of an oceanic island arc and its basinal sedimentary cover. The remnants includes arc sequence marine pyroclastic and volcanoclastic strata and a basinal turbidites. The arc was constructed on a composite basement which consist of two elements, the Alexander terrane and the Taku terrane. The ensimatic nature of arc basement is demonstrated by distinctive lithic components [Gehrels and Saleeby, 1987a ,b] and juvenile, mantle-derived magmas [Samson et al., 1989] and is reflected by a relatively small crustal volume of volcanic strata, the dominance of tholeiitic arc basalts, and relative paucity felsic volcanic strata in the Gravina sequence.

The oceanic island arc system was localized along the eastern margin of the Alexander terrane (Figure 1), where Upper Jurassic to Lower Cretaceous volcanic and basinal deposits accumulated on Upper Triassic and older strata of the Alexander terrane. Structures in the arc basement suggest both strike-slip [McClelland and Gehrels, in press] and possible convergent displacements occurred during the early and middle Mesozoic. Rocks of the eastern part of the Alexander terrane were deformed and disrupted prior to the deposition of the Gravina sequence along the Duncan Canal Shear Zone in the Petersburg area [McClelland and Gehrels, in press]. Similar relations may also occur on Chilkat Peninsula, where Upper Triassic basalt, interpreted as a

fragment of Wrangellia underlie basinal turbidites [Plafker et al., 1989] that we tentatively correlate to the Gravina sequence. Lower Mesozoic rocks of Wrangellia are interpreted to have formed in a rifted arc environment [Barker et al., 1989], which is analogous to the early Mesozoic history of the Alexander terrane. Thus, Late Jurassic arc volcanism nucleated above a composite basement, comprised of an Alexander terrane and Wrangellian rift assemblage and older structural features. The second basement component consists of the Alava sequence. Upper Paleozoic bioclastic limestone, massive to pillowed metabasaltic flows, and argillite of the Alava sequence are unconformably overlain by upper member basinal turbidites of the Gravina sequence. The tectonic affinity of the Alava sequence is unclear; however, the sequence may represent disrupted fragments of the late Paleozoic portion of the Yukon-Tanana and early Mesozoic part of the Stikine terranes [Rubin and Saleeby, in review], which form a primitive arc complex underlain by continent-derived clastic deposits [Rubin et al., 1990]. Arc basement is composite, consisting of an ensimatic rifted arc (i.e., Alexander terrane), a primitive arc complex (Stikine terrane), and continent-derived slope and rise deposits (Yukon-Tanana terrane) and forms the substrate for the upper Jurassic to lower Cretaceous pyroclastic aprons and basinal turbidites. The original dimensions of the arc system are obscured, due to late Mesozoic deformation [Rubin et al., 1990] and fragmentary preservation.

The localization of oceanic island arcs along older rifted and structurally disrupted ensimatic basement fragments is well-documented in modern island arc systems of the western Pacific [e.g., the Philippine Archipelago, in Hawkins et al., 1985 and references therein] and in ancient arc complexes of the North American Cordillera [Saleeby, 1981]. In the Philippine Islands, the modern Mindanao arc nucleated above structurally disrupted ensimatic basement fragments that marked the collision between the central and eastern Mindanao belts [Hawkins et al., 1985; Karig, 1983]. The Mindanao composite arc basement comprises crustal fragments that originated within the Pacific-Eurasian plate boundary [Karig, 1983], previously assembled by strike-slip and thrust. The analogy between the modern Mindanao arc and its composite basement with the Gravina sequence is striking.

The inception of arc volcanism recorded in the Gravina sequence probably began in the middle Late Jurassic, based on the oldest fossil ages on Gravina Island and to the north on Cape Fanshaw [Gehrels and McClelland, 1987]. Initially, basalt and basaltic andesite and pyroclastic flows of the lower member

accumulated on basinal sediments that unconformably overlie the Alexander terrane. The oldest basinal sedimentary rocks consist of rhythmically banded fine-grained turbidites interlayered with lenses of coarse detritus, that were derived from Triassic parts of the Alexander terrane. A Late Triassic through Middle Jurassic hiatus in deposition and the presence of basement-derived debris in Upper Jurassic strata suggest that the basement was subaerially exposed. The basement subsided and accumulated fine-grained basinal sediments, massive mafic lavas and pyroclastic debris. Progradation of pyroclastic aprons resulted in an upward-coarsening sequence of volcanoclastic sedimentary rocks (Figure 2). Similar marine progradational sequences in volcanoclastic sediments have been recognized in the modern Mariana Island arc [Karig, 1972], in marginal basins of the southwestern Pacific Ocean [Klein, 1974], and as an important component in marginal basins [Moore and Karig, 1975]. Rapid buildup of pyroclastic aprons implies subsidence of the basin, which allows for the transport of coarse volcanoclastic debris into the basin. Alternatively, the progradational sequence was the result of the migration of volcanism towards the basin. In either case, no simple pattern of volcanogenic sedimentation emerges from the available data.

A thick succession of epiclastic and tuffaceous turbidites blanket the lower volcanic sequence. The shift from volcanic to predominantly epiclastic deposition marks a fundamental change in the evolution of the Gravina basin. The turbidites were deposited on a varied substrate, including the Alava sequence and lower volcanic member of the Gravina sequence, indicating that the Alexander terrane and Alava sequence were amalgamated prior to the deposition of the upper member. The presence of Late Jurassic granitoid cobbles in channel-fill deposits imply erosion and uplift of the older arc edifice. Fine-grained epiclastic debris was also shed from the dissected arc. Interstratified tuffaceous turbidites record continued volcanism. Lack of quartz-rich terrigenous deposits indicates bathymetric or paleogeographic isolation from a continental source area.

The age and timing of uplift and erosion of the older arc edifice and resulting influx of epiclastic debris probably occurred in the Early Cretaceous. The Gravina sequence is young as Albian [Berg et al., 1972] and may be as young as Cenomanian (D. Brew, personal comm., 1987). Uplift and erosion of the basin may have been related to tectonic instability along western margin of the Alexander terrane. Mid-Cretaceous contractional deformation of the Gravina sequence has been documented in southeast Alaska

[Rubin et al., 1990]. The uplift and erosion of adjacent parts of the Gravina belt may have marked the onset of mid-Cretaceous compression and collapse of the basinal sequence. Thick volumes of epiclastic debris records a fundamental change in the basin evolution and signals the onset of mid-Cretaceous orogenic activity.

On a regional scale, the timing of volcanism and epiclastic sedimentation in the Gravina sequence varies along strike. Further to the north (Figure 1), in the Juneau region, epiclastic strata form the base of the Gravina sequence and are overlain by metabasaltic lavas and pyroclastic rocks [Brew and Ford, 1985]. The mafic volcanic strata are younger than the underlying epiclastic rocks and are dominantly Early Cretaceous in age [Brew and Karl, 1987]. Preliminary major-element geochemical analyses suggest that the metabasalt formed in a rift environment [Ford and Brew, 1987]. Similar geologic relations are present in the eastern Alaska Range where Upper Jurassic to Lower Cretaceous volcanic and basinal strata form a thick and continuous section. The stratigraphically lowest rocks, consisting of Upper Jurassic shallow water marine sedimentary rocks overlain by marine turbidites and conglomerate, lie unconformably over Paleozoic and Mesozoic rocks of Wrangellia and contain coarse detritus that is derived from the underlying basement [Berg et al., 1972]. Neocomian arc-related volcanic strata of the overlying Chisana Formation consist of submarine and non-marine mafic and intermediate flows, volcanoclastic rocks and shallow marine argillite [Barker, 1987; Richter and Jones, 1976]. Thus, the inception of volcanic activity in the eastern Alaska Range and in the Juneau area is younger than volcanic activity recorded in the Ketchikan area.

The deeper levels of the Upper Jurassic magmatic arc are exposed only locally, in both the St. Elias Mountains of the Yukon and British Columbia and in the Coast Range, northwestern British Columbia. Recent studies conducted in the Coast Ranges of western British Columbia have revealed a deeper level of exposure of the Late Jurassic magmatic arc than in southern southeastern Alaska [Crawford et al., 1987; Hollister et al., 1987; Woodsworth et al., 1983]. Here, Late Jurassic plutons intrude the Alexander terrane and represent the roots of a magmatic arc [Armstrong, 1988; Van der Heyden, 1987]. Only a thin metamorphic selvage of the Upper Jurassic volcanic cover is preserved in northwestern British Columbia, whereas to the north in southeast Alaska, a relatively thick, partly low-grade volcanic section is preserved. Deeper levels of the arc also are preserved to the north in the St. Elias Range and the southern Yukon

Territory. Late Jurassic to earliest Cretaceous calc-alkaline plutonism occurred throughout the Alexander terrane and locally within Wrangellia [Dodds and Campbell, 1988]. Coeval calc-alkaline plutonism also extended into southern Alaska [MacKevett, 1978; Hudson, 1983] and northern southeastern Alaska [Brew and Morrell, 1987]. Volcanic strata of this age have not been recognized within the belt; however, the Upper Jurassic and Lower Cretaceous arc-related strata of the Gravina sequence may represent the upper crustal levels of the Late Jurassic plutonic belt.

In summary, deeper levels of the Late Jurassic and Early Cretaceous magmatic arc represented by the plutonic rocks exposed in western British Columbia and in southern Alaska and northern southeast Alaska. Calc-alkaline plutons of this age have not been recognized in southeast Alaska [Brew and Morrell, 1983], where only coeval upper crustal volcanic strata are exposed. The differences in exposure of Early Cretaceous crustal levels between southeast Alaska and western British Columbia is probably due to both along strike variations of mid-Cretaceous thrust faulting and differential post mid-Cretaceous uplift, extension and erosion. This interpretation may explain the paucity of Upper Jurassic volcanic rocks in western British Columbia, Yukon, and southern Alaska.

CONCLUSIONS

Basaltic to andesitic lavas and pyroclastic strata between southeastern and southern Alaska delineate a Late Jurassic to Early Cretaceous arc system. The inception of arc volcanism was probably middle Late Jurassic to Late Jurassic. The arc was constructed across a composite basement consisting of the Alexander and Wrangellia terrane, and likely correlatives of the Stikine and Yukon-Tanana terranes, forming a pre-Late Jurassic tie between Insular superterrane and the western margin of North America. The volcanic strata are dominated by tholeiitic arc basalts which formed as pyroclastic aprons that were shed from the flanks of submarine volcanos. Fine- to coarse-grained epiclastic turbidites consist were deposited in a submarine fan setting adjacent to dissected volcanic centers. Uplift and erosion of the arc is locally recorded by abundant Late Jurassic coarse granitic cobbles in the clastic basinal deposits. Volcanic activity was diachronous along the length of the oceanic island arc and may reflect segmentation of the arc or can incomplete preservation. Subsequently, the volcanic and basinal rocks were deformed during a major intra-arc contractional event

during mid-Cretaceous time, accompanied by emplacement of a distinctly younger (90-100 Ma) arc-related plutonic suite.

REFERENCES

- Armstrong, R.L., Mesozoic and early Cenozoic magmatic evolution of the Canadian Cordillera, Spec. Pap. Geol. Soc. Am., 218, 55-91, 1988.
- Beikman, H.M., Geologic map of Alaska, U.S. Geol. Surv. Spec. Map, 1980.
- Berg, H.C., Geologic map of Annette Island, Alaska, U.S. Geol. Surv. Misc. Map I-684, 1972.
- Berg, H.C., Geology of Gravina Island, Alaska, U.S. Geol. Surv. Bull., 1373, 41 pp., 1973.
- Berg, H.C., Elliott, R.L., and Koch, R.D., Geologic map of the Ketchikan and Prince Rupert quadrangles, Alaska, U.S. Geol. Surv. Misc. Invest. Series, Map 1-1807, 1988a.
- Berg, H.C., Jones, D.L., and Richter, D.H., Gravina-Nutzotin belt: Tectonic significance of an upper Mesozoic sedimentary and volcanic sequence in southern and southeastern Alaska, U.S. Geol. Surv. Prof. Pap., 800-D, D1- D24., 1972.
- Brew, D.A., Loney, R.A., and Muffler, L.J.P., Tectonic history of southeastern Alaska, in A symposium on the tectonic history and mineral deposits of the western Cordillera in British Columbia and neighboring part of the United States, Can. Inst. Mining and Metallurgy Spec. Vol. 8, 149-170, 1966.
- Brew, D.A., and Karl, S.M., Reexamination of the contacts and other features of the Gravina belt, southeastern Alaska, U.S. Geol. Surv. Circ. 1016, 143-146, 1987.
- Brew, D.A., and Morrell, R.P., Intrusive rocks and plutonic belts in southeastern Alaska, U.S.A., Circum-Pacific Plutonic terranes, edited by J.A. Roddick, Geol. Soc. Am. Mem. 159, 171- 194, 1983.
- Brooks, A.H., Preliminary report on the Ketchikan mining district, Alaska, with a reconnaissance of Chickaman River, U.S. Geol. Surv. Prof. Pap., 1, 120 pp., 1902.
- Buddington, A.F., and Chapin, T., Geology and mineral deposits of southeastern Alaska, U.S. Geol. Surv. Bull., 800, 398 pp., 1929.
- Busby-Spera, C.J., Evolution of a Middle Jurassic back-arc basin, Cedros Island, Baja California, Evidence from a marine volcanoclastic apron, Geol. Soc. Am. Bull., 100, 218-233, 1988a.
- Busby-Spera, C.J., Speculative tectonic model for the early Mesozoic arc of the southwest Cordilleran United States, Geology, 16, 1121-1125, 1988b.
- Cameron, A.E., Smith, D.H., and Walker, R.I., Mass spectrometry of nanogram-size samples of lead, Ana. Chem., 41, 525-526, 1969.
- Chapin, T., The structure and stratigraphy of Gravina and Revillagigedo Islands, Alaska, U.S. Geol. Surv. Prof. Pap., 120-D, 83-100, 1918.
- Crawford, M.L., Hollister, L.S., and Woodsworth, G.J., Crustal deformation and regional metamorphism across a terrane boundary, Coast Plutonic Complex, British Columbia, Tectonics, 6, 343-361, 1987.

- Dodds, C.J., and Campbell, R.B., Potassium-argon ages of mainly intrusive rocks in the Saint Elias Mountains, Yukon and British Columbia, Geol. Surv. Can. Pap., 87-16, 43 pp., 1988.
- Ewart, A., The mineralogy and petrology of Tertiary-recent orogenic volcanic rocks: with special reference to the andesite-basaltic compositional range, Andesites, Orogenic andesites and related rocks, edited by R.S. Thorpe, pp. 25-98, John Wiley and Sons, New York, 1982.
- Gabrielse, H., Major dextral transcurrent displacements along the Northern Rocky Mountain trench and related lineaments in north-central British Columbia, Geol. Soc. Am. Bull., 96, 1-14, 1985.
- Gabrielse, H. and Wheeler, J.O., Tectonic framework of southern Yukon and northwestern British Columbia, Geol. Surv. Can. Pap., 60-24, 37, 1961.
- Garcia, M O., Criteria for the identification of ancient volcanic arcs, Earth Sci. Rev., 14, 147-165, 1978.
- Gehrels, G.E., and McClelland, W.C., Outline of the Taku terrane and Gravina belt in the Cape Fanshaw-Windham Bay region of central southeastern Alaska, Geol. Soc. Am. Abstr. Programs, 20, 163, 1987.
- Gehrels, G.E., McClelland, W.C., Samson, S.D., Patchett, P.J. and Jackson, J.L., Ancient continental margin assemblage in the northern Coast Mountains, southeast Alaska and northwest Canada, Geology, 18, 208-211, 1990.
- Gehrels, G.E., and Saleeby, J.B., Geologic framework, tectonic evolution and displacement history of the Alexander terrane, Tectonics, 6, 151-173, 1987a.
- Gehrels, G.E., and Saleeby, J.B., Geology of Annette, Gravina, and Duke islands, southeastern Alaska, Can. J. Earth Sci., 24, 866-881, 1987b.
- Gill, J., Orogenic andesites and plate tectonics, 385 pp, Springer Verlag, New York, 1981.
- Grantz, A., Jones, D.L., and Lamphere, M.A., Stratigraphy, paleontology, and isotopic ages of upper Mesozoic rocks in the southwestern Wrangell Mountains, Alaska, U.S. Geol. Surv. Prof. Pap., 550-C, C39-C47, 1966.
- Harland, W.B., Cox, A.V., Lewellyn, P.G., Pickton, C.A.G., Smith, A.G., and Walters, R., A Geologic time scale, 131 pp., Cambridge University Press, Cambridge, 1982.
- Harper, G.D., and Wright, J.E., Middle to Late Jurassic tectonic evolution of the Klamath Mountains, California-Oregon, Tectonics, 3, 759-772, 1984.
- Hawkins, J.W., Moore, G.F., Villamor, R., Evans, C., and Wright, E., Geology of the composite terrane of east and central Mindanao, Circum-Pacific Council for Energy and Mineral Resources, Earth Sci. Ser., 1, 437-463, 1985.
- Hollister, L.S., Grissom, G.C., Peters, E.K., Stowell, H.H., and Sisson, V.B., Confirmation of empirical correlation of Al in hornblende with pressure of solidification of calc-alkaline plutons, Am. Min., 72, 231-239, 1987.
- Howell, D.G., Jones, D.L., and Schermer, E.R., Tectonstratigraphic terranes of the Circum-Pacific region, Tectonstratigraphic terranes of the Circum-Pacific region, edited by D.G. Howell, Circum-Pacific council for energy and mineral resources, pp. 3-30, Earth Sci. Ser., 1, Houston, Texas, 1985.
- Hudson, T., Calc-alkaline plutonism along the Pacific rim of Southern Alaska, in Roddick, J.A., ed., Circum-Pacific Plutonic terranes, Geol. Soc. Am. Mem., 159, 159-1170, 1983.

- Jaffey, A.H., Flynn, K.F., Glendenin, L.E., Bentley, W.C., and Essling, A.M., Precision measurement of half-lives and specific activities of ^{235}U and ^{238}U , Phys. Rev. C, **4**, 1889-1906, 1971.
- Karig, D.E., Accreted terranes in the northern part of the Philippine Archipelago, Tectonics, **2**, 211-236, 1983.
- Karig, D.E., and Moore, G.F., Tectonically controlled sedimentation in marginal basins, Earth Planet. Sci. Lett., **26**, 233-238, 1975.
- Karl, S.M., Johnson, B.R., and Lamphere, M.A., New K-Ar ages for plutons on western Chichagof Island on Yakobi Island, U.S. Geol. Surv. Circ., **1016**, 147-149, 1988.
- Kay, R.W., Volcanic arc magmas: Implications of a melting-mixing model for element recycling in the crust-upper mantle system, J. Geol., **88**, 497-522, 1980.
- Klein, G. de V., The control of depositional depth, tectonic uplift, and volcanism on sedimentation processes in backarc basins of the western Pacific, J. Geol., **93**, 1-25, 1985.
- Krogh, T.E., A low-contamination method for hydrothermal decomposition of zircon and extraction of U and Pb for isotopic age determinations, Geochim. Cosmochim. Acta, **37**, 485-494, 1973.
- Lamphere, M. A., and Jones, D.L., Cretaceous time scale from North America, Contributions to the geologic time scale, edited by G. V. Cohee, M.F. Glaessner, and H.D. Hedberg, pp. 259-268, AAPG Studies in Geology, **6**, American Association of Petroleum Geologists, Houston, Texas, 1978.
- Loney, R.A., Brew, D.A., Muffler, L.J.P., and Pomeroy, J.S., Reconnaissance geology of Chichagof, Baronof, and Kruzof Islands, southeastern Alaska, U.S. Geol. Surv. Prof. Pap., **792**, 105 pp., 1973.
- MacKevett, E.M., Jr., Geologic map of the McCarthy quadrangle, Alaska, U.S. Geol. Surv. Map, **I-1031**, 1978.
- Mattinson, J.M., U-Pb ages of zircon: a basic examination of error propagation, Chemical Geology, **66**, 151-162, 1987.
- McClelland, W.C., and Gehrels, G.W., Characteristics of the Taku terrane (TT) and Gravina belt (GB) in the Petersburg region, central southeastern Alaska, Geol. Soc. Am. Abstr. Programs, **20**, 211, 1988.
- McClelland, S.M., and Taylor, S.R., Role of subducted sediments in island-arc magmatism: Constraints from REE patterns, Earth Planet. Sci. Lett., **54**, 423-430, 1981.
- Monger, J.W.H., and Berg, H.C., Lithotectonic terrane map of western Canada and southeastern Alaska, U.S. Geol. Surv. Misc. Field Studies Map, **MF-1874-B**, 12 pp., 1985.
- Monger, J.W.H., Price, R.A., and Tempelman-Kluit, J.D., Tectonic accretion and the origin of the two major metamorphic and plutonic belts in the Canadian Cordillera, Geology, **10** (2), 70-75, 1982.
- Nakamura, N., Determination of REE, Ba, Fe, Mg, Na, and K in carbonaceous and ordinary chondrites, Geochim. Cosmochim. Acta, **38**, 757-775, 1974.
- Oldow, J.S., Bally, A.W., Avé Lallemant, H.G., Leeman, W.P., Phanerozoic evolution of the North American Cordillera: United States and Canada, The Geology of North America, in The Geology of North America - an overview, A, edited by A.W. Bally, and A.R. Palmer, pp. 139-232, Geological Society of America, Boulder, Colo., 1989.
- Pavlis, T.J., Origin and age of the Border Ranges Fault of southern Alaska and its bearing on the Late Mesozoic tectonic evolution of Alaska, Tectonics, **1**, 343-368, 1982.

- Pearce, J.A., and Cann, J.R., Tectonic setting of basic volcanic rocks determined using trace element analyses, Earth Planet. Sci. Lett., **19**, 290-300, 1973.
- Pearce, J.A., Trace element characteristics of lavas from destructive boundaries, in Thorpe, R.S., ed., Andesites, Orogenic andesites and related rocks, John Wiley and sons, New York, 525-547, 1982.
- Pearce, J.A., Role of the sub-continental lithosphere in magma genesis at active continental margins, Continental basalts and mantle xenoliths, edited by C.J. Hawkesworth and M.J. Norry, pp. 230-259, Shiva, Orpington (London), and Birkhauser Boston, Cambridge, Massachusetts, 1983.
- Plafker, G., Nockleberg, W.J., and Lull, J.S., Bedrock geology and tectonic evolution of the Wrangellia, Peninsular, and Chugach terranes along the trans-Alaskan crustal transect in the Chugach Mountains and southern Copper River Basin, Alaska, J. Geophys. Res., **94**, 4255-4295, 1989a.
- Plafker, G., Blome, C.D., and Silberling, N.J., Reinterpretation of lower Mesozoic rocks on the Chilkat Peninsula, Alaska, as a displaced fragment of Wrangellia, Geology, **17** (1), 3-6, 1989b.
- Rubin, C.M., and Saleeby, J.B., The inner boundary zone of the Alexander terrane in southern SE Alaska, A newly discovered thrust belt, Geol. Soc. Am. Abstr. Programs, **19**, 455, 1987a.
- Rubin, C.M., and Saleeby, J.B., The inner boundary zone of the Alexander terrane in southern SE Alaska, Part 1: Cleveland Peninsula to southern Revillagigedo Island, Geol. Soc. Am. Abstr. Programs, **19**, 826, 1987b.
- Rubin, C.M., and Saleeby, J.B., A new perspective on what is the Taku terrane in southern SE Alaska, Geol. Soc. Am. Abstr. Programs, **20**, 226, 1988.
- Rubin, C.M., and Saleeby, J.B., Tectonic framework of upper Paleozoic and lower Mesozoic Alava sequence: A revised view of the polygenetic Taku terrane in southern southeast Alaska, Can. J. Earth Sci., in review.
- Rubin, C.M., Saleeby, J.B., Cowan, D.S., Brandon, M.T., and McGroder, M.F., Regionally extensive mid-Cretaceous west-vergent thrust system in the northwestern Cordillera: Implications for continent-margin tectonism, Geology, **18** (3), 276-280, 1990.
- Rubin, C.M., Miller, M.M., and Smith, A.E., Tectonic development of Cordilleran mid-Paleozoic volcanoplutonic complexes: Evidence for convergent margin tectonism, Geol. Soc. Am. Spec. Pap., **225**, in press.
- Saleeby, J.B., Accretionary tectonics of the North American Cordillera, Ann. Rev. Earth Planet. Sci., **15**, 45-73, 1983.
- Saleeby, J.B., The inner boundary zone of the Alexander terrane in southern SE Alaska: Part II southern Revillagigedo Island (RI) to Cape Fox (CF), Geol. Soc. Am. Abstr. Programs, **19**, 828, 1987.
- Saleeby, J.B., and Rubin, C.M., The western margin of the Coast Plutonic Complex (CPC) in southernmost SE Alaska, Geol. Soc. Am. Abstr. Programs, **21**, 139, 1989.
- Samson, S.D., McClelland, W.C., Patchett, P.J., and Gehrels, G.E. Nd isotopes and Phanerozoic crustal genesis in the Canadian Cordillera, Nature, **337**, 705-709, 1989.
- Smith, P.S., Notes on the geology of Gravina Island, Alaska, U.S. Geol. Surv. Prof. Pap., **95**, 97-105, 1915.
- Terra, F., and Wasserburg, G.S., U-Th-Pb systematics in three Apollo 14 Basalts and the problems of the initial Pb in lunar rocks, Earth Planet. Sci. Lett., **14**, 281-304, 1972.

- Thompson, R.N., Magmatism of the British Tertiary province, *Scottish Journal of Geology*, v. 18, p. 49-107, 1982.
- Thorpe, R.S., Andesites: Orogenic andesites and related rocks, 724 pp., John Wiley and sons, New York, 1982.
- Van Der Heyden, P., Tectonic evolution of the Coast Plutonic Complex, British Columbia: Implications of new U-Pb and K-Ar dates, Geol. Soc. Am. Abstr. Programs, 20, 239, 1988.
- Wheatley, M., and Rock, N.M.S., SPIDER: A Macintosh program to generate normalized multi-element "spidergrams," Am. Min., 73, 919-921, 1988.
- White, W.M., and Dupré, B., Sediment subduction and magma genesis in the Lesser Antilles: Isotopic and trace element constraints, J. Geophys. Res., 91, 5927-5941, 1986.
- Winchester, J.A., and Floyd, P.A., Geochemical discrimination of different magma series and their differentiation products using immobile elements, Chem. Geol., 20, 325-343, 1973.
- Woodsworth, G.J., Crawford, M.L., and Hollister, L.S., Metamorphism and structure of the Coast Plutonic Complex and adjacent belts, Prince Rupert and Terrace areas, British Columbia, Geol. Assoc. Can. Field Trip Guidebook 14, 62 pp., 1983.
- Wright, F.E., and Wright, C.W., The Ketchikan and Wrangell mining districts, Alaska, U.S. Geol. Surv. Bull., 347, 210 pp., 1908.
- York, D., Least-squares fitting of a straight line with correlated errors, Earth Planet. Sci. Lett., 5, 320-324, 1969.

ACKNOWLEDGEMENTS. Parts of this research were supported by National Science Foundation Grants EAR 86-05386 and EAR 88-034834 (to Saleeby), additional support (to Rubin) was provided by a Geological Society of America Penrose Grant, a Sigma-Xi grant-in-aid, the U.S. Geological Survey, Alaska Branch, and by the U.S. Forest Service, Ketchikan Ranger District. We thank Fred Barker, Darell Cowan, John Garver, Meghan Miller, Bill McClelland, and George Plafker for helpful discussions. We also thank Fred Barker (U.S.G.S.) for providing the geochemical analyses for the Gravina sequence volcanic rocks.

**GEOLOGIC AND STRUCTURAL HISTORY OF THE WESTERN METAMORPHIC
ROCKS OF THE COAST PLUTONIC COMPLEX, CLEVELAND PENINSULA -
REVILLAGIGEDO ISLAND, SOUTHERN SOUTHEAST ALASKA**

Charles M. Rubin and Jason B. Saleeby Division of Geological and Planetary Sciences, California
Institute of Technology, Pasadena, California, 91125

Submitted to the Bulletin of the Geological Society of America

ABSTRACT

Rocks exposed west of the Coast Plutonic Complex in southeast Alaska form an imbricate thrust belt that affected the tectonic boundary between two of the largest allochthonous crustal fragments in the North American Cordillera; the Insular superterrane and the Intermontane superterrane. In the Alexander terrane (Insular superterrane), lower Paleozoic metavolcanic and metasedimentary rocks (Descon Formation) and dioritic plutons are unconformably overlain by Lower Devonian clastic strata (Karheen Formation). These rocks are overlain locally by Upper Triassic basalt, rhyolite and marine clastic strata (Hyd Group). Upper Jurassic and Lower Cretaceous metavolcanic and metasedimentary strata of the Gravina sequence unconformably overlie the Alexander terrane and the upper Paleozoic and lower Mesozoic Alava sequence. The Gravina sequence forms a structural package that is over 15 km thick. These strata record intermittent arc volcanism along the eastern edge of the Alexander terrane. The Gravina sequence is structurally overlain by upper Paleozoic and lower Mesozoic basaltic strata, marble, and argillite (Alava sequence), and locally lower Paleozoic clastic and volcanic strata, and orthogneiss (Kah Shakes sequence); together, these constitute the Taku terrane (Intermontane superterrane?). These rocks were deformed in the mid-Cretaceous and this tectonism was broadly coeval with arc magmatism. Deformation involved the emplacement of west-directed thrust nappes over a structurally intact and relatively unmetamorphosed basement. The Paleozoic and lower Mesozoic Alexander terrane forms the structural basement for much of the thrust belt, along a moderate, northeast-dipping ramp. Mid-Cretaceous tonalite, granodiorite and quartz diorite intrude rocks of the thrust belt and are locally affected by the deformation. Mid-Cretaceous deformation occurred during two episodes that were contemporaneous with the emplacement of large sill-like plutons. Older

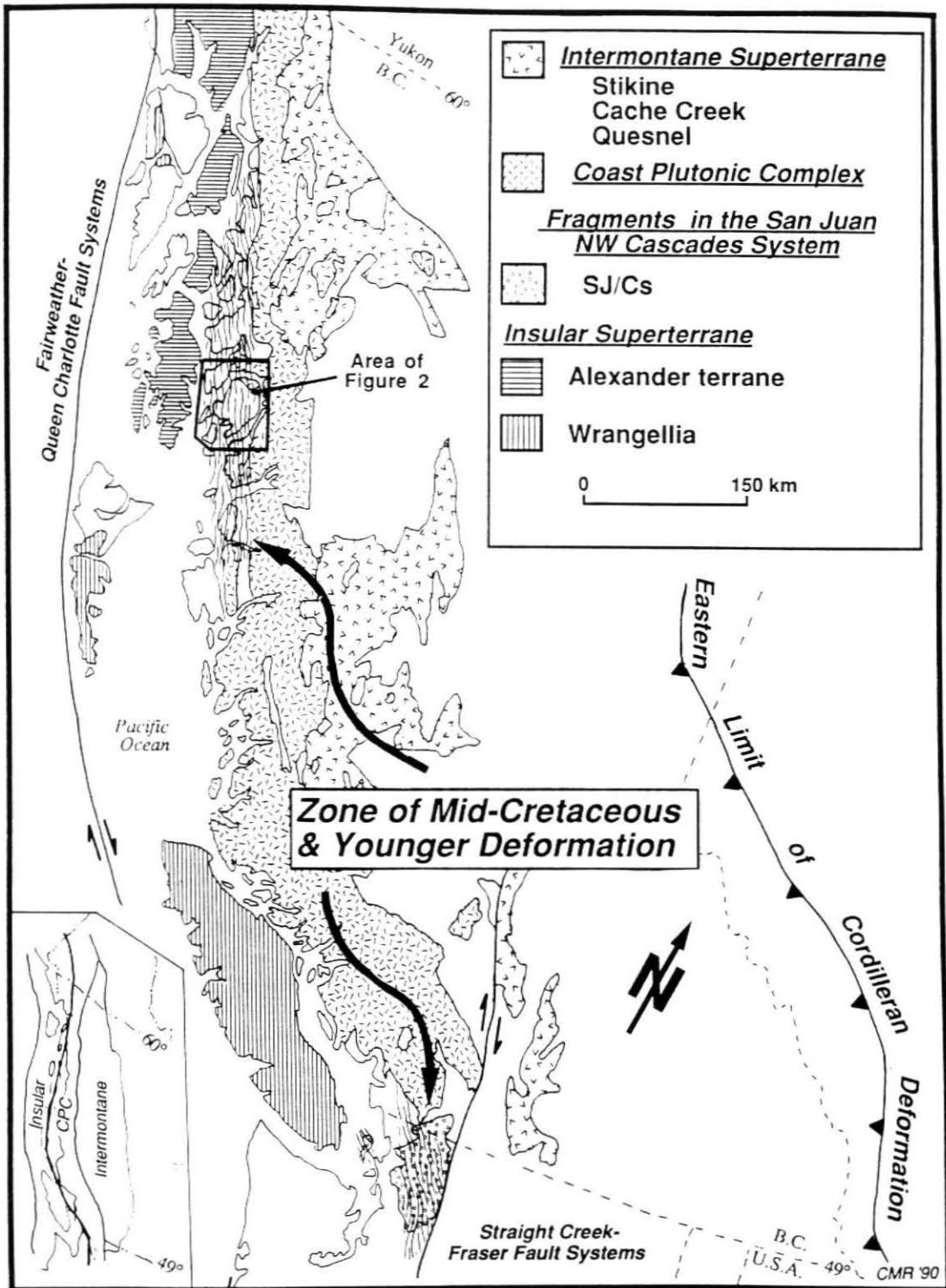
structures record ductile southwest-vergent folding and faulting, regional metamorphism, and contain a well-developed axial-planar foliation. The second generation structures developed during the later stages of southwest-directed reverse faulting that juxtaposes rocks of contrasting metamorphic pressures and temperatures.

Structural, stratigraphic and geochronologic data suggest that regional-scale deformation in southeast Alaska occurred between 113 Ma and 89 Ma. Rocks in the thrust belt were uplifted regionally by 70 Ma, with an average uplift rate of ≈ 0.9 mm/yr. Deformation involved the collapse of a marginal basin(s) and a magmatic arc, and overprinted the older tectonic boundary between the Insular superterrane and the late Mesozoic western margin of North America (at that time the Intermontane superterrane). Contractional deformation along the length of the thrust belt was broadly coeval with arc magmatism, and thus records intra-arc tectonism. Late Paleocene to Early Eocene igneous activity and deformation subsequently affected the thrust belt.

INTRODUCTION

The western metamorphic framework rocks of the Coast Plutonic Complex represent a structurally imbricated zone that extends along strike for at least 1500 km (Figure 1). Detailed structural, stratigraphic, and geochronologic data on these metamorphic rocks are critical for understanding the accretionary history of the Pacific northwest Cordillera. The metamorphic rocks contain mantle-derived, juvenile crustal material represented by the Alexander terrane on the west to continentally-derived slope and rise deposits of the North American craton on the east. One of the outstanding tectonic problems in the northwestern Cordillera is the nature of the boundary between allochthonous ensimatic crustal fragments consisting of the Alexander and Wrangellian terranes and the western margin of late Mesozoic North America. This study area provides a strategic link across this boundary. Distinctive stratigraphic sequences recognized in the thrust belt record the late Mesozoic continent-margin history of western North America. Recent work (Crawford et al., 1987; Rubin et al., 1990) shows that these regionally metamorphosed rocks form a late Mesozoic fold and thrust belt and involve both crystalline basement and its volcanic and basinal cover. This orogenic zone

Figure 1: Regional geologic map of study area, with study area in inset. Zone of mid-Cretaceous and younger deformation stippled.



has only been recently recognized (Monger et al., 1982; Crawford et al., 1987; Rubin et al., 1990) and is a major element in the Mesozoic evolution of the western North America. Deformation began in the mid-Cretaceous and was broadly coeval with arc magmatism, involving the emplacement of west-directed thrust nappes over a structurally intact and relatively unmetamorphosed basement. The presence of inverted metamorphic isograds beneath thrust faults indicates that hot metamorphic and plutonic rocks were translated over a relatively cold basement. The Paleozoic and lower Mesozoic Alexander terrane forms the structural basement to the thrust belt, along a shallowly north- to northeast-dipping ramp.

In this paper, we describe the deformed strata, establish the timing of deformation in relation to isotopically-dated plutons (Table 1), and outline the structural chronology of the thrust belt in southern southeast Alaska. Our studies have focused on a transect of the Paleozoic and Mesozoic metamorphic framework rocks, exposed west of the Coast Plutonic Complex (Figure 1). The data presented in this paper are based upon detailed geologic field mapping along the shorelines and ridges of Cleveland Peninsula, Revillagigedo, Annette, Gravina, and smaller adjacent islands (Figure 2). We describe the deformation that has affected this area. By establishing the structural setting of syn- and post-tectonic plutons, and with the use of zircon geochronology, we are able to establish the absolute timing and tectonic setting of thrust belt evolution.

GEOLOGIC SETTING

The Alexander terrane forms the structural basement for most of the rocks that lie west of the Coast Plutonic Complex. The Alexander terrane consists of a structurally intact lower Paleozoic ensimatic arc sequence overlain by middle Paleozoic clastic and carbonate strata which are unconformably capped by an Upper Triassic rift assemblage (Gehrels and Saleeby, 1987a). In most areas, rocks of the Alexander terrane are only slightly deformed and are not highly metamorphosed (Gehrels and Saleeby, 1987a, b), except near the eastern boundary where it is overprinted by late Mesozoic deformational structures. East of, and depositionally overlying the Alexander terrane, lie Upper Jurassic to Lower Cretaceous marine

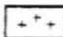

Table 1: Pb-U geochronologic sample locations from the Ketchikan area and descriptions of intrusive rocks.

Sample #	Latitude	Longitude	Field setting	Zircon properties
84JR18	55° 30' 00"	131° 59' 6"	Non-foliated, medium-grained trondhjemite dike - intrudes greenschist facies metavolcanic rocks and marble	2:1; Sub=An>Eu; irregular shapes; colorless, grey-tint, inclusions common.
86CR111	55° 31' 24"	132° 1' 61"	Slightly altered and foliated medium-grained quartz diorite in a heterogeneous sequence of diorite, amphibolite, hornblende, and pyroxenite	2:1; Sub>Eu>An; irregular shapes; colorless, grey- to pink-tint; inclusions common
88CR14	55° 59' 57"	132° 3' 51"	Non-foliated, medium-grained biotite granodiorite, part of the Eaton Point Pluton	3:1, Eu>Sub>An; colorless, pink-tint inclusion free
88CR15	55° 54' 15"	132° 11' 6"	Massive, very fine-grained gabbroic pods and dikes that cross-cut Union Bay Ultramafic Complex hornblende	3:1, Eu>Sub>An; colorless, pink-tint inclusion free
88CR24	55° 57' 58"	132° 51' 13"	Non-foliated, medium-grained porphyritic granodiorite	3:1, Eu>Sub>An; colorless, pink-tint inclusion free



Notes: Eu, euhedral; Sb, subhedral; An, anhedral. 2:1, length:width ratios of zircon grains.
Color determined under reflected light.

Figure 2: Geologic map showing distribution of geologic units, major structures, and zircon sample locations on Cleveland Peninsula, Revillagigedo and adjacent islands. BI = Bell Island Pluton, BP = Bushy Point Pluton, MB = Moth Bay Pluton, EP = Eaton Point Pluton, AB = Alava Bay, CI = Carol Inlet, GI = George Inlet, and POW = Prince of Wales Island, SB = Spacious Bay. BMT = Black Mountain Thrust, NRSZ = northern Revillagigedo Island fault zone, SRSZ = southern Revillagigedo Island fault zone. Adapted from Berg (1972, 1973; parts of Annette and Gravina Islands), Gehrels and Saleeby (1987a,b; Prince of Wales Island, parts of Annette, Duke, and Gravina islands), C.M. Rubin (unpublished mapping, 1985, 1986, 1987; Cleveland Peninsula and adjacent islands); C.M. Rubin and J.B. Saleeby (unpublished mapping, 1986, 1987, 1988; Revillagigedo and adjacent Islands).


PALEOCENE AND YOUNGER (?) INTRUSIVE ROCKS

-  Tonalite, quartz diorite, & granodiorite
-  Pegmatite dike swarm


MIDDLE CRETACEOUS INTRUSIVE ROCKS

-  Tonalite, granodiorite, diorite, & gabbro
-  Zoned ultramafic complexes


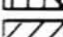



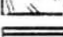
U. JURASSIC & L. CRETACEOUS GRAVINA SEQUENCE

-  Metamorphosed tuff, greywacke, argillite, conglomerate, basalt-andesite tuff, breccia & pillow flows, & hypabyssal intrusive rocks


U. PALEOZOIC & L. MESOZOIC ALAVA SEQUENCE

-  Metamorphosed mafic pillow flows, tuff & breccia, argillite, marble, & quartzite


PALEOZOIC & L. MESOZOIC ALEXANDER TERRANE

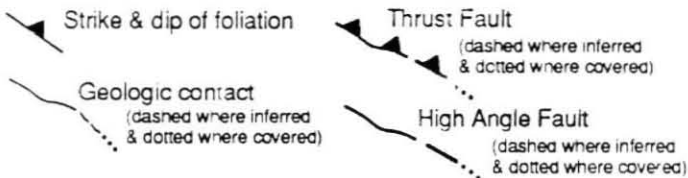
-  Triassic conglomerate, siltstone, limestone, basalt, & rhyolite \ Gabbro
-  Devonian conglomerate, sandstone, siltstone, & marble
-  Ordovician-Silurian basaltic andesite tuff, breccia, pillowed flows, & hypabyssal rocks
-  Silurian trondhjemite & local diorite
-  Ordovician-Silurian tonalite, diorite, & gabbro
-  Cambrian & older (?) meta-igneous rocks

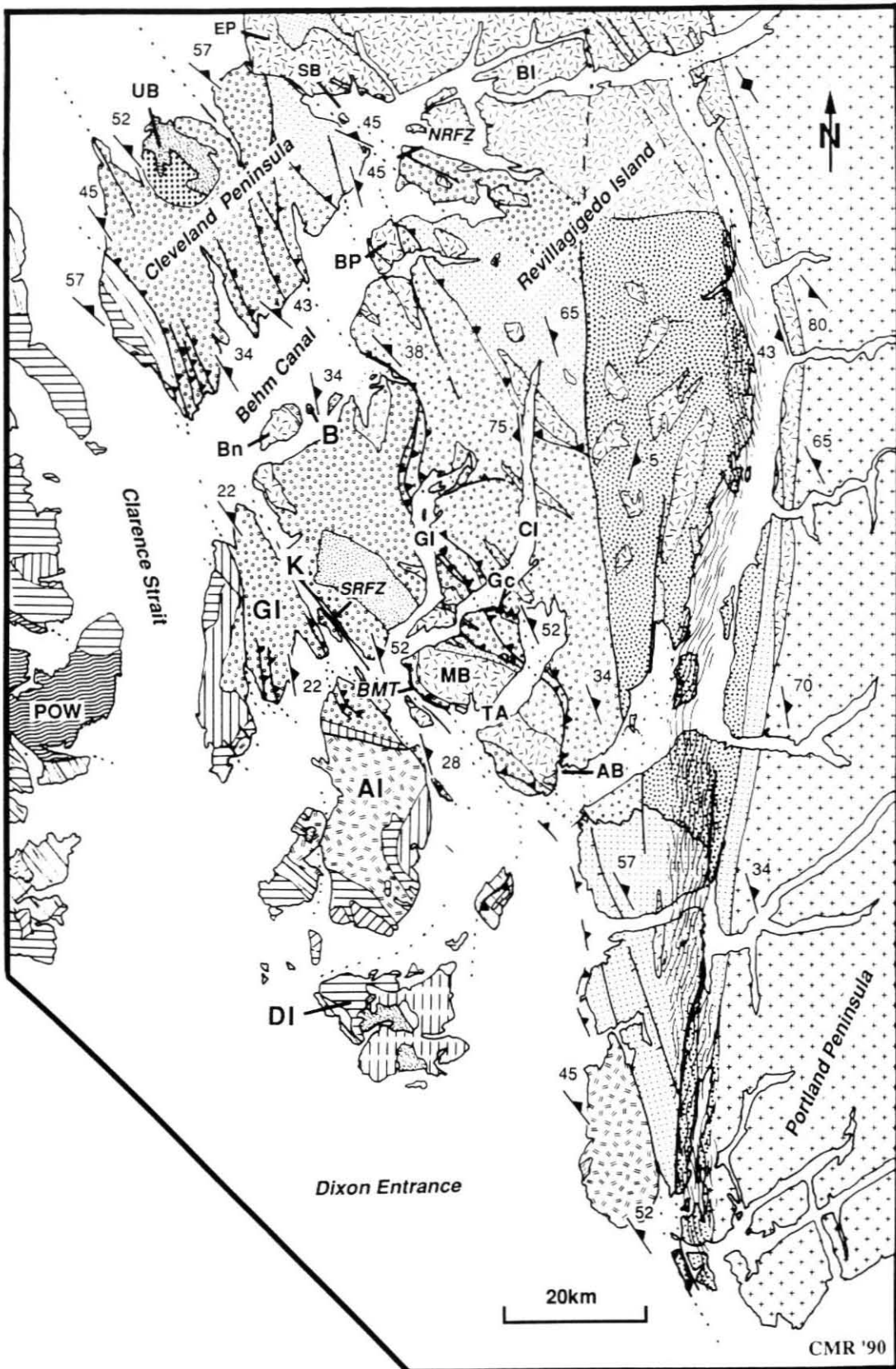
PALEOZOIC KAH SHAKES SEQUENCE

-  Devonian orthogneiss, lower Paleozoic quartz-bearing psammitic rocks, silicic metavolcanic rocks, amphibolite, metapelite, quartzite & marble

EAST BEHM CANAL GNEISS COMPLEX

-  Lower Paleozoic, tonalite gneiss, diorite gneiss, amphibolite, & psammitic gneiss





pyroclastic and basinal strata of the Gravina sequence. Structurally overlying the Alexander terrane and Gravina sequence is the middle Paleozoic and lower Mesozoic Alava sequence, and lower to mid-Paleozoic Kah Shakes sequence (formerly part of the Taku terrane of Berg et al., 1988). Locally, channel-fill deposits of the Gravina sequence overlie the Alava sequence and thus form an overlap between the Alexander terrane and the Alava sequence. The Kah Shakes sequence locally occupies higher structural levels on northeast Cleveland Peninsula, western Revillagigedo Island and northwestern Portland Peninsula (Figure 3), and consists of lower Paleozoic meta-silicic tuff, quartzite, marble, metabasalt, calc-silicate, and orthogneiss.

A regionally extensive mid-Cretaceous west-vergent thrust belt occurs along parts of the eastern boundary of the Alexander terrane (Figure 3), where it imbricates the Gravina and is juxtaposed against the Alava sequence. The orogenic zone consists of an imbricate series of west-vergent thrust sheets and on Cleveland Peninsula the imbricated package has a total structural thickness of over 15 km. Based on field relations and geochronology discussed here, the thrust belt was active over a relatively short period of time, and was broadly coeval with arc magmatism. These structures affected the original tectonic boundary between two of the largest crustal fragments in the North American Cordillera which at these latitudes consist of the Insular and Intermontane superterrane (terrane I and II of Monger et al., 1982).

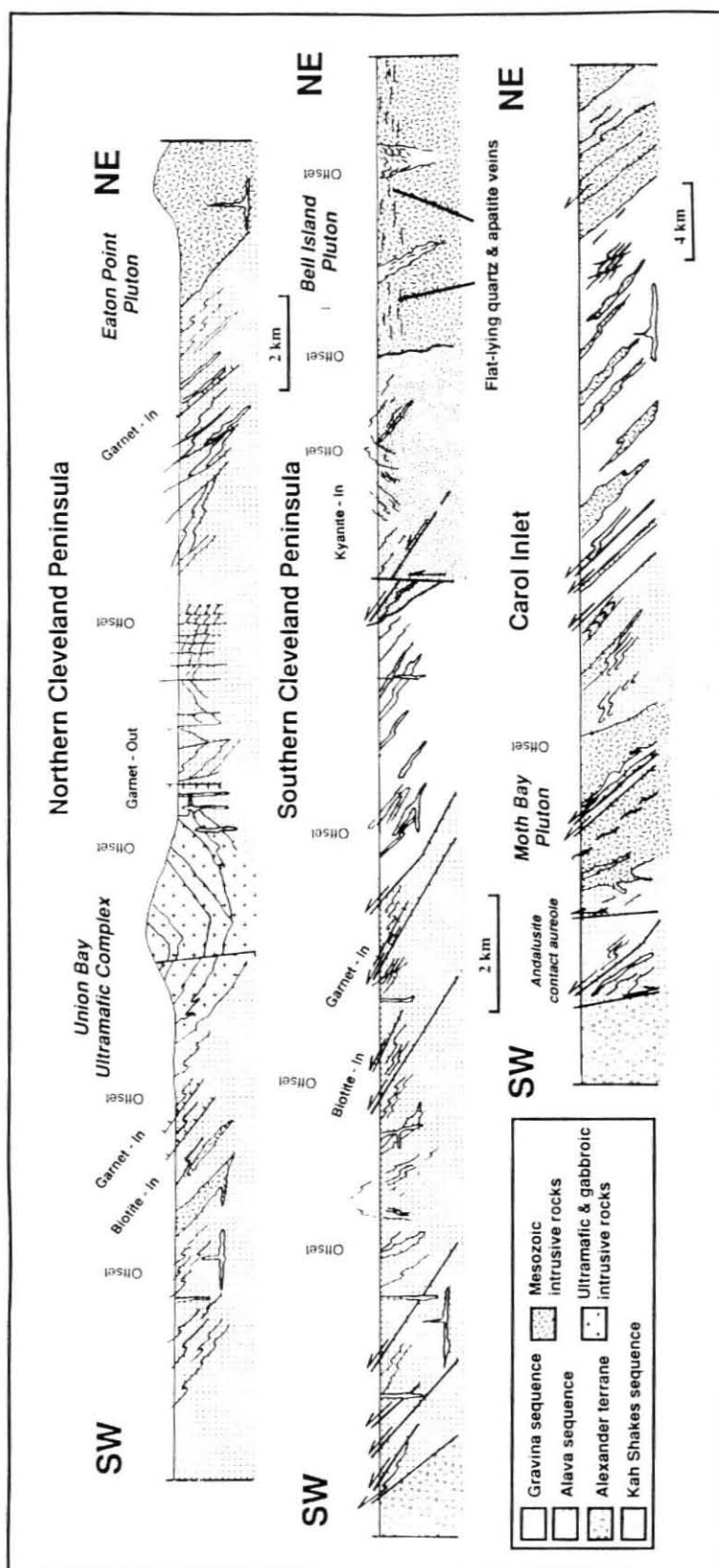
GEOLOGIC FRAMEWORK

Alexander terrane

Descon Formation

The southern portion of Cleveland Peninsula and, in part, the western side of Revillagigedo Island are underlain by metavolcanic rocks, with subordinate phyllite and marble of Ordovician - Early Silurian (?) age (Figure 2). The lower contact of this mafic sequence is not exposed. The upper contact is faulted against the Upper Jurassic to Lower Cretaceous Gravina sequence and is depositionally overlain by the Devonian Karheen Formation on western Cleveland Peninsula. The minimum age of metavolcanic rocks on Cleveland Peninsula is constrained by a cross-cutting trondhjemite dike, with single-fraction U-Pb

Figure 3: Geologic cross-sections: (A) northern Cleveland Peninsula; (B) southern Cleveland Peninsula; (C) Carol Inlet.



zircon age of 443 ± 4 (84JR18, Tables 1 and 2). Although there was insufficient material to obtain multiple analyses, the internally concordant Late Ordovician age is quite similar to ages of meta-igneous rocks of the Descon Formation on Prince of Wales Island (Saleeby et al., 1984). Similar metavolcanic and metasedimentary rocks on central and southern Prince of Wales Island range in age from Early Ordovician to Early Silurian and are assigned to the Descon Formation (Eberlein et al., 1983; Herreid et al., 1978; Gehrels and Saleeby, 1987 a, b). Based on similar rock types, stratigraphic position, and age, we assign the mafic metavolcanic and metasedimentary strata on southwestern Cleveland Peninsula to the Descon Formation. There is a possibility that the metavolcanic rocks on southern Cleveland Peninsula could represent slightly deformed Wales Group; however, inasmuch as the Wales Group lies regionally beneath the Descon Formation, such an interpretation does not fundamentally affect our analysis.

On Cleveland Peninsula, the Descon Formation consists of lower greenschist facies metabasalt flows, breccia, and tuff. The mafic metavolcanic strata contain euhedral augite and feldspar phenocrysts in a pale to dark green tuffaceous matrix comprising albite, chlorite, epidote, and white mica. The mafic metavolcanic strata are locally interlayered with marble and argillite. Marble beds range in thickness between 1 and 3 m, which is also typical of the Wales Group. The Descon Formation in this region contains a greater proportion of mafic metavolcanic rocks than are present in correlative strata on Prince of Wales Island. No fossils have been recovered from these lower Paleozoic rocks on Cleveland Peninsula.

Metaplutonic Complex

Metamorphosed gabbro, diorite, plagioclase and quartz porphyritic granodiorite, and orthogneiss underlie much of southwestern Cleveland Peninsula (Figure 2). Plagioclase and quartz porphyritic granodiorite occurs as homogeneous, massive to foliated bodies containing oligoclase, quartz and interstitial microperthite, and minor hornblende. Heterogeneous bodies of foliated and layered diorite, quartz diorite, basalt, and gabbro consist of texturally varied, fine- to medium-grained plagioclase, hornblende, biotite, and minor quartz. Minor hornblende and clinopyroxene sills and dikes intrude the igneous complex, that displays complex intrusive relations. Interlayered foliated dikes and sills of diorite, gabbro,

Table 2. ZIRCON ISOTOPIC AGE DATA

Sample	Fraction† (μm)	Concentrations (ppm)			Atomic Ratios		Isotopic ages (Ma) \pm		
		Amount Analyzed (mg)	238 U	206 Pb*	$\frac{206\text{Pb}}{204\text{Pb}}$	$\frac{206\text{Pb}^*}{238\text{U}}$	$\frac{207\text{Pb}^*}{235\text{U}}$	$\frac{206\text{Pb}^*}{238\text{U}}$	$\frac{207\text{Pb}^*}{235\text{U}}$
84JR18	45-62	0.6	130	7.9	7110	0.072890(44)	0.05403	438.0	438.7
86CR111	45-62	2.7	1167	53.1	42995	0.052550(36)	0.40425	330.2	344.7
	46-80	2.3	991	49.2	50280	0.053064(34)	0.44088	359.3	370.9
	>80	1.0	1201	67.1	5742	0.064319(54)	0.49498	401.9	408.3
88CR14	<25	3.6	692	8.9	6955	0.014784(10)	0.09850	94.6	95.4
	25-45	5.2	898	11.2	7421	0.014368(09)	0.09524	91.9	92.3
	45-62	9.0	725	9.5	5532	0.014976(10)	0.09897	95.8	95.8
88CR15	62-80	3.2	483	6.3	5925	0.014928(08)	0.09923	95.5	96.0
	80-100(a)	3.7	587	6.9	6889	0.013470(07)	0.08925	86.3	86.8
	80-100(b)	2.7	433	5.1	12982	0.013477(07)	0.08918	86.3	86.7
	100-120	3.2	493	5.8	10950	0.013676(07)	0.09074	87.6	88.2
88CR24	62-80	7.5	752	9.7	7598	0.014910(10)	0.09852	95.4	95.4
	80-100	5.9	870	11.3	6468	0.014942(10)	0.09847	95.6	95.4
	>100	2.9	536	6.9	9036	0.014935(10)	0.09129	95.6	95.9
84GR03	45-80	4.3	1160	14.3	8037	0.014910(09)	0.09406	90.7	91.3
	80-100	6.3	449	5.7	412	0.014082(11)	0.09331	90.2	90.6

* Radiogenic: nonradiogenic correction based upon 40 picogram blank Pb (1:18.78; 15.61; 38.50) and initial Pb approximations: 206/204 = 48.6; 207/204 = 15.6; 208/204 = 38.2.

† Fractions separated by grain size and magnetic properties. Magnetic properties are given as non-magnetic split at side/front slopes for 1.7 amps on Franz Isodynamic Separator. Samples hand-picked to 99.9% purity prior to dissolution. Dissolution and chemical extraction technique modified from Krogh (1973).

§ Decay constants used in age calculation: $\lambda^{238\text{U}} = 1.55125 \times 10^{-10}$, $\lambda^{235\text{U}} = 9.8465 \times 10^{-10}$ (Jaffey et al., 1971); $^{238}\text{U}/^{235}\text{U}$ atom=137.88. Uncertainties (\pm) in radiogenic ratios calculated by quadratic sum of total derivatives of ^{238}U and $^{206}\text{Pb}^*$ concentration and $^{207}\text{Pb}^*/^{206}\text{Pb}^*$ equations with error differentials defined as follows: (1) Isotope ratio determinations from standard errors (δ/n) of mass spectrometer runs plus uncertainties in fractionation corrections based on multiple runs of NBS 981, 983, and U500 standards; (2) Spike concentrations from range of deviations in multiple calibrations with normal solutions; (3) Spike compositions from external precisions of multiple isotope ratio determinations; (4) Uncertainty in natural $^{238}\text{U}/^{235}\text{U}$ from Chen and Wasserburg (1981); and (5) Nonradiogenic Pb isotopic compositions from uncertainties in isotope ratio determinations of blank Pb and uncertainties in composition of initial Pb from estimates of regional variations based on references given above and consideration of rock type.

88CR15: (a) and (b) are replicate analyses

and basalt are cross-cut by porphyritic intrusive bodies. The plutonic rocks intrude screens and septa of metasedimentary rocks that are part of the Descon Formation. Here, quartz porphyritic and diorite gneiss intrude foliated augite-phyric metabasalt and marble. All intrusive units are, in turn, cross-cut by leucogabbro and diorite pods and sills, and quartz and feldspar veins. Zircon from a foliated metadiorite dike yields a U-Pb age of 445 ± 8 Ma (88CR111, Tables 1 and 2). The metaplutonic rocks exposed on Cleveland Peninsula are similar in composition, texture, lithology, and intrusive relations to metaplutonic rocks exposed to the west across Clarence Strait on Kaasan Peninsula (Eberlein et al., 1983). Based on these geologic relations, and the continuity of exposure along the southwestern side of Cleveland Peninsula and the east side of Kaasan Peninsula, the metaplutonic rocks on Cleveland Peninsula are interpreted to be correlative with similar rocks on Kaasan Peninsula.

Karheen Formation

Coarse-grained clastic strata unconformably overlie metaplutonic rocks on the shoreline south of Niblack Hollow on western Cleveland Peninsula (Figure 2), and consist of interbedded siliceous argillite and micaceous limestone overlain by pebble to cobble conglomerate. Conglomerate beds occur as distinctive layers that overlie, and are interbedded with, banded siliceous argillite and consist of beds 30-50 cm thick. Clasts are matrix-supported and are usually less than 5 cm in diameter in a argillaceous limestone matrix. Clasts consist of rounded and subangular plutonic and volcanic clasts, and vein quartz material. Basaltic sills and dikes intrude the sequence. No fossils have been recovered from the clastic sequence. On the basis of similarities of stratigraphic position and lithology, the clastic strata are interpreted as part of the Lower Devonian conglomeratic part of the Karheen Formation, exposed on central Prince of Wales Island (Eberlein et al., 1983). On Prince of Wales Island, similar strata consisting of pebble to cobble conglomerate, limestone, shale, and greywacke unconformably overlie metaplutonic diorite rocks (Eberlein et al., 1983). The conglomeratic strata record uplift and erosion of Ordovician and Silurian rocks during the Klakas orogeny (Gehrels et al., 1983).

Hyd Group

Upper Triassic strata on Annette and Gravina islands consist of limestone, fine- to coarse- grained clastic sedimentary rocks, and basalt to rhyolite volcanic rocks (Berg, 1972, 1973). These rocks unconformably overlie pre-Devonian strata of the Alexander terrane and are unconformably overlain by the Upper Jurassic to Lower Cretaceous Gravina sequence (see discussion below). The Upper Triassic strata have been recently described by Gehrels et al. (1987). Upper Triassic strata of the Alexander terrane are not present on Cleveland Peninsula and Revillagigedo Island.

Gravina sequence

Upper Jurassic and Lower Cretaceous strata structurally overlie lower Paleozoic rocks on southeastern Cleveland Peninsula, and locally lie unconformably over Triassic rocks on Annette and Gravina Islands (Figure 2; Berg, 1972, 1973; Brew and Karl, 1987; Rubin and McClelland, 1989; Rubin and Saleeby, in prep.). These strata belong to the Gravina-Nutzotin belt (Berg et al., 1972), which we informally call the Gravina sequence in southern southeastern Alaska. The sequence is exposed along the eastern margin of the Alexander terrane in much of southeast Alaska (Figure 1). Near Ketchikan, the Gravina sequence consists of two distinctive members; however, stratigraphic thickness is uncertain due to complex deformation and thrust faulting.

On Cleveland Peninsula, the lower contact of the Gravina sequence is not exposed and is in thrust contact with the Descon Formation of the Alexander terrane. Here, the Gravina sequence has an approximate structural thickness of 15 km. The lower member consists of argillite, calcareous argillite, waterlaid coarse pyroclastic deposits, tuff, lavas, and minor intrusive rocks. Pyroclastic volcanic deposits dominate the lower member on Cleveland Peninsula and contain massive to pillowed flows and flow breccia, commonly with clasts that are angular to subangular in shape. Augite and hornblende phenocrysts are present in both the matrix and clasts. Crystal-rich tuff and tuffaceous argillite are also present on Cleveland Peninsula, Annette, Gravina, Revillagigedo, and adjacent islands. Typically, crystal tuff consists of euhedral augite \pm hornblende phenocrysts in a pale green tuffaceous matrix containing augite, hornblende, epidote, clinozoisite, albite, and white mica. Texturally-diverse, hypabyssal dioritic bodies intrude the

lower member as tabular bodies that parallel regional trends on northern Annette Island and southeastern Cleveland Peninsula. The contact between the diorite and enclosing volcanic rocks lacks a well-defined contact aureole, and is texturally and compositionally gradational. The age of the lower member is poorly constrained and, based on lithologic and stratigraphic similarities with Upper Jurassic strata exposed on Gravina Island (Berg, 1973), the lower member on Cleveland Peninsula is interpreted as Late Jurassic in age.

The upper member consists of argillite, tuff, slate, and conglomerate and is well-exposed on Cleveland Peninsula, Revillagigedo, Gravina, and adjacent islands. The lower contact of the member is not exposed; however, locally the upper member overlies both the lower member of the Gravina sequence and unconformably overlies the upper Paleozoic and lower Mesozoic Alava sequence (discussed below). The upper contact is not exposed and is in fault contact with adjacent terranes. Lithologic units consist of argillaceous and tuffaceous turbidites and pebble to cobble conglomerate, with a total structural thickness of 900 meters. Conglomerate beds occur in a distinctive mappable horizon, exposed between southeastern Cleveland Peninsula and southeastern Revillagigedo Island. The clasts are ellipsoidal, have been partly affected by younger deformation, and range in size from 3 to 18 cm in diameter. In places, boulder-sized clasts up to 40 cm in diameter occur. The clasts consist of fine- to coarse-grained leucocratic quartz diorite, granodiorite, volcanic porphyry, argillite, and minor marble and quartz vein material. The clasts yield Pb-U zircon ages of 154 Ma to 158 Ma (Rubin and Saleeby, in review, chapter 2). These Late Jurassic ages for the granitic clasts provide a maximum age for deposition. Based on geologic relations with similar strata exposed to the north and sparse fossil data in the Ketchikan area (Berg et al., 1972), an Early Cretaceous age (after the time scale of Lanphere et al., 1978) is inferred for the upper member clastic and tuffaceous strata.

Taku terrane

Alava sequence

The Alava sequence (formerly part of the the Taku terrane of Berg et al., 1978) is a distinctive upper Paleozoic and lower Mesozoic stratified sequence and, along with the Gravina sequence, forms the eastern boundary zone of the Alexander terrane along its 300 km extent. We have abandoned using the term "Taku

terrane," to describe the polydeformed and metamorphosed strata exposed on the west side of the Coast Plutonic Complex because numerous elements of the Taku terrane as originally defined by Berg et al. (1978), can now be reassigned to either the Alexander terrane, Gravina sequence or the "Kah Shakes sequence." The remainder belongs to the Alava sequence which is well-exposed from Portland Peninsula to the northeast shoreline on Cleveland Peninsula (Figure 2). The Alava sequence is fault bounded on the east by lower to middle Paleozoic orthogneiss, and intruded by Cretaceous and younger foliated tonalite and granodiorite.

The Alava sequence, in southern southeast Alaska, consists of two members, an Upper Pennsylvanian and Lower Permian metavolcanic and metasedimentary assemblage and a Middle to Upper Triassic mixed metasedimentary and metavolcanic assemblage (Silberling et al., 1981; Orchard, personal communication). The lower part of the sequence consists of massive crinoidal marble interlayered with black argillite and phyllite and mafic metavolcanic lava, breccia, tuff, pillowed flows, and minor quartzite. Carbonaceous and siliceous nodular limestone, argillite, mafic metavolcanic tuff, breccia, and pillowed flows make up the distinctive upper member. The base of the Alava sequence is nowhere exposed and the sequence either structurally overlies the Gravina sequence or Alexander terrane. Locally, the epiclastic strata of the Gravina sequence unconformably overlie the Alava sequence.

Based on lithology, broad age constraints, and tectonic setting, the Alava sequence might be correlative with the upper Paleozoic parts of the Yukon-Tanana terrane (Rubin and Saleeby, in review). The laterally continuous upper Paleozoic marble horizons in the Alava sequence resemble Yukon-Tanana lithologies more closely than similar age strata in Wrangellia. In this context, the lower Mesozoic portion of the Alava sequence is correlated with the Triassic portion of the Stikine terrane (e.g., Stuhini Group). The presence of Kah Shakes affinity quartzite interlayered with Alava metabasalt supports this later interpretation (Saleeby, in preparation).

Alternatively, the Alava sequence is possibly correlative to the upper Paleozoic and lower Mesozoic parts of Wrangellia that are exposed in the eastern Alaska Range. In this context, the Alava sequence may represent a metamorphic vestige of Wrangellia. Similar strata previously assigned to the

Taku terrane on southern Chilkat Peninsula, north of Juneau, are now considered part of Wrangellia (Figure 1; Plafker et al., 1988).

Kah Shakes sequence

The Kah Shakes sequence (formerly parts of the Taku and Tracy Arm terranes of Berg et al., 1978) comprises the westernmost framework rocks of the Coast Plutonic Complex, and forms screens and septa within the Coast Plutonic Complex (Saleeby and Rubin, 1990; Figures 1 and 2). As with the Alava sequence, we have abandoned terrane nomenclature to describe rocks exposed west of the Coast Plutonic Complex. Regionally metamorphosed and polydeformed strata previously assigned to separate terranes can now be reinterpreted in the context of detailed geologic mapping, ongoing geochronology and geochemistry.

The Kah Shakes sequence is best exposed on the western shoreline of Portland Peninsula. The sequence is bounded on the west by a thrust fault in which the Alexander terrane and perhaps the Alava sequence form lower plates, and is intruded on the east by the voluminous Cretaceous and Tertiary Plutonic rocks of the Coast batholithic belt. On southernmost Revillagigedo Island, the Kah Shakes sequence structurally overlies the Alexander terrane along an east-dipping thrust fault. The sequence consists of a thick succession of quartzite and carbonate-rich turbidites, siliceous and quartz-feldspathic schist, subordinate metabasalt, pelitic schist, and orthogneiss (Figure 4). Orthogneiss, exposed to the south on Portland Peninsula, displays complex zircon systematics and has unique Proterozoic zircon inheritance, unlike the lower Paleozoic intrusive rocks of the Alexander terrane (Saleeby and Rubin, 1989, 1990). Based on lithologic similarities, mid-Paleozoic intrusive ages, the presence of Proterozoic zircon inheritance, spatial proximity, and tectonic setting, the Kah Shakes sequence is interpreted as correlative with the Yukon-Tanana terrane, which is now recognized within roof pendants and metamorphic screens as far south as latitude 59°, east of Juneau (Wheeler and McFeely, 1987).

Figure 4: Amphibolite-facies rocks of quartzite and marble in the Kah Shakes sequence, exposed north of Rudyerd Inlet on the east-side of Behm Canal.



Intrusive Rocks

Mid-Cretaceous (?) mafic and ultramafic Rocks

Mid-Cretaceous (?) mafic and ultramafic bodies underlie part of Cleveland Peninsula, Revillagigedo and Duke islands (Figure 2). The ultramafic complexes form a linear belt that spans approximately 560 km, from southern southeast Alaska to northwestern British Columbia (Taylor, 1967). The complexes intrude rocks of the Alexander terrane, Gravina and Alava sequences. The bodies occur as zoned ultramafic complexes ranging in composition from dunite, in the center, to pyroxenite and hornblende pyroxenite on the outer border (Taylor, 1967; Irvine, 1967, 1974). The Duke Island ultramafic complex, located east of the late Mesozoic deformational front, is moderately to highly deformed and yields a Pb-U zircon age on a pegmatite of 108 Ma (J. Saleeby, in review). Zircon from saussuritized gabbroic pods and veins that cross-cut a hornblende in the Union bay Ultramafic Complex (Table 1) yield a discordant U-Pb age of 86.5 ± 5 Ma (88CR15, Table 2). K-Ar analyses on hornblende and biotite for the ultramafic bodies yield 100 Ma to 110 Ma cooling ages (Lanphere and Eberlein, 1966), which is consistent with the U-Pb zircon age of the Duke Island pegmatite.

Quartz diorite and granodiorite

Northern Revillagigedo Island and Cleveland Peninsula are underlain by a composite batholith composed of massive to foliated, medium- to coarse-grained hornblende quartz diorite and granodiorite (Figure 2). The Bell Island Pluton on northern Revillagigedo and Bell Islands, and northern Cleveland Peninsula are part of the composite body (Figure 2). Sub-horizontal dikes and veins of light grey to tan, weathering quartz-feldspar pegmatite and subordinate agmatite are present throughout the batholith. The rocks contain varying proportions of plagioclase, microcline, quartz, green hornblende, and brown biotite. Apatite, zircon, sphene, ilmenite, and magnetite occur as accessory minerals. A leucocratic quartz diorite (Table 1; Bell Island Pluton) yields U-Pb zircon age of 90.5 ± 7 Ma (Table 2). The age of the Bell Island Pluton is consistent with a preliminary U-Pb zircon age of 89 Ma reported by Arth et al. (1988). K-Ar analyses yield hornblende cooling ages that range from 86 to 55.5 Ma, and biotite cooling ages that range from 74 to 49 Ma (Smith and Diggles, 1981). The batholith intrudes the Gravina sequence on northern

Cleveland Peninsula, the Kah Shakes sequence on east Behm Canal, and the Alava sequence on western Revillagigedo Island.

Plagioclase porphyritic granodiorite, quartz diorite, and tonalite

Elongate stocks, plutons, sills, and dikes of plagioclase porphyry and quartz diorite intrude much of Revillagigedo and adjacent islands and Cleveland Peninsula (Figure 2). The Eaton Point Pluton, exposed on northern Cleveland Peninsula is assigned to this unit. Locally, the rocks contain tan plagioclase phenocrysts, which make up to 50% of the rock, and range between 1 and 4 cm in diameter. The groundmass contains fine-grained quartz, microcline, biotite, minor hornblende, epidote, and garnet. Commonly, euhedral garnet occurs within cores of plagioclase, but it also occurs within the groundmass. Anhedral to euhedral epidote is interstitial to plagioclase crystals. The plutons intrude metasedimentary and metavolcanic rocks assigned to the Gravina and Alava sequences, and locally the Alexander terrane (?), and have narrow contact aureoles that overprint the metamorphic foliation. The sills and dikes are sub-concordant to foliation and locally cross-cut the metamorphic framework rocks, increasing in abundance towards the east. A medium-grained granodiorite yields a U-Pb zircon age of 95.8 Ma (88CR14, Tables 1 and 2) for the Eaton Point Pluton. A plagioclase porphyritic granodiorite phase of the Eaton Point Pluton yields a U-Pb age of 95.5 Ma (88CR24, Tables 1 and 2). K-Ar analyses yield 86.9 Ma (hornblende) and 82 Ma (biotite) cooling ages (Smith and Diggles, 1981).

Epidote-hornblende tonalite, quartz diorite, and granodiorite

Epidote-bearing granodiorite, quartz diorite, and tonalite occur as elongate plutons on southwestern and part of northeastern Revillagigedo Island (Figure 2). These distinctive plutons continue as a belt farther north into the Petersburg and Juneau area (Figure 1; Brew and Morrell, 1983; Brew, 1988). The petrology and mineral chemistry of these epidote-bearing plutons are discussed by Zen (1985, 1988), Zen and Hammarstrom (1984), and Hollister et al. (1987). The rocks are characterized by apple-green epidote and contain quartz, plagioclase, microcline, hornblende, biotite, and locally garnet. Magnetite, ilmenite, apatite, zircon, sphene, and allanite occur as accessory minerals. The plutons are usually massive in the

interior and-foliated along its margins and intrude the Gravina and Alava sequences, and locally the Alexander terrane (?). The intrusive bodies display intrusive contacts and are locally in fault contact with adjacent metasedimentary and metaplutonic rocks. U-Pb zircon ages for the plutons range between 95 Ma and 101 Ma, and locally zircon systematics reveal Proterozoic inheritance (e.g., the Moth Bay Pluton; Rubin and Saleeby, 1988). A Hornblende $\text{Ar}^{40}/\text{Ar}^{39}$ plateau age of 97 Ma is reported by Sutter and Crawford (1985) for the Moth Bay Pluton.

Lamprophyre dikes

A northeast-trending swarm of lamprophyre dikes intrudes the metamorphic framework rocks and most intrusive rocks on Cleveland Peninsula and Revillagigedo and adjacent smaller islands (Figure 2). The dikes intrude a pluton with Pb-U ages that range between 19 Ma and 32 Ma (Arth et al., 1988) and are cross-cut by Pleistocene volcanic rocks (Smith, 1973). The dikes are linear, undeformed, and vary in thickness between .5 m and 2.5 m. The rocks are mineralogically and texturally variable, and contain fine-grained equigranular altered plagioclase, brown amphibole, clinopyroxene, calcite, and chlorite. Major- and trace-element geochemistry are reported by Lull and Plafker (1987) and are chemically indistinguishable from continental flood basalt.

Cenozoic deposits

Columnar-jointed lava flows, flow breccia, and local volcanic cones and plugs cover parts of Revillagigedo and adjacent smaller islands. Most of these lavas are post-glacial in age, based on the presence of unconsolidated ash and pumice that locally cover parts of glaciated ridges, and the preservation of volcanic cones and plugs undisturbed by glacial activity. Pre-glacial volcanic activity is reported by Berg et al. (1978). K-Ar whole-rock and plagioclase analyses of basalts yield ages of ≈ 5 Ma and ≈ 0.5 to 1.0 Ma (Smith and Diggles, 1981).

STRUCTURAL GEOLOGY AND METAMORPHISM

Only recently have mid-Cretaceous basement-involved thrust faults and associated nappe structures been recognized in southern southeast Alaska (Berg et al., 1988; Crawford et al., 1987; Rubin et al., 1990; Rubin and Saleeby, in review). Deformation of lower Paleozoic to mid-Cretaceous supracrustal and plutonic rocks in the region is localized along the eastern boundary of the Alexander terrane, and is characterized by an imbricate series of west- to southwest-vergent thrust sheets. Based on regional geologic and geochronologic relations, the west-vergent fold and thrust system was active between about 113 and 89 Ma (Rubin and Saleeby, 1988a). Younger intrusive rocks do not display the mid-Cretaceous thrust-related fabrics. Both the younger intrusive rocks and the rocks affected by mid-Cretaceous deformation were subsequently affected by Late Paleocene to Early Eocene deformation and associated uplift (Hollister, 1982; Crawford et al., 1987; Gehrels and McClelland, 1988). K/Ar cooling ages from biotite and hornblende in plutonic rocks yield ages of 74 and 81.8 Ma, respectively (Smith and Diggles, 1981) and are interpreted as a minimum uplift age for the thrust belt. Deformation and metamorphism which preceded mid-Cretaceous orogenesis are discussed by McClelland and Gehrels (in review), and appear to represent pre-Late Jurassic dextral strike-slip dismemberment of the Alexander terrane.

Mid-Cretaceous deformation occurred during two main episodes that correspond with the emplacement of sill-like plutonic bodies. Older fabrics record ductile southwest-vergent folding and faulting, regional metamorphism, whereas younger fabrics are characterized by crenulation cleavage, thrust faulting and associated folding. Structural style varies along the strike of the orogenic zone and between structural levels due to changes in rock type, overall metamorphic grade, and proximity to plutonic rocks. Due to changes in bulk-rock volume, the presence of ductile strain and associated plastic flow, and the absence of exposed step-up angles along thrust faults, cross-sections cannot be rigorously balanced.

Internal Structure of the Thrust Belt

First-generation thrust faults

The lowest thrust sheets consist of lower Paleozoic schist, marble, and meta-igneous rocks of the Alexander terrane (Figure 3A, B). These rocks are characterized by mesoscopic folding, non-penetrative foliation and

thrust faulting, and display lower-greenschist facies mineral assemblages. Early deformational fabrics (D_1) are characterized by mesoscopic northeast dipping foliation surfaces (S_1) and a bedding-foliation intersection lineation (L_{0x1}). Thrust faults trend northwest and dip moderately to the northeast. The Gravina sequence structurally overlies the Alexander terrane, and on Cleveland Peninsula the sequence consists of six separate west-vergent thrust sheets (Figure 3A). The basal thrust fault separating the Alexander terrane from the Gravina sequence cross-cuts the metamorphic foliation, displays a cataclastic fabric (Figure 4), and juxtaposes shallowly-dipping Gravina sequence argillite over the moderately-dipping lower Paleozoic Descon Formation of the Alexander terrane (Figure 5). Lower Paleozoic and Upper Proterozoic crystalline rocks of the Alexander terrane form structural basement. In general, thrust faults trend northeast and their orientation generally follows the regional metamorphic foliation (Figure 2). There is a predominance of moderate, northeast-dipping foliation surfaces (Figure 6A) which are axial planar to asymmetric, west- to southwest vergent folds. These asymmetric folds are truncated by thrust faults and appear kinematically linked to the thrust faults. In well-bedded strata, compositional layering and foliation are commonly subparallel, whereas massive volcanic flows and breccias do not display a foliation and deform as rigid bodies. Foliation parallels flattening fabrics that are well-developed within conglomeratic horizons. The S_1 foliation is defined by mica grains and elongate, slightly flattened plagioclase grains that are parallel to sub-parallel to compositional layering. Rocks of the Gravina sequence are structurally overlain to the northeast, along the Pt. Francis fault system, by upper greenschist facies rocks belonging to the upper Paleozoic and lower Mesozoic Alava sequence. Moderately-dipping, west- to southwest-vergent ductile fault zones are characteristic of the structurally higher thrust sheets. There is a predominance of moderate northeast-dipping foliation surfaces (S_1), which are axial planar to asymmetric, west- to southwest-vergent folds (Figure 6 B, C). These asymmetric folds are truncated by thrust faults (Figure 7) and appear to be kinematically linked, as above, to thrust faults. The Alava sequence is, in part, structurally overlain by amphibolite facies rocks assigned to the lower Paleozoic Kah Shakes sequence. Kah Shakes rocks are characterized by attenuated fold limbs and a moderately developed down-dip elongation lineation that is parallel to fold axes. On northern Cleveland Peninsula and northeast Revillagigedo Island (Figure 2) Kah Shakes foliation trends northwest, whereas on Portland Peninsula foliation strikes north-south.

Figure 5: Geologic sketch map of the contact between the Alexander terrane and the Gravina sequence, exposed in an unnamed cove, northeast of Caamano Point, southern Cleveland Peninsula. Regional location shown in inset. (Ketchikan C-6 quadrangle)

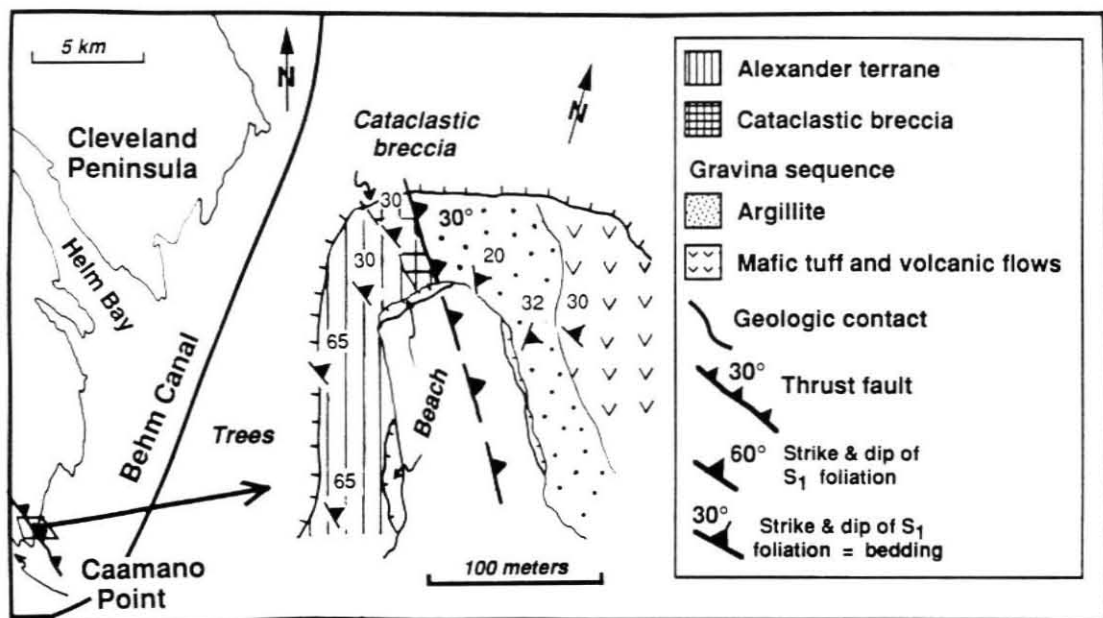


Figure 6: Lower-hemisphere, equal-area plot showing: (A) Poles to foliation surfaces on northwest Cleveland Peninsula; (B) Poles to foliation surfaces on southern Cleveland Peninsula; (C) Trend and plunge of small-scale folds, and poles to foliation surfaces in higher level thrust nappes on northern Cleveland Peninsula; and (D) Poles to foliation surfaces and trend and plunge of elongation lineation in higher level thrust nappes.

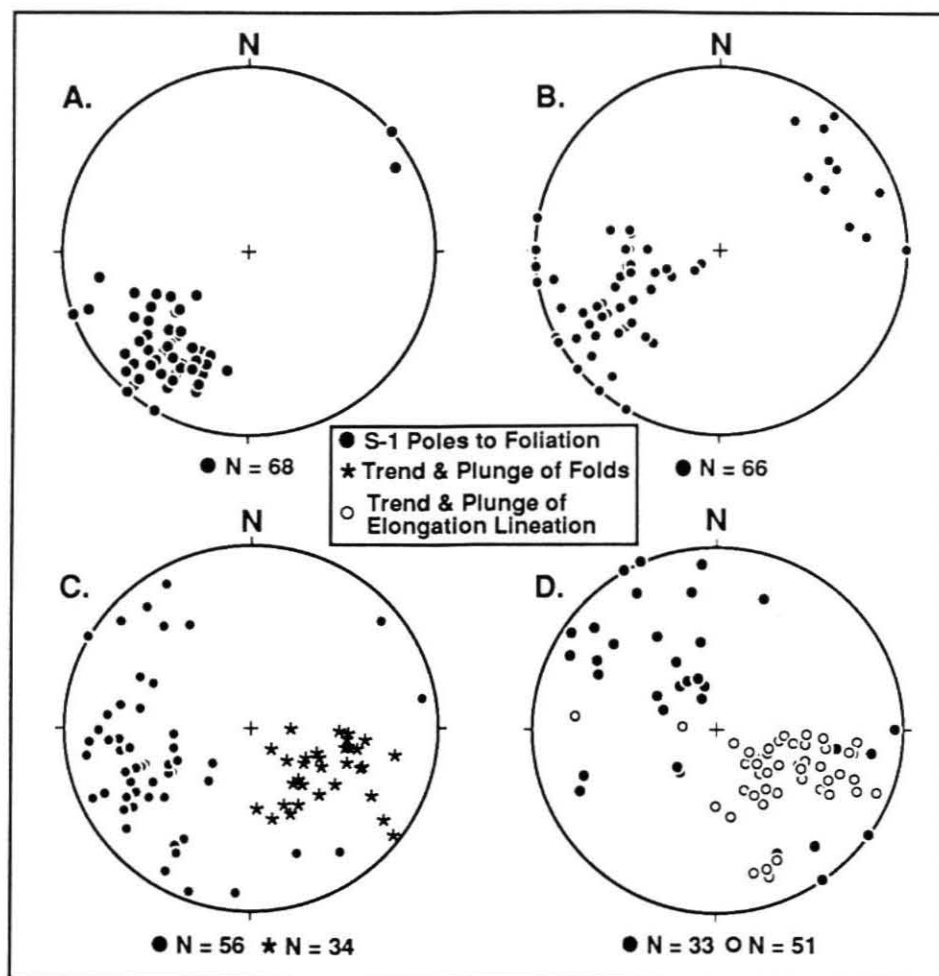
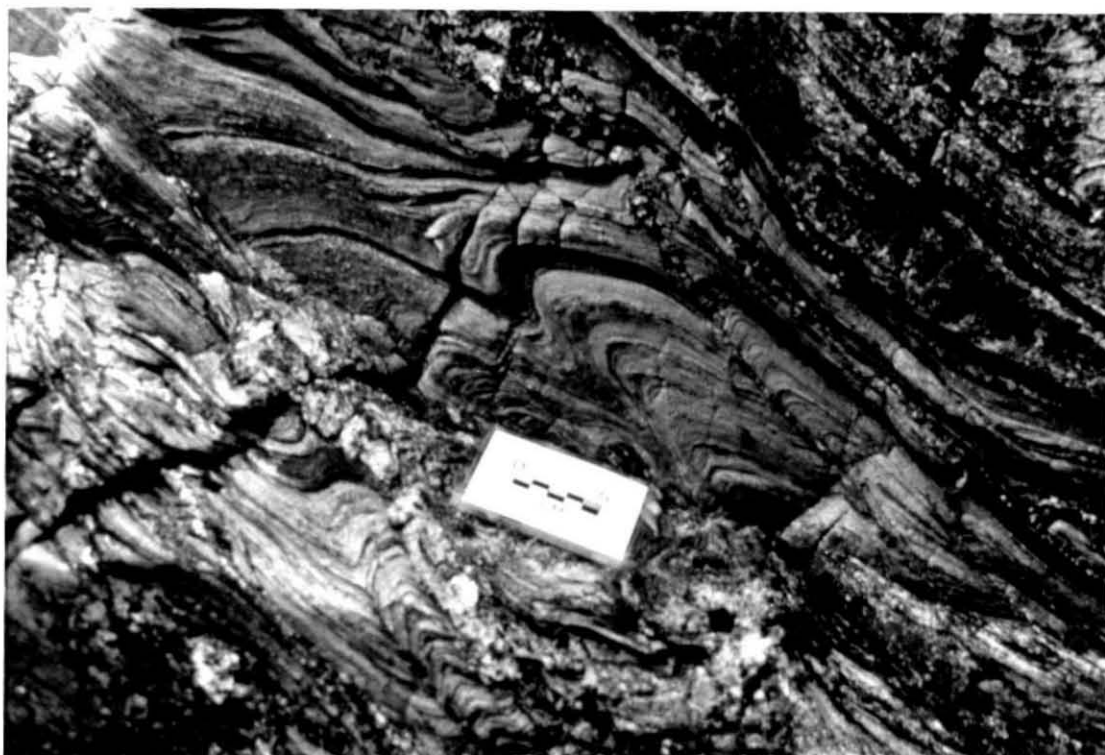


Figure 7: Asymmetric folds truncated by moderately-dipping thrust faults in the Permian part of the Alava sequence, exposed on Revillagigedo Island. This fault zone places Permian marble and metabasalt over Triassic carbonaceous pelitic schist.



Metamorphic grades increase from lower to higher structural levels. In the lowest structural level, phyllite in the Gravina sequence contains white mica, chlorite, epidote, plagioclase, and calcite which are typical of lower greenschist facies metamorphism. Fossils are preserved in carbonaceous limestone and argillite. Contact metamorphic aureoles are present, and are best observed on Spire Island located northeast of Annette Island (Figure 2). Relict andalusite, replaced by white mica, occurs in phyllite in a narrow zone adjacent to the Spire Island diorite, which indicates low pressure and high temperature conditions. Garnet porphyroblasts occur in phyllite of the Gravina sequence adjacent to the Union Bay Ultramafic Complex. Here, the regional fabric, defined by the planar orientation of biotite and white mica, overprints the contact metamorphic aureole. This suggests that the emplacement of the ultramafic complex preceded regional metamorphism. Mafic volcanic rocks are widespread in the lower structural levels and contain relict euhedral phenocrysts of clinopyroxene, hornblende, and plagioclase in a fine-grained microgranular matrix of relict pyroxene, amphibole, and metamorphic actinolite, chlorite, epidote, albite, quartz, white mica, and calcite, which is typical of low-temperature greenschist-facies metamorphism. Relict clinopyroxene and hornblende phenocrysts in the volcanic strata are unstrained and are partially replaced by chlorite and white mica. Preliminary oxygen isotopic analyses (C. Rubin and H. P. Taylor, Jr., unpublished data) on mafic phenocrysts indicate preservation of primary igneous $\delta^{18}\text{O}$ values which imply that the phenocrysts did not exchange with hydrothermal fluids. The presence of andalusite in contact aureoles, lower greenschist facies metamorphic mineral assemblages, combined with the presence of abundant relict phenocrysts in volcanic strata implies pressures no greater than 3.5 kb (e.g., Holdaway, 1971) and temperatures less than 400 ° C (e.g., Turner, 1981) in the lower structural levels.

Towards the east, in successively higher structural levels, biotite and garnet appear indicating upper greenschist facies metamorphism. Locally, staurolite is present in pelitic strata and hornblende-plagioclase-garnet \pm epidote mineral assemblages are present in mafic metavolcanic rocks. These lower amphibolite mineral assemblages, combined with pressure estimates obtained for the Moth Bay Pluton, based on aluminium content in hornblende (Zen and Hammarstrom, 1984) and the experimental calibration of Johnson and Rutherford (1989) imply pressure of 5 to 6 Kb and temperatures of \approx 550° C. Pressure estimates for the Bushy Point Pluton, located to the northeast (Figure 2; Zen and Hammarstrom, 1984)

using the same geobarometer, yield pressures in excess of 6.2 Kb. In higher structural levels, on northern Cleveland Peninsula and Revillagigedo Island (Figure 2), kyanite \pm sillimanite schist occur as bladed crystals up to 1 cm long which cross-cut the dominant northeast trending foliation. The presence of kyanite-staurolite mineral assemblages, mid-crustal level plutons (e.g., Bushy Point Pluton), and the occurrence of tonalite sills and dikes that lack contact aureoles suggest upper amphibolite temperatures of at least 550° C and pressures \approx 6-7 kb (e.g., Turner, 1981) in the higher structural thrust sheets.

Second-generation Thrust Faults

Black Mountain Fault Zone

The Black Mountain Fault Zone, exposed on southwestern Revillagigedo Island between Thorne Arm and Carol Inlet (Figures 2 and 8), is a major structural boundary in the Ketchikan area. The fault zone dips moderately northeastward and juxtaposes mid-Cretaceous tonalitic sills, dikes and a large pluton, along with their host rocks, over non-deformed mid-Cretaceous sills and dikes, and Gravina sequence metasedimentary and metavolcanic rocks (Figure 3B). To the northwest, the fault zone cuts tonalitic sills and segments of the Moth Bay Pluton. Regional metamorphic and structural fabrics are cross-cut by the fault zone. Fabrics produced by simple shear are well-preserved in the fault zone. Igneous rocks in the fault zone commonly display blastomylonitic textures and locally relict igneous textures are completely overprinted by ultramylonite consisting of very fine-grained quartz-bioite-epidote mineral assemblages. Rotated plagioclase porphyroclasts, asymmetric recrystallized tails, and S-C fabrics in the igneous rocks suggest top to the northwest or a sinistral-reverse sense of motion. Brecciated, oblate clasts of weakly-deformed plutonic rocks (Figure 9) are surrounded by a foliated micaceous, locally mylonitic matrix and commonly display S-C fabrics which indicate a similar sense of shear. The timing of motion on the Black Mountain fault is constrained by differing lines of evidence. The fault zone affects plutonic rocks with a Pb-U zircon of 101 Ma (Rubin and Saleeby, 1988), so this much of the deformation must have post-dated the emplacement of the pluton. Contact mineral assemblages locally overprint blastomylonitic fabrics in the fault zone, implying that contact metamorphism overlapped in time with faulting.

Figure 8: Geologic cross-section across the Black Mountain fault zone, exposed on southwestern Revillagigedo Island.

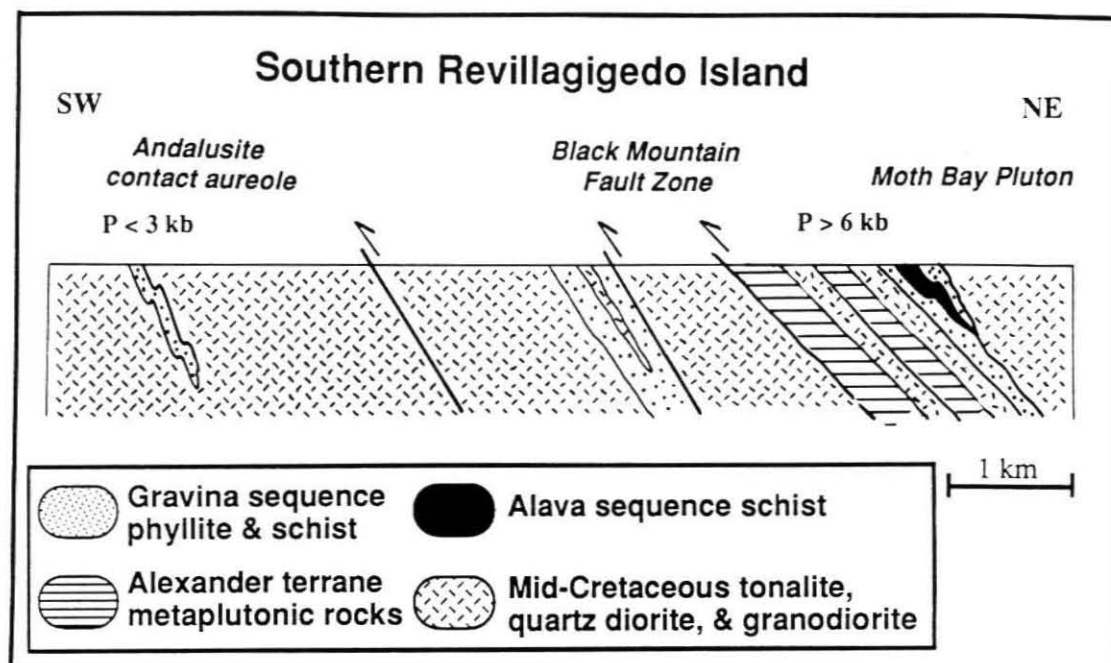
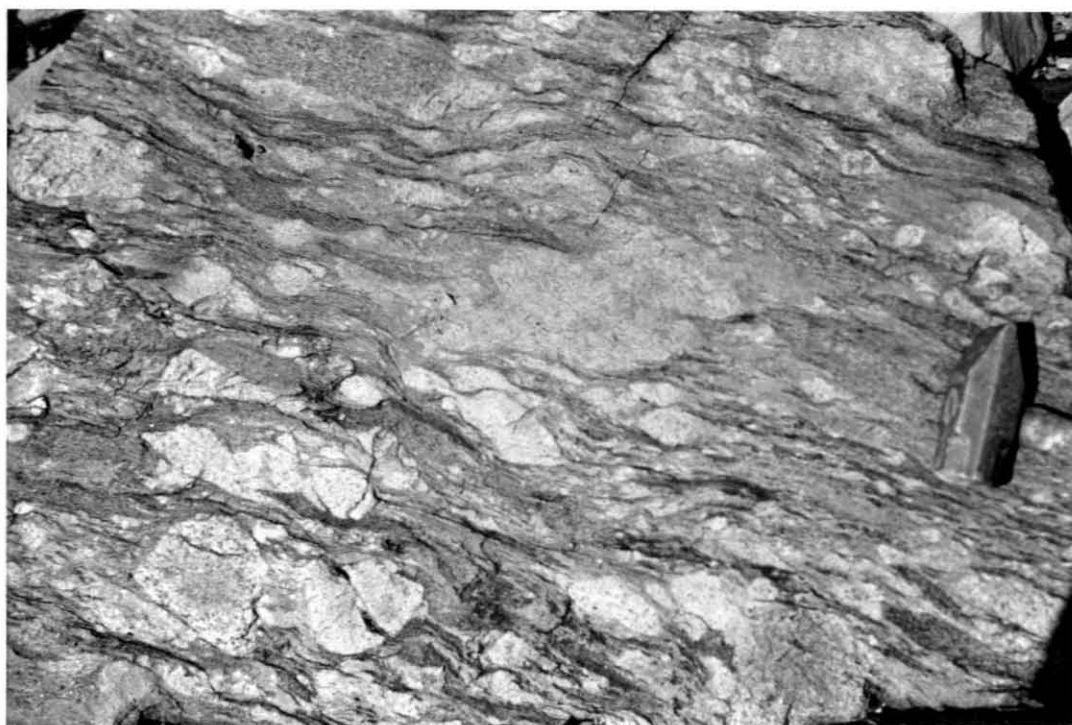


Figure 9: Weakly deformed tonalitic clasts in a mylonitic matrix. These fabrics developed within the Black Mountain Fault zone on southern Revillagigedo Island.



The amount of displacement on the fault zone is difficult to estimate; however, by using differences in metamorphic and igneous pressures on rocks exposed on either side of the fault, a qualitative displacement estimate can be obtained. The presence of kyanite-staurolite schist gives a minimum pressure of 5.5 kb for the hanging wall metasedimentary rocks. Based on aluminum contents in hornblende from the Moth Bay Pluton (Hammarstrom and Zen, 1986) and using the experimental calibration of Johnson and Rutherford (1989), a pressure range from 5.0 to 6.0 kb is recorded for the pluton exposed in the upper plate of the thrust. The extreme ranges in pressure may be due to variability of Al^T in hornblende. These pressures are in agreement with those recorded in metamorphic mineral assemblages from upper plate lithologies. Based on the presence of an andalusite contact aureole and associated regional lower greenschist facies mineral assemblages, a maximum pressure of 3.0 to 3.5 Kb is inferred for the footwall region. Assuming that the pressure estimates are correct and were locked in prior to faulting, the hanging wall was uplifted 14 km with respect to the footwall. A minimum dip-slip displacement of approximately 24 km is inferred across the Black Mountain Fault zone, assuming the fault was not subsequently rotated during post-Cretaceous time. Concurrent translational displacement across the fault cannot be quantified; however, substantial sinistral displacement is likely.

Third-generation ductile fault zones

Steeply-dipping, north- to northeast-dipping ductile fault zones cross-cut the earlier (S_1) fabrics in the eastern and northern part of the thrust belt (Figure 2). The fault zones are characterized by a strongly developed foliation which reorient earlier S_1 fabrics. Two such mid-Cretaceous to Late Paleocene (?) fault zones are exposed on Revillagigedo Island, the southern Revillagigedo fault zone on the west and the northern Revillagigedo fault zone, exposed to the north (Figure 2).

Structural relations suggest that reverse faulting occurred after F_1 folding and associated thrust faulting, and possibly during the late stages of the emplacement of the mid-Cretaceous tonalite plutons. The relationships between thrust faulting, regional metamorphism, and later reverse faulting described below suggest that these are likely the result of a single progressive deformational event.

Northern Revillagigedo Island Fault Zone

The Northern Revillagigedo Island fault zone is exposed on northern Revillagigedo Island (Figure 2). Here, earlier northwest-trending S_1 fabrics (regional foliation) are preserved within a compositionally-banded biotite schist and are completely transposed and tightly refolded within a series of ductile shear zones (Figure 10). The metamorphic rocks are cut by numerous quartz veins in which northwest-trending S_1 quartz veins are folded and attenuated; later quartz veins form along the axial surfaces of S_2 folds. Most axial planes of S_2 folds trend between $N40^\circ$ to $60^\circ W$ and dip between 70° to the northeast to vertical. Folds in banded biotite schist are disharmonic, generally tight to isoclinal and commonly asymmetric. The fold axes trend $S40^\circ$ to $80^\circ E$ and plunge moderately to the southeast. The limbs of the folds are extremely attenuated and locally display isolated asymmetric floating hinges. A well-developed elongation lineation is associated with S_2 foliation, and trends $S40^\circ$ to $60^\circ E$, plunging moderately to steeply to the southeast.

The Northern Revillagigedo Island fault zone separates supracrustal metamorphic sequences of widely differing metamorphic grade. In the footwall block, south of the fault zone, supracrustal rocks display garnet greenschist-facies mineral assemblages, whereas to the north, in the hanging wall, kyanite-bearing amphibolite grade schist and the mid-Cretaceous Bell Island pluton are present. Based on these geologic relations, top to the west or a reverse-sense of motion is recorded across the fault. The magnitude of displacement on the fault zone is difficult to estimate, due to the absence of stratigraphic cut-offs along the fault zone. A minimum of displacement of 7 km between the hanging wall and footwall is inferred based on metamorphic pressure estimates on pelitic supracrustal rocks exposed on either side of the fault zone. Sinistral displacement across the fault cannot be quantified; however, substantial displacement may be likely.

Southern Revillagigedo Fault Zone

The Southern Revillagigedo Fault Zone is exposed along southwest side of Revillagigedo Island (Figure 2). The fault strikes approximately $N20^\circ$ - $30^\circ W$ and dips moderately to the northeast. Southwest-vergent asymmetric folds trend $S60^\circ$ - $70^\circ E$ and plunge moderately to the southeast (Figure 11 A). Rocks in the fault zone consist of highly deformed argillite and tuffaceous argillite interlayered with thin marble

Figure 10: Geologic sketch of transposed foliation (S1) and associated isoclinal folds in banded kyanite schist along the Northern Revillagigedo fault zone. Elongation lineation dips moderately to the southeast.

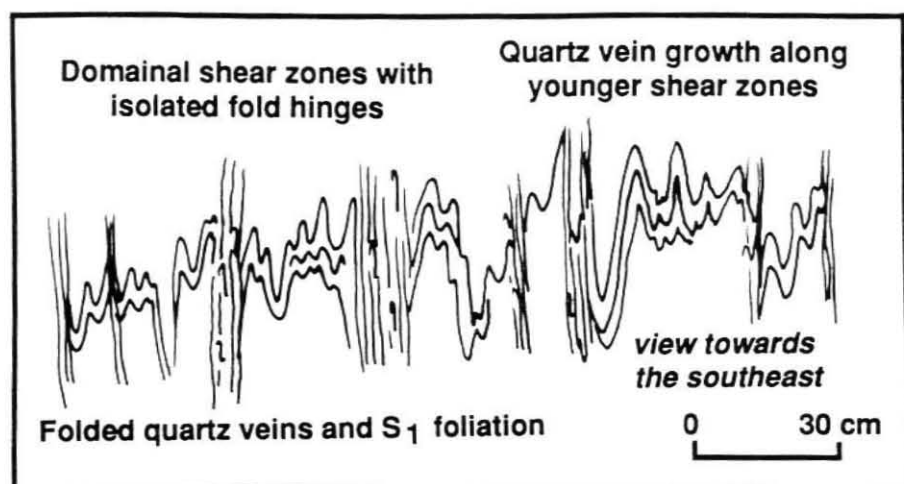
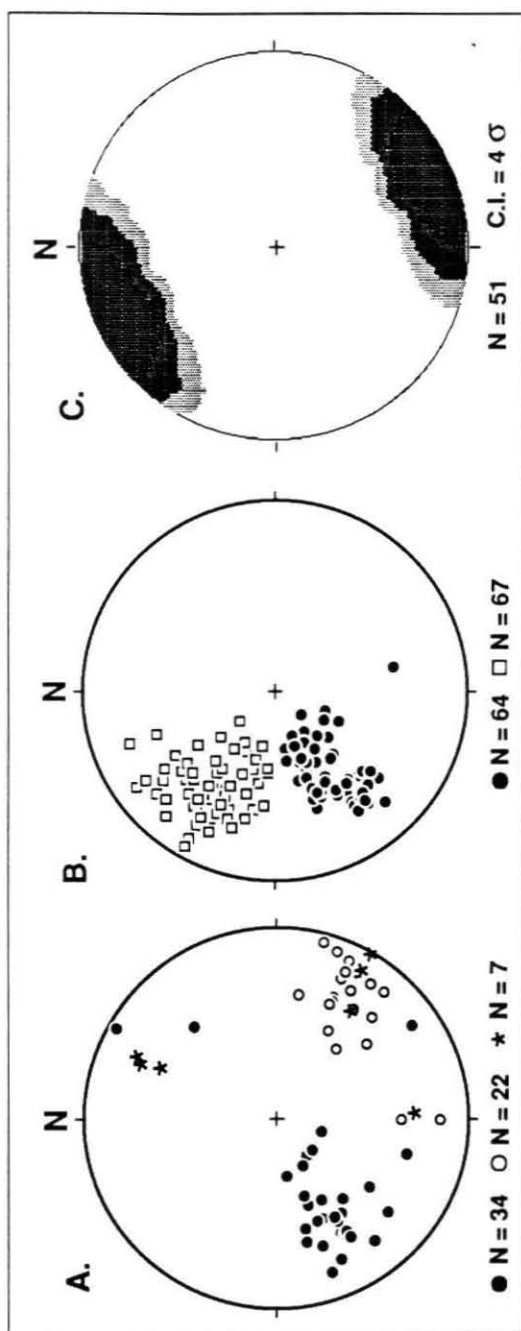


Figure 11: Lower hemisphere equal-area plot showing: (A) Poles to foliation surfaces, small-scale folds, and lineations along the southern Revillagigedo fault zone; (B) Poles to foliation surfaces and small-scale folds of D₁ and D₂ fabrics; (C) Contour of poles to dike orientation. C.I. = confidence interval, after Kamb (1959). ● = S₁ foliation; □ = S₂ foliation; * = trend and plunge of small scale folds; O = trend and plunge of lineation.

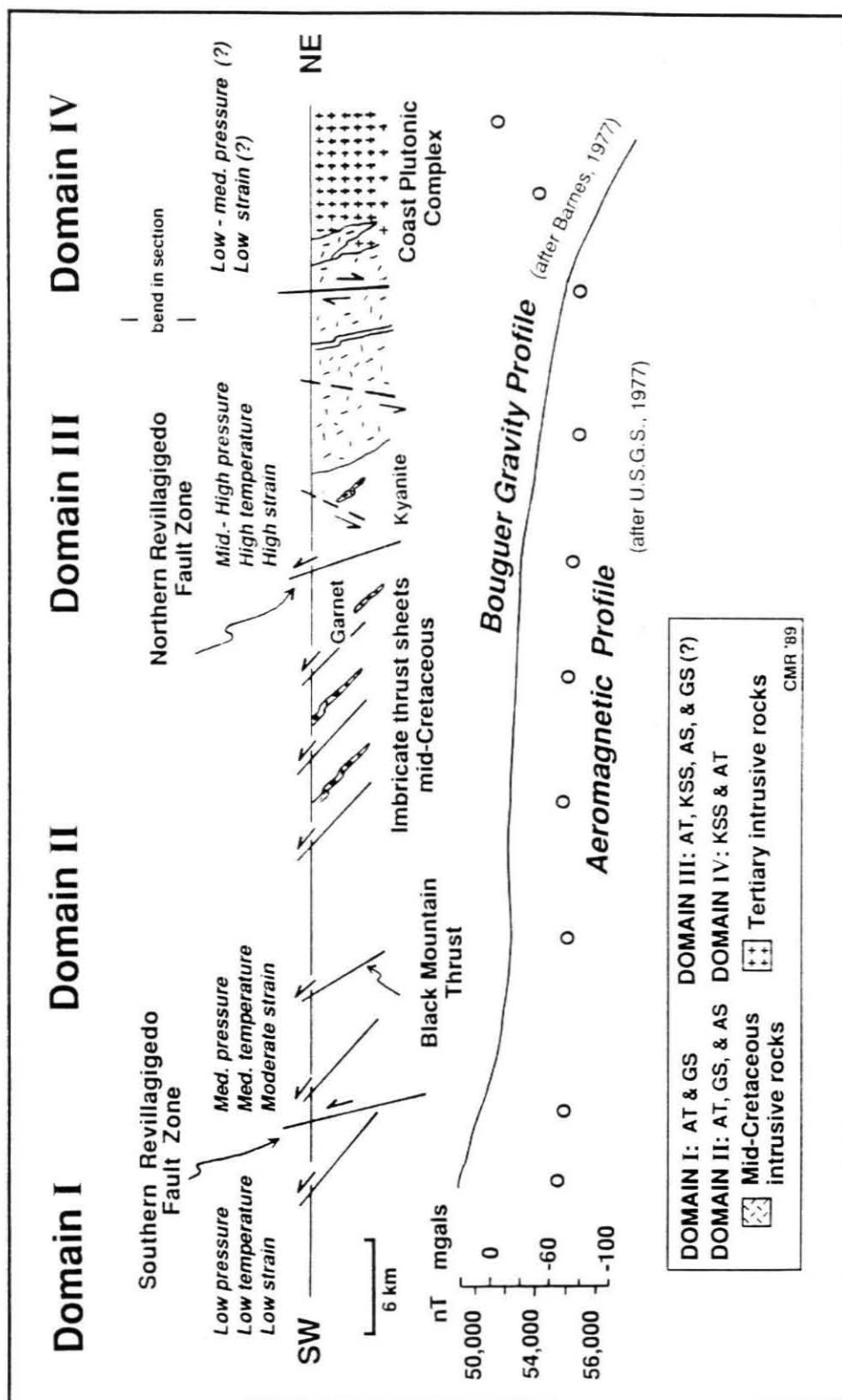


lenses. Numerous quartz veins are present in the fault zone. The southern Revillagigedo fault zone separates rocks of differing metamorphic and grade. In the footwall, rocks are well-bedded and are characterized by lowermost greenschist facies mineral assemblages and unstrained relict phenocrysts. Based on these relations, the footwall block appears to have undergone minor finite strain and metamorphism. In contrast, the upper plate contains rocks that locally have biotite-grade greenschist facies mineral assemblages, well-developed foliation surfaces, and are intruded by numerous sills and dikes of deformed diorite. As the fault zone is approached, abundant quartz veins appear in the metamorphosed hanging-wall lithologies. A top to the west, or reverse sense of motion is recorded across the Southern Revillagigedo fault zone.

Zonation of the Thrust Belt

These high angle reverse faults divide the thrust belt into three mid-Cretaceous structural domains (Figure 12). The subsurface geometry of the thrust faults and ductile reverse faults are not accurately known. By combining available geologic and petrologic constraints, a reasonable and internally consistent subsurface geometry can be constructed. Domain # 1, located on the western portion of the thrust belt, consists of rocks which have undergone little finite strain and which contain low temperature and pressure metamorphic mineral assemblages. Typically, rocks in this domain are well bedded and consist entirely of the Alexander terrane and Gravina sequence. The central region, domain # 2, consists of imbricate thrust nappes of rocks that are assigned to the Alexander terrane, and Gravina and Alava sequences. The rocks display well-developed metamorphic fabrics and contain medium pressure and temperature-sensitive metamorphic minerals. The appearance of mid-Cretaceous tonalite and granodiorite is characteristic of this domain. Higher pressure and temperature mineral assemblages are recorded by rocks in domain # 3 which consists of the Alexander terrane, and Kah Shakes, Alava, and Gravina sequences. Here, amphibolite metamorphic facies rocks are dominant. Well-developed elongation lineations, highly attenuated fold limbs, and polyphase fabrics characterize this domain. Metamorphic rocks contain a high proportion of tonalitic sills and dikes, and locally lit-par-lit textures are well developed in the high grade gneisses of domain # 3.

Figure 12: Aeromagnetic and gravity profiles and geologic cross-section across the western wall rocks of the Coast Plutonic Complex showing the major mid-Cretaceous structural domains. AT = Alexander terrane; GS = Gravina sequence; AS = Alava sequence; KSS = Kah Shakes sequence.



Typically, these rocks are intruded by Late Paleocene intrusive rocks and are overprinted by Early Tertiary extensional deformation.

Further mid- Cretaceous shortening was accommodated through the development of crenulation cleavage and is best exposed on the western shore of Revillagigedo Island. This fabric is defined by mesoscopic, northeast trending space cleavage (S_2), S_1 - S_2 intersection lineation (L_{1x2}), and associated west- to northwest-vergent asymmetric kink folds (Figure 11B). The cleavage forms small-scale folds in phyllite, whereas in massive metavolcanic rocks, a planar widely-spaced cleavage is present (Figure 11B). The cleavage is defined by the concentration of phyllosilicates in fold limbs. New mineral growth parallel to the kink fold axial planes consist of fine-grained biotite and garnet. Quartz grains are recrystallized and slightly flattened to the axial planes.

Late Paleocene Deformation

Paleocene and younger (?) deformation has affected rocks on the western margin of the Coast Plutonic Complex (Figure 2). Here, the eastern edge of the Alexander terrane and the Alava sequence appear to deepen in level of exposure and are dominated by low to moderate east- to west-dipping sheets of schist, gneiss, and phyllonite, termed the east Behm Canal gneiss complex (Saleeby, 1987; Saleeby and Rubin, 1990). Northeast-plunging elongation lineations are common; however, late tectonic recrystallization overprints this fabric. There is a predominance of moderate west-dipping foliation surfaces which are axial planar to asymmetric east-verging folds. These east-verging fabrics have re-oriented earlier mid-Cretaceous fabrics. Late Paleocene pegmatite dikes are highly deformed and are affected by these east- and west-dipping structures (Saleeby and Rubin, 1989). Exposure of the gneiss complex might be related to a reversal in vergence during Paleocene time, when deep levels of the mid-Cretaceous thrust system were transported upwards along east-vergent structures.

A swarm of hornblende-bearing diabase dikes cross-cut all structures and fabrics. These dikes trend northeast (Figure 11C) and mark a regional change in the overall tectonic setting during Miocene time.

DISCUSSION AND TECTONIC HISTORY

Three major lithotectonic assemblages, which include the Alexander and Taku terranes and the Gravina sequence, are present along a northwest-trending belt on the western side of the Coast Plutonic Complex. The upper Paleozoic portion of the Alava sequence represents the westernmost extent of the Yukon-Tanana terrane, which is interpreted as a continental margin assemblage of slope and rise deposits and dismembered fragments of a mid- to late Paleozoic arc system. The lower Mesozoic part of the Alava sequence has lithologic similarities to parts of the Stikine terrane. Structural basement is composite and consists of the Alexander and Taku (Alava and Kah Shakes sequences) terranes. The Alexander terrane forms depositional basement to the Gravina sequence; locally the epiclastic strata of the Gravina sequence lie unconformably over the late Paleozoic and lower Mesozoic Alava sequence, thus forming an overlap between the two basement constituents (e.g., Alexander terrane and Alava sequence). These data suggest the Alexander terrane was adjacent to the western margin of North America prior to deposition of the Upper Jurassic to Lower Cretaceous Gravina sequence. Primary relations between the Kah Shakes and Alava sequences are uncertain, although quartzite is interlayered with Alava marble on southeast Revillagigedo Island suggesting possible depositional relations.

The record of deposition and deformation within this belt spans an interval of almost 70 m.y., from the Late Jurassic to Late Cretaceous time. Beginning in the Late Jurassic, primitive arc-type (?) basaltic to basaltic andesite volcanic rocks of the Gravina sequence were deposited on basinal epiclastic strata that unconformably overlie Triassic and older portions of the Alexander terrane, and the late Paleozoic and lower Mesozoic Alava sequence (e.g., Yukon-Tanana and Stikine terranes; Rubin and Saleeby, 1989; Rubin and Saleeby, in review). Coarse-grained epiclastic and distal volcanic basinal strata of the Gravina sequence overlie the older volcanic rocks. Provenance for the coarse-grained epiclastic strata indicates uplift erosion of the older plutonic arc edifice, probably within an extensional tectonic setting. Beginning immediately after the deposition Gravina sequence, zoned mafic and ultramafic complexes were emplaced into rocks of the Alexander terrane on Duke and Annette Islands (e.g., the Duke Island ultramafic complex) and the Gravina sequence (e.g., the Union Bay ultramafic complex), and are present as numerous smaller bodies that intrude adjacent terranes. These enigmatic bodies form a linear belt parallel to the Gravina

sequence along the eastern edge of the Alexander terrane and may have been emplaced during the onset of mid-Cretaceous deformation, possibly in an extensional setting.

After the deposition of the Gravina sequence and during the emplacement of the zoned ultramafic complexes, significant mid-Cretaceous deformation and metamorphism affected these rocks and their basement components. Mid-Cretaceous deformation is recorded on Cleveland Peninsula, Revillagigedo Island, and the eastern portions of Annette, Gravina and adjacent islands. During the mid-Cretaceous, Gravina arc and basinal strata were imbricated together with their composite basement of the Alexander and Taku terranes along a series of moderately-dipping west to southwest-vergent thrust sheets. Asymmetric west to southwest-vergent folds formed during this faulting. Thrust sheets of the lower Paleozoic Kah Shakes sequence commonly overlie the Alexander terrane and Gravina and Alava sequence nappes; however locally on Portland Peninsula, the Kah Shakes sequence structurally underlies deformed Alexander terrane. Complex thrust geometries and out of sequence thrust faults may result from the reactivation of different primary basement components. This deformation is recorded in southern southeast Alaska by: (1) west- to southwest-vergent thrust faulting; (2) pervasive metamorphism, ranging from lower greenschist to amphibolite facies mineral assemblages; (3) emplacement of calc-alkaline sills, dikes, and plutons; (4) high angle reverse faulting; and (4) uplift that records at least 14 km of vertical transport by Late Cretaceous time. Available age constraints from Revillagigedo and adjacent islands indicate that this deformational event began in the Albian (≈ 113 Ma), the age of the youngest strata involved in thrust faulting, and must have ceased by ≈ 70 Ma, based on biotite K-Ar cooling ages (Smith and Diggles, 1981) from mid-Cretaceous plutons. During the mid-Cretaceous, Gravina arc and basinal strata was imbricated together with their composite basement of the Alexander and Taku terranes along a series of moderately-dipping west- to southwest - vergent thrust sheets. Asymmetric west - to southwest - vergent folds formed during this faulting. Complex thrust geometries and out of sequence thrust faults may result from the reactivation of different primary basement components. The presence of thrust sheets composed of crystalline basement may imply a zone of decoupling within middle levels of the continental crust during the mid-Cretaceous. The extent of northeast-directed underthrusting of the Gravina sequence and its composite basement beneath

the Yukon-Tanana terrane is difficult to assess; however, it is possible that these thrust sheets extend as a subhorizontal décollement beneath northwest British Columbia and western Yukon Territory.

The emplacement of mid-Cretaceous sills, dikes, and elongate plutons was broadly coeval with deformation; however, the details of the relation between deformation and pluton emplacement is quite complicated. These calc-alkalic intrusive rocks formed in response to plate convergence along the western margin of the Alexander terrane and represent the mid-crustal levels of a mid-Cretaceous continent-margin arc (Barker and Arth, 1984). Steeply-dipping reverse faults became active perhaps during the late stages of thrust faulting. Vertical motion on these faults resulted in the juxtaposition of differing crustal levels across the thrust belt and was perhaps responsible for the initial uplift of the deeper levels of the arc by the latest Cretaceous, reflected by an average uplift rate of ≈ 0.59 mm/yr. (Rubin and Saleeby, in review). Highly-deformed Late Paleocene to Early Eocene tonalitic and granodioritic intrusives are present on eastern Revillagigedo Island and western Portland Peninsula, and belong to a discontinuous belt of sills and elongate plutons that were intruded into overthickened crust along the western flank of the Coast Plutonic Complex. Rapid uplift accompanied the emplacement of these plutons (Hollister, 1982; Crawford et al., 1987) and may record the gravitational collapse of the mid-Cretaceous thrust belt.

Limited gravity and aeromagnetic data along the trend of the thrust belt help define the present day deeper crustal structure (Barnes, 1972a, b; 1977; U.S.G.S., 1977), which record the mid-Cretaceous and younger deformation. The dramatic decrease in Bouguer gravity anomaly values, from about +10 mgal in the non-deformed portions of the Alexander terrane to about -115 mgal in the interior of the thrust belt, along the western edge of the Coast Plutonic Complex (Figure 14) may reflect a thickened crust and associated large volumes of granitic material. The lowest Bouguer gravity anomalies coincide with the progressive thickening of the thrust wedge and the presence of mid-Cretaceous and younger intrusive rocks. A steep magnetic field gradient from the low magnetic strata of non-deformed Alexander terrane on the west to the highly magnetic eastern portions of the thrust belt and the western edge of the Coast Plutonic Complex (U.S.G.S., 1977) mirrors the Bouguer gravity gradient. Bouguer gravity data (Barnes, 1977) suggest a crustal thickness of ≈ 25 -30 km beneath the southeast Alaska archipelago (e.g., Alexander terrane and Gravina sequence) and a maximum thickness of 45 km below the crest of the Coast Plutonic Complex.

A northeast-trending swarm of Miocene to Oligocene mafic dikes cuts all Cretaceous and Early Tertiary structural elements and records northwest-southeast extension. This dike swarm may reflect regional extension associated with the opening of the Hecate Straits during the Late Tertiary. The modern structural setting is dominated by dextral strike-slip motion on the Queen Charlotte Fault system.

The mid-Cretaceous southeast Alaska orogen was characterized by thrust faulting, metamorphism and the emplacement of arc-related tonalitic and granodioritic material. Igneous activity and deformation appears to have been broadly coeval, suggesting an intra-arc setting. Mid-Cretaceous rocks exposed at the surface today were formed in middle crustal levels of a continent-marine arc and involved large-scale reworking of an earlier tectonic boundary between the Alexander terrane and the western margin of North America. The most penetrative deformation occurs where structural reactivation of differing basement components, such as the Alexander terrane and the Kah Shakes sequence, resulted in complex fault geometries. Development of the Early Tertiary tonalitic to granitic plutons followed mid-Cretaceous crustal shortening and uplift. These crustal elements formed the lithospheric framework for the Eocene Coast Batholith.

ACKNOWLEDGMENTS

Parts of this research were supported by National Science Foundation Grants EAR 86-05386 and EAR 88-034834 (to Saleeby). Additional support (to Rubin) was provided by a Geological Society of America Penrose Grant, a Sigma-Xi Grant-In-Aid, the U.S. Geological Survey, Alaska Branch, and by the U.S. Forest Service, Ketchikan Ranger District. We thank Fred Barker, Henry Berg, Dave Brew, Darrel Cowan, Maria Lucia Crawford, John Garver, George Gehrels, Linc Hollister, Meghan Miller, Bill McClelland, Jim Monger, George Plafker, and Margi Rusmore for helpful discussions on southeast Alaska stratigraphy and tectonics. Jeff Marshall assisted in mapping part of the area during the summer of 1987; Mark Fahnestock and Jon Nourse provided able field assistance during the summer of 1986.

REFERENCES

- Arth, J.G., Barker, F., and Stern, T.W., 1988, Coast Batholith and Taku plutons near Ketchikan, Alaska: Petrography, geochronology, geochemistry, and isotopic character: *American Journal of Science* v, 288-A, p. 461-489.
- Barker, F., and Arth, J.G., 1984, Preliminary results, Central Gneiss Complex of the Coast Plutonic batholith, southeastern Alaska: the roots of a high-K, calc-alkaline arc?: *Physics of the Earth and Planetary Interiors*, v. 35, p. 191-189.
- Barnes, D.F., 1972a, Simple Bouguer gravity anomaly map of Ketchikan 1:250,000 quadrangle, southeastern Alaska, showing station locations, anomaly values, and generalized 10-milligal contours: Geological Survey Open-File Map, 1 sheet.
- Barnes, D.F., 1972b, Simple Bouguer gravity anomaly map of Craig 1:250,000 quadrangle, southeastern Alaska, showing station locations, anomaly values, and generalized 10-milligal contours: Geological Survey Open-File Map, 1 sheet.
- Barnes, D.F., 1977, Interpretation of the available gravity, in Brew, D.A., Kimball, A.L., Grybeck, D., and Still, J.C., eds., *Mineral Resources of the Tracy Arm-Fords Terror wilderness study area and vicinity*: Geological Survey Open-File Report 77-649. 300 p.
- Berg, H.C., 1972, Geologic map of Annette Island, Alaska: U.S. Geological Survey Miscellaneous Geologic Investigations Map I-684, scale 1:63,000, 8 p.
- Berg, H.C., 1973, Geology of Gravina Island, Alaska: U.S. Geological Survey Bulletin 1373, 41 p.
- Berg, H.C., and Cruz, E.L., 1982, Map showing locations of fossil collections and related samples in the Ketchikan area and Prince Rupert quadrangles, southeastern Alaska: U.S. Geological Survey Open-File Report 82-1088, 1 sheet, scale 1:250,000, 27 p.
- Berg, H.C., Elliott, R.L., and Koch, R.D., 1988a, Geologic map of the Ketchikan and Prince Rupert quadrangles, Alaska: U.S. Geological Survey Miscellaneous Investigations Series, Map 1-1807, 1 sheet, scale 1:250,000.

- Berg, H.C., Jones, D.L., and Richter, D.H., 1972, Gravina-Nutzotin belt: Tectonic significance of an upper Mesozoic sedimentary and volcanic sequence in southern and southeastern Alaska: U.S. Geological Survey Professional Paper 800-D, p. D1- D24.
- Brew, D.A., and Karl, S.M., 1987, Reexamination of the contacts and other features of the Gravina belt, southeastern Alaska, *in* Galloway, J.P., and Hamilton, T.D., eds., *Geologic studies in Alaska by the U.S. Geological Survey during 1987*, U.S. Geological Survey Circular 1016, p. 143-146.
- Crawford, M.L., and Crawford, W.A., 1986, Formation of tectonic sutures, southeastern Alaska: Geological Society of America Abstracts with Programs, v. 18, p. 97.
- Crawford, M.L., Hollister, L.S., and Woodsworth, G.J., 1987, Crustal deformation and regional metamorphism across a terrane boundary, Coast Plutonic Complex, British Columbia: *Tectonics*, v. 6, p. 343-361.
- Eberlein, G.D., Churkin, M., Jr., Carter, C., Berg, H.C., and Ovenshine, A.L., 1983, Geology of the Craig quadrangle, Alaska, U.S. Geological Survey Open-File Report 83-91, scale 1:250,000, 53 p.
- Gehrels, G.E., and McClelland, W.C., 1988, Outline of the Taku terrane and Gravina belt in the Cape Fanshaw-Windham Bay region of central southeastern Alaska: Geological Society of America Abstracts with Programs, v. 20, p. 163
- Gehrels, G.E., and Saleeby, J.B., 1987, Geology of Prince of Wales Island, southeastern Alaska: Geological Society of America Bulletin: v. 98, p. 123-137.
- Gehrels, G.E., Saleeby, J.B., and Berg, H.C., 1987, Geology of Annette, Gravina, and Duke Islands, southeastern Alaska: *Canadian Journal of Earth Sciences*, v. 24, p. 866-881.
- Gehrels, G.E., McClelland, W.C., Samson, S.D., Patchett, P.J., and Jackson, J.L., 1990, Ancient continental margin assemblage in the northern Coast Mountains, southeast Alaska and northwest Canada: *Geology*, v. 18, p. 208-211.
- Harland, W.B., Cox, A.V., Lewellyn, P.G., Pickton, C.A.G., Smith, A.G., and Walters, R., 1982, *A Geologic time scale*: Cambridge, England, Cambridge University Press, Cambridge, 131 p.

- Herreid, G., Bundtzen, T.K., and Turner, D.L., 1978, Geology and geochemistry of the Craig A-2 quadrangle and vicinity, Prince of Wales Island, southeastern Alaska: Alaska Division of Geological and Geophysical Surveys Geological Report 48, 49 p.
- Holdaway, M.J., 1971, Stability of andalusite and the aluminum silicate phase diagram: *American Journal of Science*, v. 271, p. 97-131.
- Hollister, L.S., 1982, Metamorphic evidence for rapid (2mm/yr) uplift of a portion of the Central Gneiss Complex, Coast Mountains, British Columbia: *Canadian Mineralogist*, v. 20, p. 319-332.
- Irvine, T.N., 1967, The Duke Island ultramafic complex, southeastern Alaska, *in* Wyllie, P.J., ed., *Ultramafic and related rocks*, John Wiley and sons, New York, p. 84-97.
- Irvine, T.N., 1974, Petrology of the Duke Island ultramafic complex, southeastern Alaska: *Geological Society of America Memoir* 138.
- Jaffey, A.H., Flynn, K.F., Glendenin, L.E., Bentley, W.C., and Essling, A.M., 1971, Precision measurement of half-lives and specific activities of ^{235}U and ^{238}U : *Physical. Reviews C*, v. 4, p. 1889-1906.
- Johnson, M.C., and Rutherford, M.J., 1989, Experimental calibration of aluminium-in-hornblende geobarometer with application to Long Valley caldera (California) volcanic rocks: *Geology*, v. 17, p. 837-841.
- Kamb, W.B., 1959, Theory of preferred orientation developed by crystallization under stress: *Journal of Geology*, v. 67, p. 153-170.
- Krogh, T.E., 1973, A low-contamination method for hydrothermal decomposition of zircon and extraction of U and Pb for isotopic age determinations: *Geochimica Cosmochimica Acta*, v. 37, p. 485-494.
- Lanphere, M.A., and Eberlein, G.D., 1966, Potassium-argon ages of magnetite-bearing ultramafic complexes in southeastern Alaska: *Geological Society of America Special Paper* 87, p. 94.
- Lull, J.S., and Plafker, G., 1987, Geochemistry and petrography of lamprophyre dike rocks of the Coast Mountains, southeastern Alaska: *in* Galloway, J.P., and Hamilton, T.D., eds., *Geologic studies in Alaska by the U.S. Geological Survey during 1987*: U.S. Geological Survey Circular 1016, p. 169-173.

- Mattinson, J.M., 1987, U-Pb ages of zircon: a basic examination of error propagation: *Chemical Geology*, v. 66, p. 151-162.
- Monger, J.W.H., Price, R.A., and Tempelman-Kluit, J.D., 1982, Tectonic accretion and the origin of the two major metamorphic and plutonic belts in the Canadian Cordillera: *Geology*, v. 10, p. 70-75.
- Rubin, C.M., and Saleeby, J.B., 1987, The inner boundary zone of the Alexander terrane in southern SE Alaska: Part 1: Cleveland Peninsula to southern Revillagigedo Island. *Geological Society of America Abstracts with Programs*, v. 19, p. 826.
- Rubin, C.M., and Saleeby, J.B., 1988, A new perspective on what is the Taku terrane in southern SE Alaska: *Geological Society of America Abstracts with Programs*, v. 20, p. 226.
- Rubin, C.M. and Saleeby, J., 1990, Tectonic framework of the Upper Paleozoic and Lower Mesozoic Alava sequence: A revised view of the polygenetic Taku terrane in southern southeast Alaska: *Canadian Journal of Earth Science*, in review.
- Rubin, C.M., Saleeby, J.B., Cowan, D.S., Brandon, M.T., and McGroder, M.F., 1990, Late Mesozoic compressional tectonism: Development of a west-vergent thrust system in the northwestern Cordillera: *Geology*, v. 18, p. 276-280.
- Saleeby, J.B., 1987, The inner boundary zone of the Alexander terrane in southern SE Alaska: Part II southern Revillagigedo Island (RI) to Cape Fox (CF): *Geological Society of America Abstracts with Programs*, v. 19, p. 828.
- Saleeby, J.B., and Rubin, C.M., 1989, The western margin of the Coast Plutonic Complex (CPC) in southernmost SE Alaska: *Geological Society of America Abstracts with Programs*, v. 21, p. 139.
- Saleeby, J.B., and Rubin, C.M., 1990. The East Behm Canal Gneiss Complex (southern southeast Alaska) and some insights into basement tectonics along the Insular suture belt: *Geological Association of Canada Abstracts with Programs*, in press.
- Silberling, N.J., Wardlaw, B.R., and Berg, H.C., 1982, New paleontologic age determinations from the Taku terrane, Ketchikan area, southeastern Alaska, *in* Coonard, W.L. eds., *The U.S. Geological Survey in Alaska: accomplishments during 1980*: U.S. Geological Survey Circular 844, p. 117-119.

- Smith, J.G., 1973, A Tertiary lamprophyre dike province in southeastern Alaska: Canadian Journal of Earth Science, v. 10, p. 408-420.
- Smith, J.G., and Diggles, M.F., 1981, Potassium-argon determinations in the Ketchikan and Prince Rupert quadrangles, southeastern Alaska: U.S. Geological Survey Open-File Report 78-73N, p. 1-6.
- Sutter, J.F., and Crawford, M.L., 1985, Timing of metamorphism and uplift in the vicinity of Prince Rupert, British Columbia: Geological Society of America Abstracts with Programs, v. 17, p. 411.
- Taylor, H.P. Jr., 1967, The zoned ultramafic complexes of southeastern Alaska, *in* Wyllie, P.J., ed., Ultramafic and related rocks, John Wiley and sons, New York, p. 209-230.
- Terra, F., and Wasserburg, G.S., 1972, U-Th-Pb systematics in three Apollo 14 Basalts and the problems of the initial Pb in lunar rocks: Earth and Planetary Science Letters, v. 14, p. 281-304.
- Turner, F.J., 1981, Metamorphic Petrology, Second Edition, New York, 524 p.
- United States Geological Survey, 1977, Aeromagnetic map of the Ketchikan, Prince Rupert, and northeastern Craig quadrangles, Alaska: U.S. Geological Survey Open-File Report Map 77-359, scale 1:250,000, 1 sheet.
- Wheeler, J.O., and McFeely, P., 1987, Tectonic assemblage map of the Canadian Cordillera: Geological Survey of Canada Open-File Report 1565.
- York, D., 1969, Least-squares fitting of a straight line with correlated errors: Earth Planetary Science Letters, v. 5, p. 320-324.
- Zen, E-an, 1985, Implications of magmatic epidote-bearing plutons on crustal evolution in the accreted terranes of northwestern North America: Geology, v. 12, p. 266-269.
- Zen, E-an, 1988, Tectonic significance of high-pressure plutonic rocks in the westerns (sic) cordilleran of North America, *in* Ernst, W.G., ed., Metamorphism and crustal evolution of the western United States, Rubey volume vii, Prentice Hall, p. 41-68.
- Zen E-an, and Hammarstrom, J.M., 1984, Magmatic epidote and its petrologic significance: Geology, v. 12, p. 515-528.

CHAPTER 4**TECTONIC FRAMEWORK OF THE UPPER PALEOZOIC AND LOWER MESOZOIC ALAVA SEQUENCE: A REVISED VIEW OF THE POLYGENETIC TAKU TERRANE IN SOUTHERN SOUTHEAST ALASKA**

Charles M. Rubin and Jason B. Saleeby, California Institute of Technology, Pasadena, California, 91125

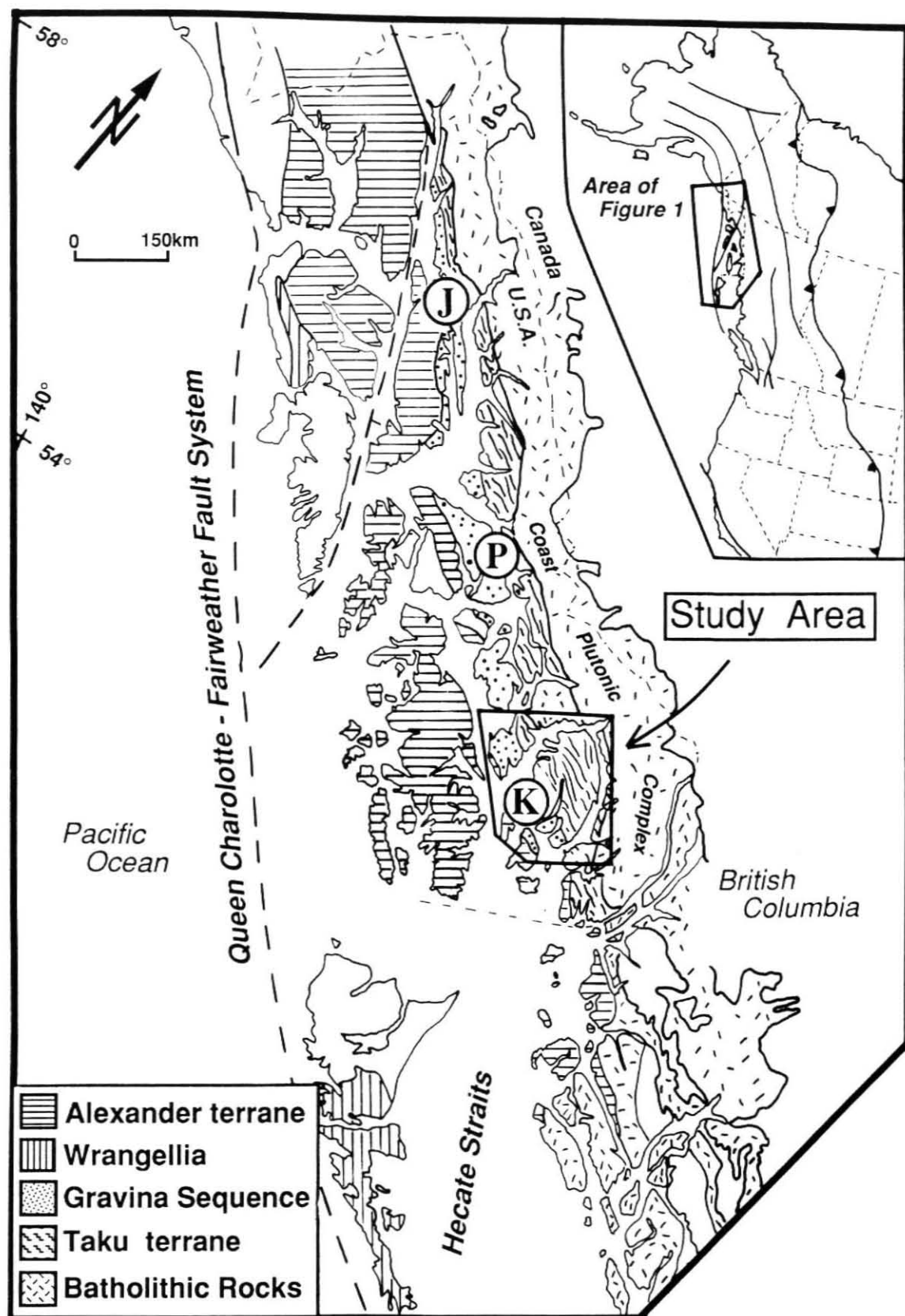
Invited paper, Canadian Journal of Earth Science

Fragments of upper Paleozoic and lower Mesozoic metavolcanic and metasedimentary sequences of the Taku terrane are recognized along a narrow belt in southeast Alaska and form a distinct lithotectonic package in the Ketchikan area. The upper Paleozoic and lower Mesozoic rocks, called the Alava sequence, consist of crinoidal and argillaceous marble, carbonaceous phyllite, argillite, mafic flows, pillow breccia, pyroclastic tuff, and quartzite. These strata are unconformably overlain by Upper Jurassic to Lower Cretaceous fine- to coarse-grained epiclastic rocks of the Gravina sequence. The Upper Paleozoic part of the Alava sequence is probably correlative with the Yukon-Tanana terrane. The Middle and Upper Triassic portion of the Alava sequence may represent a metamorphic vestige of the Stikine terrane, now exposed on the western flank of the Coast Plutonic Complex. These data suggest that the Stikine and Alexander terranes were juxtaposed prior deposition of the Upper Jurassic and Lower Cretaceous Gravina sequence. Thus, the western boundary between rocks of North American affinity and allochthonous ensimatic crustal fragments of the Alexander and Wrangellian terranes lies west of the Coast Plutonic Complex.

Introduction

The stratigraphic affinity and tectonic setting of metamorphic rocks exposed on the western flank of the Coast Plutonic Complex (Fig. 1) have been the subject of much debate. These rocks have been assigned to the Taku terrane by Monger and Berg (1987) and Berg et al. (1978) and suggest that the Taku terrane is distinct from the Alexander and Wrangellia terranes to the west and the Stikine terrane to the east. The Taku terrane consists of polydeformed and metamorphosed strata that are exposed along much of the

Figure 1: Location map of the Taku terrane in the northwestern Cordillera, showing regions and features referred to in text. K = Ketchikan, P = Petersburg, J = Juneau. Study area inset for Figure 2. Adapted from Beikman (1980); Monger and Berg (1987); Wheeler and McFeely (1987); Wheeler et al. (1988).



western flank of the Coast Plutonic Complex and comprises a belt that extends for nearly 700 km across southeastern Alaska (Monger and Berg 1987), the coastal regions of northwestern British Columbia (Berg et al. 1978), and southwest Yukon Territory (Fig. 1; Campbell and Dodds 1983). Recently, Plafker et al. (1989) correlated some Taku strata with Wrangellia, whereas Brew and Ford (1984) place parts of Taku into the Alexander terrane. Similarly, parts of Taku have been assigned to the Stikine terrane (Rubin and Saleeby 1988). The tectonic affinity of the Taku terrane thus remains unclear.

This paper presents a revised interpretation of the upper Paleozoic and lower Mesozoic portion of the Taku terrane in the Ketchikan area (Figs. 1 and 2) which indicates lithologic and age similarities with the Yukon-Tanana and Stikine terranes. Much of what has been mapped as Taku terrane in southernmost southeast Alaska consists of metamorphosed Gravina sequence and Alexander terrane (Rubin and Saleeby, 1987a, b; Saleeby 1987), which was, in part, first suggested by Brew and Ford (1984). We present new geologic and geochemical data for the upper Paleozoic and lower Mesozoic parts of the Taku terrane, which we call the Alava sequence, exposed on Cleveland Peninsula and Revillagigedo Island (Fig. 2).

Geologic Setting

The Alava sequence is part of a NW-trending belt of metamorphic and plutonic rocks that are exposed along the western margin of the Coast Plutonic Complex. The belt consists of three major assemblages that are juxtaposed along E- to NE-dipping thrust faults. These assemblages are as follows: (1) The Alexander terrane and its Upper Triassic and Upper Jurassic to Lower Cretaceous volcanic and sedimentary cover, (2) The upper Paleozoic and lower Mesozoic Alava sequence, and (3) The lower Paleozoic Kah Shakes sequence. To the west, rocks of the Upper Jurassic and Lower Cretaceous Gravina sequence depositionally overlie the Alexander terrane (Rubin and McClelland 1989; Rubin and Saleeby in review). The Upper Jurassic and Lower Cretaceous Gravina sequence forms a series of west-vergent imbricate thrust sheets and is structurally overlain by Pennsylvanian, Permian, and Triassic rocks of the Alava sequence along a NE-dipping thrust fault on Cleveland Peninsula (Fig. 2). Rocks of the Alava sequence can be traced northward into the Petersburg and Juneau areas, where they are assigned to the Taku terrane (Brew and Grybeck 1984).

Figure 2: Geologic sketch map showing distribution of geologic units, major structures, and sample locations in the Ketchikan area. AB = Alava Bay, CI = Carol Inlet, GI = George Inlet, and POW = Prince of Wales Island. Adapted from Berg (1972, 1973; parts of Annette and Gravina Islands), Gehrels and Saleeby (1987a,b; Prince of Wales Island, parts of Annette, Duke, and Gravina Islands), C.M. Rubin (unpublished mapping, 1985, 1986, 1987; Cleveland Peninsula and adjacent islands); C.M. Rubin and J.B. Saleeby (unpublished mapping, 1986, 1987, 1988; Revillagigedo and adjacent Islands). Inset shows location of Figure 3.

PALEOCENE AND YOUNGER (?) INTRUSIVE ROCKS

Tonalite, quartz diorite, & granodiorite



Pegmatite dike swarm

MIDDLE CRETACEOUS INTRUSIVE ROCKS

Tonalite, granodiorite, diorite, & gabbro



Zoned ultramafic complexes

U. JURASSIC & L. CRETACEOUS GRAVINA SEQUENCE

Metamorphosed tuff, greywacke, argillite, conglomerate, basalt-andesite tuff, breccia & pillow flows, & hypabyssal intrusive rocks

U. PALEOZOIC & L. MESOZOIC ALAVA SEQUENCE

Metamorphosed mafic pillow flows, tuff & breccia, argillite, marble, & quartzite

PALEOZOIC & L. MESOZOIC ALEXANDER TERRANE

Triassic conglomerate, siltstone, limestone, basalt, & rhyolite \ Gabbro



Devonian conglomerate, sandstone, siltstone, & marble



Ordovician-Silurian basaltic andesite tuff, breccia, pillowed flows, & hypabyssal rocks



Silurian trondhjemite & local diorite



Ordovician-Silurian tonalite, diorite, & gabbro



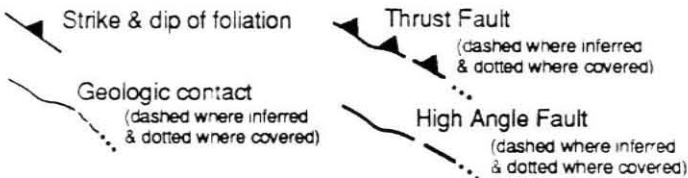
Cambrian & older (?) meta-igneous rocks

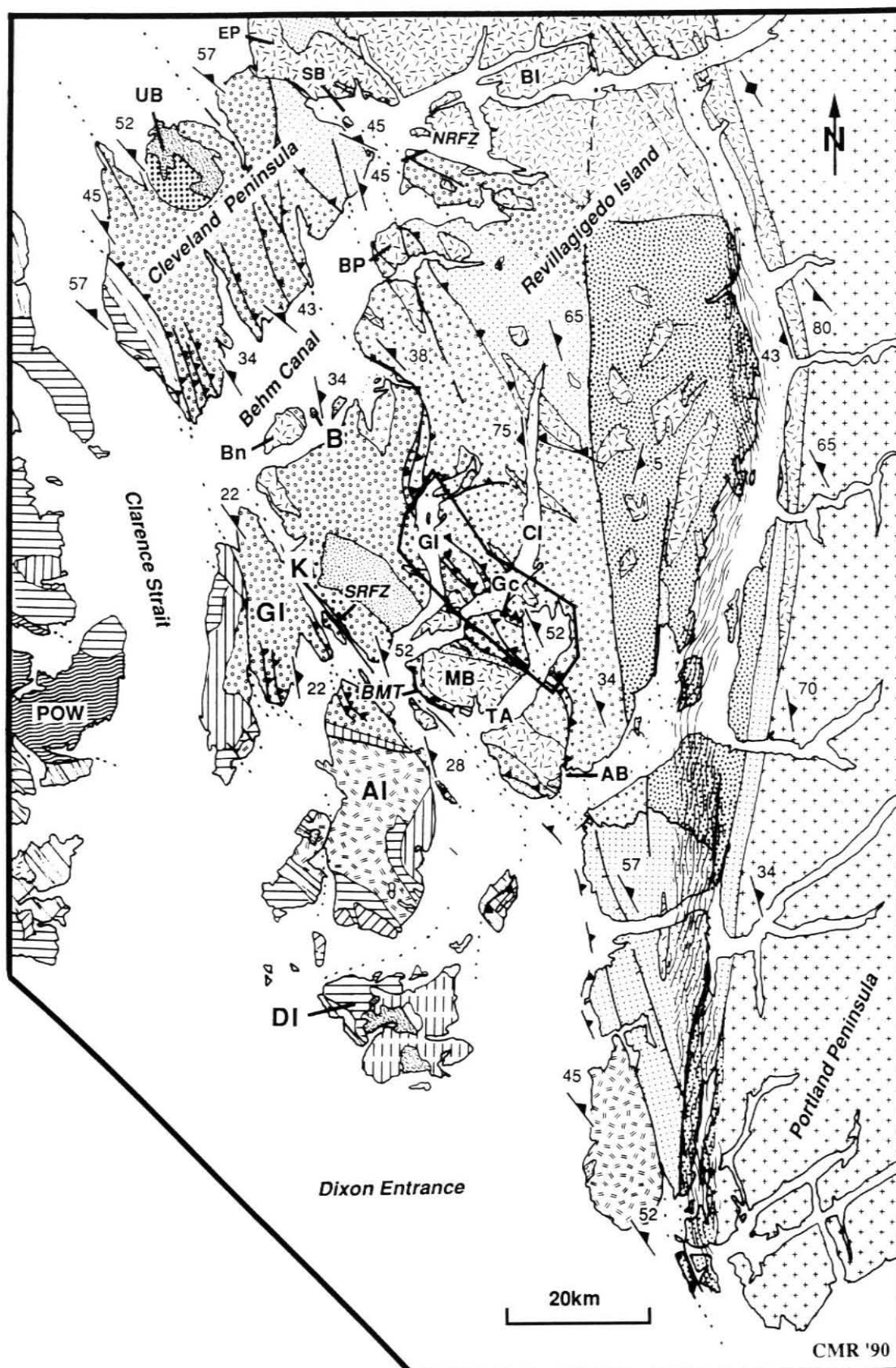
PALEOZOIC KAH SHAKES SEQUENCE

Devonian orthogneiss, lower Paleozoic quartz-bearing psammitic rocks, silicic metavolcanic rocks, amphibolite, metapelite, quartzite & marble

EAST BEHM CANAL GNEISS COMPLEX

Lower Paleozoic, tonalite gneiss, diorite gneiss, amphibolite, & psammitic gneiss





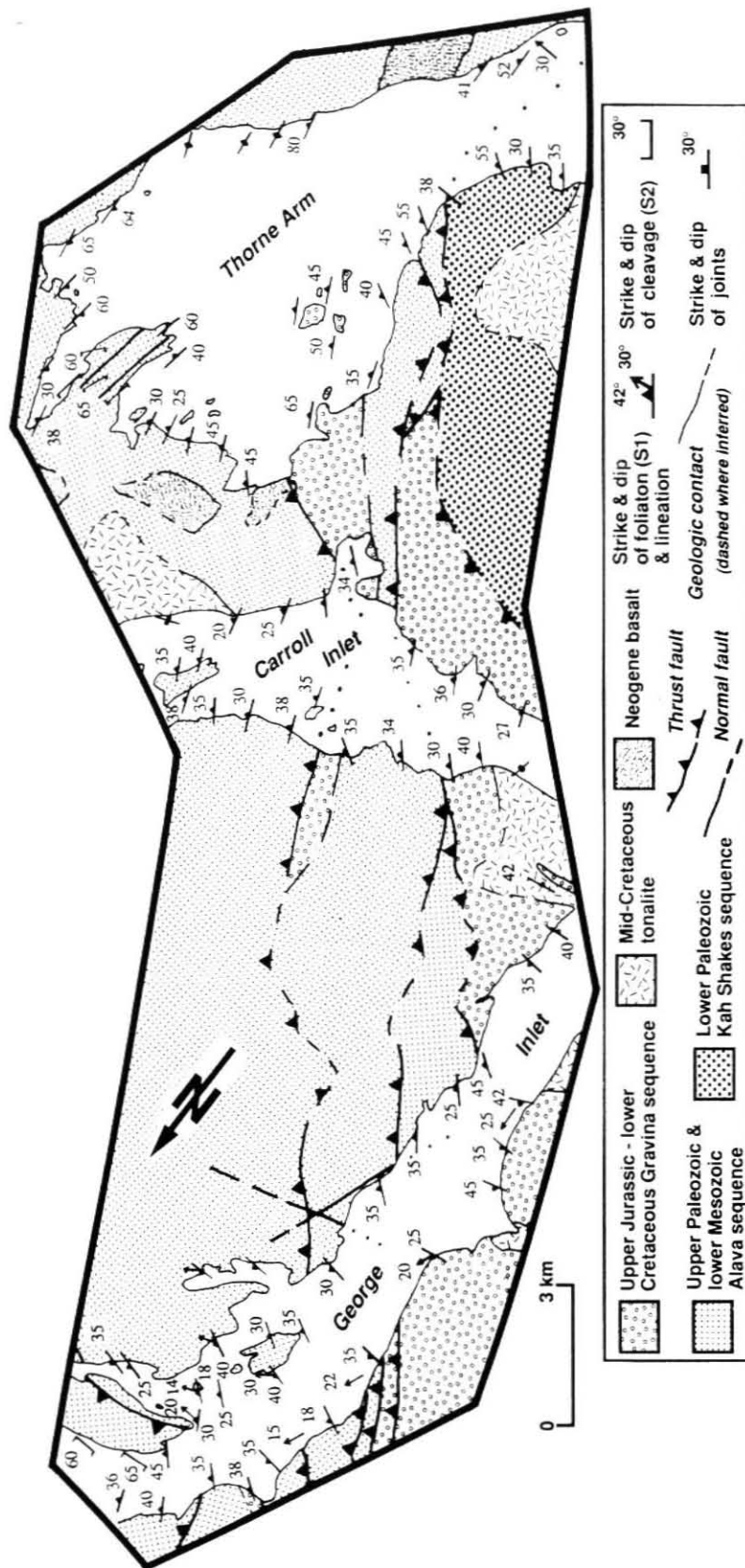
The Alava sequence on Cleveland Peninsula and west-central Revillagigedo Island, is structurally overlain along a NE-dipping thrust fault by amphibolite facies quartz-rich metasedimentary rocks, orthogneiss, metabasalt, meta-psammatic rocks, and marble. We informally call these rocks the Kah Shakes sequence, which previously constituted part of the Taku terrane. To the south on Portland Peninsula, rocks of the Kah Shakes sequence appear in lower structural levels and are overlain by Alava rocks (Saleeby and Rubin 1989). It is possible that the contact is a folded unconformity; however, the geologic relations remain unclear. These quartz-rich metasedimentary rocks are age correlative with the Yukon-Tanana terrane (Gehrels et al. 1990; Saleeby and Rubin 1989, 1990) and record deposition in a slope and continental rise setting. Primary relations between the Kah Shakes and Alava sequences are uncertain, although quartzite is interlayered with Alava marble on southeast Revillagigedo Island, suggesting early depositional relations.

These supracrustal sequences were affected by mid-Cretaceous metamorphism and thrust faulting (Rubin et al. 1990), coeval with the emplacement of tabular tonalitic plutons, sills, and dikes. Subsequently, they were strongly deformed and locally intruded by Paleocene and younger plutons of the Coast Plutonic Complex.

Alava Sequence

Stratigraphic relations presented here for the southernmost part of the Alava sequence, on Revillagigedo Island and Cleveland Peninsula, focuses on the least deformed and metamorphosed rocks of the Alava sequence. Rocks of the Alava sequence are difficult to characterize stratigraphically due to structural imbrication, greenschist to amphibolite facies metamorphism, and sparse age control. The sequence is distinguished by key stratigraphic units that include upper Paleozoic metasedimentary and metavolcanic rocks, and Middle Triassic metasedimentary rocks that are exposed on the eastern shore of George Inlet on southwestern Revillagigedo Island (Figs. 2 and 3). These key stratigraphic units are correlated by distinctive lithologies throughout the Ketchikan area.

Figure 3: Geologic sketch map of central Revillagigedo Island from C.M. Rubin (unpublished mapping) and Berg et al. (1988). Location of map shown in Figure 2.



*Stratigraphy**Unit 1: Upper Paleozoic metasedimentary and metavolcanic rocks*

The upper Paleozoic portion of the Alava sequence is characterized by metamorphosed pillow basalt, mafic tuff, and crinoidal marble. These strata show penetrative foliation, ductile folding, and middle greenschist to amphibolite facies metamorphic mineral assemblages. The unit extends from the south on Revillagigedo Island to Cleveland Peninsula in the north (Fig. 2). The lower contact of the unit is not exposed and at most localities the base of the Alava sequence is in fault contact with the Alexander terrane or Gravina sequence. The top of the unit is designated at the base of the overlying, slightly metamorphosed Triassic carbonaceous phyllite, argillaceous limestone, and basalt. The upper Paleozoic portion of the Alava sequence is divided into four groups, but their stratigraphic sequence is obscured by younger deformation: (1) lavas and argillite, (2) water-laid breccia and tuff, (3) interlayered marble and quartzite, (4) crinoidal marble. Upper Paleozoic rocks of the Alava sequence are easily distinguished from discontinuous basalt-limestone sequences in the Alexander terrane by thick, laterally continuous crinoidal marble horizons interlayered with pillow basalt.

Metamorphosed mafic flows and crinoidal marble dominate unit 1. Typically, the mafic flows are pillowed, and are interlayered with black argillite which occur in units generally less than 10 m in structural thickness. The lavas are locally massive and aphyric. The fine-grained mafic breccia contains generally monolithologic clasts as coarse as 20 cm that are angular to sub-angular in shape, and have the same composition as the matrix. Thickness varies from 2 to 10 meters. Bedding is characteristically massive; however, tectonic deformation may obscure original bedding features. Metabasalt consists of fine-grained hornblende, actinolite, albite, chlorite, epidote-clinozoisite, white mica, and minor quartz. Mafic lavas and marble can be traced southeastward into Alava bay (Fig. 2), where crinoidal marble is interlayered with centimetre-scale layers of metaquartzite.

Marble is massive to finely laminated and is commonly interbedded with metabasalt and argillite (Fig. 4 and 5); it weathers light-brown, pale-blue, and light-grey (Fig. 5) and contains crinoid columnals up to 1 cm in diameter. Locally, crinoid stems up to 2.5 cm long are preserved. Late Early

Figure 4: Schematic structural-stratigraphic section of the Alava sequence in George Inlet.

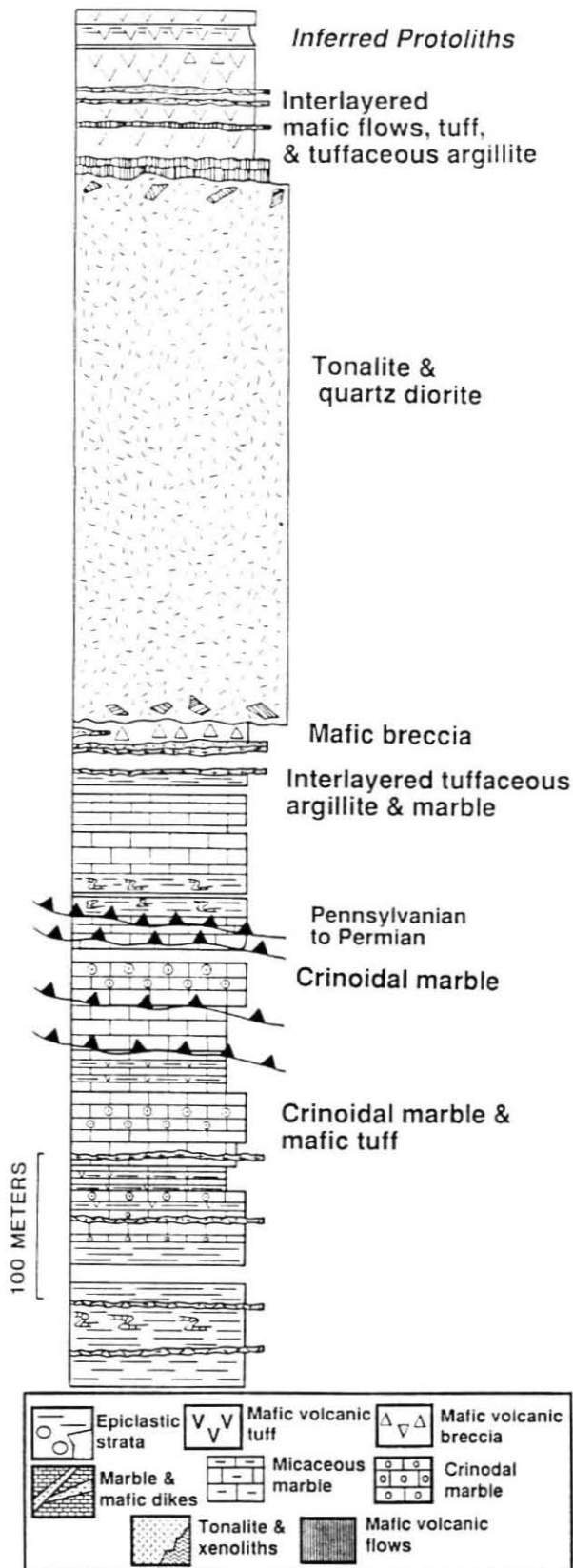


Figure 5: Early Late Permian crinoidal marble of the Alava sequence on Carol Inlet, Revillagigedo Island.



Pennsylvanian to late Permian conodonts and late Early Permian brachiopods have been reported from this unit (Berg and Cruz 1982; Silberling et al. 1982).

Unit 2: Lower Mesozoic metasedimentary and metavolcanic rocks

The lower Mesozoic portion of the Alava sequence is characterized by carbonaceous phyllite, fine-grained argillaceous limestone, metabasalt, and mafic breccia, and tuff. This unit has been identified only on central Revillagigedo Island where it has been affected by non-penetrative foliation, pressure solution, and greenschist facies metamorphism. The lower contact of the unit is not exposed. Based on the lower degree of deformation and metamorphism, and stratigraphic continuity in the Triassic rocks, it is inferred to rest unconformably on the upper Paleozoic part of the Alava sequence. The top of the unit is generally not exposed and is structurally imbricated with older portions of the Alava sequence. On the western shore of Carol Inlet, however, Upper Jurassic to Lower Cretaceous coarse-grained epiclastic rocks of the Gravina sequence appear to unconformably overlie the Alava sequence (Fig 6). Lithologies in the lower Mesozoic portion of the Alava sequence are divided into two groups: (1) mafic lavas, breccia, and tuff, (2) argillaceous and siliceous limestone and black phyllite. Lower Mesozoic rocks of the Alava sequence are distinguished from similar lithologies in the older portions of the Alava sequence by the presence carbonaceous and siliceous limestone. The mafic flows are pillowed or locally massive and aphyric. Lithic fragments within the pyroclastic deposits consist of marble, phyllite, and felsic (?) metavolcanic angular to sub-angular clasts in an aphyric tuffaceous matrix. The proportion of matrix is generally 50% and clast-supported fabrics are not observed.

Carbonaceous and argillaceous limestone dominate unit 2. Typically, fragments of halobiid bivalves (*Daonella*) are preserved in black siliceous concretions in a fissile, foliated limestone (Silberling et al. 1982). The concretions are typically 3 cm in diameter, but locally are up to 6 cm in diameter. Crinoidal limestone, containing well-preserved *Pentacrinites* (Fig. 7), phyllite, and pyritic slate also occur in unit 2. Late Middle Triassic conodonts, halobiid bivalves, and ammonites have been reported for unit 2 (Berg and Cruz 1982; Silberling et al. 1982).

Figure 6: Schematic structural-stratigraphic section showing geologic relations between the Upper Jurassic to Early Cretaceous Gravina sequence and the Alava sequence on Carol Inlet, Revillagigedo Island.

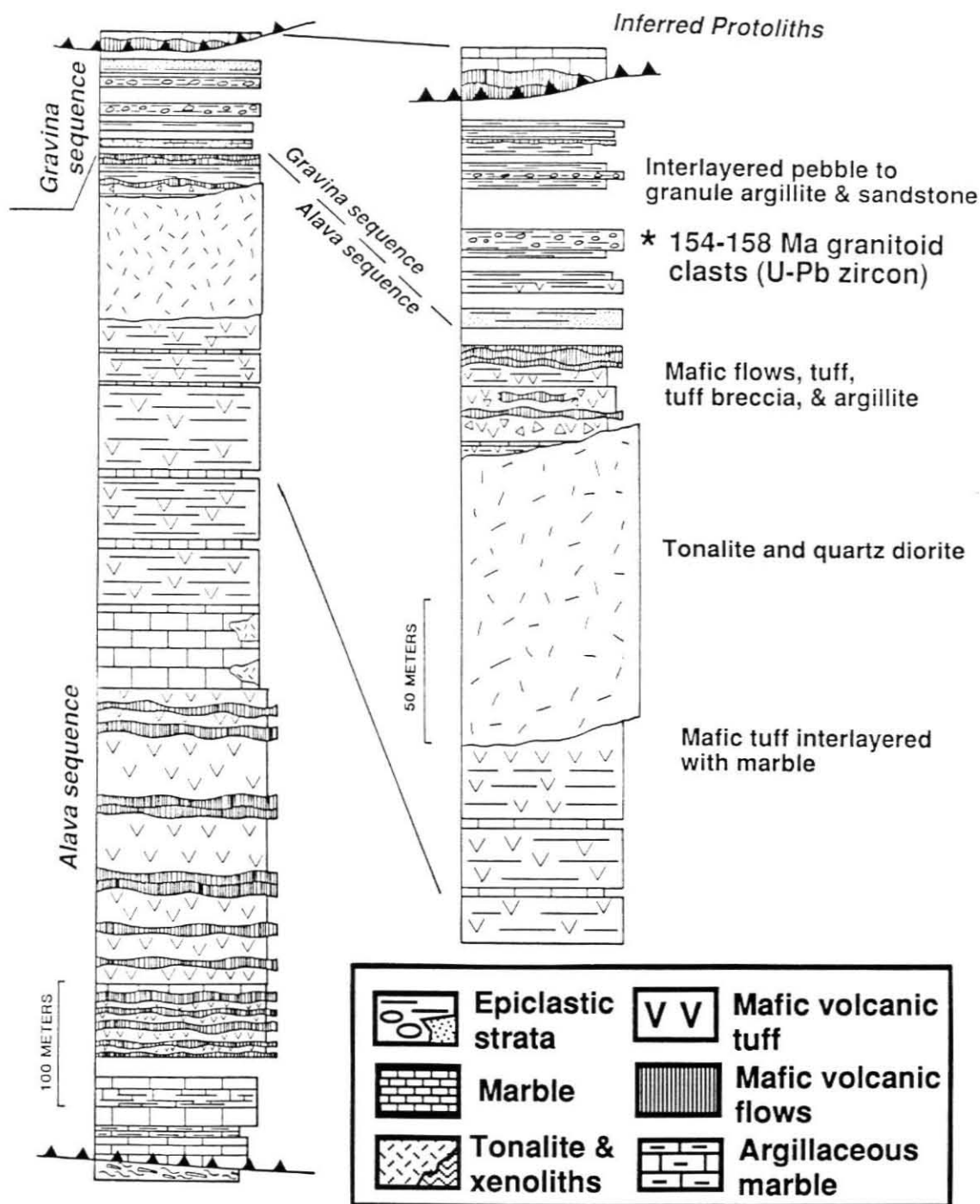
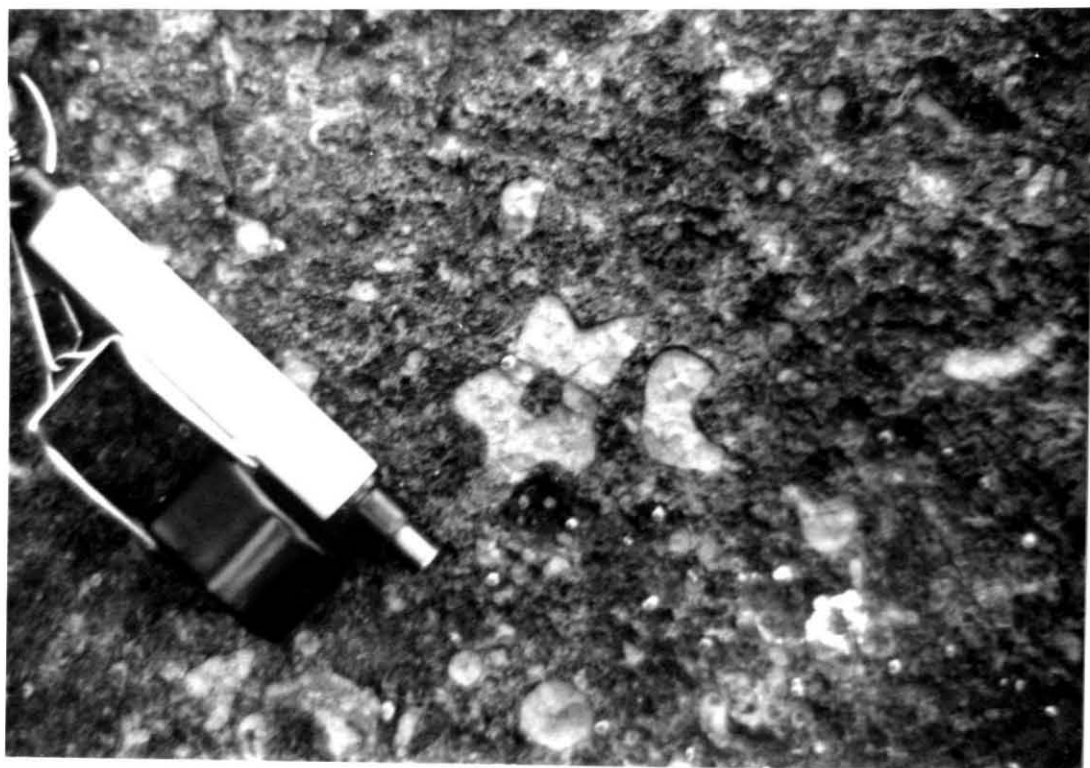


Figure 7: Late Middle Triassic crinoidal limestone containing well-preserved *Pentacrinites* on George Inlet, Revillagigedo Island.



Depositional Setting

Although the upper Paleozoic and lower Mesozoic metasedimentary and metavolcanic sequences are highly deformed and lack adequate age control, the dominance of pillowed lava and marble indicates deposition in a submarine environment. On George and Carol Inlet, the Upper Paleozoic part of the Alava sequence contains large volumes of mafic lava flows which are pillowed and largely unbroken, which might have formed in a proximal position to an inferred vent on the seafloor. Whereas on the northern end of Thorne Arm pillow lavas are interstratified with mafic pillow breccia and tuff, which suggests that a fissure might have extended along the volcanic apron. Preliminary trace element geochemistry suggest that the lavas are transitional between volcanic arc tholeiite and MORB (see geochemistry below). The metavolcanic rocks interfinger with crinoidal marble indicating moderately shallow water deposition punctuated by mafic volcanism. Well-preserved crinoid columns in marble imply a relatively low-energy environment. Metabasalt and marble laterally grade into interlayered quartzite, marble, and metabasalt, suggesting an adjacent mature source terrane.

Because rocks of the Alava sequence contain an incomplete and fragmentary record, the late Paleozoic and early Mesozoic volcanic evolution and depositional histories can only be inferred. Trace-element geochemistry is only an approximate guide to the petrotectonic setting of tholeiitic basalts. Thus, the discrimination between back-arc-basin basalt, MORB, and forearc eruptions is difficult. Based on geologic relations, limited trace element geochemistry, and regional considerations, Paleozoic rocks of the Alava sequence might have been deposited adjacent to a rifted arc or within a back arc basin. The quartzite horizons represent episodic influx of continent-derived detritus, perhaps from the adjacent Kah Shakes sequence. Mafic volcanism and carbonate deposition recorded by Middle and Upper Triassic strata of the Alava sequence occurred in a shallow marine setting. Well-preserved ammonites and bivalves in argillaceous limestone carbonaceous phyllite imply a relatively low-energy, organic-rich environment adjacent to a land-mass.

Magmatic affinities of metabasalts

Trace element geochemistry from Alava sequence metabasalts shed light on their petrotextonic setting. For mafic volcanic rocks that have undergone low grade metamorphism, a useful method to classify and discriminate magmas erupted in different tectonic settings is to examine the concentration of trace elements such as Ti, Zr, Y, Cr, and V (Table 1; Pearce 1980, 1982; Pearce and Cann 1973). The criteria used to distinguish tectonic affinities of magmas are derived from empirically determined values from a variety of modern plate tectonic settings (Pearce 1982; Pearce and Norry 1979). High field strength elements that are relatively immobile during seafloor alteration and greenschist facies metamorphism are used (Cann 1970; Humphris and Thompson 1978).

Based on trace element patterns, most Alava sequence lavas are typical of mid-ocean-ridge basalts (MORB), some typical of modern island arc tholeiites, and some typical of within-plate basalts (Fig. 8; Pearce 1982). On a Cr/Y plot, the data plot either in the high-Y part of the arc tholeiite field or in the high-Y part of the MORB field; however, two samples fall into the within-plate field (Fig. 8A). The metabasalts might best be described as transitional between the IAT and MORB field. Cr abundances are generally high, which is characteristic of MORB. Ti/Zr ratios are high and plot within the MORB field (Fig. 6B; Pearce and Cann 1973). Metabasalts have Ti/Zr ratios in the range of MORB and IAT; however, a few samples fall out the the expected fields (Fig. 8C).

In summary, trace-element abundances for Cr, Zr, Ti, Y, and V, combined with significant amounts of mafic metavolcanic rocks and interbedded marble indicate that the Alava sequence metavolcanic rocks may represent a rifted arc tholeiite sequence. These geochemical variations are similar to immature rifted arcs of the western Pacific (Gill 1981). Mafic rocks from the MORB tholeiite suite are distinguished by high Ti/V ratios and high abundances of Ti, Cr, Zr, and Ni (e.g., Basaltic Volcanism Study Project 1981; Gill 1981), which also characterize the Alava sequence metavolcanics.

Regional correlations

Regionally-significant components of the Alava sequence in the Ketchikan area include: (1) Pennsylvanian to Permian crinoidal marble intercalated with pelitic phyllite, (2) Permian metabasaltic

Table 1. Analyses of metabasalts from the Alava sequence (ppm)

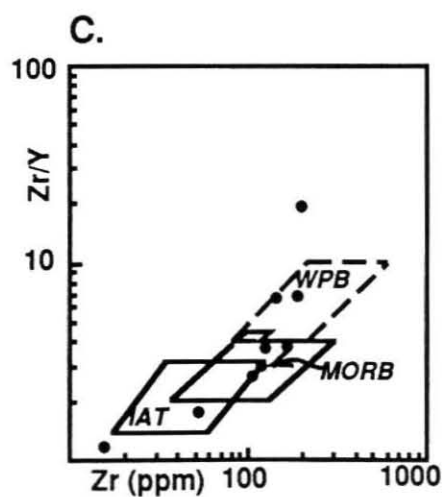
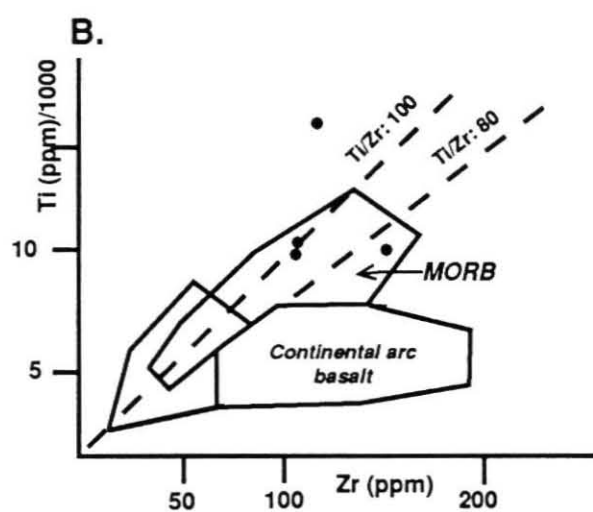
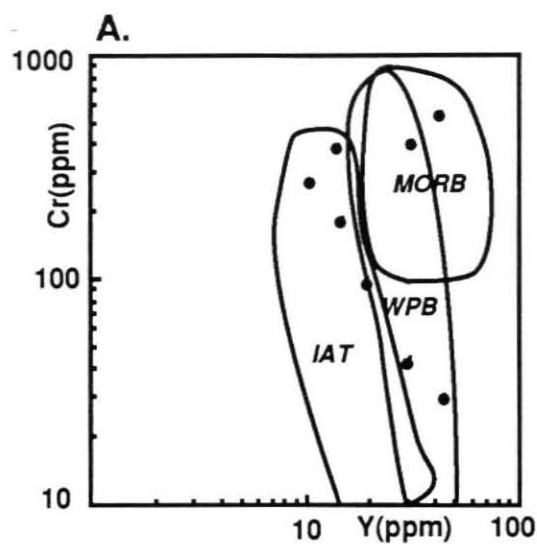
	Ti	V	Ni	Cr	Zr	Y	Sr	"Rb
84JR32*	22644	150	63	185	128	15	237	N/A
87CR62*	38343	337	111	100	178	21	45	N/A
86CR202*	41130	498	58	551	133	42	1298	N/A
87CR41*	39030	206	5308	271	211	11	1010	N/A
84JR37*	33460	397	8909	414	165	31	35	N/A
86CR206*	65700	407	501	-	67	42	31	N/A
87CR41°	9353	N/A	116	"392	16	14	1000	37
87CR57°	10731	N/A	15	"30	120	44	148	2
87CR63°	10311	N/A	17	"44	123	30	445	11

* Trace elements analyzed by ICAP at University of California, Riverside.

° Trace elements were analyzed by EDXRF at the U. S. Geological Survey, Denver, Colorado.

" Rb analyzed by XRF at the U.S. Geological Survey, Denver, Colorado.

Figure 8: Trace element discrimination diagrams showing data from fresh pillowed metabasalts of the Alava sequence. MORB = mid-ocean-ridge basalt field. WPB = within-plate basalt field. IAT = island-arc tholeiite field. (A) Cr-Y discrimination diagram of Pearce (1982). (B) Ti-Zr discrimination diagram of Pearce and Cann (1973). (C) ZR/Y-Zr discrimination diagram of Pearce (1980).

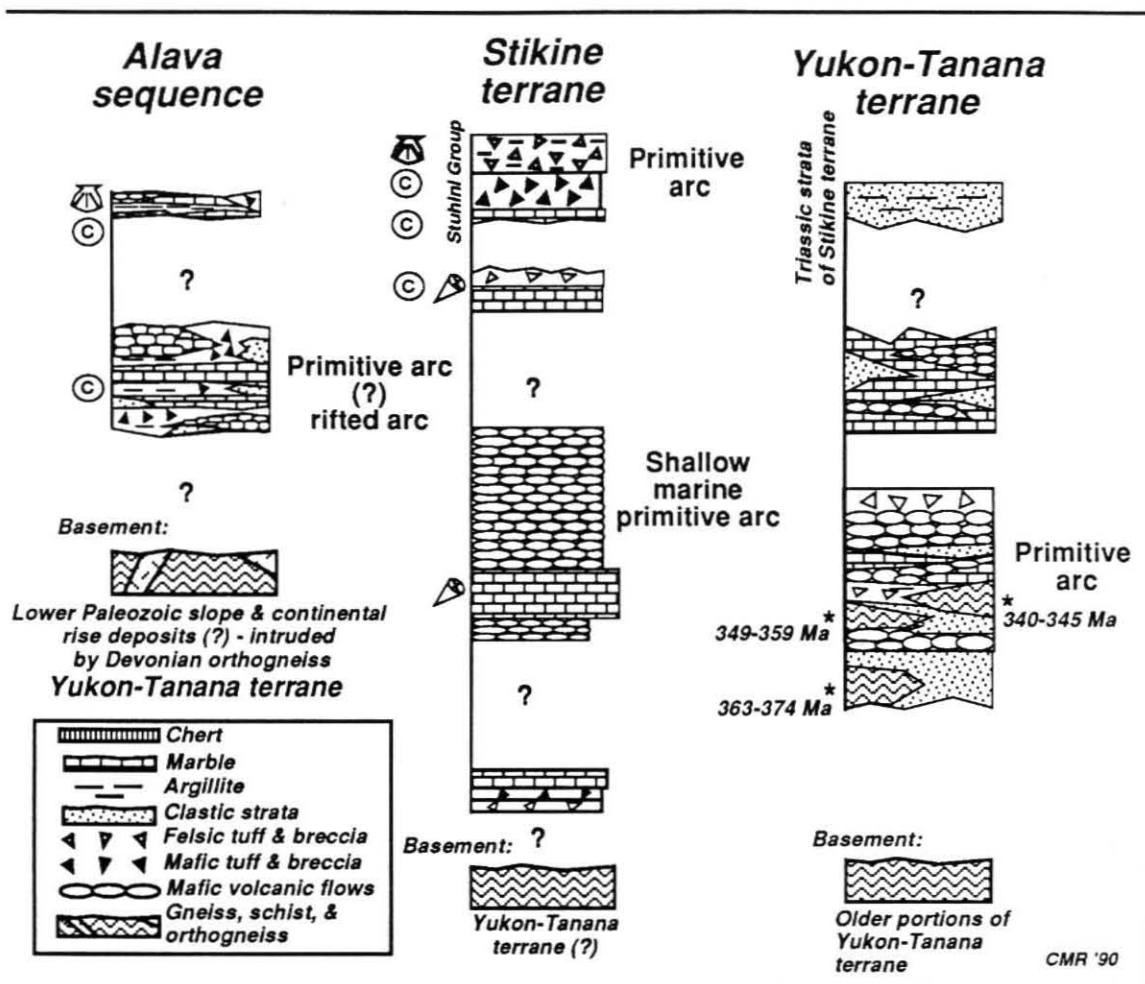


pillow flows, tuff, and breccia, (3) Permian massive metabasalt flows, crinoidal marble, and interlayered quartzite, and (4) Upper Middle Triassic carbonaceous limestone, phyllite, basalt, and basaltic breccia. In addition, differences in the intensity of deformation and metamorphic grade between the Upper Paleozoic and lower Mesozoic parts of the Alava sequence suggest that significant deformation and associated metamorphism occurred prior to the deposition of lower Mesozoic strata of the Alava sequence. The inferred unconformity between the two Alava components has been obscured as the result of mid-Cretaceous and younger deformation and metamorphism.

There are four regionally extensive terranes in the northwest Cordillera that have rocks of the same age, Wrangellia, the Alexander, Stikine, and Yukon-Tanana terranes. Salient lithologic and age constraints are shown in Figure 9. To the west lies the Alexander terrane and Wrangellia (Fig. 1). Wrangellia consists of a lower to mid-Paleozoic island arc assemblage overlain by a remarkably uniform sequence of Upper Triassic submarine to subaerial tholeiitic basalt that was deposited in a rift setting adjacent to an active arc (Barker et al. 1989; Monger and Berg 1987). The Alexander terrane contains a relatively complete lower Paleozoic ensimatic arc sequence overlain by middle Paleozoic clastic and carbonate strata and a Upper Triassic rift-related assemblage (Gehrels and Saleeby, 1987a). Sm-Nd studies show that the Alexander terrane is composed of Phanerozoic, juvenile crust (Samson et al. 1989). The Alexander terrane and Wrangellia were contiguous during the Middle Pennsylvanian (Gardner et al. 1988). To the east, lies the Stikine and Yukon-Tanana terranes. The Yukon-Tanana terrane consists predominantly of a mid- to late Paleozoic arc assemblage built on continental crust (Aleinikoff et al. 1981, 1986; Mortensen and Jilson 1985). The westernmost part of the Stikine terrane consists of an upper Paleozoic primitive volcanic arc, platformal carbonate, and basinal strata (Monger 1977) and an Upper Triassic primitive volcanic arc, shallow water carbonate, and clastic strata, called the Stuhini Group (Anderson 1989; Monger 1980).

The Pennsylvanian and Permian components of the Alava sequence share some general lithologic features with the Yukon-Tanana terrane, whereas the lower Mesozoic portion shares some general lithologic and depositional features of the Mesozoic parts of both the Stikine terrane and Wrangellia (Fig. 9). It is apparent that additional biostratigraphic and igneous age control is necessary for a unique

Figure 9: Correlation chart for mid-Paleozoic and lower Mesozoic volcanic and basinal assemblages in the Pacific northwest Cordillera. References used in constructing this chart include Anderson (1989), Berg and Cruz (1982), Gehrels and Saleeby (1987), Lowe et al. (1982), Monger (1977), Mortensen and Jilson (1985), Richter (1976), Richter and Dutro (1975), Silberling et al. (1982), Weber et al. (1978), and Werner (1977, 1978).



correlation with adjacent terranes. Nevertheless, first-order stratigraphic similarities exist between the Alava sequence and the Yukon-Tanana and Stikine terranes. In general, the Pennsylvanian and Permian volcanic-sedimentary strata of Alava and Yukon-Tanana share many common elements. Upper Paleozoic metabasalt, marble, and important occurrences of quartzite characterize these two sequences. Pennsylvanian to Permian fossiliferous marble, interlayered mafic metavolcanic rocks, quartzite of the Alava sequence can be reasonably correlated with Upper Paleozoic elements of the Yukon-Tanana terrane exposed to the north in the Yukon Territory (Fig. 9; Monger and Berg 1987; Mortensen and Jilson 1985). Quartz-rich sediments are abundant throughout the Yukon-Tanana terrane (Dusel-Bacon and Aleinikoff 1985; Mortensen and Jilson 1985; Tempelman-Kluit 1979). Upper Carboniferous and Lower Permian limestone deposits in the Sicker Group of Wrangellia lack interstratified mafic lavas and pelitic phyllite, and the characteristic quartzite (Fig. 1; Brandon et al. 1986; Muller 1980); therefore, they are not equivalent. Laterally-continuous upper Paleozoic marble horizons in the Alava sequence are not present in the adjacent Alexander terrane (Gehrels and Saleeby 1987). Furthermore, quartz-rich sedimentary rocks have not been identified in either Wrangellia (Jones et al. 1977; Muller 1980) or the Alexander terrane (Gehrels and Saleeby 1987).

The Ladinian to Carnian part of the Alava sequence is poorly preserved, making correlations tentative. Halobia-bearing carbonaceous limestone, phyllite, and metabasalt are common constituents of Upper Triassic Stuhini Group of the Stikine terrane (Anderson 1989; Grove 1986; Monger 1980). In detail, however, there are many stratigraphic differences between the Alava sequence and the Stuhini Group. The late Middle Triassic strata of the Alava sequence might represent a lateral facies of the Stuhini Group. In addition, the inferred unconformity between the late Middle Triassic strata and the underlying late Paleozoic rocks of the Alava sequence is similar to geologic relations seen in the Triassic of the Stikine terrane. There, an unconformity is recognized between the Triassic portion of Stikine and the underlying Yukon-Tanana terrane (Mortensen and Jilson 1985; Werner 1977, 1978).

Alternatively, these strata could be correlative with the Middle to Upper Triassic strata of Wrangellia. Ladinian strata of Wrangellia on the Queen Charlotte Islands include siliceous and calcareous shale, Daonella-bearing shale and abundant basaltic sills which overlie Pennsylvanian and Lower Permian limestone (Brandon et al. 1986; Carlisle and Suzuki 1974). Similarly, to the north in the eastern Alaska

Range, Upper Triassic Wrangellian strata are comparable to the Upper Triassic argillaceous limestone of the Alava sequence, except that they lack basaltic sills (Lowe et al. 1982; Richter 1976; Richter and Dutro 1975). Because the Triassic strata of the Alava sequence rest on rocks of continental derivation (i.e., Yukon-Tanana terrane), their correlation with the Triassic of Wrangellia is considered unlikely.

In summary, lithologic similarities between the late Paleozoic portion of the Alava sequence and the Yukon-Tanana terrane, and the presence of an inferred pre-Middle Triassic unconformity in both strata of the Alava sequence and in the Yukon-Tanana and Stikine terranes suggest shared stratigraphic history throughout late Paleozoic and early Mesozoic time.

Regional Tectonic Implications

The interpretation that correlative rocks of the Yukon-Tanana and Stikine terranes occur on the western flank of the Coast Plutonic Complex has fundamental implications for the accretionary evolution and Mesozoic crustal structure of the northwestern Cordillera. Strike-slip deformation accounts for at least 350 km of northwards translation of these terranes with respect to North America (Price and Carmichael 1986), thus their current tectonic setting with respect to the Cordilleran continental margin may be the result of late Mesozoic and early Cenozoic tectonism. Based on palinspastic restoration of late Mesozoic and early Tertiary deformation, the paleo-continental margin of North America, which consisted of attenuated continental crust, must have extended farther to the west by at least 200 km (Brown et al. 1986). Presumably, oceanic crust that was overlain by continent-derived slope and rise deposits was situated outboard of the attenuated North American continental crust. These continent-derived slope and rise deposits are probably represented by the quartz-rich metasediments, marble, and pelitic strata of the Yukon-Tanana terrane (Gehrels et al. 1990; Rubin et al. in press). The recognition of Paleozoic continent-derived slope and rise deposits on the western flank of the Coast Plutonic Complex suggests that remnants of paleo-continental margin extended further to the west than previously thought. This interpretation implies that the presence of Paleozoic oceanic lithosphere overlain by continent-derived slope and rise deposits might, in part, form basement to the Coast Plutonic Complex and extend along its western flank. In addition, the western metamorphic belt of the Coast Plutonic Complex marks a fundamental boundary between North

American continental crust and its Late Paleozoic fringing arc system, and ensimatic, juvenile crust of the Insular superterrane. This boundary coincides with a regionally extensive mid-Cretaceous thrust belt (Rubin et al. 1990). Geologic ties between the Alava and Gravina sequences suggest that mid-Cretaceous deformation overprints the boundary and is not related to the collision of the westward Insular superterrane with North America.

The recognition that the Upper Jurassic and Lower Cretaceous Gravina sequence overlies both the Alexander terrane and Alava sequence raises important questions about the timing of accretion of the Insular superterrane to North America, which is thought to have taken place in the mid-Cretaceous (Monger et al. 1982). The juxtaposition of the Alexander, Stikine, and Yukon-Tanana terranes prior to the deposition of the Gravina sequence requires a pre-Late Jurassic tie between the Alexander terrane and the western margin of the Stikine terrane. This interpretation is supported by the Early to Middle Jurassic deformation documented by McClelland and Gehrels (in press) which may record the initial juxtaposition of the Alexander terrane with the western margin of the Stikine terrane.

In summary, the upper Paleozoic portion of the Alava sequence represents the westernmost extent of the Yukon-Tanana terrane, which is interpreted as a continental margin assemblage of slope and rise deposits and dismembered fragments of a mid- to late Paleozoic arc system. The lower Mesozoic part of the Alava sequence has lithologic similarities to both Wrangellia and the Stikine terrane. Based on regional considerations, however, the Triassic portion of Alava sequence is tentatively correlated with the lower Mesozoic part of the Stikine terrane. Upper Jurassic and Lower Cretaceous volcanic and basinal sedimentary rocks of the Gravina sequence unconformably overlie both the Alava sequence and Alexander terrane, forming a pre-Late Jurassic overlap between the Insular and Intermontane superterranes. In addition, the western boundary between rocks of North American affinity and allochthonous ensimatic crustal fragments is west of the Coast Plutonic Complex and is presently exposed along a series of west-vergent thrust faults in southeast Alaska. In this view, the collision of Insular superterrane and the concurrent closure of a late Mesozoic oceanic basin is not required to explain the stratigraphic, structural, and metamorphic relations seen in southeast Alaska and western British Columbia. Mid-Cretaceous

deformation and magmatism seen throughout the northwestern Cordillera can now be re-evaluated in light of the new data presented here.

Acknowledgements

Field and laboratory work for southeast Alaska regional studies has been supported by the U.S. National Science Foundation Grants EAR 86-05386 and EAR 88-03834 (to JBS). Additional support (to CMR) was provided by Geological Society of America Penrose Grants, a Sigma-Xi grant-in-aid, and by the U.S. Geological Survey, Alaska Branch. We thank Fred Barker (U.S.G.S.) and David Marrett (University of California, Riverside) for geochemical analyses. We thank George Gehrels, Bill McClelland, Meghan Miller, and Margi Rusmore for helpful discussions on Alaskan geology.

ALEINIKOFF, J.N., DUSEL-BACON, C., FOSTER, H.L., and FUTA, K. 1981. Proterozoic zircon from augen gneiss, Yukon-Tanana upland, east-central Alaska. *Geology*, **9**: 649-473.

ALEINIKOFF, J.N., DUSEL-BACON, C., and FOSTER, H.L. 1986. Geochronology of augen gneiss and related rocks, Yukon-Tanana terrane, east-central Alaska. *Geological Society of American Bulletin*, **97**: 626-637.

ANDERSON, R.G. 1989. A stratigraphic, plutonic, and structural framework for the Iskut River map area, northwestern British Columbia, *In* Current research, Part E: Geological Survey of Canada, Paper 89-1E, p. 145-154.

BARKER, F., SUTHERLAND-BROWN, A., BUDAHN, J.R., AND PLAFKER, G. 1989. Back-arc with frontal-arc component origin of Triassic Karmutsen basalt, British Columbia, Canada. *Chemical Geology*, **75**: 81-102.

BASALTIC VOLCANISM STUDY PROJECT. 1981. Basaltic volcanism on the terrestrial planets. Pergamon Press, New York, United States.

BEIKMAN, H.M. 1980. Geologic map of Alaska: U.S. Geological Survey Special Map, scale 1: 2,500,000, 2 sheets.

- BERG, H.C. 1972. Geologic map of Annette Island, Alaska. U.S. Geological Survey Miscellaneous Geologic Investigations Map I-684, scale 1:63,000, 8 p.
- 1973, Geology of Gravina Island, Alaska. U.S. Geological Survey Bulletin 1373, 41p.
- BERG, H.C., and CRUZ, E.L. 1982. Map showing locations of fossil collections and related samples in the Ketchikan area and Prince Rupert quadrangles, southeastern Alaska. U.S. Geological Survey Open-File Report 82-1088, scale 1:250,000, 27p.
- BERG, H.C., JONES, D.L., and CONEY, P.J. 1978. Pre-Cenozoic tectonostratigraphic terranes of southeastern Alaska and adjacent area. U.S. Geological Survey Open-File Report 78-1085.
- BERG, H.C., ELLIOTT, R.L., and KOCH, R.D. 1988. Geologic map of the Ketchikan and Prince Rupert quadrangles, Alaska. U.S. Geological Survey Miscellaneous Investigations Series, Map 1-1807, scale 1:250,000.
- BRANDON, M.T., COWAN, D.S., and VANCE, J.A. 1988. The Late Cretaceous San Juan thrust system, San Juan Islands, Washington. Geological Society of America Special Paper 221, 81 p.
- BREW, D. A., and FORD, A.B. 1984. Tectonostratigraphic terranes in the Coast plutonic-metamorphic complex, southeastern Alaska. In The U.S. Geological Survey in Alaska: accomplishments during 1982. Edited by K.L. Reed, and S. Bartsch-Winkler. U.S. Geological Survey Circular 939, pp. 90-93.
- BROWN, R.L., JOURNEAY, J.M., LANE, L.S., MURPHY, D.C., and JONES, C.J. 1986. Obduction, backfolding and piggyback thrusting in the metamorphic hinterland of the southeastern Canadian Cordillera. *Journal of Structural Geology*, 8: 255-268.
- CAMPBELL, R.B., and DODDS, C.J. 1983. Tatshenshini River map area (114P). Geological Survey of Canada, Open-file 926.
- CANN, J.R. 1970. Rb, Sr, Y, Zr, and Nb in some ocean floor basaltic rocks. *Earth and Planetary Sciences Letters*, 19: 7-11.
- CARLISLE, D., and SUZUKI, T. 1974. Emergent basalt and submarine carbonate clastic sequences including the Upper Triassic *Dilleri* and *Welleri* zones on Vancouver Island. *Canadian Journal of Earth Science*, 11: 245-289.

- DUSEL-BACON., and ALEINIKOFF, J.N. 1985. Petrology and tectonic significance of augen gneiss from a belt of Mississippian granitoids in the Yukon-Tanana terrane, east-central Alaska. *Geological Society of America Bulletin*, **96**: 411-425.
- GARDNER, M.C., BERGMAN, S.C., CUSHING, G.W., MACKEVETT, E.M. JR., PLAFKER, G., CAMPBELL, R.B., DODDS, C.J., MCCLELLAND, W.C., and MUELLER, P.A. 1988. Pennsylvanian pluton stitching of Wrangellia and the Alexander terrane, Wrangell Mountains, Alaska. *Geology*, **16**: 967-971.
- GEHRELS, G.E., and SALEEBY, J.B. 1987a. Geology of Prince of Wales Island, southeastern Alaska. *Geological Society of America Bulletin*, **98**: 123-137.
- 1987b. Geology of Annette, Gravina, and Duke Islands, southeastern Alaska. *Canadian Journal of Earth Sciences*, **24**: 866-881.
- GEHRELS, G.E., MCCLELLAND, W.C., SAMSON, S.D., PATCHETT, P.J. and JACKSON, J.L. 1990. Ancient continental margin assemblage in the northern Coast Mountains, southeast Alaska and northwest Canada. *Geology*, **18**: 208-211.
- GILL, J. 1981. *Orogenic andesites and plate tectonics*. Springer Verlag, New York, 385p.
- GROVE, E.W. 1986. Geology and mineral deposits of the Unuk River-Salmon River-Anyox area. British Columbia Ministry of Energy, Mines and Petroleum Resources, Bulletin 63, 434 p.
- HARLAND, W.B., COX, A.V., LEWELLYN, P.G., PICKTON, C.A.G., SMITH, A.G. and WALTERS, R. 1982. *A Geologic time scale*. Cambridge, England, Cambridge University Press, 131 p.
- HUMPHRIS, S.E., and THOMPSON, G. 1978. Trace-element mobility during hydrothermal alteration of oceanic basalt. *Geochimica et Cosmochimica Acta*, **42**: 127-136.
- JONES, D.L., SILBERLING, N.J., and HILLHOUSE, J.W. 1977. Wrangellia -- a displaced terrane in northwestern North America. *Canadian Journal of Earth Science*, **14**: 2565-2577.
- LOWE, P.C., RICHTER, D.H., SMITH, R.L., and SCHMOLL, H.R. 1982. Geologic map of the Nabesna B-5 quadrangle, Alaska. U.S. Geological Survey Quadrangle Map, Map GQ-1566, scale 1:63,360.

- MCCLELLAND, W.C., and GEHRELS, G.E. 1990. Geology of the Duncan Canal shear zone and its bearing on the accretionary history of the Alexander terrane, southeastern Alaska. Geological Society of America Bulletin, in press.
- MONGER, J.H.W. 1980. Upper Triassic stratigraphy, Dease Lake and Tulsequah map areas, northwestern British Columbia. Geological Survey of Canada Paper 80-1B, pp. 1-9.
- MONGER, J.W.H., and BERG, H. 1987. Lithotectonic terrane map of western Canada and southeastern Alaska. U.S. Geological Survey Miscellaneous Field Studies Map MF 1874B, scale 1: 2,500,000.
- MONGER, J.W.H., PRICE, R.A. and TEMPELMAN-KLUIT, J.D. 1982. Tectonic accretion and the origin of the two major metamorphic and plutonic belts in the Canadian Cordillera, *Geology*, 10: 10-75.
- MORTENSEN, J.K., and JILSON, G.A. 1985. Evolution of the Yukon-Tanana terrane: Evidence from southeastern Yukon Territory. *Geology*, 13: 806-810.
- MULLER, J.E. 1980. The Paleozoic Sicker Group of Vancouver Island, British Columbia. Geological Survey of Canada Paper 79-30.
- PEARCE, J.A. 1980. Geochemical evidence for the genesis and eruptive setting of lavas from Tethyan ophiolites. *In* Ophiolites. Edited by A. Panayiotou. International Ophiolite Symposium Proceeding, Cyprus, Ministry of Agriculture and Natural Resources, Geological Survey Department.
- PEARCE, J.A. 1982. Trace element characteristics of lavas from destructive boundaries, *In* Andesites: Orogenic andesites and related rocks. Edited by R.S. Thorpe, John Wiley and sons, New York, pp. 525-547.
- PEARCE, J.A., and CANN, J.R. 1973. Tectonic setting of basic volcanic rocks determined using trace element analyses. *Earth and Planetary Science Letters*, 19: 290-300.
- PEARCE, J.A., and NORRY, M.J. 1979. Petrogenetic implications of Ti, Ar, Y, and Nb variations in volcanic rocks. *Contributions to Mineralogy and Petrology*, 69: 33-47.
- PLAFKER, G., BLOME, C.D., and SILBERLING, N.J. 1989. Reinterpretation of lower Mesozoic rocks on the Chilkat Peninsula, Alaska, as a displaced fragment of Wrangellia. *Geology*, 17: 3-6.

- PRICE, R.A. and CARMICHAEL, D.M. 1986. Geometric test for Late Cretaceous-Paleocene intracontinental transform faulting in the Canadian Cordillera. *Geology*, **14**: 468-471.
- RICHTER, D.H. 1976. Geologic map of the Nabesna quadrangle, Alaska. U.S. Geological Survey Miscellaneous Investigations Series, Map 1-932, 1 sheet, scale 1:250,000.
- RICHTER, D.H., AND DUTRO, J.T. 1975. Revision of the Type Mankomen Formation (Pennsylvanian and Permian), Eagle Creek area, Eastern Alaska Range, Alaska. U.S. Geological Survey Bulletin 1395-B.
- RUBIN, C.M., and SALEEBY, J.B. 1987a. The inner boundary zone of the Alexander terrane in southern SE Alaska: A newly discovered thrust belt. *Geological Society of America Abstracts with Programs*, **19**: 455.
- _____. 1987b. The inner boundary zone of the Alexander terrane in southern SE Alaska, Part 1: Cleveland Peninsula to southern Revillagigedo Island. *Geological Society of America Abstracts with Programs*, **19**: 826.
- _____. 1988. A new perspective on what is the Taku terrane in southern SE Alaska. *Geological Society of America Abstracts with Programs*, **20**: 226.
- RUBIN, C.M., and MCCLELLAND, W.C. 1989. The Gravina Belt: Remnants of a mid-Mesozoic oceanic arc in southern southeast Alaska. *Eos, Transactions, American Geophysical Union*, **70**: 1308.
- RUBIN, C.M. SALEEBY, J.B., COWAN, D.S., MCGRODER M.F. and BRANDON, M.T. 1990. Late Mesozoic compressional tectonism: Development of a west-vergent thrust system in the northwestern Cordillera. *Geology*, **18**: 276-280.
- RUBIN, C.M., MILLER, M.M., and SMITH, G.M. 1990. Tectonic development of Cordilleran mid-Paleozoic volcano-plutonic complexes. In *The paleogeography of the Klamath Mountains, Sierra Nevada, and adjacent areas*. Edited by D.S. Harwood and M.M. Miller. Geological Society of America Special Paper 225, in press.
- SALEEBY, J.B., and RUBIN, C.M. 1989. The western margin of the Coast Plutonic Complex (CPC) in southernmost SE Alaska. *Geological Society of America Abstracts with Programs*, **21**: 139.

- 1990. The East Behm Canal Gneiss Complex (southern southeast Alaska) and some insights into basement tectonics along the Insular suture belt. Geological Association of Canada Abstracts with Programs, in press.
- SAMSON, S.D., MCCLELLAND, W.C., PATCHETT, P.J., and GEHRELS, G.E. 1989. Nd isotopes and Phanerozoic crustal genesis in the Canadian Cordillera. *Nature*, **337**: 705-709.
- SILBERLING, N.J., WARDLAW, B.R., and BERG, H.C. 1982. New paleontologic age determinations from the Taku terrane, Ketchikan area, southeastern Alaska. *In* The U.S. Geological Survey in Alaska: accomplishments during 1980. Edited by W.L. Coonard. U.S. Geological Survey Circular 844, pp. 117-119.
- TEMPELMAN-KLUIT, D.J. 1979. Transported cataclasite, ophiolite and granodiorite in Yukon: Evidence of arc-continent collision. Geological Survey of Canada Paper 79-14, 27p.
- WEBER, F.R., FOSTER, H.L., KEITH, T.E.C., and DUSEL-BACON, C. 1978. Preliminary geologic map of the Big Delta quadrangle, Alaska. U.S. Geological Survey Open-File Report 78-529A.
- WERNER, L.J. 1977. Metamorphic terrane, northern Coast Mountains west of Atlin Lake, British Columbia. Geological Survey of Canada Paper 77-1A, pp. 267-269.
- 1978. Metamorphic terrane, northern Coast Mountains west of Atlin Lake, British Columbia. Geological Survey of Canada Paper 78-1A, pp. 69-70.
- WHEELER, J.O., and McFEELY, P. 1987. Tectonic assemblage map of the Canadian Cordillera. Geological Survey of Canada Open-File Report 1565.
- WHEELER, J.O., BROOKFIELD, A.J., GABRIELSE, H., MONGER, J.W.H., TIPPER, H.W. and WOODSWORTH, G.J. 1988. Terrane map of the Canadian Cordillera: Canadian Geological Survey Open-File Report 1894.

CHAPTER 5

Thrust tectonics and Cretaceous intracontinental shortening in southeast Alaska

C M. Rubin and J B. Saleeby, California Institute of Technology, Pasadena, California, 91125

submitted to Thrust Tectonics, Geological Society of London

Abstract

An imbricate thrust belt that extends along strike for over 2000 km overprints the tectonic boundary between two of the largest allochthonous crustal fragments (Intermontane and Insular superterrane) in the North American Cordillera and affects rocks west of the Coast Plutonic Complex in southeast Alaska and western British Columbia. Deformation was broadly coeval with mid-Cretaceous magmatism and involved the emplacement of west-directed thrust nappes over a structurally intact and relatively unmetamorphosed basement. The Palaeozoic and lower Mesozoic Alexander terrane forms structural basement for much of the thrust belt, along a moderately northeast-dipping ramp.

Mid-Cretaceous deformation occurred during two main episodes that were contemporaneous with the emplacement of tabular plutonic bodies. Older structures record ductile southwest-vergent folding and faulting, regional metamorphism, and contain a well-developed axial-planar foliation. Second generation structures include southwest-directed reverse faults that juxtapose contrasting metamorphic grades and refold earlier structures.

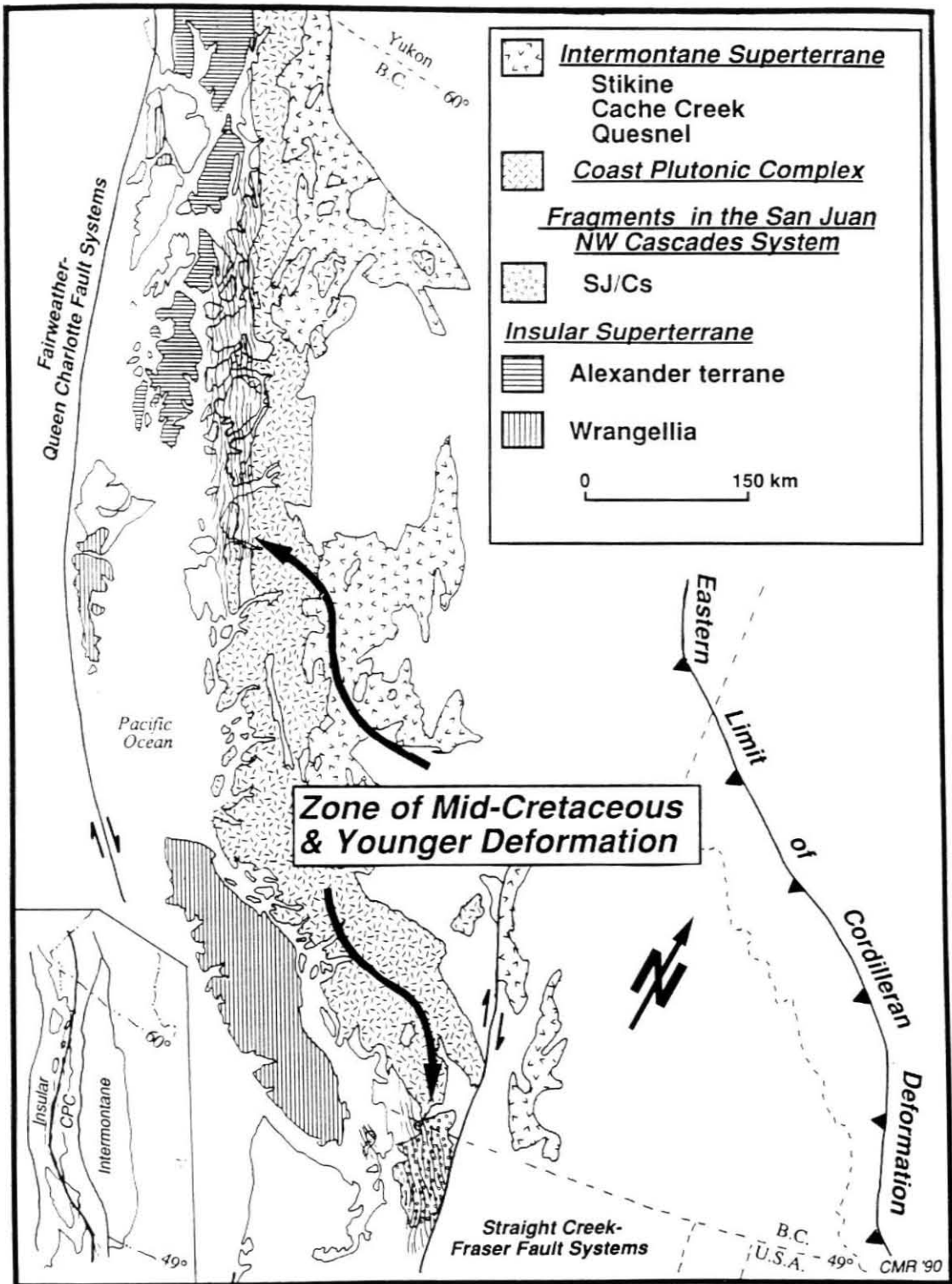
Structural, stratigraphic and geochronologic data suggest that regional-scale deformation in southeast Alaska occurred between 113 Ma and 89 Ma. Rocks in the thrust belt were regionally uplifted by 70 Ma, at an average rate of ≈ 0.9 mm/yr. Deformation involved the collapse of marginal basin(s) and a magmatic arc, overprinting the older tectonic boundary between the Insular superterrane and the late Mesozoic western margin of North America (i.e., the Intermontane superterrane). Contractual deformation along the length of the thrust belt was broadly coeval

with arc magmatism, and thus records intra-arc tectonism. Late Paleocene to Early Eocene deformation and uplift may mark the transition from contractional to extensional tectonism and perhaps records the collapse of tectonically thickened crust.

The western metamorphic belt of the Coast Plutonic Complex of the North American Cordillera comprises a northeast-trending zone from western British Columbia to northern southeast Alaska (latitude 49° - 59°; Fig. 1). The belt is characterized by widespread Cretaceous crustal shortening, metamorphism, and deep erosion (Crawford et al. 1976; Rubin et al. 1990). Thrust sheets in the belt show extensive basement involvement, including both juvenile, ensimatic elements of the Alexander terrane and continent-derived North American slope and rise deposits. The involvement of crystalline basement in thrust sheets and large thrust displacements imply that deformation affected the upper and middle crust and not just a thin, detached sedimentary cover. There is ample evidence for abundant thickening in the late Mesozoic; furthermore by analogy to similar orogenic belts (e.g., the present day Andes, Suarez et al. 1983), an anomalously thickened crust existed by the late Mesozoic time.

The tectonic evolution of the western metamorphic belt in western Canada and southeast Alaska has been discussed by numerous workers (Hollister 1982; Monger et al. 1982; Crawford et al. 1987; Rubin et al. 1990). Two principal tectonic interpretations have been invoked to explain the extensive late Mesozoic deformation that extends for over 2000 km, mostly along the western side of the Coast Plutonic Complex: (1) deformation resulted from the collision of allochthonous terranes (e.g., the Alexander terrane and Wrangellia) against the western margin of Mesozoic North America, or (2) deformation occurred in an intra-arc setting (see Rubin et al. 1990). Most workers agree, however, that the mid-Cretaceous and younger calc-alkaline plutons originated in a convergent-margin setting (Armstrong, 1988). In this paper, we present an overview of the mid-Cretaceous structural history and speculate on the younger Paleocene deformational framework of the western metamorphic belt of the Coast Plutonic Complex in southern southeast Alaska, between latitudes 55° and 56° N (Fig. 1).

Figure 1: Map showing the major lithotectonic elements and the region of mid-Cretaceous and younger deformation in southeast Alaska. Inset shows superterrane and intervening Coast Plutonic Complex (CPC). SJ/Cs = San Juan Islands - northern Cascades.



Tectonic framework

The western North American Cordillera can be subdivided into two N-NW-trending lithotectonic belts, the Intermontane and Insular superterrane (Fig. 2). The Intermontane superterrane, consisting of lower Palaeozoic continent-derived slope and rise deposits, and upper Palaeozoic to lower Mesozoic ensimatic arc assemblages, probably formed adjacent to North America (Miller 1987; Rubin et al. in press). The superterrane was accreted to North America in Early to Middle Jurassic time (Monger et al. 1982) and thus formed the western margin of the North American continent during Cretaceous time. The Insular superterrane, consisting of juvenile, mantle-derived volcanic arc and rift assemblages is separated from the Intermontane superterrane to the west by the Coast Plutonic Complex (Fig. 1). The Insular superterrane, extending for over 2000 km along strike, has no apparent paleogeographic relation to North America until the Cretaceous (Monger et al. 1982; Saleeby 1983; Gehrels & Saleeby 1987a).

The tectonic boundary between the two superterrane generally coincides with the western metamorphic belt of the Coast Plutonic Complex (Fig. 1). A regionally extensive mid- to Late Cretaceous thrust belt affected both superterrane and involved the stripping of the upper part of continental and ensimatic crust beneath an underthrust Insular superterrane. Differing structural levels are exposed throughout the belt, from high-grade gneiss on the east, to low-grade phyllite on the west, making this a unique area to study thrust tectonics.

Geologic and stratigraphic setting

The Alexander terrane forms structural basement to the thrust belt and consists of a structurally intact lower Palaeozoic ensimatic arc sequence overlain by middle Palaeozoic clastic and carbonate strata (Fig. 3, Gehrels & Saleeby 1987a). These rocks are capped by an Upper Triassic rift assemblage (Fig. 3, Gehrels & Saleeby 1987b). In most areas, rocks of the Alexander terrane are only slightly deformed and are not highly metamorphosed (Gehrels & Saleeby 1987), except near the eastern boundary where the Alexander terrane is overprinted by late Mesozoic

Figure 2: Generalized distribution of the Intermontane and Insular superterrane and the miogeocline of the northern Cordillera (modified after Monger et al. 1982; Monger & Berg 1987; Wheeler et al. 1988; Miller 1987). Also shown are some large-strike-slip faults. Initial Sr 0.706 isopleth from Kistler & Peterman (1973), Farmer & DePaolo (1983) and Armstrong (1988).

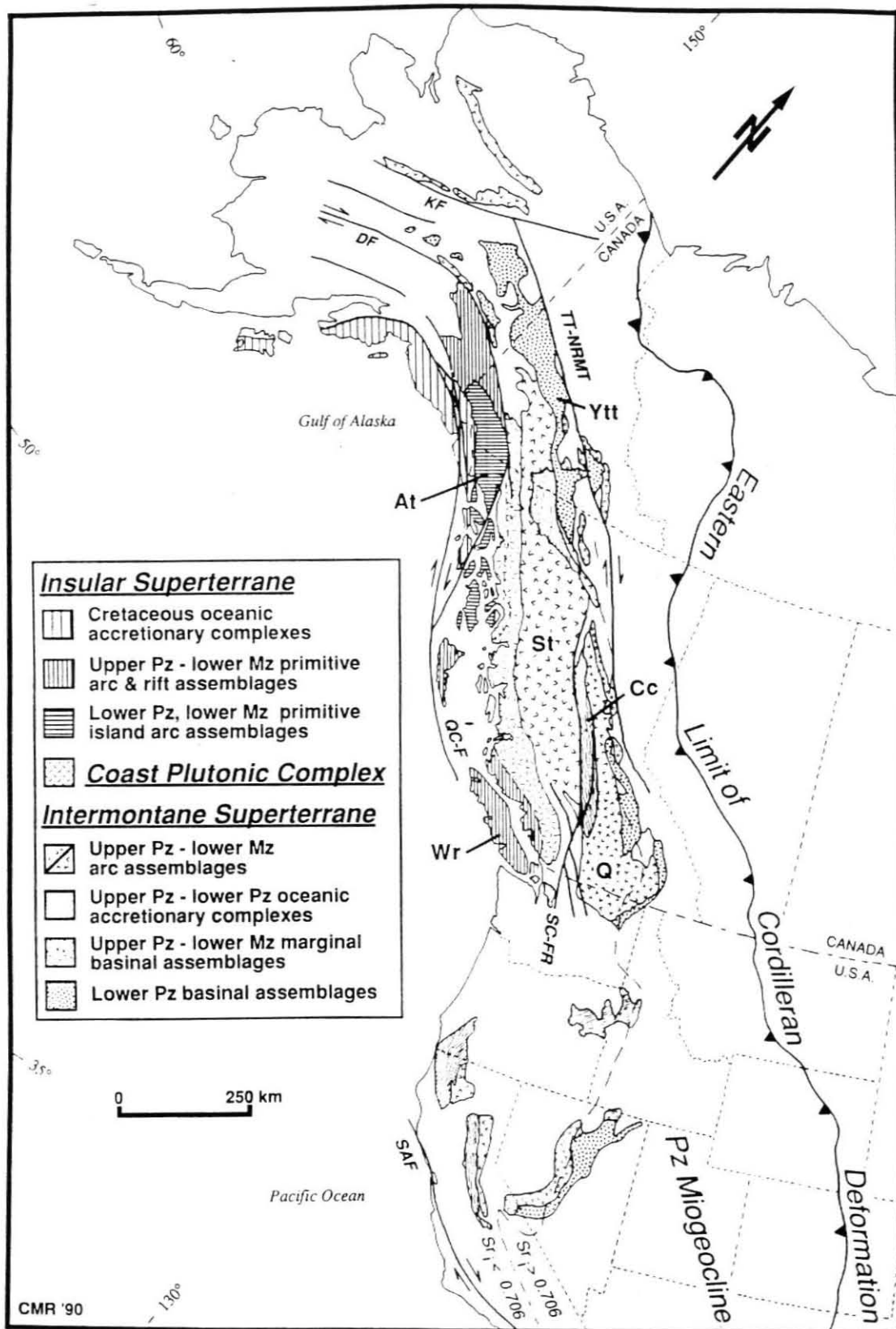
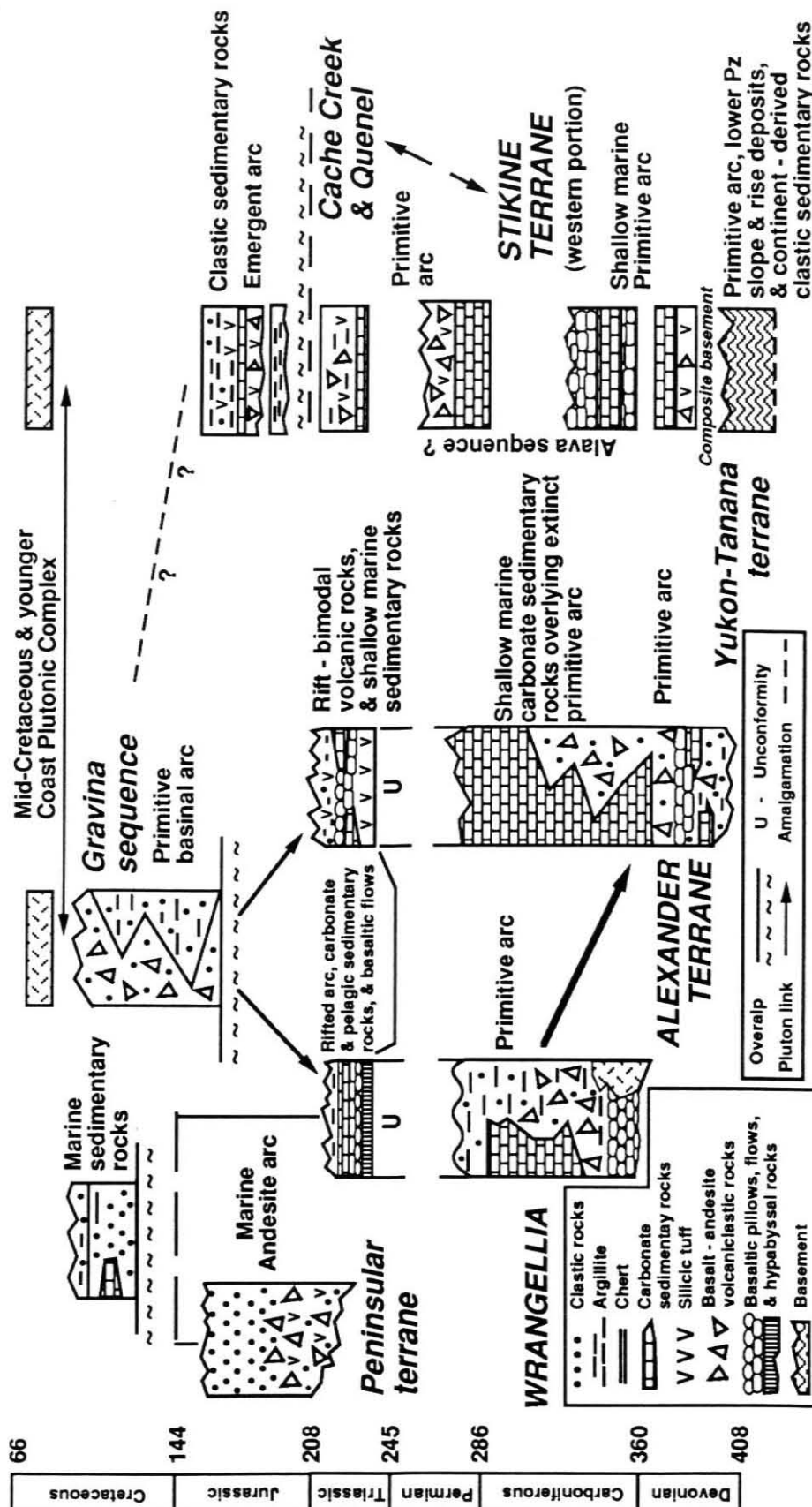


Figure 3: Petrotectonic and structural histories of the Intermontane and Insular superterrane of British Columbia and southern Alaska (modified from Saleeby 1983; Gardner et al. 1986; Miller 1987; Anderson 1989).

Insular Superterrane

Intermontane Superterrane



deformational structures. East of and depositionally overlying the Alexander terrane lie Upper Jurassic and Lower Cretaceous marine pyroclastic and basinal strata of the Gravina sequence (Fig. 3, Berg et al. 1988). The pyroclastic and basinal strata constitute the remnants of an oceanic island arc system that was constructed on the Alexander terrane (Rubin & McClelland 1989). Middle Palaeozoic and lower Mesozoic rocks of the Alava sequence structurally overlies rocks of the Alexander terrane and the Gravina sequence (Fig. 3). Locally, channel-fill and turbidite deposits of the Gravina sequence unconformably overlie the Alava sequence and thus form an overlap between the Alexander terrane and the Alava sequence. The Alava sequence consists of three lithotectonic units, (1) Pennsylvanian and Permian mafic metavolcanic tuff and flows and massive crinoidal marble interbedded with black phyllite, (2) localized sequences of quartzite, mafic metavolcanic rocks, and marble, and (3) upper Middle Triassic carbonaceous marble, mafic metavolcanic tuff, breccia, and flows. The original stratigraphic relations and distribution of the Alava sequence are obscured by mid-Cretaceous and younger deformation, thus their stratigraphic correlation with adjacent terranes is uncertain. Based upon lithostratigraphy, age considerations, and tectonic setting, the Alava sequence is similar to the upper Palaeozoic and lower Mesozoic Stikine terrane (Intermontane superterrane, Rubin & Saleeby 1988). The presence of quartzite precludes a stratigraphic correlation with juvenile, age-equivalent elements of Wrangellia.

The Kah Shakes sequence occupies even higher structural levels in the northern portions of the thrust belt and consists of lower Palaeozoic quartzite, marble, amphibolite, calc-silicate rocks, and mid-Palaeozoic orthogneiss. The presence of detrital zircon from quartz-rich meta-psammitic rocks yielding Proterozoic upper intercept U-Pb ages (Saleeby & Rubin 1989; Gehrels et al. 1990) and Precambrian inheritance in zircon from orthogneiss implies an old continental source for some of the terrigenous rocks in the Kah Shakes sequence. The older portions of the Kah Shakes sequence represent outer shelf and continental rise deposits derived from the North American continent. The sequence may have formed depositional basement to the Alava sequence. Negative ϵ_{Nd} values and high initial Sr values for correlative

rocks to the north support the interpretation that the Kah Shakes sequence has an old continental component in its source (Samson et al. 1989).

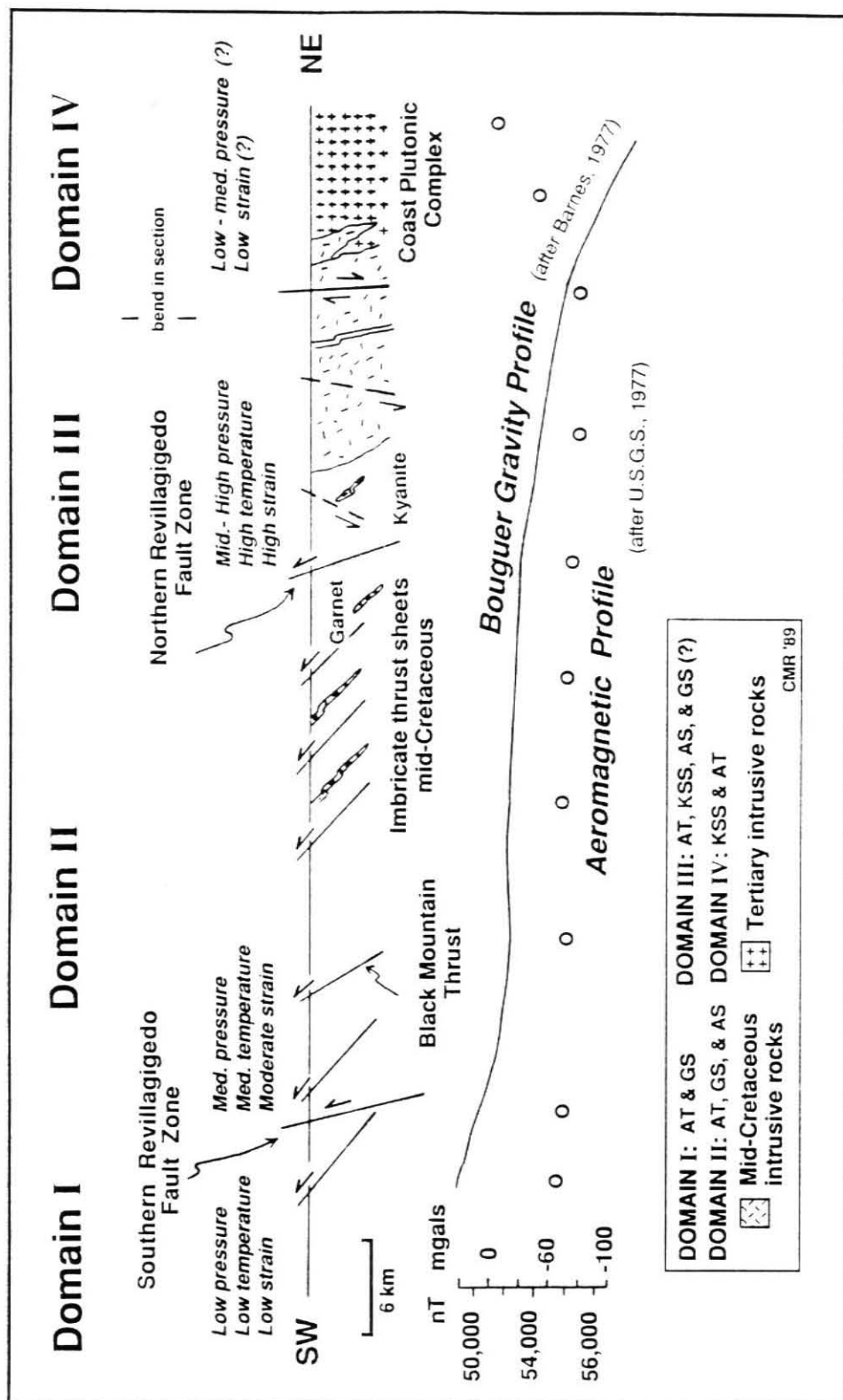
Rocks in the thrust belt were intruded by mafic-ultramafic complexes, epidote-bearing tonalite, quartz diorite and granodiorite plutons, sills and dikes that range in age from ≈ 110 to 89 Ma (U-Pb ages on zircon, Rubin & Saleeby 1987a, b; Arth et al. 1988). Such plutons that yield ages of ≈ 100 Ma or less crosscut the earlier regional metamorphic fabric; 95-101 Ma plutons are cut by thrust faults, and 90 Ma plutons crosscut thrust faults. A belt of Early Paleocene to Early Eocene plutons occurs east of the thrust belt (Smith & Diggles, 1981); fabrics in these younger rocks reflect Tertiary deformation (Saleeby & Rubin 1989). Geochemical and isotopic data indicate that all the intrusive rocks have continental- magmatic affinities (Arth et al. 1988).

Internal structure of the thrust belt

Based on differences in metamorphic grade, strain history, and stratigraphy, the northern part of the thrust belt can be divided into four major structural domains (Fig. 4), three of which are described here. The structurally lowest thrust sheets (domain I) consist of lower greenschist facies supracrustal and metaigneous rocks of the lower Palaeozoic Alexander terrane and Upper Jurassic and Lower Cretaceous Gravina sequence. These rocks have been overthrust by upper greenschist and lower amphibolite grade rocks of the middle to lower Palaeozoic Kah Shakes sequence and the upper Palaeozoic and lower Mesozoic (?) Alava sequence (Domain II). The third structurally higher allochthonous unit consists of amphibolite grade rocks of the Kah Shakes sequence, interlayered with abundant tonalite sills and dikes (domain III). Metamorphic grade dramatically increases with structural level. Structural basement to domain I and II consist of the Alexander terrane, whereas in the higher nappe complexes, basement appears to be imbricated and composite, consisting of both the Alexander terrane and Kah Shakes sequence.

In contrast, structural styles and the stacking order of thrust sheets are different in the southern portion of the thrust belt. Here, the structurally lowest thrust sheets consist of lower Paleozoic supracrustal and meta-igneous rocks of the Alexander terrane. These rocks are

Figure 4: Geologic cross-section, aeromagnetic, and gravity profiles across the western metamorphic belt of the Coast Plutonic Complex showing the mid-Cretaceous structural domains. Late Paleocene-Eocene fabrics do not strongly overprint this area. AT = Alexander terrane; GS = Gravina sequence; AS = Alava sequence; KSS = Kah Shakes sequence.

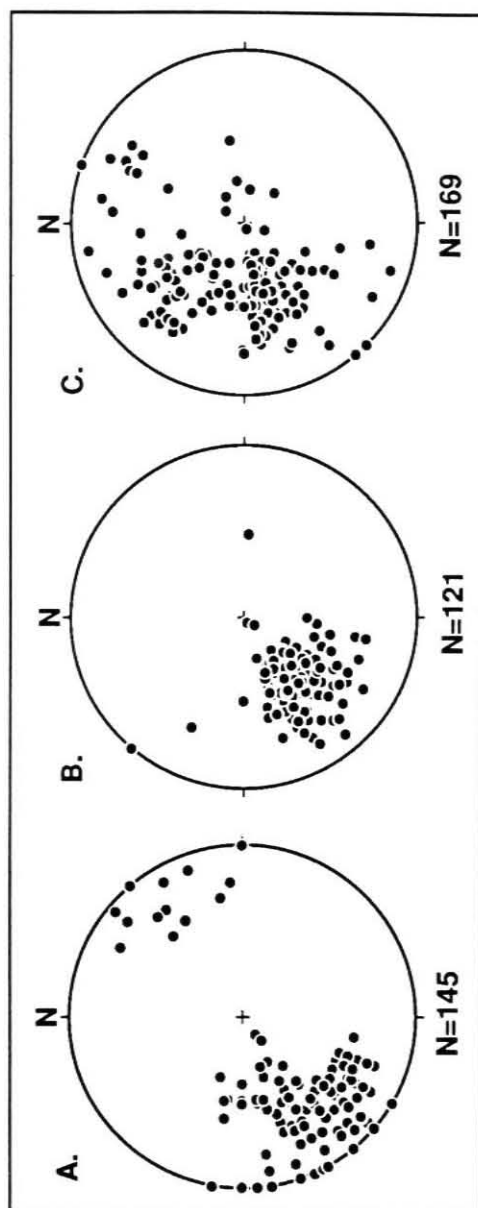


structurally overlain by siliceous schist, orthogneiss, and marble of the middle to lower Palaeozoic Kah Shakes sequence. Upper Jurassic to Lower Cretaceous metaturbidites of the Gravina sequence structurally overlie the Kah Shakes sequence. These rocks are overthrust by lower amphibolite grade rocks of the upper Palaeozoic and lower Mesozoic (?) Alava sequence.

Non-penetrative foliation and lower greenschist facies mineral assemblages, mesoscopic folding and thrust faulting characterize domain I. Thrust faults strike NW and dip moderately to the NE. Rocks in the thrust sheets display a dominant NE striking foliation (Fig. 5) that is parallel or subparallel with original bedding surfaces. Foliation is axial-planar to west-vergent asymmetric folds that are in turn cut by thrust faults. We interpret these west-vergent folds to be kinematically linked to the thrust faults and to have formed contemporaneously with faulting. Domain I is characterized by low-temperature and pressure regional metamorphic mineral assemblages, andalusite-bearing contact metamorphic aureoles, and unstrained fossils and relict phenocryst assemblages. Preliminary finite strain studies on the shapes of deformed pebbles in coarse-grained meta-conglomerates of the Gravina sequence indicate the rocks are comparatively weakly deformed, with R_{XZ} ratios of 5:1 or smaller. Based on these data, rocks in domain I show little finite strain and did not experience temperatures greater than 400° C or pressures over 3 kb.

Domain II lies structurally above domain I and is composed largely of imbricate thrust sheets consisting of lower Palaeozoic and lower Mesozoic supracrustal rocks of the Alava sequence, Upper Jurassic (?) and lower Cretaceous metasedimentary rocks of the Gravina sequence, and locally lower Palaeozoic orthogneiss of the Alexander terrane. Some of these rocks (i.e., Alava sequence) may have been originally part of the Intermontane superterrane (Fig. 3) and were thrust over the Alexander terrane and its Upper Jurassic and lower Cretaceous volcanic-sedimentary cover. The overall structural relations between the Alava and Gravina sequences on central Revillagigedo Island is best described as an imbricate series of thrust sheets with intervening Kah Shakes basement thrust slabs. Stratigraphic control is based on isotopically dated (Pb-U zircon) clasts in laterally continuous Gravina sequence metaturbidites, distinctive Permian fossiliferous marble and Middle Triassic carbonaceous marble horizons in the

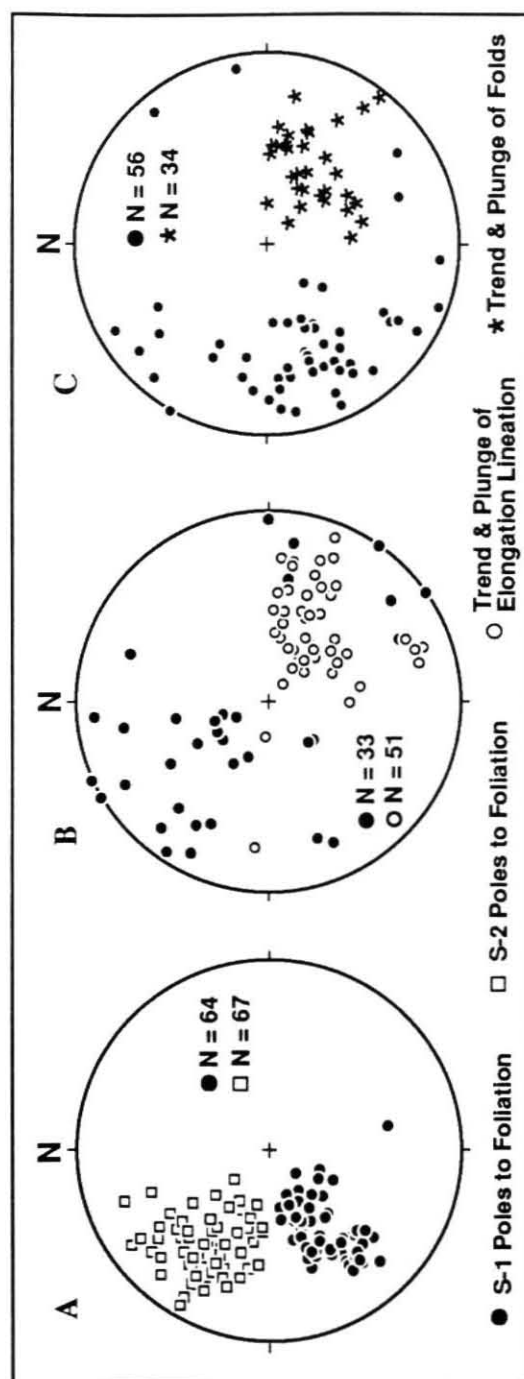
Figure 5: Lower-hemisphere, equal-area plot showing poles to foliation surfaces domain I, (A) northwest Cleveland Peninsula, (B) Annette Island, (C) Gravina Island.



Alava sequence. The thrust that separates domains I and II ramps to deeper structural and stratigraphic levels and dips moderately towards the east. Meta-igneous pebble- to cobble-conglomerate in the Gravina sequence show flattening fabrics that parallel foliation surfaces. Numerous deformed tonalite and quartz diorite sills and dikes are present in domain II and probably emplaced broadly with thrust faulting (Hollister & Crawford 1986). The contemporaneity of $\text{Ar}^{40}/\text{Ar}^{39}$ hornblende cooling ages from metamorphic rocks (Sutter & Crawford 1985) and U-Pb zircon ages in the tonalitic plutons and sills (Rubin & Saleeby 1988; Saleeby 1988) support the synchronicity of metamorphism, thrust faulting, and igneous activity. Thrust faults commonly ramp along weak horizons and are composed of marble phacoids in a penetratively-cleaved phyllonite. Where thrust faults pass through a relatively competent marble, flat-ramp-flat geometries are formed. Class 1C and similar style class 2 folds (fold classification after Ramsay & Huber 1987) with axial planes dipping moderately towards the NE are common in domain II (Fig. 6). The folds affect bedding and verge to the NW. Lineations are defined by the intersection of bedding and cleavage and dip moderately to the NE (Fig. 6a). A wide range of rock compositions produce a range of mineral assemblages; white mica-biotite-quartz-plagioclase-chlorite \pm garnet \pm calcite are common in psammitic rocks, whereas in metabasalts hornblende-biotite-plagioclase-epidote-chlorite assemblages are common. Locally, staurolite and kyanite are present, thus spanning upper greenschist to lower amphibolite facies. In summary, domain II is characterized by upper greenschist to amphibolite facies metamorphic mineral assemblages and yield pressures ranging from 5 to 6 kb. Therefore, higher pressure and temperature conditions were attained in domain II than in domain I.

The structurally higher thrust sheets, exposed in domain III, do not have simple thrust geometries that are observed in domains I and II. Domain III is characterized by polydeformed, isoclinally folded, amphibolite-facies supracrustal and meta-igneous rocks. This domain exhibits large-scale stratigraphic inversion and sheath folds that form crystalline nappe complexes. Well-developed moderately-dipping elongation lineations that parallel fold axes (Fig. 6b, c), highly attenuated fold limbs, retrograde thrust slices, and amphibolite facies metamorphic rocks

Figure 6: Lower-hemisphere, equal-area plot showing, (A) poles to foliation and cleavage in domain II, (B) poles to foliation and trend and plunge of small-scale folds in domain II, and (C) poles to foliation and trend and plunge of elongation lineation in domain III.



characterize domain III. Similar style class 2 and 3 folds are common in this domain. Metamorphic mineral assemblages include hornblende-plagioclase \pm biotite \pm garnet in mafic gneiss, quartz-plagioclase-biotite-kyanite in pelitic strata, and quartz-plagioclase-biotite-orthoclase-garnet commonly is present in medium-grained psammatic gneiss. Steep N- to NE-dipping ductile reverse faults cross-cut the earlier regional fabrics. These fault zones are characterized by a strongly developed foliation that transposes the earlier fabrics. The orientation of the faults at depth is not accurately known; however, based on limited kinematic indicators (e.g., s-c fabrics, fold vergence) and the juxtaposition of rocks with differing metamorphic grade along fault zones, a consistent sense of motion can be constructed (Fig. 4). Reverse faults, such as the northern Revillagigedo fault zone (Fig. 4), have a minimum separation of 10 km, based on contrasting metamorphic grades. Late Cretaceous uplift and erosion of the western part of the orogenic belt was most likely accommodated along these reverse faults. In the southern and eastern portions of the thrust belt, subsequent Paleocene and younger deformation has re-oriented mid-Cretaceous fabrics. Here, deep structural levels of the west-vergent thrust belt were transported upwards along steeply dipping east-vergent faults. These east-vergent structures record Paleocene crustal shortening; however, the overall tectonic setting may have been extensional.

Timing of mid-Cretaceous orogenic events

Age constraints for the timing of deformation come from plutons which cross-cut and are affected by structural fabrics. The earliest phase of thrust faulting is present in domains I and II, which are overthrust by 101 Ma hornblende-bearing tonalite and granodiorite (U-Pb zircon age, Rubin & Saleeby 1987). Deformed intrusive rocks of similar age that intrude the Alexander terrane are exposed to the west (Saleeby unpublished data) and indicate that thrust faulting was active prior to 100 Ma. Thrust faulting continued to \approx 90 Ma (U-Pb zircon), the age of the youngest plutons affected by thrust-related deformation. The age of the youngest strata involved in thrust faulting is Albian (Berg et al. 1972) and to the north may be as young as Cenomanian

(Brew, oral comm. 1988). Thus, much of the deformation occurred between the Albian and Turonian, approximately between 113 Ma and 89 Ma (time scale after Harland et al. 1982).

Uplift, erosion, and foredeep development

Cooling rates can be calculated from U-Pb data from zircon, K/Ar and $\text{Ar}^{40}/\text{Ar}^{39}$ data from hornblende and biotite. Zircon yielding dates of 101 Ma is inferred to have crystallized between 1000° C and 850° C based on the solidus temperature of an understaturated tonalite (Huang & Wyllie 1986). Hornblende from the same intrusive body in the western part of the thrust belt yield $\text{Ar}^{40}/\text{Ar}^{39}$ cooling ages of 97 Ma (Sutter & Crawford 1985), and are inferred to have retained argon at $530^{\circ} \pm 40^{\circ}$ C (Harrison & McDougall 1980). These data yield a cooling rate between 112°C/m.y. to 75°C/m. Hornblende and biotite from the eastern part of the thrust belt yield K/Ar cooling ages of 89 Ma and 82 Ma respectively (Smith & Diggles 1981) and yield a cooling rate of 70°C/m.y to 30°C/m.y.

Inferred uplift rates can be calculated from K/Ar cooling ages on hornblende and biotite (Smith & Diggles 1982), U-Pb zircon ages (Rubin & Saleeby 1987a,b) from tonalitic plutons that have well constrained barometry, and certain assumptions about the thermal structure of the mid-Cretaceous crust. A tabular tonalite pluton (Bushy Point pluton) yielding U-Pb ages of 95 Ma is inferred to have crystallized at a depth of ≈ 25 km. The pressure estimate is based on Al^{T} content in hornblende (Hammarstrom & Zen 1986) and the experimental calibration of the Al^{T} in hornblende barometer (Rutherford & Johnson 1989). Hornblende and biotite from the surrounding country rock yield a K/Ar cooling ages of 80.2 ± 4 Ma and $83.0 \text{ Ma} \pm 2.5$ Ma and are inferred to have retained argon at $280^{\circ} \pm 40^{\circ}$ C and $530^{\circ} \pm 40^{\circ}$ C respectively (Harrison 1981; Harrison & McDougall 1980). Assuming a mid-Cretaceous geothermal gradient of $\approx 25^{\circ}\text{C}/\text{km}$, these data imply an apparent uplift rate of ≈ 0.9 km/m.y. To the south, the inferred mid-Cretaceous average uplift rate is ≈ 0.58 mm/yr (Zen 1988), which is comparable with the inferred uplift rates in the Ketchikan area. These uplift rates are comparable with modern orogenic uplift and erosion rates (see Dahlen and Suppe 1988).

Synorogenic to post orogenic marine and nonmarine foredeep sequences are represented by the Upper Cretaceous Queen Charlotte and Nanaimo Groups in western British Columbia. The Nanaimo Group consists of Turonian to Maastrichtian (≈ 90 Ma to 65 Ma) marine and non-marine sandstone, conglomerate, and mudstone, approximately 2.5 km thick, that unconformably overlies rocks of Wrangellia (Muller & Jeletsky 1970). The Late Cretaceous Nanaimo conglomerates contain metamorphic clasts that were derived from thrust sheets exposed to the east indicating that both metamorphism and thrust faulting occurred prior to the Late Cretaceous (see Brandon et al. 1989). Similarly, the Queen Charlotte Group consist of Albian to probably Coniacian (≈ 113 Ma to 87.5 Ma) marine fine- to very coarse-grained clastic strata that is approximately 3 km thick (Sutherland-Brown 1968). Metamorphic and igneous clasts in the Queen Charlotte Group were derived from the Coast Plutonic Complex (Yagishita 1985), perhaps recording loading due to the emplacement of thrust nappes. These synorogenic deposits represent the westward dispersal of sediments that were derived from the uplifted thrust belt (Yagishita 1985). The presence of strong lithosphere beneath the Insular superterrane might have prevented the development of deep basins, thus shallow foredeep basins were formed as the crust was flexed down by the weight of the thrust sheets. The foredeep deposits record average sedimentation rates between ≈ 0.15 mm/yr. (Queen Charlotte Group) and ≈ 0.2 mm/yr (Nanaimo Group, Brandon et al. 1988) and show that erosion rates in the mid-Cretaceous are about 0.2 to 0.5 mm/yr. These rates are consistent with inferred Late Cretaceous uplift rates in the Prince Rupert and Ketchikan areas.

Implications for basement tectonics and convergent margin tectonics

Major differences in the structural styles present in southeast Alaska and many mountain belts characterized by thin-skin deformation (e.g., Canadian Rockies) reflect fundamental differences in basement deformation, level of crustal exposure during deformation, and subsequent tectonic evolution. Mid-Cretaceous thrust and reverse faults in southeast Alaska dip

between 40° and 70° and affect predominantly crystalline basement. This type of structural style may be analogous to present day deformation in the high Andes (Suarez et al. 1983) and Himalaya (Molnar 1984). The few recent thrust faults recognized in the high Andes (e.g., Pariahuanea fault) dip steeply, with seismic activity no deeper than 20 km (Philip & Megard 1977). This style of faulting is analogous to the mid-Cretaceous faulting in the thrust belt in southeast Alaska. Similarly, some fault plane solutions show steeply-dipping thrust faults in the Himalaya. There, the northern margin of India is presently underthrusting Asia, forming a crustal-scale duplex (Molnar 1984) which effectively delaminated the continental crust under India. In a similar fashion, the moderately dipping thrust faults in southeast Alaska formed in response to the underthrusting of the Alexander terrane under the western continental margin of North America. Both the high Andes and Himalaya have also undergone very different styles of deformation during their tectonic evolution, in which back-folding or "retrocharriage" occurred during the later stages of thrust faulting. In this context, the eastward dipping faults and foliation surfaces in the eastern portion of the thrust belt in southeast Alaska may be analogous to the modern day structural reversals seen in the Andes or Himalaya. Although the analogy between the mid-Cretaceous thrust system and the Andes or Himalaya might be imperfect, the mid-Cretaceous thrust system might represent a hybrid example between the two modern analogues. The presence of both coeval igneous activity (Andes), contractional tectonism between two continental fragments (Himalayas), and the transport of crystalline slabs along thrust faults in the mid-Cretaceous point to an intermediate view between the two modern analogs.

Beneath most of the western wall rocks of the Coast Plutonic Complex, the present day crustal thickness is less than 30 km (Barnes 1972a, b, 1977) and locally may be as thin as 25 km (Yorath et al. 1985). Based on an emplacement pressure of $\approx 6-7$ kb for 100 Ma plutons (Hammarstrom & Zen 1986; Rubin & Saleeby 1988), the crust was at least 25 km thick. Due to subsequent thrust and reverse faulting, the mid-Cretaceous (90 Ma) crust may have been 50 to 60 km thick. The estimate of mid-Cretaceous crustal thickness is consistent with the present-day thickness of 25 to 30 km, plus the amount of crust removed to expose Cretaceous mid-crustal

rocks. This estimate is in accord with crustal thickness in regions which have undergone similar styles of crustal-thickening, such as the hinterland of the Canadian Rockies (Monger & Price 1979; Monger et al. 1985). Subsequent erosion and uplift of the thrust belt in an extensional setting during Paleocene and Eocene time might have subsequently thinned the crust; however, the available constraints on present crustal structure and magnitude of extension are poorly known. Rapid early Tertiary uplift rates of about 2 km/m.y. have been inferred for the western flank of the Coast Plutonic Complex (Hollister 1982), although the uplift has been ascribed to contractional tectonism (Hollister 1982; Crawford et al. 1987). Extensional tectonism is documented on the west flank of the Coast Plutonic Complex, where thrust-related fabrics are truncated by east-dipping Tertiary extensional faults (McClelland et al. 1990). Thus by analogy with regions of active extension (e.g., high Andes), tectonically thickened mid-Cretaceous crust may have collapsed and subsided due the gravitational potential of a high mountain belt. Abundant mid-Cretaceous and younger sills and plutons and a moderate geothermal gradient resulted in hot, thermally weakened crust which effectively reduced the overall strength of the crust.

Locally, the emplacement of arc-derived calc-alkaline magmas was coeval with mid-Cretaceous deformation. Thus, mid-Cretaceous contractional tectonism occurred in an intra-arc setting. Addition of voluminous early- to mid-Tertiary plutons coincided with and succeeded erosion, uplift, and inferred extension of the tectonically thickened and thermally weakened crust. The mid-Cretaceous to Early Tertiary tectonic history reflects contractional and extensional events occurring in an convergent-margin setting. Changes in overall plate convergence rates and the rate of subduction may explain differing structural styles. Examples of other thrust belts that have been affected by a spectrum of structural styles can be found in the Himalaya (Gansser 1964), western Alps (Royden & Burchfiel 1989), and the Andes (Jordan et al. 1983).

Controversy exists concerning the role of collision of allochthonous crustal elements (e.g., the Alexander terrane and Wrangellia) in late Mesozoic deformation of the northwest Cordillera (Monger et al. 1982; Crawford et al. 1987; Pavlis 1989; Rubin et al. 1990). The absence

of an accretionary wedge and high-pressure metamorphic terranes, combined with the lack of evidence for an intervening late Mesozoic oceanic crust between the Insular and Intermontane superterrane at these latitudes is an important constraint for collisional tectonic models. There is no general agreement in plate tectonic models that explain mid-Cretaceous and younger deformation; however, deformation and igneous activity occurred in a magmatic arc setting. In this view, the collision of exotic tectonic elements and the concurrent closure of a late Mesozoic oceanic basin is not required to explain the stratigraphic, structural, and metamorphic relations seen in southeast Alaska and western British Columbia.

ACKNOWLEDGEMENTS

CMR is grateful for long discussions with Maria Lucia Crawford, Bill McClelland, Meghan Miller, and Margi Rusmore on Alaskan Cordilleran tectonics. Field and laboratory work for southeast Alaska regional studies have been supported by the U.S. National Science Foundation Grants EAR 86-05386 and EAR 88-03834 (to JBS); additional support (to CMR) was provided by Geological Society of America Penrose Grants, a Sigma-Xi grant-in-aid, and by the U.S. Geological Survey, Alaska Branch. Some of the work reported here was part of a doctoral thesis by C.M.R. at Caltech.

REFERENCES

- Anderson, R.G. 1989 A stratigraphic, plutonic, and structural framework for the Iskut River map area, northwestern British Columbia, in Current research, Part E: Geological Survey of Canada, Paper 89-1E, p. 145-154.
- Armstrong, R.L. 1988 Mesozoic and early Cenozoic magmatic evolution of the Canadian Cordillera, *in* Clark, S.P., Jr, et al., eds., Processes in continental lithospheric deformation: Geological Society of America Special Paper 218, p. 55-91.

- Arth, J.G., Barker, F., & Stern, T.W. 1988 Coast Batholith and Taku plutons near Ketchikan, Alaska: Petrography, geochronology, geochemistry, and isotopic character: *American Journal of Science* v, 288-A, p. 461-489.
- Barnes, D.F. 1972a Simple bouguer gravity anomaly map of Prince Rupert 1:250,000 quadrangle, southeastern Alaska, showing station locations, anomaly values, and generalized 10-milligal contours: U.S. Geological Survey Geophysical Open-File Map., 1 sheet..
- 1972b Simple bouguer gravity anomaly map of Ketchikan 1:250,000 quadrangle, southeastern Alaska, showing station locations, anomaly values, and generalized 10-milligal contours: U.S. Geological Survey Geophysical Open-File Map, 1 sheet..
- 1977 Bouguer gravity map of Alaska: U.S. Geological Survey Geophysical Investigations Map GP-913., 1 sheet, scale 1:2,500,000.
- Berg, H.C., Jones, D.L., & Richter, D.H. 1972 Gravina-Nutzotin belt: Tectonic significance of an upper Mesozoic sedimentary and volcanic sequence in southern and southeastern Alaska: U.S. Geological Survey Professional Paper 800-D, p. 1-24.
- , Elliott, R.L., & Koch, R.D. 1988a Geologic map of the Ketchikan and Prince Rupert quadrangles, Alaska: U.S. Geological Survey Miscellaneous Investigations Series, Map 1-1807, 1 sheet, scale 1:250,000.
- Brandon, M.T., Cowan, D.S., & Vance, J.A. 1988 The Late Cretaceous San Juan thrust system, San Juan Islands, Washington: Geological Society of America Special Paper 221, 81 p.
- Crawford, M.L., Hollister, L.S., & Woodsworth, G.J. 1987 Crustal deformation and regional metamorphism across a terrane boundary, Coast Plutonic Complex, British Columbia: *Tectonics*, v. 6, p. 343-361.
- Dahlen, F.A., & Suppe, J. 1988 Mechanics, growth, and erosion of mountain belts, in Clark, S.P., Burchfiel, B.C., Suppe, J., eds., *Processes in continental lithospheric deformation*: Geological Society of America Special Paper 218, p.161- 178.

- Farmer, G.L. & DePaolo, D.J. 1983 Origin of Mesozoic and Tertiary granite in the western United States and implications for pre-Mesozoic crustal structure - 1. Nd and Sr isotopic studies in the geocline of the Northern Great Basin: *Journal of Geophysical Research*, v. 88, p. 3379-3401.
- Garner, M.C., Bergman, S.C., Cushing, G.W., MacKevett, E.M., Plafker, G., Campbell, R.B., Dodds, C.J., McClelland, W.C., & Mueller, P.A. 1988 Pennsylvanian pluton stitching of Wrangellia and the Alexander terrane, Wrangell Mountains, Alaska: *Geology*, v. 16, p. 967-971,
- Gansser, A. 1964 *Geology of the Himalayas*: London, Wiley - Interscience, 289 p.
- Gehrels, G.E. & Saleeby, J.B. 1987a Geologic framework, tectonic evolution, and displacement history of the Alexander terrane: *Tectonics*, v. 6, p. 151-173.
- , & Saleeby J.B. 1987b *Geology of Prince of Wales Island, southeastern Alaska*: Geological Society of America Bulletin, v. 98, p. 123-137.
- , McClelland, W.C., Samson, S.D., Patchett, P.J. & Jackson, J.L. 1990 Ancient continental margin assemblage in the northern Coast Mountains, southeast Alaska and northwest Canada: *Geology*, v. 18, p.208-211.
- Hammarstrom, J.M. & Zen, E. 1986 Aluminum in hornblende: An empirical igneous geobarometer: *American Mineralogist*, v. 71, p. 1297-1313.
- Harland, W.B., Cox, A.V., Lewellyn, P.G., Pickton, C.A.G., Smith, A.G. & Walters, R. 1982 *A Geologic time scale*: Cambridge, England, Cambridge University Press, 131 p.
- Harrison, T.M. 1981 The diffusion of ^{40}Ar in hornblende: *Contributions to Mineralogy and Petrology*, v. 78, p. 324-331.
- & McDougall I. 1980 Investigations of an intrusive contact, northwest Nelson, New Zealand-I. Thermal, chronological, and isotopic constraints: *Geochimica et Cosmochimica Acta*, v. 44, p. 1985-2003.
- Hollister, L.S. 1982 Metamorphic evidence for rapid uplift of a portion of the central gneiss complex, Coast Mountains, B.C.: *Canadian Mineralogist*, v. 20, p. 319-332.

- & Crawford, M.L. 1986 Melt-enhanced deformation: A major tectonic process: *Geology*, v. 14, p. 358-561.
- Huang, W.L. & Wyllie, P.J. 1986 Phase relationships of gabbro-tonalite-granite-water at 15 kb with applications to differentiation and anatexis: *Am. Mineral.* v. 71, p. 301-316.
- Jordan, T., Isacks, B., Allmendinger, R., Brewer, J., Ramos, V. & Ando, C. 1983 Andean tectonics related to the geometry of the subducted plate: *Geological Society of America Bulletin*, v. 94, p. 341-346.
- Kistler, R.W. & Peterman, Z.E. 1973 Variations in Sr, Rb, K, Na and initial $^{87}\text{Rb}/^{86}\text{Sr}$ in Mesozoic granitic rocks and intruded wall rocks in central California: *Geological Society of America Bulletin*, v. 84, p. 3489-3512.
- McClelland, W.,C., Gehrels, G.E., Samson, S.D. & Patchett, P.J. 1990 Geologic and structural relations along the western flank of the Coast Mountains batholith: Stikine River to Cape Fanshaw, central SE Alaska: *Geological Society of Canada Abstract with Programs*, in press.
- Miller, M.M. 1987 Dispersed remnants of a northeast Pacific fringing arc -- Upper Paleozoic island arc terrane of Permian McCloud faunal affinity, western U.S.: *Tectonics*, v. 6, p. 807-830.
- Molnar, P. 1984 Structure and tectonics of the Himalaya: Constraints and implications of geophysical data: *Ann. Rev. Earth Planet. Sci.*, v. 12, p. 489-518.
- Monger, J.W.H. & Berg, H. 1987 Lithotectonic terrane map of western Canada and southeastern Alaska: U.S. Geological Survey Miscellaneous Field Studies Map MF 1874B, scale 1:2,500,000.
- , & Price, R.A. 1979 Geodynamic evolution of the Canadian Cordillera - progress and problems: *Canadian Journal of Earth Science*, v. 16, p. 770-791.
- , Price, R.A. & Tempelman-Kluit, J.D. 1982 Tectonic accretion and the origin of the two major metamorphic and plutonic belts in the Canadian Cordillera: *Geology*, v. 10, p. 70-75.
- , Clowes, R.M., Price, R.A., Simony, P.S., Riddihough, R.P. & Woodsworth, G.J. 1985 B-2 Juan de Fuca plate to the Alberta plains: *Geological Society of America Decade of North American Geology Centennial Continent/Ocean Transect 7*, scale 1:1,000,000, 21 p.

- Muller, J.E. & Jeletzky, J.A. 1970 Geology of the Upper Cretaceous Nanaimo Group, Vancouver Island and Gulf Islands, British Columbia: Geological Survey of Canada Paper 69-27, 77 p.
- Pavlis, T. 1989 Middle Cretaceous orogenesis in the northern Cordillera: A mediterranean analog: *Geology*, v. 17, p. 947-950.
- Philip, H. & Megard, F. 1977 Structural analysis of the superficial deformation of the 1969 Pariahuanca earthquake (central Peru): *Tectonophysics*, v. 38, p. 259-278.
- Royden, L. & Burchfiel, B.C. 1989 Arc systematic variations in thrust belt style related to plate boundary processes? (The western Alps versus the Carpathians): *Tectonics*, v. 8, p. 51-61.
- Rubin, C.M & Saleeby, J.B. 1987a The inner boundary zone of the Alexander terrane in southern SE Alaska: A newly discovered thrust belt: *Geological Society of America Abstracts with Programs*, v. 19, p. 455.
- & Saleeby, J.B. 1987b The inner boundary zone of the Alexander terrane in southern SE Alaska, Part 1: Cleveland Peninsula to southern Revillagigedo Island: *Geological Society of America Abstracts with Programs*, v. 19, p. 826.
- & Saleeby, J.B. 1988 A new perspective on what is the Taku terrane in southern SE Alaska: *Geol. Soc. Am. Abst. with Prgms.*, v. 20, p. 226.
- & McClelland, W.C. 1989 The Gravina Belt: Remnants of a mid-Mesozoic oceanic arc in southern southeast Alaska: *Eos, Transactions, American Geophysical Union*, p. 1308.
- , Saleeby, J.B., Cowan, D.S., McGroder M.F. & Brandon, M.T. 1990 Late Mesozoic compressional tectonism: Development of a west-vergent thrust system in the northwestern Cordillera: *Geology*, v. 18, p. 276-280..
- , Miller, M.M. & Smith, G.M. 1990 Tectonic development of Cordilleran mid-Paleozoic volcano-plutonic complexes, in Harwood, D.S., and Miller, M.M., eds., *The paleogeography of the Klamath Mountains, Sierra Nevada, and adjacent areas: Geological Society of America Special Paper 255*, in press.
- Saleeby, J.B. 1983 Accretionary tectonics of the North American Cordillera: *Annual. Reviews in Earth and Planetary Sciences*, v. 15, p. 45-73.

- , & Rubin, C.M. 1989 The western margin of the Coast Plutonic Complex (CPC) in southernmost SE Alaska: *Geol. Soc. Am. Abst. with Prgms.*, v. 21, p. 139.
- Samson, S.D., McClelland, W.C., Patchett, P.J. & Gehrels, G.E. 1989 Nd isotopes and Phanerozoic crustal genesis in the Canadian Cordillera: *Nature*, v. 337, p.705-709.
- Smith, J.G. & Diggles, M.F. 1981 Potassium-argon determinations in the Ketchikan and Prince Rupert quadrangles, southeastern Alaska: *U.S. Geological Survey Open-File Report 78-73N*, p. 1-6.
- Suarez, G., Molnar, P. & Burchfiel, B.C. 1983 Seismicity, fault plane solutions, depth of faulting, and active tectonics of the Andes of Peru, Ecuador, and southern Columbia: *Journal of Geophysical Research*, v. 88, p. 10403-10428.
- Sutherland-Brown, A 1968 *Geology of the Queen Charlotte Islands British Columbia*, British Columbia Department of Mines and Petroleum Resources Bulletin 54, 226 p.
- Sutter, J.F. & Crawford, M.L. 1985 Timing of metamorphism and uplift in the vicinity of Prince Rupert, British Columbia and Ketchikan, Alaska: *Geol. Soc. Am. Abst. with Prgms.*, v 17, p. 411.
- Yagishita, K. 1985 Evolution of a provenance as revealed by petrographic analyses of Cretaceous formations in the Queen Charlotte Islands, British Columbia, Canada: *Sedimentology*, v. 32, p. 671-684.
- Yorath, C.J., Woodsworth, G.J., Riddihough, R.P., Currie, R.G., Hyndman, R.D., Rogers, G.C., Seemann, D.A. & Collins, A.D. 1985 Continent - Ocean transect B1: Intermontane Belt (Skeena Mountains) to Insular Belt (Queen Charlotte Islands): *Geological Society of America Decade of North American Geology Centennial Continent/Ocean Transect 8*, scale 1:1,000,000, 7 p.
- Wheeler, J.O., Brookfield, A.J., Gabrielse, H., Monger, J.W.H., Tipper, H.W. & Woodsworth, G.J. 1988 Terrane map of the Canadian Cordillera: *Canadian Geological Survey Open-File Report 1894*, scale 1:2,000,000.

Zen, E. 1988 Tectonic significance of high-pressure plutonic rocks in the westerns Cordillera of North America p. 41-68, in Ernst, W.G., ed., Metamorphism and crustal evolution of the western United States, Rubey volume VII, Prentice Hall, Englewood Cliffs, New Jersey. W

CHAPTER 6

REGIONALLY EXTENSIVE MID-CRETACEOUS WEST-VERGENT THRUST SYSTEM IN THE NORTHWESTERN CORDILLERA: IMPLICATIONS FOR CONTINENT-MARGIN TECTONISM

C.M. Rubin, J.B. Saleeby, D.S. Cowan, M.T. Brandon, and M.F. McGroder.

published in Geology, March, 1990

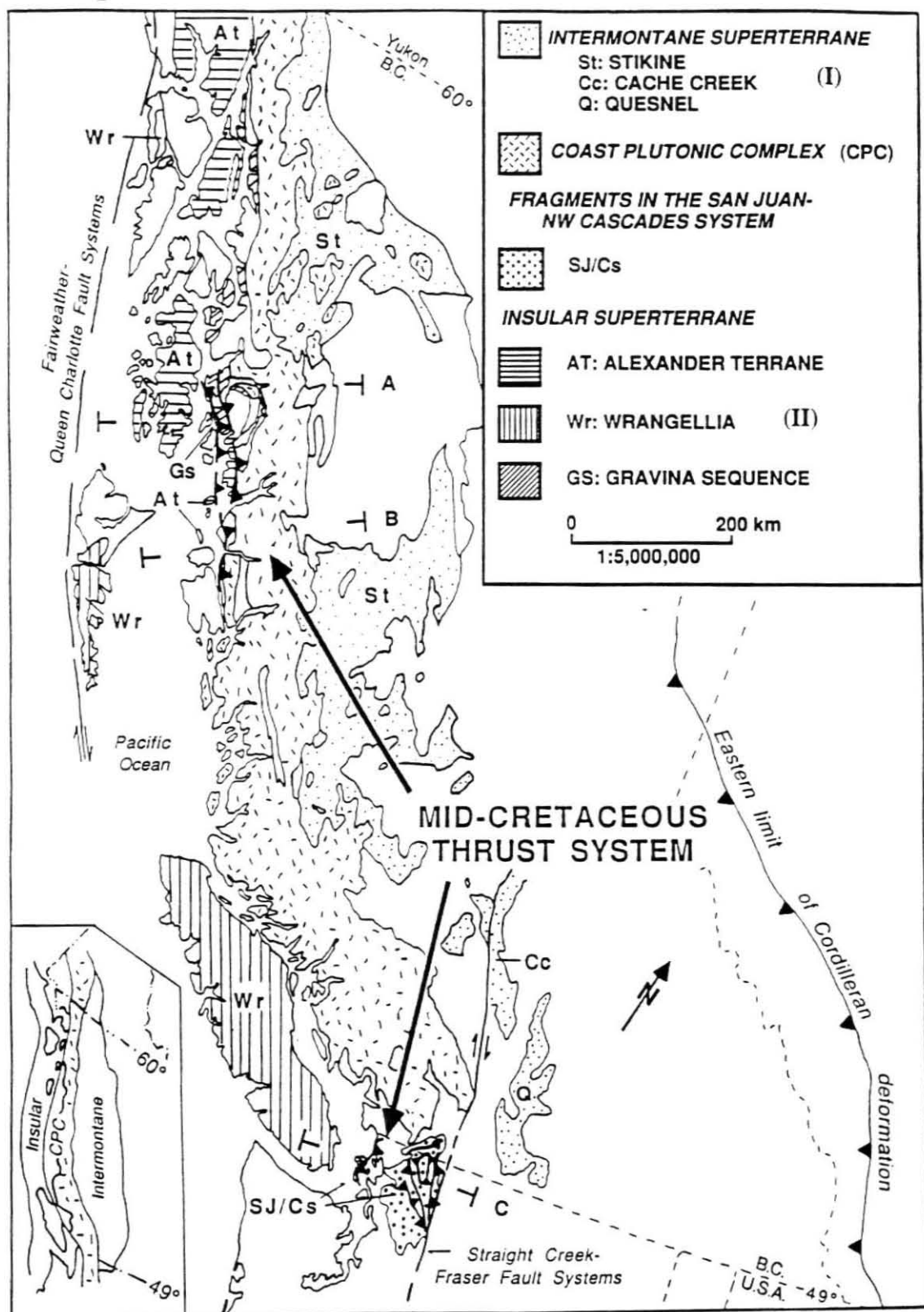
ABSTRACT

The Intermontane-Insular superterrane boundary zone represents a fundamental crustal boundary separating the two largest allochthonous crustal fragments in the North American Cordillera. Structural, stratigraphic, and geochronologic relations along this boundary indicate that substantial west-vergent compression and concomitant crustal thickening occurred there in mid-Cretaceous time. This orogenic zone extends for more than 1200 km along strike length, between southern southeast Alaska and northern Washington. In southern southeast Alaska and northwest British Columbia, rocks of the Insular superterrane were imbricated along a series of west- to southwest-vergent thrust faults. In northern Washington and southwestern British Columbia a wide zone encompassing the margins of the two superterrane as well as numerous intervening smaller fragments was shortened principally along west-vergent thrusts. Known geologic relations do not discriminate among existing tectonic models that explain the origin of the mid-Cretaceous thrust system.

INTRODUCTION

Mesozoic high-grade metamorphism and magmatism have long been documented in the northwestern Cordillera and were accompanied by thrust faulting. We propose that a mid-Cretaceous thrust system extends for more than 1200 km along strike, between southern southeast Alaska and northern Washington. Deformation affected rocks that range in age from Early Paleozoic to mid-Cretaceous. Collectively, these rocks mostly belong to the Intermontane and Insular superterrane (terrane I and II of Monger et al., 1982; Fig. 1). We review structural, stratigraphic, and geochronologic relations that suggest that a west-vergent fold and thrust system developed along the boundary between the two superterrane from

Figure 1. Distribution of mid-Cretaceous thrust system in northwestern Cordillera after Brandon et al. (1988); Brandon (1989); Crawford et al. (1987); Rubin and Saleeby (1987a, and 1987b). Terranes I and II of Monger et al. (1982).



about 100 to 85 Ma and involved both crystalline basement and supracrustal rocks.

TECTONIC FRAMEWORK

Many of the lithotectonic elements constituting the western Cordillera between lat. 40° and 60°N can be grouped into the Intermontane and Insular superterrane (Fig. 1). The composite Intermontane superterrane consists of Stikine, Cache Creek, and Quesnel terranes and was accreted to North America in Middle Jurassic time (Monger et al., 1982), and thus formed the western margin of the continent during the Cretaceous. The Insular superterrane consists of the Wrangellia and Alexander terranes and lies parallel to and west of the Intermontane superterrane. North of 49°N, the boundary between the two is largely obscured by the Coast Plutonic Complex, whereas to the south, the superterrane are separated partly by the crystalline core of the north Cascades, including the Skagit metamorphic suite.

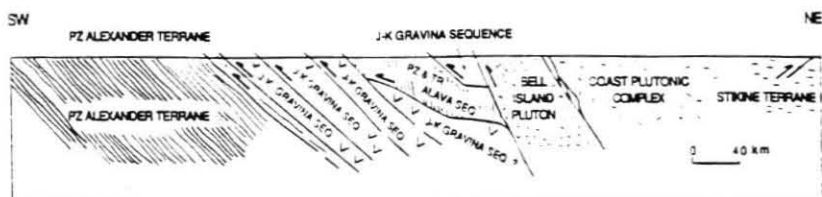
Together with earlier work (Misch, 1966; Crawford and others, 1987), our geologic field studies in southern southeast Alaska and northern Washington show that contemporaneous mid- to Late Cretaceous west-vergent thrust faulting occurred locally along parts of the superterrane boundary (Fig. 1). In southern southeast Alaska, the thrust belt is localized along the eastern edge of the Alexander terrane and consists of an imbricate series of west-vergent thrust sheets with a total structural thickness of more than 20 km (Fig. 2A; Rubin and Saleeby, 1987a). West-vergent folds and thrust faults are present along the inner boundary zone of the Alexander terrane, near Prince Rupert, British Columbia (Fig. 2B; Crawford and others, 1987). In the San Juan Islands and northwest Cascades, an imbricate west-vergent thrust system (Fig. 2C; Brandon et al., 1988) affects a variety of terrane including some probably derived from the two superterrane. Compressional deformation and regional metamorphism that affected the two superterrane are complex and vary in detail along strike of the boundary; however, the similarities in structural styles and timing of thrusting are remarkable.

SOUTHERN SOUTHEAST ALASKA

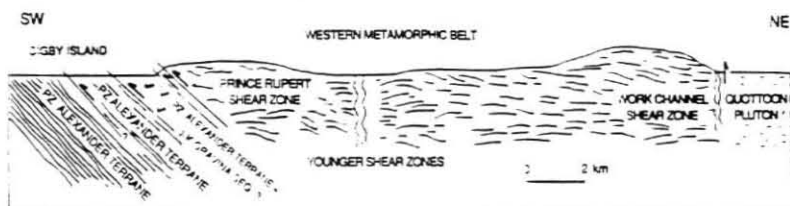
The Insular superterrane in southern southeast Alaska consists of the lower Paleozoic to lower Mesozoic Alexander terrane, the Upper Jurassic-Lower Cretaceous Gravina sequence, and the upper

Figure 2. Structural transects across the mid-Cretaceous thrust system. PZ = Paleozoic, P = Permian, MZ = Mesozoic, TR = Triassic, J = Jurassic, K = Cretaceous, UK = Upper Cretaceous. A: After Rubin and Saleeby (1987a, 1987b) and unpublished mapping by Rubin and Saleeby. B: After work of Crawford et al., (1987). C: After Brandon et al. (1988) and Brandon (1989). Locations of cross sections are shown in Figure 1.

A. SOUTHERN SOUTHEAST ALASKA - CLEVELAND PENINSULA

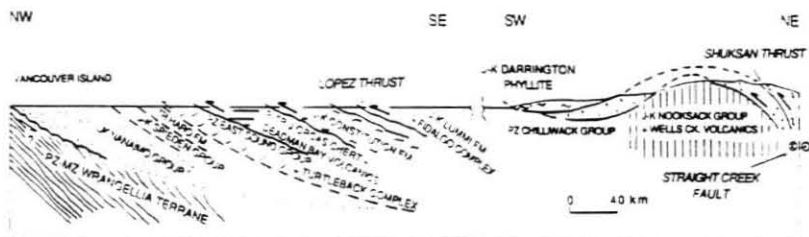


B. WESTERN BRITISH COLUMBIA - PRINCE RUPERT AREA



C. SAN JUAN ISLANDS

NORTHWEST CASCADES & FOOTHILLS



Paleozoic and lower Mesozoic Alava sequence, which includes metavolcanic rocks, marble, and argillite formerly assigned to parts of the Taku terrane (Monger and Berg, 1987; Berg et al., 1988). In most areas, rocks of the Alexander terrane are only slightly deformed and are not highly metamorphosed (Gehrels and Saleeby, 1987a), except along the eastern margin where they are overprinted by mid-Cretaceous compressional structures (Saleeby et al., 1985; Rubin and Saleeby, 1987a). East of and depositionally overlying the Alexander terrane lies the Upper Jurassic to Lower Cretaceous Gravina sequence which consists of marine pyroclastic and volcanoclastic debris and epiclastic rocks (C. Rubin and J. Saleeby, unpublished mapping), although the depositional nature of the contact has been questioned by Brew and Karl (1987). The youngest fossils obtained from the Gravina sequence in the Ketchikan region are Albian in age (Berg et al., 1972). Structurally overlying the Alexander terrane and the Gravina sequence is the Alava sequence. The Alava sequence is also depositionally overlain by the Gravina sequence; however, in most places the contact is an east-dipping thrust fault in southern southeastern Alaska (C. Rubin and J. Saleeby, unpublished mapping).

The Alexander terrane and the Gravina and Alava sequences were intruded by mafic-ultramafic complexes, epidote-bearing tonalite, quartz diorite and granodiorite plutons. The plutons, sills and dikes range in age from 101 to 89 Ma (Pb-U ages on zircon; Rubin and Saleeby, 1987a, 1987b; Arth et al., 1988). All these plutons crosscut the earlier regional metamorphic fabric; 95-101 Ma plutons are cut by thrust faults, and 90 Ma plutons crosscut thrust faults. A belt of Late Cretaceous to Early Paleocene plutons occurs east of the thrust belt (Smith and Diggles, 1981); fabrics in these younger rocks reflect Tertiary deformation. Mesozoic and Tertiary fabrics are differentiated by orientation and their relations to radiometrically dated plutons.

Our regional studies in the Ketchikan area indicate that rocks of the Alexander terrane and the Gravina and Alava sequences were imbricated along a series of west-vergent thrust sheets (Fig. 2a; Berg et al., 1988). The structurally lowest thrust sheets consist of lower Paleozoic schist, marble, and meta-igneous rocks of the Alexander terrane. Low to medium greenschist facies rocks of the Gravina sequence structurally overlie the Alexander terrane; the sequence consists of six separate east-dipping thrust sheets. Higher grade Alava-sequence schist and imbricated Gravina sequence occupy higher structural positions.

Mesoscopic deformation is characterized by folding, cleavage formation, and thrust faulting. Mesoscopic asymmetric folds are related to a northeast-dipping axial planar cleavage. The mesoscopic folds are associated with moderately dipping ductile thrust faults. Together, these structures and fabrics record widespread compressional deformation and a protracted history of crustal shortening. Syntectonic metamorphism ranges from lower greenschist to amphibolite facies. Increasing strain and metamorphic grade occur structurally upward.

Age constraints for the timing of deformation come from the relation between plutons and regional structural fabrics. Locally, mylonitic tonalite and granodiorite crosscut metamorphic fabrics associated with folding and are in turn cut by thrust faults. These plutons yield ages from 95 to 101 Ma (Pb-U ages on zircon, Arth et al., 1988; Rubin and Saleeby, 1987a, 1987b). Granodiorite plutons that crosscut thrust faults yield Pb-U zircon ages of 89 to 91 Ma (Arth et al., 1988; Rubin and Saleeby, 1987a). Thus, thrust faulting was still active during or after 95 Ma and terminated by 90 Ma. On the basis of our geochronologic constraints, the age of the youngest strata involved in deformation (Berg et al., 1972), and the geologic time scale of Harland et al. (1982), thrust faulting must have begun between Albian and Early Cenomanian time and ceased by the Turonian. Geochemical and isotopic data indicate that all the intrusive rocks have continental-arc-related magmatic affinities (Arth et al., 1988), suggesting an intra-arc setting for the mid-Cretaceous deformation.

WESTERN BRITISH COLUMBIA

Two of the lithotectonic assemblages described above from southern southeast Alaska are also represented in the mountains west of Prince Rupert, British Columbia. Low-grade metamorphic rocks of the westernmost western metamorphic belt are correlated with the Alexander terrane (Fig. 1; Woodsworth et al., 1983; Woodsworth and Orchard, 1985). These rocks are overlain by carbonaceous argillite and conglomerate which are similar to rocks of the Gravina sequence exposed in the Ketchikan area (Crawford et al., 1987). All these rocks are affected by thrust faults and associated west-vergent folds (Fig. 2B; Crawford and Hollister, 1982; Crawford et al., 1987). Metamorphic grade increases from west to east, with the highest grade rocks occupying the highest structural levels (Crawford and Hollister, 1982). The mid-Cretaceous

Ecstall pluton is intruded into kyanite-bearing schist and migmatitic gneisses which form the structurally highest thrust sheets (Crawford et al., 1987). Magmatic flow lineation and oriented mafic inclusions within the Ecstall pluton are parallel to both the pluton margin and the regional foliation of the surrounding country rock and are thought to be syntectonic fabrics (Crawford and Hollister, 1982; Crawford et al., 1987).

Constraints for the timing of deformation come from mid- to Late Cretaceous plutons. The Ecstall pluton was generated and emplaced during thrust faulting and associated deformation (Crawford et al., 1987), and yields a Pb-U zircon age of 98 ± 4 Ma (Woodsworth et al., 1983). K/Ar biotite cooling ages of 96 and 84 Ma from nondeformed plutons (Hutchison, 1982) give a minimum age for the cessation of deformation and metamorphism in the westernmost part of the thrust belt.

To the west, in the Queen Charlotte Islands, the mid- to Upper Cretaceous rocks of the Queen Charlotte Group consist of marine and nonmarine sandstone, conglomerate, and shale (Sutherland-Brown, 1968). Provenance and paleocurrent indicators suggest an eastern source made up of volcanoclastic and plutonic debris shed off the flanks from an active magmatic arc and its basement complex (Sutherland-Brown, 1968; Yagishita, 1985). The Upper Cretaceous foredeep deposits of the Queen Charlotte Group probably represent late orogenic sediments that were derived from the thrust system.

In both southern southeast Alaska and western British Columbia, mid-Cretaceous regional-scale deformation affected rocks of the Insular superterrane. Emplacement of mid-Cretaceous arc-related quartz-diorite, tonalite, and granodiorite plutons was broadly synchronous with this deformation, suggesting an intra-arc setting for the mid-Cretaceous deformation. Thrust-related deformation in southeast Alaska is constrained as pre-Turonian and, in western British Columbia, as pre-Cenomanian.

NORTHWESTERN WASHINGTON AND SOUTHERN BRITISH COLUMBIA

In northern Washington and southern British Columbia, the San Juan-northwest Cascades thrust system consists of thrust sheets lying west of the steeply dipping Straight Creek-Fraser fault (Fig. 1; Misch, 1966; Brown, 1987; Brandon et al., 1988; Brandon, 1989; Journeay, 1989). Thrust sheets contain diverse rock units ranging in age from early Paleozoic to latest Early Cretaceous. In the San Juan Islands,

the stacking order, from structurally lowest to highest, is as follow: lower to upper Paleozoic tonalite, gabbro, and volcanogenic rocks of the Turtleback terrane; Permian to Lower Jurassic chert, basalt and limestone of the Deadman terrane; Upper Jurassic to Lower Cretaceous volcanoclastic sedimentary rocks and interbedded chert and basalt of the Constitution Formation; and the Decatur terrane, including the Middle-Late Jurassic Fidalgo ophiolite and its upper Mesozoic clastic cover (Fig. 2C; Brandon et al., 1988). Thrust sheets in the northwest Cascades include (Fig. 2C) Middle Jurassic(?) Wells Creek Volcanics and their volcanoclastic cover of Upper Jurassic and Lower Cretaceous Nooksack group; upper Paleozoic and Triassic Chilliwack Group and overlying strata; and, structurally highest, the Shuksan Metamorphic Suite, comprising Jurassic (?) metasedimentary and metabasaltic rocks that were metamorphosed to greenschist or blueschist facies during the Late Jurassic and Early Cretaceous (Misch, 1966; McGroder and Miller, 1989). Most of the rocks in the thrust system record high P/low T metamorphism, which resulted from tectonic burial that accompanied contractional imbrication and crustal thickening.

The age of thrusting is based on several lines of evidence. In the San Juan Islands, the youngest rocks involved in the deformation are Late Albian age (99-101 Ma, time scale of Harland et al., 1982). Santonian (ca. 84 Ma) strata of the Nanaimo Group, which mostly postdate thrusting, contain clasts derived from some of the metamorphosed units in the thrust sheets (Brandon et al., 1988). In the Cascades, east of the Straight Creek Fault, the 88 Ma Mount Stuart batholith (Pb-U zircon; J. Magloughlin, personal commun., 1988; analyzed by P. van der Heyden) intruded a post-96 Ma thrust fault (Miller, 1985). All available evidence suggests that the major episode of thrusting occurred between 90 and 100 Ma.

The San Juan-northwest Cascades thrust system formed a wedge that was emplaced westward over the Wrangellia terrane (Insular superterrane) in mid-Cretaceous time. This interpretation concurs with that of Misch (1966) in that the overall vergence of the system was toward the west; in contrast, Brown (1987) proposed north-northwestward tectonic transport. The Intermontane superterrane *sensu stricto* lies about 100 km east of the easternmost preserved remnants of the thrust system. The Intermontane superterrane, however, is thought to have formed the hanging wall to the thrust system (Brandon et al., 1988). The Intermontane superterrane and the thrust system are now separated by the uplifted core of the North Cascades (Skagit Metamorphic Suite of Misch, 1966; Fig. 2). Viewed broadly, the San Juan-northwest Cascades

system constitutes a wide, internally imbricated, lithologically diverse zone separating the two superterrane. Some pre-Cretaceous lithotectonic units in the thrust system (e.g., the Chilliwack Group and the Deadman Bay terrane) have tectonic affinity to rocks of the Intermontane superterrane (Brandon et al., 1988). During the mid-Cretaceous, they were imbricated with non-Intermontane lithologies. The Mount Stuart and related 80-90 Ma plutons represent a magmatic arc that was constructed across the newly formed contractional orogen.

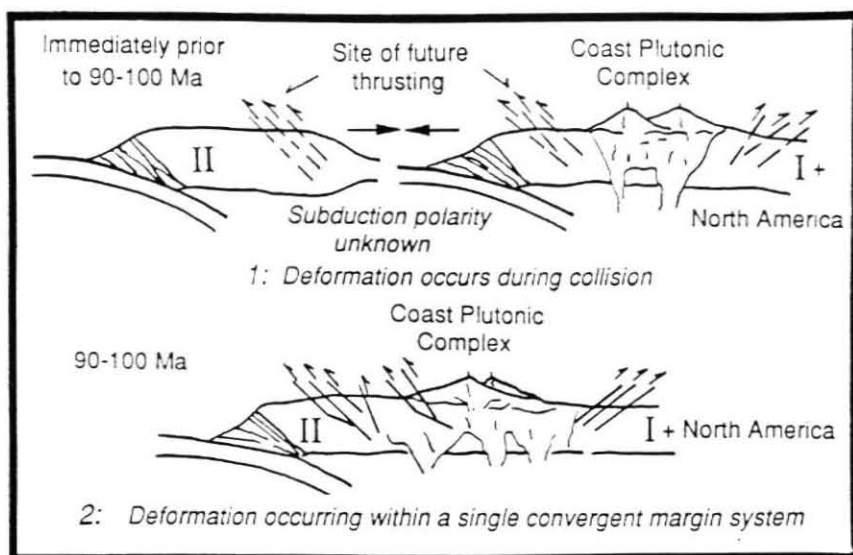
DISCUSSION

Similarities in structural style, vergence, and age of deformation among thrust systems in southeast Alaska, western British Columbia and northwestern Washington-southwestern British Columbia suggest that they are parts of a mid-Cretaceous orogenic zone that spanned at least 1200 km. Coeval east-vergent thrusting and folding are now documented in a parallel belt, east of the orogen, from north-central British Columbia (Tipper, 1969; Rusmore and Woodsworth, 1988) to north-central Washington (McGroder and Miller, 1989).

Mid-Cretaceous fold development and thrust faulting were broadly coeval with arc magmatism in that calc-alkaline plutonism occurred shortly before, perhaps during, and shortly after the structures were developed; however, older fabrics are locally present. Mid-Cretaceous plutons that are coeval with thrust faulting occur in western British Columbia (Crawford et al., 1987) and in southern southeast Alaska (Rubin and Saleeby, 1987a, 1987b). Younger plutons are more widespread. Calc-alkalic plutons that crosscut the deformational fabrics are present within both superterrane. Such magmatism persisted intermittently until at least the Eocene (Armstrong, 1988).

Two models that incorporate existing ideas explain the origin of the mid-Cretaceous thrust belt and are compatible with our current understanding of the magmatic history of the northwestern Cordillera (Fig. 3). Model 1 implies the existence of an intervening subduction zone and marginal basin between the Insular superterrane and the western margin of North America (Fig. 3). Evidence of a pre-Cretaceous subduction zone within the intervening marginal basin is not preserved, perhaps because of extensive crustal shortening. The closure along this postulated subduction zone marks the collision of the two superterrane.

Figure 3. Tectonic models for origin of mid-Cretaceous deformation within Coast Plutonic Complex. I = Intermontane superterrane; II = Insular superterrane. Model 1 adapted from Goodwin (1975) and Monger et al. (1982). Model 2 adapted from Berg et al. (1972), Monger and others (1972), Armstrong, (1988), and Van der Heyden and Woodsworth, (1988).



In this context, deformation can be viewed as a result of a collisional orogeny involving the collapse of a marginal basin system that separated the Insular superterrane from the western margin of North America. In light of the synchronicity of deformation along strike, a collisional origin implies that (1) prior to mid-Cretaceous time, the two superterrane must have been roughly parallel and had nearly linear edges, and (2) an ocean basin existed that was small and elongate parallel to the superterrane.

Model 2 implies that mid-Cretaceous crustal shortening and magmatism occurred in an intra-arc setting, above a single, east-dipping subduction zone (Fig. 3). Arc magmatism and deformation involved the collapse of a series of marginal basins and a magmatic arc. This model implies that the intervening basins were small and their collapse was not necessarily accommodated by a separate subduction zone. Deformation may have been related to changes in velocity and direction of plate motions and was a direct consequence of subduction beneath the edge of the continental margin. In this context, the thrust system overprinted the older tectonic boundary between the Insular superterrane and the North American margin. Compressional deformation was broadly coeval with arc magmatism, and thus reflects intra-arc tectonism.

In either model, subsequent to mid-Cretaceous deformation, the locus of arc magmatism migrated to the east (Armstrong, 1988) and was superimposed along the boundary between the two superterrane. The Coast Plutonic Complex was intruded along this boundary zone in response to ongoing east-dipping subduction. Synorogenic to post orogenic marine and nonmarine foredeep sequences, represented by the Upper Cretaceous Queen Charlotte and Nanaimo Groups, record westward dispersal of sediments derived from the uplifted thrust belt.

CONCLUSIONS

Structural, stratigraphic, and geochronologic relations along the Insular-Intermontane superterrane boundary suggest that a predominantly west-vergent fold and thrust belt affected the tectonic boundary between two large crustal fragments in southeast Alaska, western British Columbia, and northern Washington. This west-vergent thrust belt spans at least 1200 km in strike length. Radiometric and stratigraphic age constraints bracket thrust faulting between 101 and 88 Ma. A major continental arc subsequently formed just east of the locus of the thrust system. This arc is represented by the mid-

Cretaceous to Eocene component of the Coast Plutonic Complex. Two existing models may explain this deformation: (1) crustal shortening is attributed to the collision of the Insular superterrane to the western North American margin (e.g., Intermontane superterrane), and (2) crustal shortening occurred in an intra-arc setting following the accretion of the Insular superterrane.

REFERENCES CITED

- Armstrong, R.L., 1988, Mesozoic and early Cenozoic magmatic evolution of the Canadian Cordillera, *in* Clark, S.P., Jr., et al., eds., Processes in continental lithospheric deformation: Geological Society of America Special Paper 218, p. 55-91.
- Arth, J.G., Barker, F., and Stern, T.W., 1988, Coast Batholith and Taku plutons near Ketchikan, Alaska: Petrography, geochronology, geochemistry, and isotopic character: American Journal of Science, v. 288-A, p. 461-489.
- Berg, H.C., Jones, D.L., and Richter, D.H., 1972, Gravina-Nutzotin belt: Tectonic significance of an upper Mesozoic sedimentary and volcanic sequence in southern and southeastern Alaska: U.S. Geological Survey Professional Paper 800-D, p. 1-24.
- Berg, H.C., Elliott, R.L., and Koch, R.D., 1988a, Geologic map of the Ketchikan and Prince Rupert quadrangles, southeastern Alaska: U.S. Geological Survey Miscellaneous Investigations Series Map 1-1807, 1 sheet, scale 1:250,000.
- Brandon, M.T., 1989, Geology of the San Juan-Cascade nappes, northwestern Cascade Range and San Juan Islands, *in* Joseph, N.L., et al., eds., Geologic guidebook for Washington and adjacent areas: Washington Division of Geology and Earth Resources Information Circular 86, p. 137-151.
- Brandon, M.T., Cowan, D.S., and Vance, J.A., 1988, The Late Cretaceous San Juan thrust system, San Juan Islands, Washington: Geological Society of America Special Paper 221, 81 p.
- Brew, D.A., and Karl, S.M., 1987, A reexamination of the contacts and other features of the Gravina Belt, southeastern Alaska: U.S. Geological Survey Circular 1016, p. 143-146.

- Brown, E.L., 1987, Structural geology and accretionary history of the Northwest Cascades system, Washington and British Columbia: Geological Society of America Bulletin, v. 99, p. 210-214.
- Crawford, M.L., and Hollister, L.S., 1982, Contrast of metamorphic and structural histories across the Work Channel Lineament, Coast Plutonic Complex, British Columbia: Journal of Geophysical Research, v. 87, p. 3849-3860.
- Crawford, M.L., Hollister, L.S., and Woodsworth, G.J., 1987, Crustal deformation and regional metamorphism across a terrane boundary, Coast Plutonic Complex, British Columbia: Tectonics, v. 6, p. 343-361.
- Gehrels, G.E., and Saleeby, J.B., 1987a, Geology of Prince of Wales Island, southeastern Alaska: Geological Society of America Bulletin, v. 98, p. 123-137.
- 1987b, Geologic framework, tectonic evolution, and displacement history of the Alexander terrane: Tectonics, v. 6, p. 151-173.
- Goodwin, C.I., 1975, Imbricate subduction zones and their relationship with Upper Cretaceous to Tertiary porphyry deposits in the Canadian Cordillera: Canadian Journal of Earth Sciences, v. 12, p. 1362-1378.
- Harland, W.B., Cox, A.V., Lewellyn, P.G., Pickton, C.A.G., Smith, A.G., and Walters, R., 1982, A Geologic time scale: Cambridge, England, Cambridge University Press, 131 p.
- Hutchison, W.W., 1982, Geology of the Prince Rupert-Skeena Map area, British Columbia: Geological Survey of Canada Memoir 394, 116 p.
- Journeay, J.M., 1989, Late Mesozoic and Cenozoic fault systems of the southern coast belt: Geological Society of America Abstracts with Programs, v. 21, no. 5, p. 99.
- McGroder, M.F., and Miller, R.B., 1989, Geology of the eastern north Cascades, in Joseph, N.L., et al., eds., Geologic guidebook for Washington and adjacent areas: Washington Division of Geology and Earth Resources Information Circular 86, p. 97-111.
- Miller, R.B., 1985, The ophiolitic Ingalls Complex, north-central Cascade Mountains, Washington: Geological Society of America Bulletin, v. 96, p. 27-42.

- Misch, P., 1966, Tectonic evolution of the northern Cascades of Washington, *in* A symposium on the tectonic history and mineral deposits of the western Cordillera in British Columbia and neighboring parts of the United States: Canadian Institute of Mining and Metallurgy Special Volume 8, p. 101-148.
- Monger, J.W.H., and Berg, H., 1987, Lithotectonic terrane map of western Canada and southeastern Alaska: U.S. Geological Survey Miscellaneous Field Studies Map MF 1874B, scale 1:2,500,000.
- Monger, J.W.H., Souther, J.G., and Gabrielse, H., 1972, Evolution of the Canadian Cordillera: A plate tectonic model: *American Journal of Science*, v. 272, p. 577-602.
- Monger, J.W.H., Price, R.A., and Tempelman-Kluit, J.D., 1982, Tectonic accretion and the origin of the two major metamorphic and plutonic belts in the Canadian Cordillera: *Geology*, v. 10, p. 70-75.
- Rubin, C.M., and Saleeby, J.B., 1987a, The inner boundary zone of the Alexander terrane in southern SE Alaska: A newly discovered thrust belt: *Geological Society of America Abstracts with Programs*, v. 19, p. 455.
- 1987b, The inner boundary zone of the Alexander terrane in southern SE Alaska, Part 1: Cleveland Peninsula to southern Revillagigedo Island: *Geological Society of America Abstracts with Programs*, v. 19, p. 826.
- Rubin, C.M., Saleeby, J.B., Cowan, D.S., McGroder, M.F., and Brandon, M.T., 1988, Late Mesozoic compressional tectonism: Development of a west-vergent thrust system in the northwestern Cordillera: *Geological Society of America Abstracts with Programs*, v. 20, p. A110.
- Rusmore, M., and Woodsworth, G.W., 1988, A note on the Coast-Intermontane belt transition, Mount Waddington map area, British Columbia, *in* Current Research, Part E: Geological Survey of Canada Paper 89-1E, p. 163-176.
- Saleeby, J.B., Gehrels, G.E., and Berg, H. C., 1985, Character of the Alexander-Taku terrane boundary-Cape Fox to Cleveland Peninsula-SE Alaska: *Geological Society of America Abstracts with Programs*, v. 17, p. 406.
- Smith, J.G., and Diggles, M.F., 1981, Potassium-argon determinations in the Ketchikan and Prince Rupert quadrangles, southeastern Alaska: U.S. Geological Survey Open-File Report 78-73N, p. 1-6.

- Sutherland-Brown, A., 1968, Geology of the Queen Charlotte Islands, British Columbia, British Columbia Department of Mines and Petroleum Resources, Bulletin 54, 226 p.
- Tipper, H.W., 1969, Mesozoic and Cenozoic geology of the northeast part of Mount Waddington map-area (92N), Coast District, British Columbia: Geological Survey of Canada Paper 68-33, 103 p.
- Van der Heyden, P., and Woodsworth, G.J., 1988, Tectonic evolution of the Coast Plutonic Complex, British Columbia: Implications of new U-Pb and K-Ar dates: Geological Society of America Abstract with Programs, v. 20, p. A239.
- Woodsworth, G.J., and Orchard, M.J., 1985, Upper Paleozoic to lower Mesozoic strata and their conodonts, western Coast Plutonic complex, British Columbia: Canadian Journal of Earth Sciences, v. 22, p. 1329-1344.
- Woodsworth, G.J., Loveridge, W.D., Parrish, R.R., and Sullivan, R.W., 1983, Uranium-lead dates from the central Gneiss Complex and Ecstall pluton, Prince Rupert map area, British Columbia: Canadian Journal of Earth Sciences, v. 20, p. 1475-1483.
- Yagishita, Koji, 1985, Evolution of a provenance as revealed by petrographic analyses of Cretaceous formations in the Queen Charlotte Islands, British Columbia, Canada: Sedimentology, v. 32, p. 671-684.

ACKNOWLEDGMENTS

Parts of this research were supported by National Science Foundation Grants EAR 86-05386 and EAR 88-03834 (to Saleeby) and EAR 81-07654 and EAR 85-08239 (to Cowan); additional support (to Rubin) was provided by a Geological Society of America Penrose Grant, a Sigma-Xi grant-in-aid, and by the U.S. Geological Survey, Alaska Branch. We thank Maria Lucia Crawford, John Garver, Meghan Miller, Bill McClelland, Jim Monger, and Margi Rusmore for helpful discussions regarding Cordilleran tectonics, and Maria Lucia Crawford, Bill McClelland, and Peter van der Heyden for thorough and careful reviews of the manuscript.

APPENDIX 1

U-PB GEOCHRONOLOGIC METHODS

Laboratory methods

Zircon separation: Geochronologic samples collected from Revillagigedo Island, and Cleveland and Portland Peninsulas ranged from 15 to 70 kg of homogeneous rock that was sampled from a single outcrop. Zircons were separated from the rock mechanically and with heavy liquids, sieved to less than 165 microns, and separated magnetically on a Franz isodynamic separator. The least magnetic fractions (side-slope of 2° or less and a forward slope of 10°) were acid washed in warm concentrated HNO_3 for 30 minutes, and rinsed at least four times in warm distilled water followed by reagent-grade acetone. The zircon population was sieved in various size-fractions using silk screens that were disposed of after each use. Each zircon fraction analyzed was hand-picked under a binocular microscope, resulting in a population consisting of greater than 99% zircon. Zircons with composite grains, inclusions, fractures, etc., were removed from the population. The zircons were weighed (within 2%), placed into a previously cleaned Teflon (TFE) capsule, and rinsed in a warm ultraclean HNO_3 for 15 minutes.

Zircon dissolution and isolation of U and Pb: The procedures for dissolving zircon and isolating U and Pb are similar to those described by Krogh (1973). Significant changes from Krogh's procedure include: (1) the zircon is dissolved in HF and then redissolved in HCl in a Teflon capsule; (2) a mixed ^{235}U - ^{208}Pb tracer is added after the HCl solution has been aliquoted and the sample and spike are placed on a hot plate overnight to equilibrate; (3) uranium is removed from the columns with 0.5 N HBr, rather than H_2O ; and (4) a mixed ^{205}Pb - ^{230}Th - ^{235}U tracer is used for small samples (less than 3 mg) then added to a HF solution, diluted with concentrated HNO_3 , and then placed on a hot plate overnight to equilibrate. Finally, the solution is evaporated and re-equilibrated with 6N HCl overnight on a hot plate again.

Mass spectrometry: Isotopic analyses were conducted on either a 30.48 cm, 60°-sector Lunatic IV mass spectrometer with an accelerating voltage of ≈ 10 KV or a 35-cm VG 90° extended geometry-sector multicollector with an accelerating voltage of ≈ 8 KV. Pb was loaded with H_3PO_4 silica gel (Cameron and others, 1969) onto a previously outgassed rhenium filament and pre-heated in a laminar-flow hood. Isotopic data were collected during a 20-minute interval during which ^{208}Pb (or Pb^{205}), ^{207}Pb , and ^{206}Pb were measured on separate faraday cup collectors, and ^{204}Pb was measured on a separate Daly multiplier. Filament temperatures averaged 1350°C and the current signal averaged $\approx 10^{-11}$ amps (10^{-11} ohm resistor) of ^{206}Pb and decreased slightly during the course of the run. Uranium was loaded with H_3PO_4 and graphite and was analyzed as a uranium metal; filament temperatures were approximately 1800°C . Uranium isotopic data were collected on a multicollector faraday cup, with signal current ranging from $\approx 10^{-11}$ to 10^{-12} amps (10^{-11} ohm resistor). For most samples, 50 sets of isotope ratios were measured, with each measurement representing a 5-second integration. NBS Pb and U standards were routinely analyzed throughout the study and did not vary significantly from given NBS values (Tables A-1, A-2, and A-3).

Data analysis

The following values have been used in adjusting the measured isotopic ratios and in the age calculations:

(1) The composition and concentration of ^{235}U - ^{208}Pb tracer were measured and the compositions are as follows: $^{208}\text{Pb}/^{206}\text{Pb} = 1448 \pm 26$, $^{208}\text{Pb}/^{207}\text{Pb} = 4025 \pm 242$, $^{208}\text{Pb}/^{204}\text{Pb} = 9400 \pm 1128$ and $^{235}\text{U}/^{238}\text{U} = 17.27 \pm .05$.

The concentrations of Pb and U have been determined as follows: $7.6944 \text{ e } 10^{-7} \pm 1.8$ % Pb moles/gm, and $1.9804 \text{ e } 10^{-8} \pm 3$ % U moles/gm tracer.

(2) The composition and concentration of a mixed ^{205}Pb - ^{230}Th - ^{235}U tracer were measured and the compositions are as follows: $^{205}\text{Pb}/^{207}\text{Pb} = 3669 \pm 210$, $^{205}\text{Pb}/^{206}\text{Pb} = 3035 \pm 125$, $^{205}\text{Pb}/^{204}\text{Pb} = 12264 \pm 1200$, and $^{235}\text{U}/^{238}\text{U} = 2080 \pm 21$. The concentrations of Pb and

U have been determined as $0.4537 \times 10^{-9} \pm 6\%$ Pb moles/gm, and $2.78 \times 10^{-9} \pm 5\%$ U moles/gm.

(3) The isotopic composition of the unspiked aliquot has been adjusted for 0.04 ± 0.02 ng blank lead with a composition of $^{206}\text{Pb}/^{204}\text{Pb} = 18.78 \pm 0.30$ or $^{207}\text{Pb}/^{204}\text{Pb} = 15.61 \pm 0.22$, and $^{208}\text{Pb}/^{204}\text{Pb} = 38.5 \pm 0.60$. The amount of blank Pb was determined by isotope dilution analysis of a typical dissolution and chemical separation procedure without zircon. The blank composition has been determined through isotopic analysis of acids and dust particles in the lab.

(4) Blank U is in the 20 ng range which is negligible for U concentration determinations.

(5) The isotopic composition of the spiked aliquot has been adjusted for blank Pb by balancing both the $^{206}\text{Pb}/^{204}\text{Pb}$ and $^{206}\text{Pb}/^{207}\text{Pb}$ of the spiked and unspiked aliquots. Additional blank Pb in the spiked aliquot is assigned the composition cited above.

(6) Common Pb remaining after correction for blank Pb is interpreted as the initial Pb, and is assigned a composition of: $^{206}\text{Pb}/^{204}\text{Pb} = 18.0 \pm 1.5$, $^{207}\text{Pb}/^{204}\text{Pb} = 15.59 \pm 0.4$, $^{208}\text{Pb}/^{204}\text{Pb} = 37.8 \pm 2.0$ for Paleozoic samples, and 18.6 ± 1.5 , 15.6 ± 0.4 , and 38.0 ± 2.0 for Mesozoic samples. These values are from Doe and Zartman (1979).

(7) Constants used: $\lambda^{238} = 1.55125 \times 10^{-10}$; $\lambda^{235} = 9.8485 \times 10^{-10}$; and $^{238}\text{U}/^{235}\text{U}$ (atomic) = 137.88 (Jaffey, A.H., et al., 1971, Steiger and Jager, 1977).

Table A-1: Isotopic composition of lead in NBS 983 standard, measured by the VG mass spectrometer and other mass spectrometers at CIT, the University of California at Santa Barbara, and VG and Finnegan MAT factories. Internal precisions for all runs given as 1σ . Uncertainties for actual samples are probably higher, due to minor variations in sample purity.

SAMPLE	$^{206}\text{Pb}/^{204}\text{Pb}$	$^{206}\text{Pb}/^{207}\text{Pb}$	$^{206}\text{Pb}/^{208}\text{Pb}$
NBS 983 (given values):	2695 ± 145	14.0447 ± 79	73.43 ± 13
Lunatic II CIT 12 runs , 100 ng, JBS $ff = 1 \text{ } \mu\text{g}/\text{AMU}$	2729 ± 50	14.048 ± 10	73.43 ± 13
UCSB MAT 261 3 runs, 100 ng, JBS $ff = 1 \text{ } \mu\text{g}/\text{AMU}$	2751 ± 20	14.048 ± 8	73.142 ± 731
UCSB MAT 261 7 runs, (Mattinson, 1987)	2742	14.063	73.626
MAT 261 Factory with static JBS,50ng	2748 ± 21	14.0390 ± 9	73.346 ± 29
VG-354 Factory with static daly 10ng, JBS 100ng,JBS	2703 ± 16 2750 ± 10	14.0340 ± 6 14.0360 ± 2	73.057 ± 10 73.072 ± 7
VG SECTOR-MS 25ng, 7 runs, JBS	2729	14.0400	73.053
VG SECTOR-MS 25ng, 20 runs, CMR (Std. error %)	2708 (.043)	14.047 (.0059)	73.213 (.0107)
VG SECTOR-MS 25ng, 8 runs, CMR (Std. error %)	2699 (.0440)	14.065 (.005)	73.2 (.024)

Table A-2: Isotopic composition of lead in NBS 981 standard, measured by the VG mass spectrometer and other mass spectrometers at CIT, the University of California at Santa Barbara, the Max Planck-Institut für Chemie (Mainz), and VG and Finnegan MAT factories. Internal precisions for all runs given as 1σ . Uncertainties for actual samples are probably higher, due to minor variations in sample purity.

SAMPLE	$^{206}\text{Pb}/^{207}\text{Pb}$	$^{208}\text{Pb}/^{206}\text{Pb}$	$^{206}\text{Pb}/^{204}\text{Pb}$
NBS 981 (given values):	1.09333 ± 39	2.16812 ± 80	16.9371 ± 110
Mainz MAT 261 (Todt et al., 1984)	1.09326 ± 34	2.16715 ± 12	16.9373 ± 13
Lunatic II CIT (LTS) 100 ng $ff = 1\text{‰}/\text{AMU}$	1.0932 ± 3	2.1652 ± 4	16.948 ± 16
Lunatic IV CIT 1 run, 100 ng $ff = 1\text{‰}/\text{AMU}$	1.0940 ± 16	2.1664 ± 10	16.950 ± 20
Lunatic IV CIT 2 run, 100 ng	1.0942 ± 20	2.1642 ± 15	16.913 ± 25
UCSB MAT 261 11 runs, (Mattinson, 1987)	1.0946	2.1616	16.895
VG-MS CIT, 100ng	1.0934 ± 15	2.1675 ± 9	16.941 ± 48
VG SECTOR-MS 250ng $ff = 1\text{‰}/\text{AMU}$	1.0935 ± 10	2.1674 ± 5	16.9326 ± 49
VG SECTOR-MS 11 runs $\text{‰}/\text{AMU}$ (Std. error %)	1.0939 (.007)	2.1674 (.007)	16.9339 (.018)

Table A-3: Isotopic composition of Uranium in NBS 500 standard measured by the VG mass spectrometer at Caltech. Internal precisions for all runs given as 1σ . Uncertainties for actual samples are probably higher, due to minor variations in sample purity.

SAMPLE	$^{235}\text{U}/^{238}\text{U}$
NBS 500 (given values):	$0.99969 \pm .050$
VG SECTOR-MS 2 runs 50ng (JBS) (Std. error %)	$0.99795 (.0088)$
VG SECTOR-MS 2 runs 100ng (JBS) (Std. error %)	$0.9977 (.0379)$
VG SECTOR-MS 2 runs 100ng (JBS) (Std. error %)	$0.99985 (.0147)$
VG SECTOR-MS 16 runs 350ng (CMR) (Std. error %)	$1.00015 (.0128)$

REFERENCES

- Cameron, A.E., Smith, D.H., and Walker, R.L., 1969, Mass spectrometry of nanogram-size samples of lead: *Analytical Chemistry*, v. 41, p. 525-526.
- Doe, B.R., and Zartman, R.E., 1979, Plumbotectonics, the Phanerozoic, in Barnes, H.L. eds., *Geochemistry of hydrothermal ore deposits*: Wiley Interscience, New York, p. 22-70.
- Jaffey, A.H., Flynn, K.F., Glendenin, L.E., Bentley, W.C., and Essling, A.M., 1971, Precision measurement of half-lives and specific activities of ^{235}U and ^{238}U : *Physical Reviews C*, v. 4, p. 1889-1906.
- Krogh, T.E., 1973, A low-contamination method for hydrothermal decomposition of zircon and extraction of U and Pb for isotopic age determinations: *Geochimica Cosmochimica Acta*, v. 37, p.485-494.
- Mattinson, J.M., 1987, U-Pb ages of zircons: a basic examination of error propagation: *Chemical Geology*, v. 66, p. 151-162.
- Steiger, R.H., and Jager, E., 1977, Subcommittee on geochronology: convention on the use of decay constants in geo- and cosmochemistry: *Earth and Planetary Science Letters*, v. 36, p. 350-362.
- Todt, W., Cliff, R.A., Hanser, A., Hoffman, A.W., 1984, ^{202}Pb + ^{205}Pb double spike for lead isotopic analyses: *Terra Cognita*, v. 4, p. 209.

APPENDIX 2

ABBREVIATIONS FOR GEOLOGIC MAPS

A = andesite	h = hornblende	α = amphibolite
B = basalt	c = clinopyroxene	γ = greenschist
Dc = dacite	o = orthopyroxene	Γ = greenstone
D = diorite	b = biotite	ψ = slate
Mz = monzonite	q = quartz	ϕ = phyllite
Gd = granodiorite	p = plagioclase	σ = schist
G = granite	K = k - feldspar	β = blueschist
K = keratophyre	a = andalusite	λ = hornfels
P = peridotite	s = sillimanite	π = gneiss
R = rhyolite	m = muscovite	π = flaser gneiss
S = serpentinite	mm = mica	π = injection gneiss
T = tuff	g = garnet	ω = migmatite
Tr = trondjemite	Ch = chlorite	Ω = agmatite
Tn = tonalite	δi = silicic	$\rho\pi$ = paragneiss
U = ultramafic	\bullet = psammatic	mt = metamorphosed
	x = breccia	$o\pi$ = orthogneiss
	- = pelitic	sp = spaced
Ar = arenite	v = micro	ft = fault
Ag = argillite	\odot = porphyritic	dp = depositional
Cs = calc-silicate	v = varitextured	un = unconformity
C = chert	ϵ = enclave	in = intrusive
Cg = conglomerate	z = xenolithic	
Di = diamictite	gf = quartzofeldspathic	
Li = limestone	l = leuco	<u>Protolith</u>
M = marble	Cb = carbonaceous	mv = metavolcanic
Mr = marl		ms = metasediment
Q = quartzite		mr = metamorphic rock
W = greywacke	\approx = approximate	mx = mixed rocks
Gt = grit	∇ = deformed	
L = lava	Δ = domainal deformation	lp = lower plate
	op = overprint	up = upper plate

	Strike & dip of bedding		<u>Geologic contact</u> (dashed where inferred & dotted where covered)
	Strike & dip of foliation		<u>Thrust Fault</u> (dashed where inferred & dotted where covered)
	Strike & dip cross-cutting cleavage		<u>High Angle Fault</u> (dashed where inferred & dotted where covered)
	Strike & dip of joints		Shear zone (\pm dip)
	Mylonitic foliation		
	Cataclastic foliation		
	Trend & plunge of lineation		
	Trend & plunge of small- scale folds		

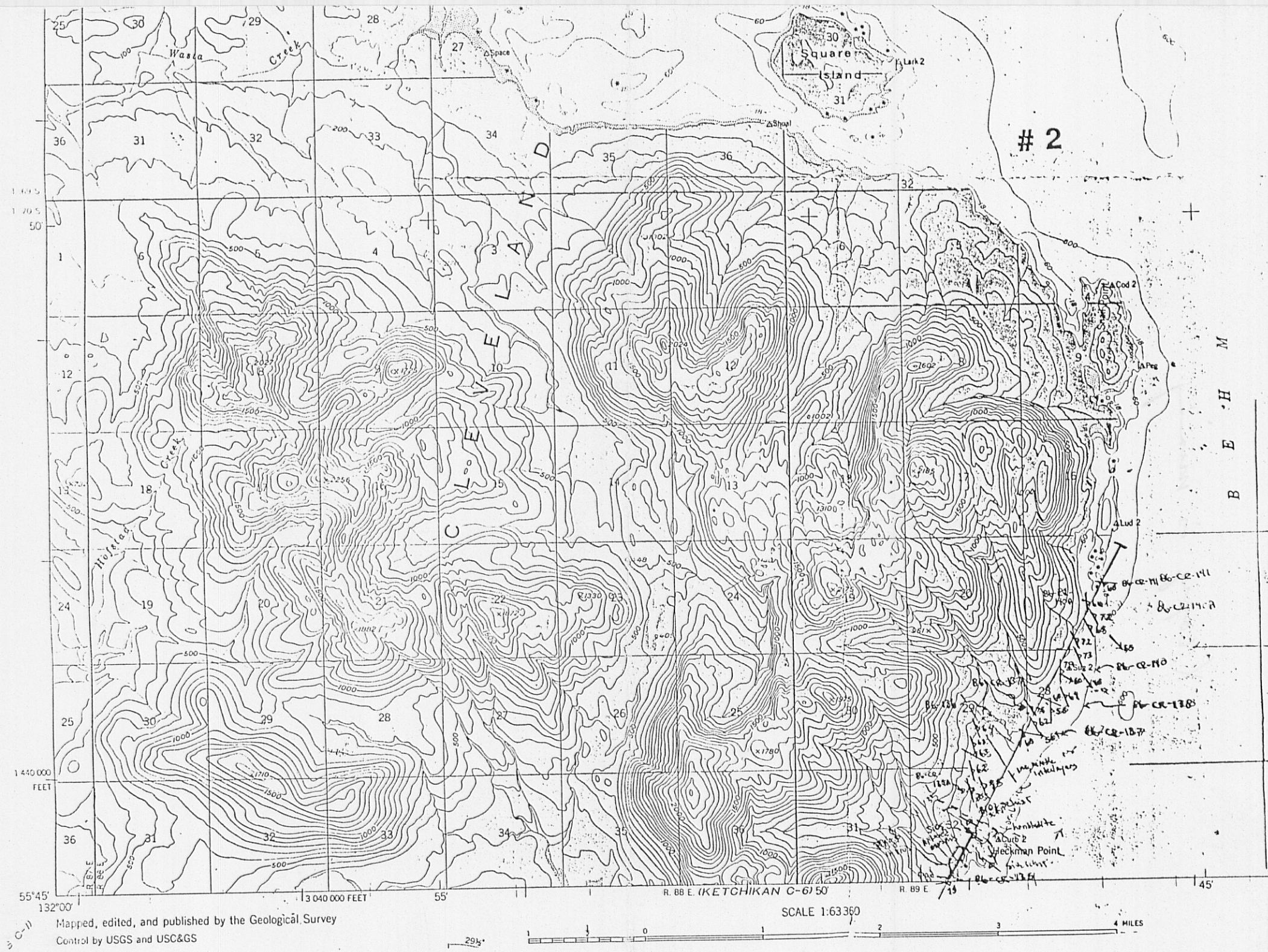


ETCHIKAN D-6

1830

55°4

132°00



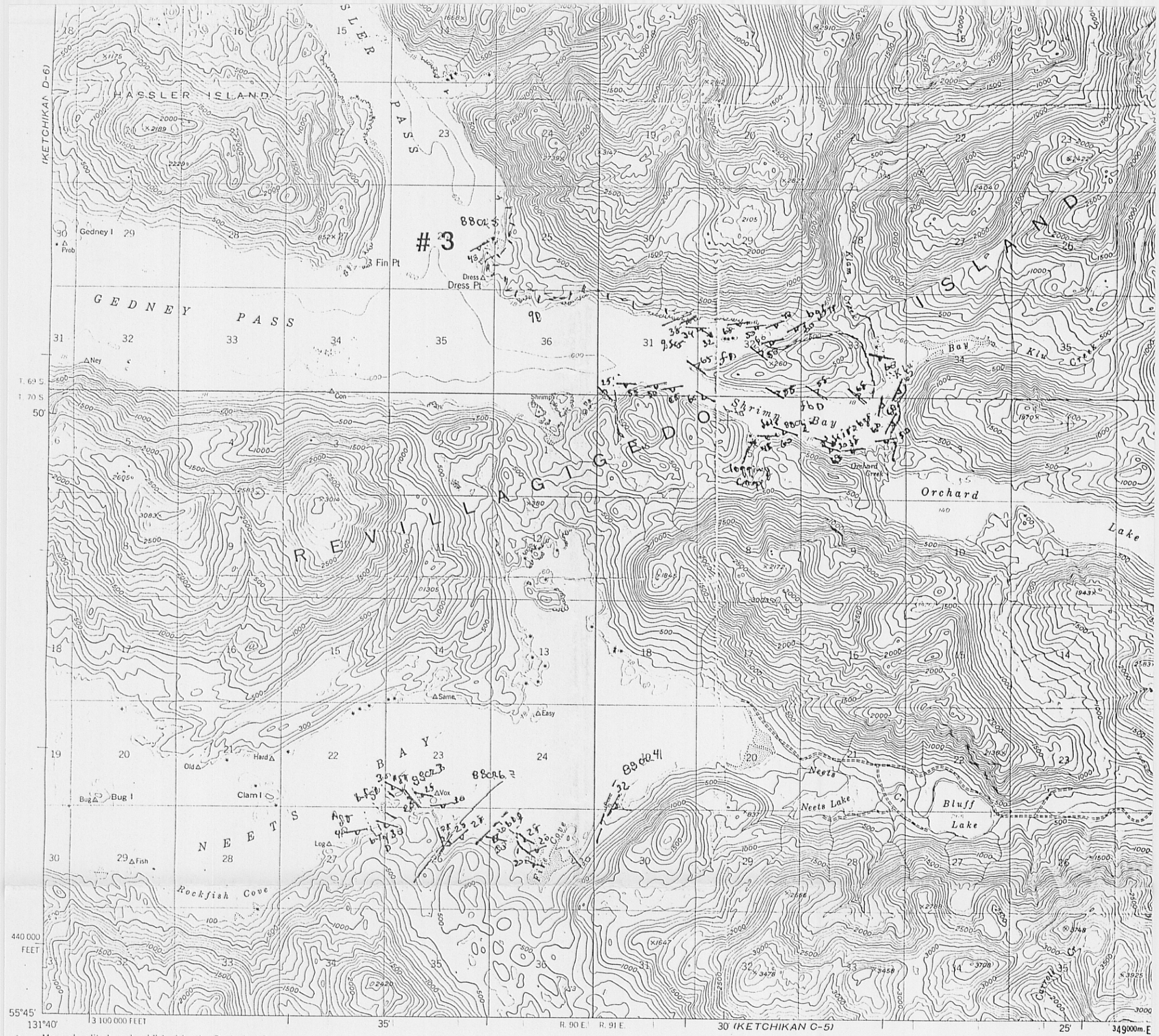


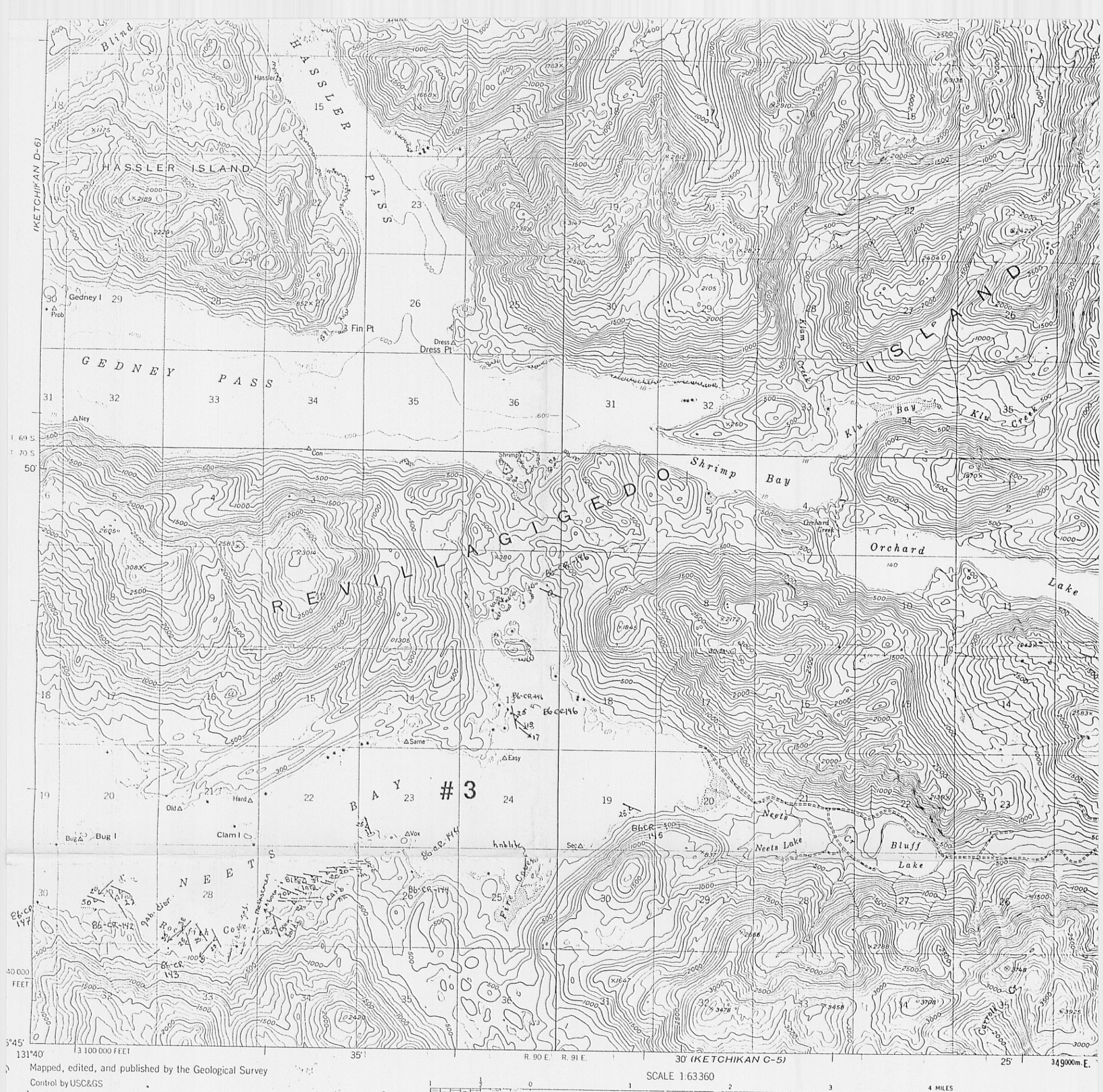


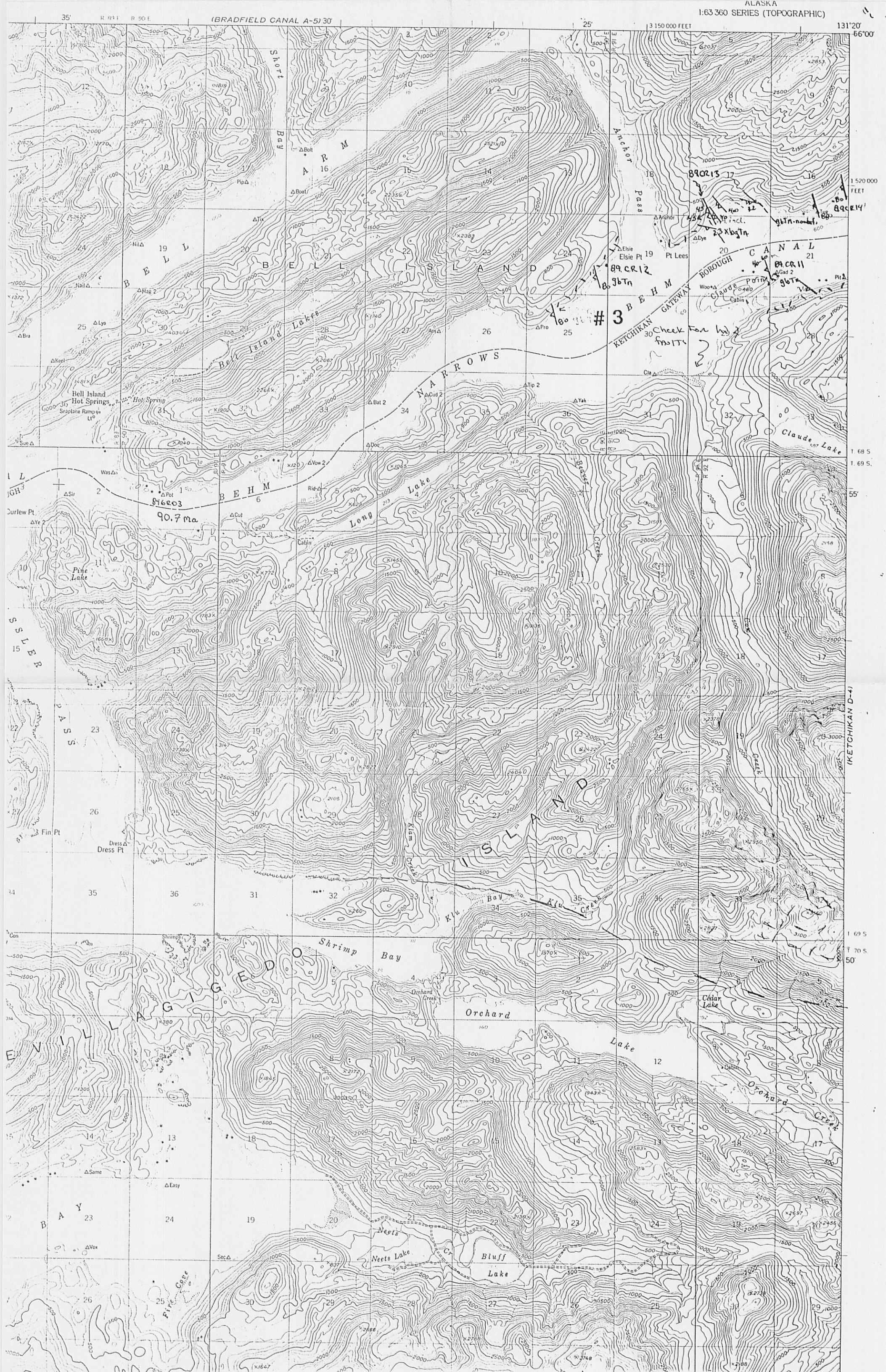
131°40' 3 100 000 FEET 35° R 90 E. R 91 E. 30 (KETCHIKAN C-5) 25° 34900

Mapped, edited, and published by the Geological Survey
Central Office

SCALE 1:63360 4 MILES





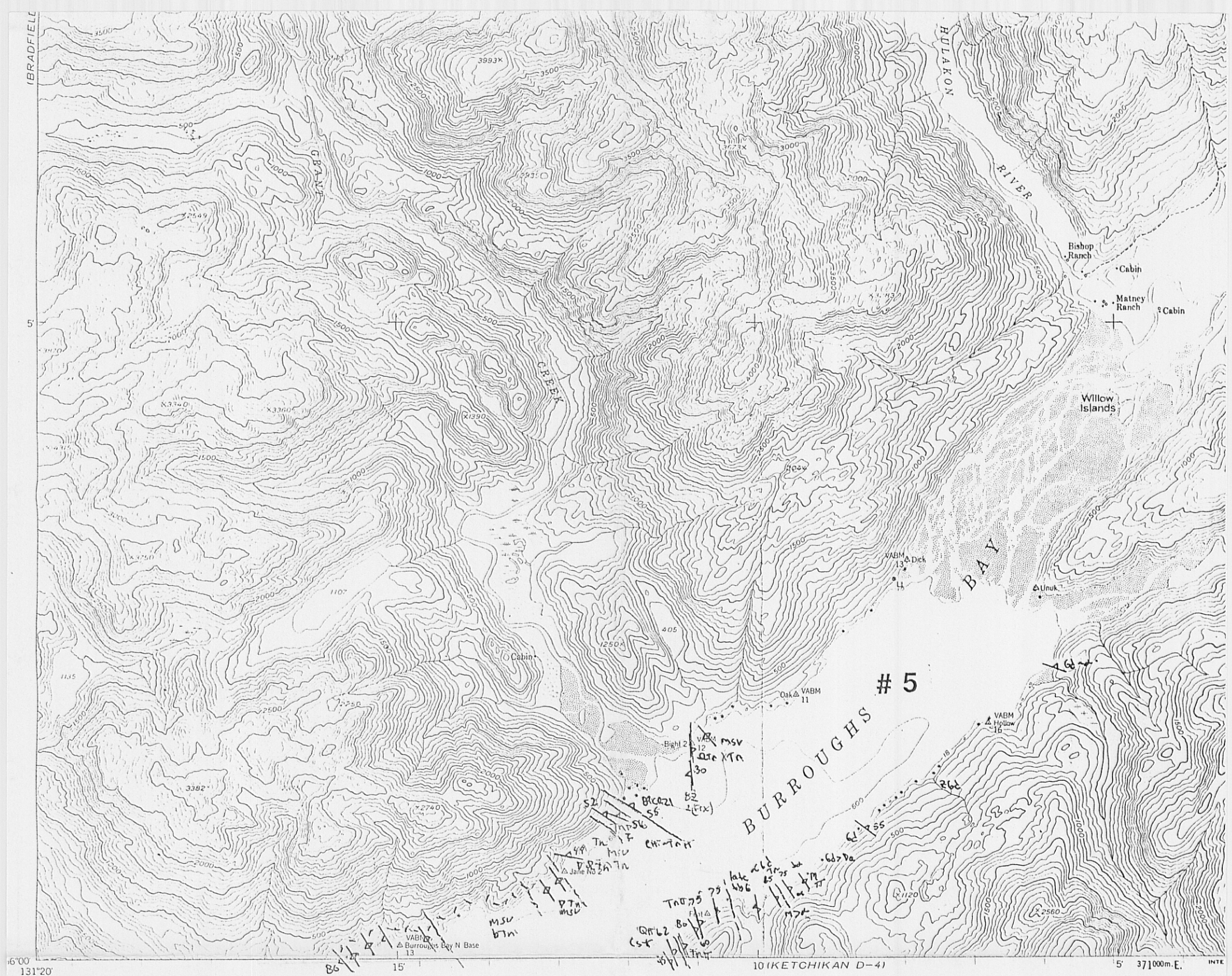




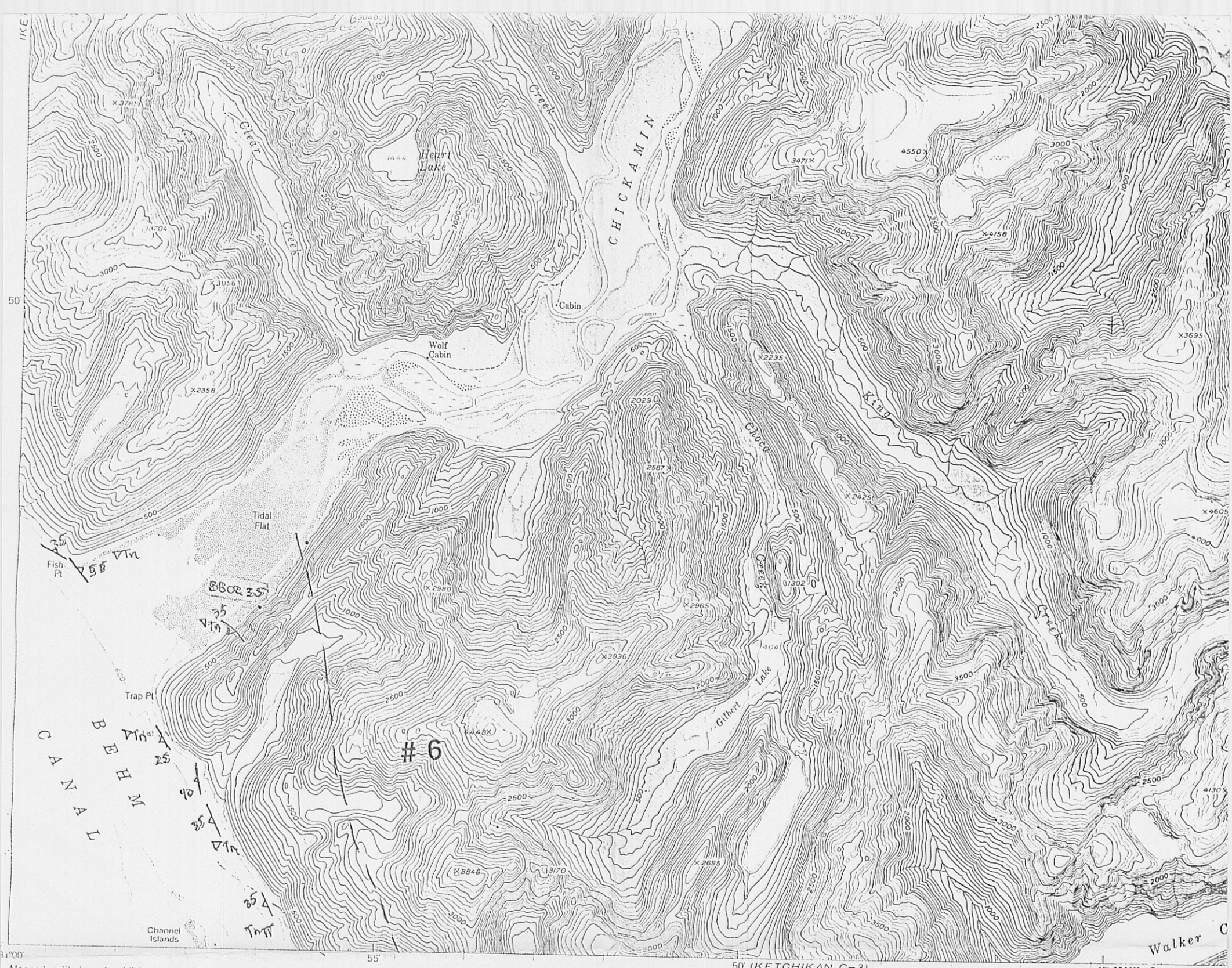
UNITED STATES
DEPARTMENT OF THE INTERIOR
GEOLOGICAL SURVEY

KETCHIKAN (D-4) QUADRANGLE
ALASKA
1:63,360 SERIES (TOPOGRAPHIC)





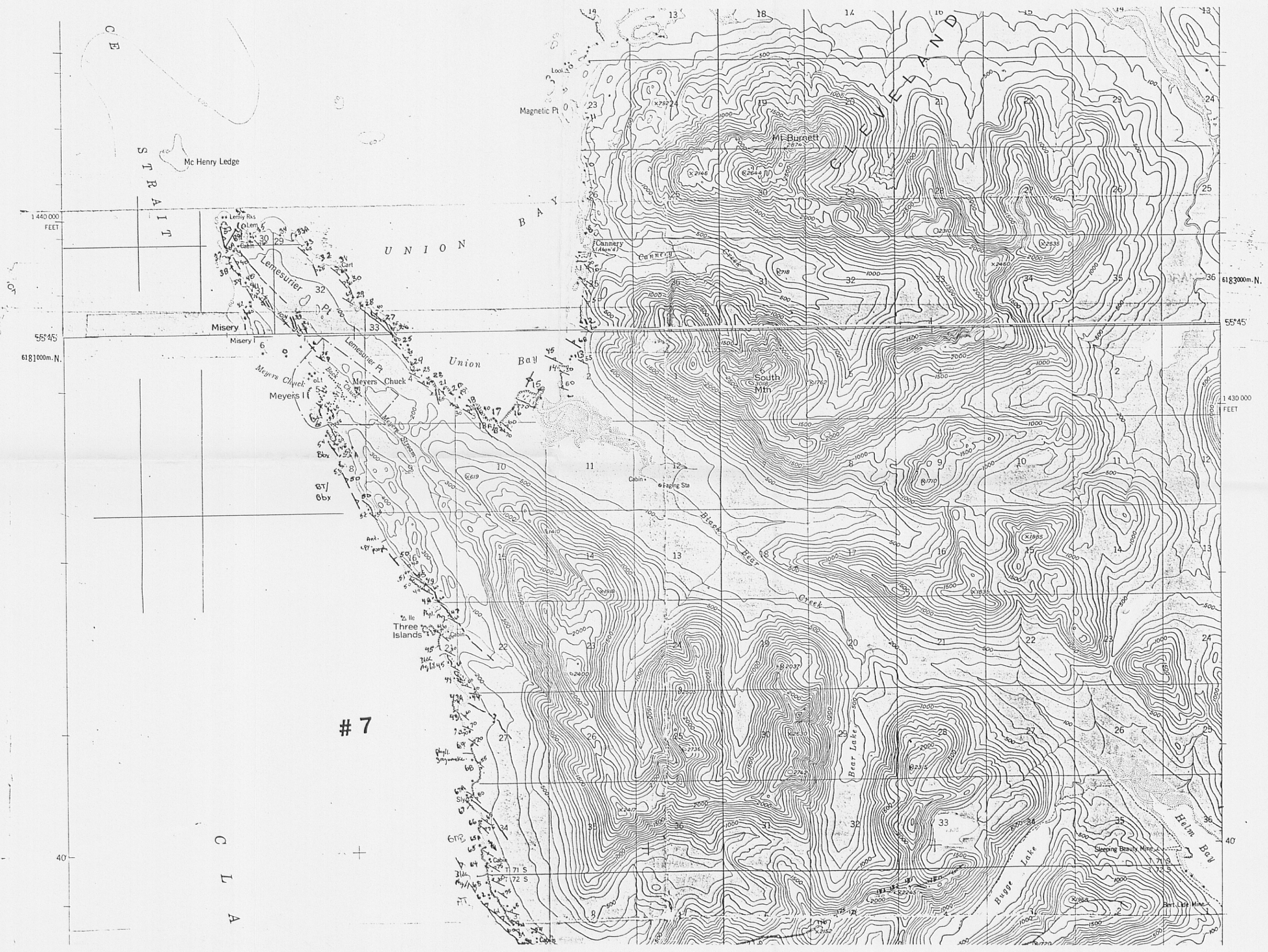
Maped, edited, and published by the Geological Survey



Mapped, edited, and published by the Geological Survey

50 IKETCHIKAN C-31
SCALE 1:63,360

45° 39' 1000m. E. INTERIOR.



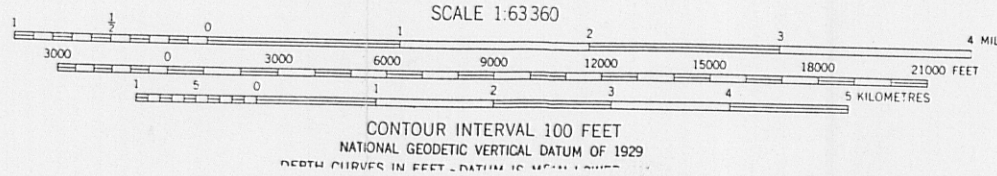
7



7

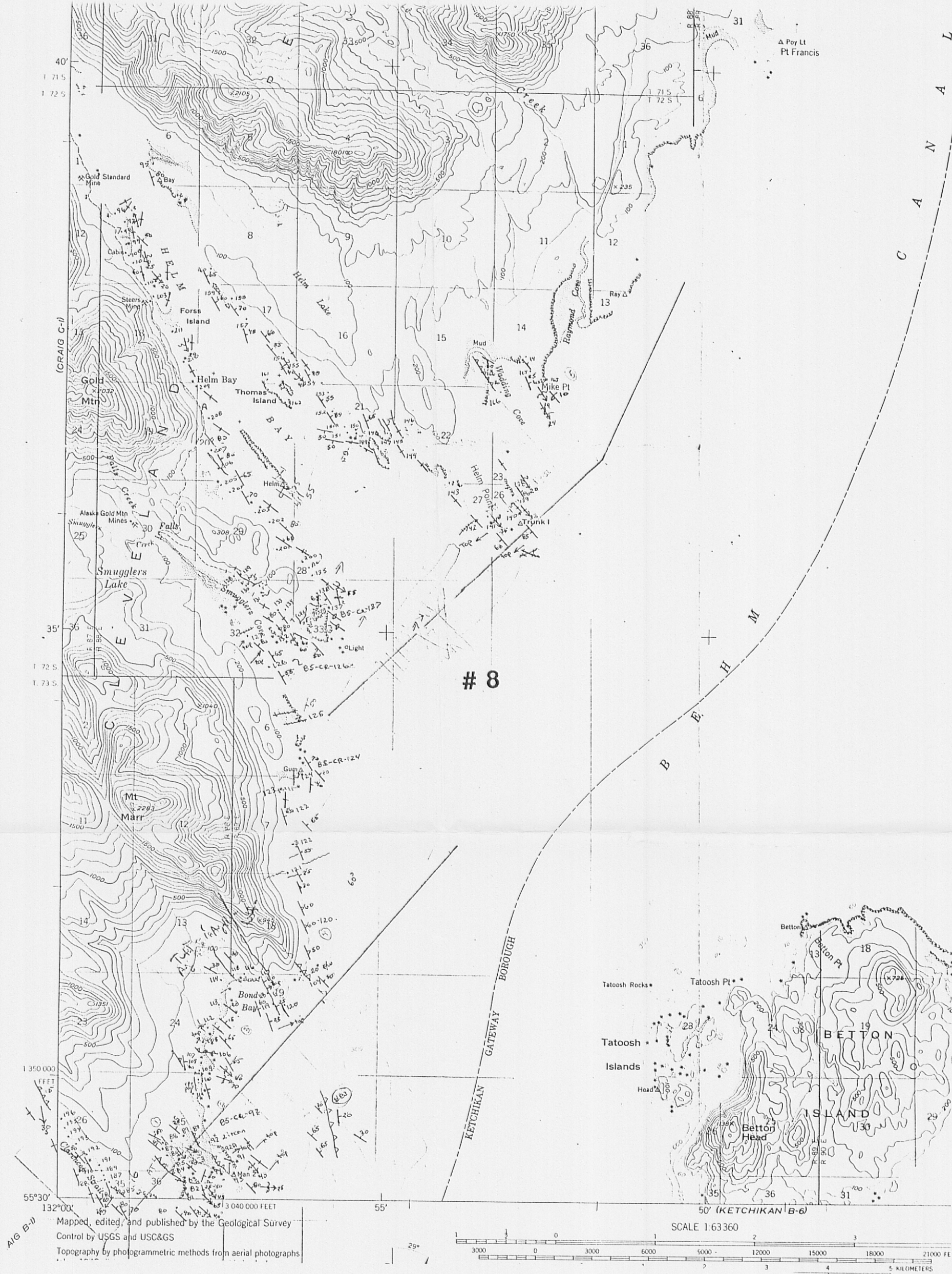


Maped, edited, and published by the Geological Survey
Control by USGS and USC&GS
Topography by photogrammetric methods from aerial photographs
taken 1948, field annotated 1950. Map not field checked
Selected hydrographic data compiled from USC&GS Charts 8076
(1:10,000 scale), 8079 (1:79,334 scale), 8102 (1:229,376 scale),
8124, and 8142. This information is not intended for navigational purposes
Universal Transverse Mercator projection, 1927 North American datum



ROAD CLASSIFICATION
Trails





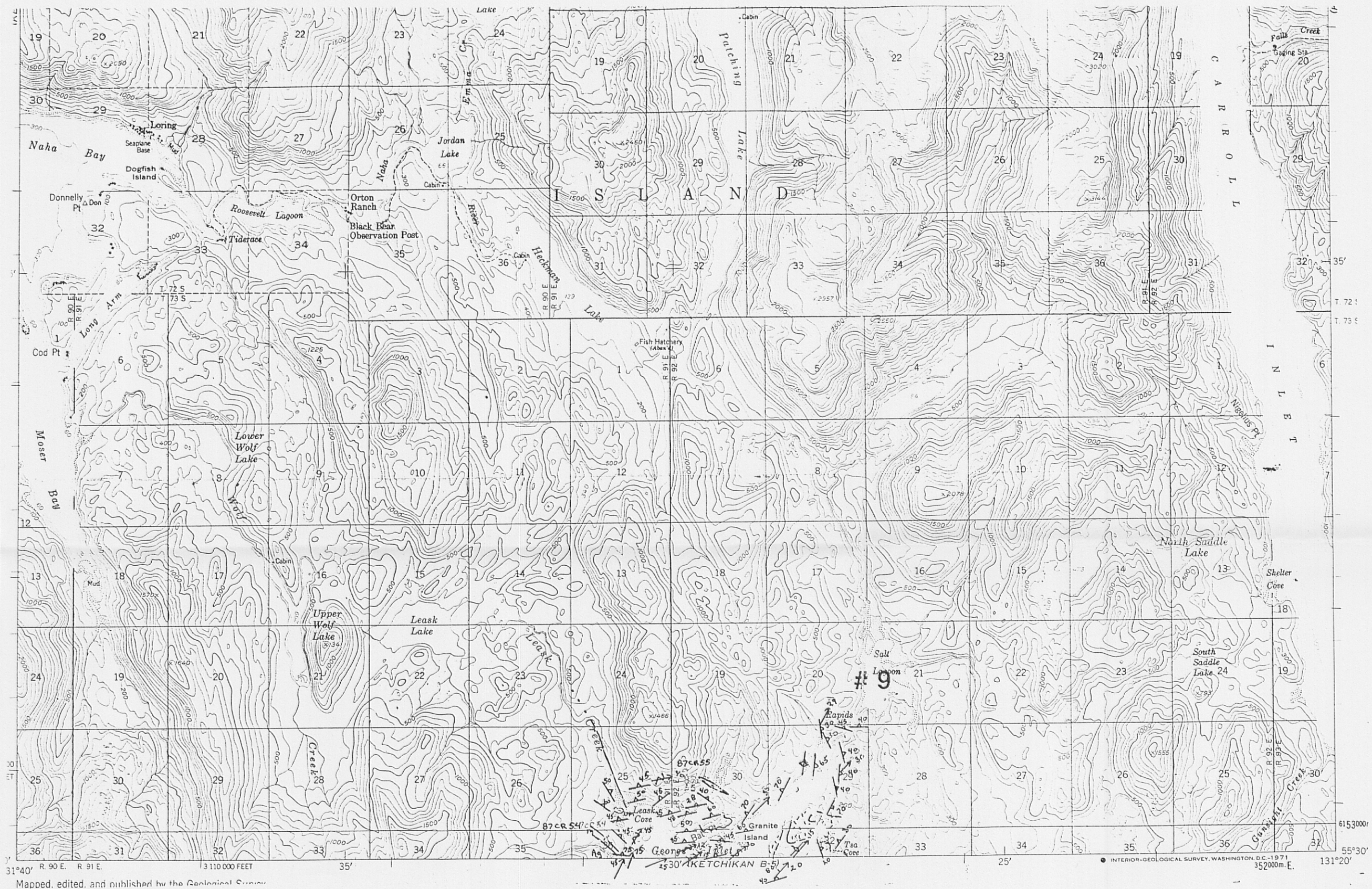




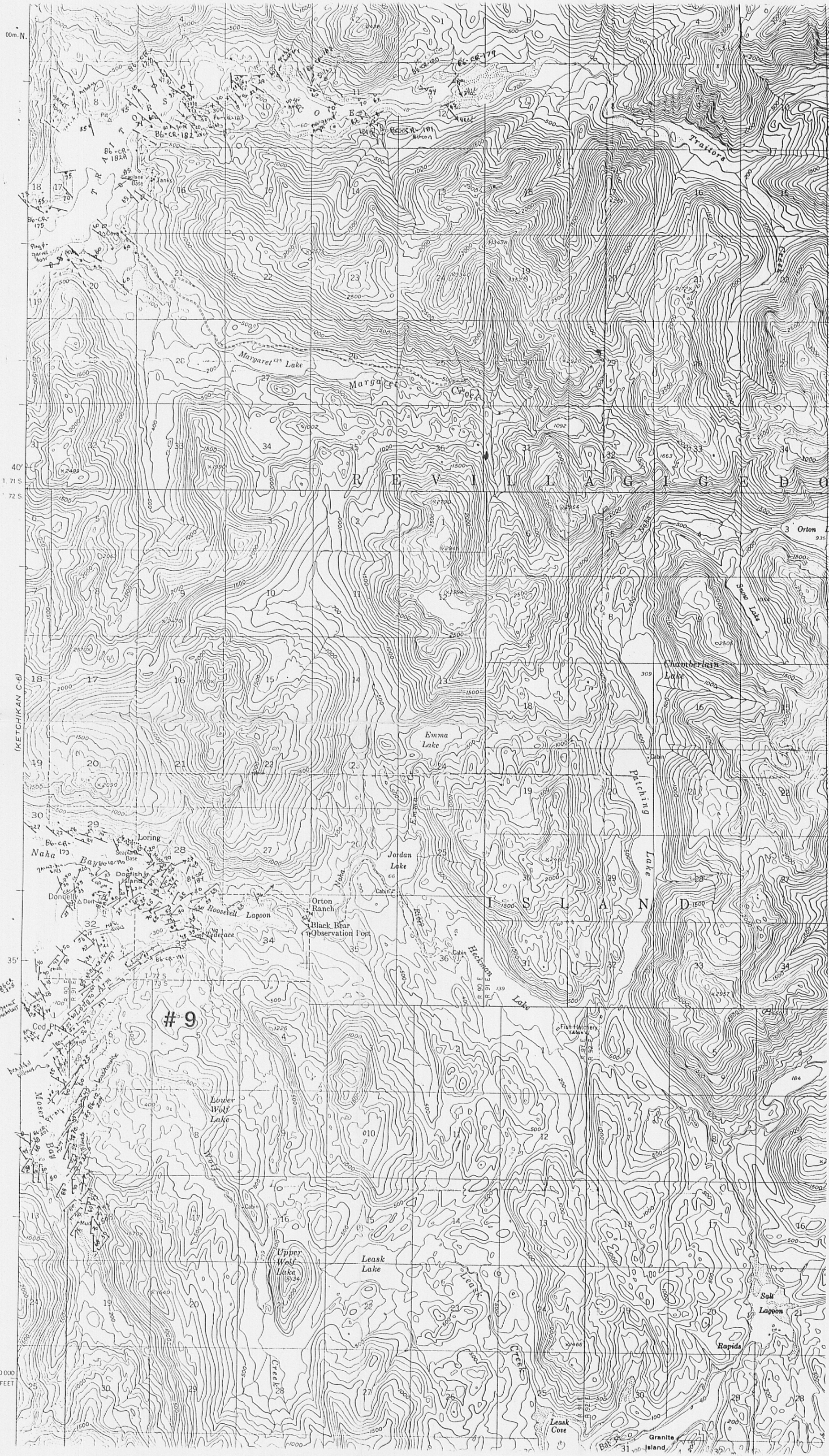






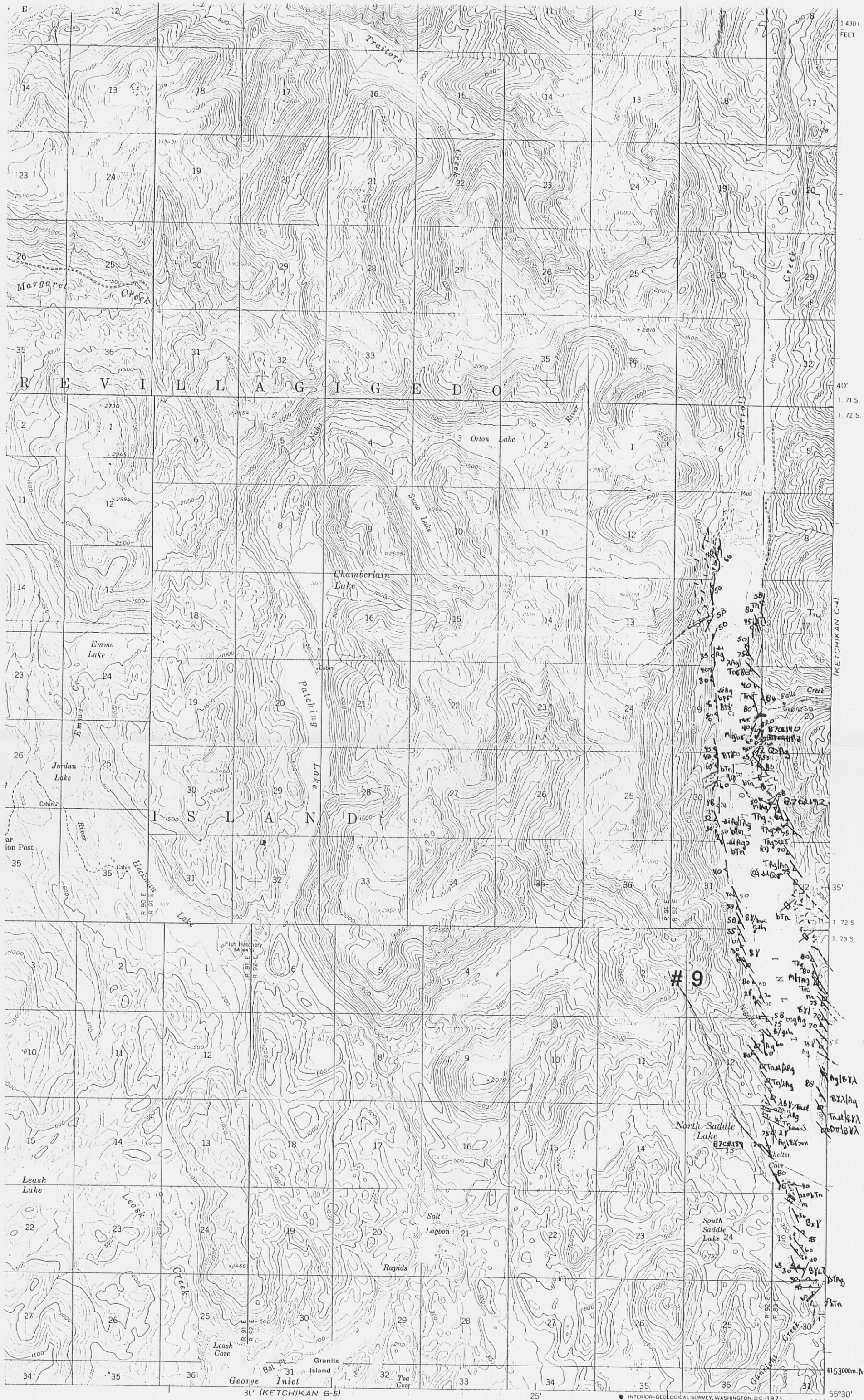


Mapped, edited, and published by the Geological Survey





app, eared, and published by the Geological Survey



1430
FEET

40'
T. 71 S.
T. 72 S.

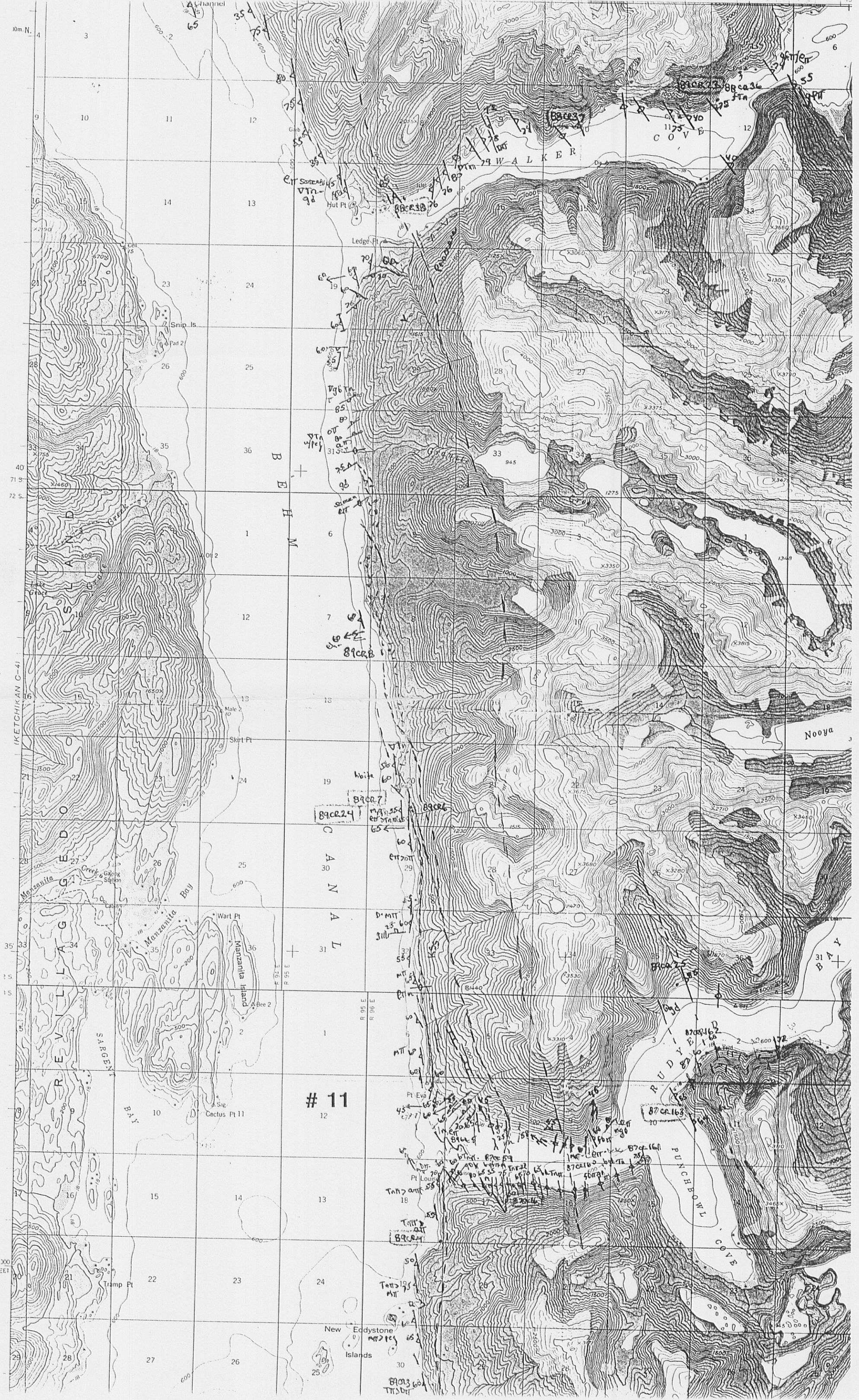
(KETCHIKAN C-4)

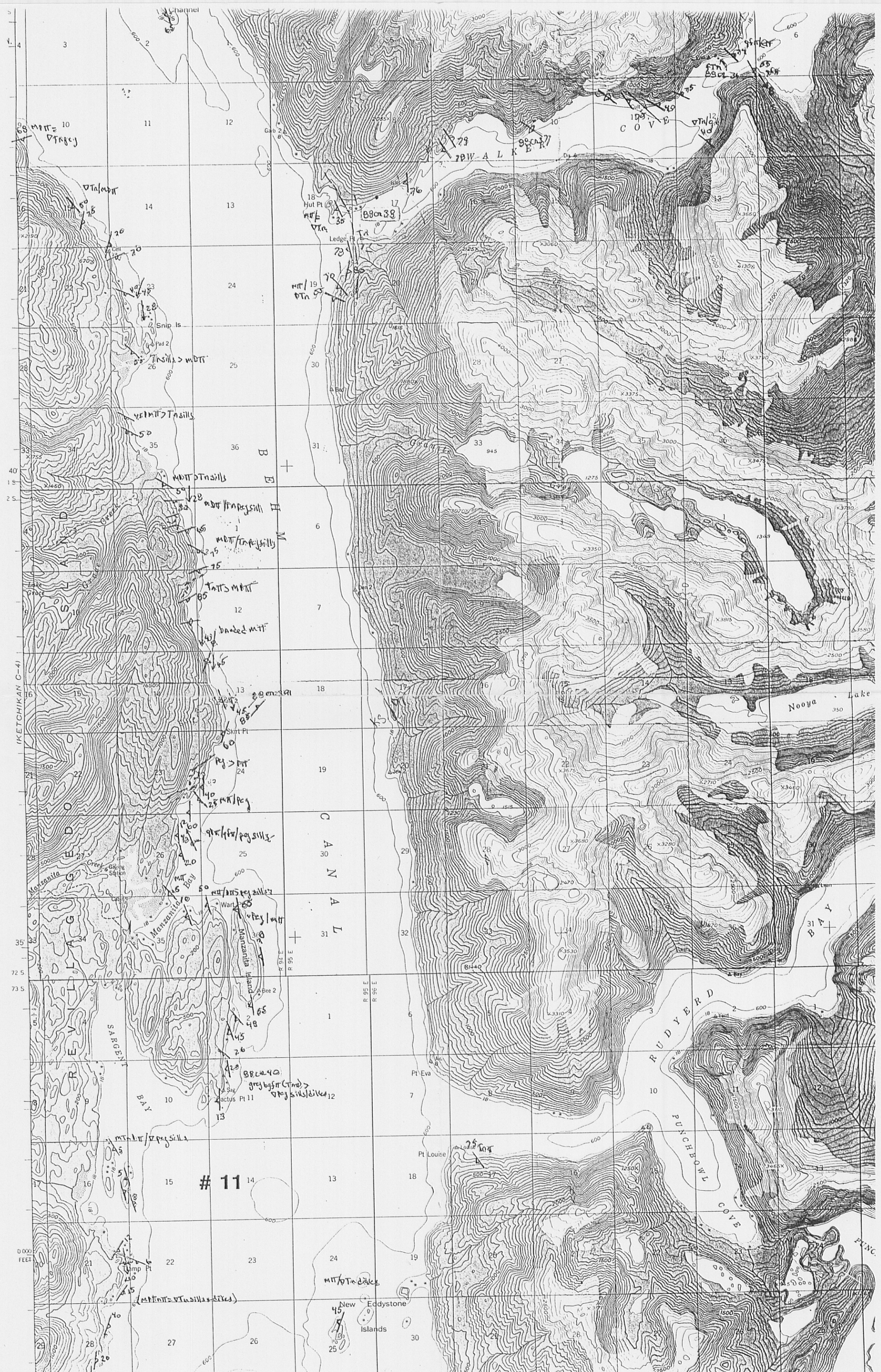
35'
T. 72 S.
T. 73 S.

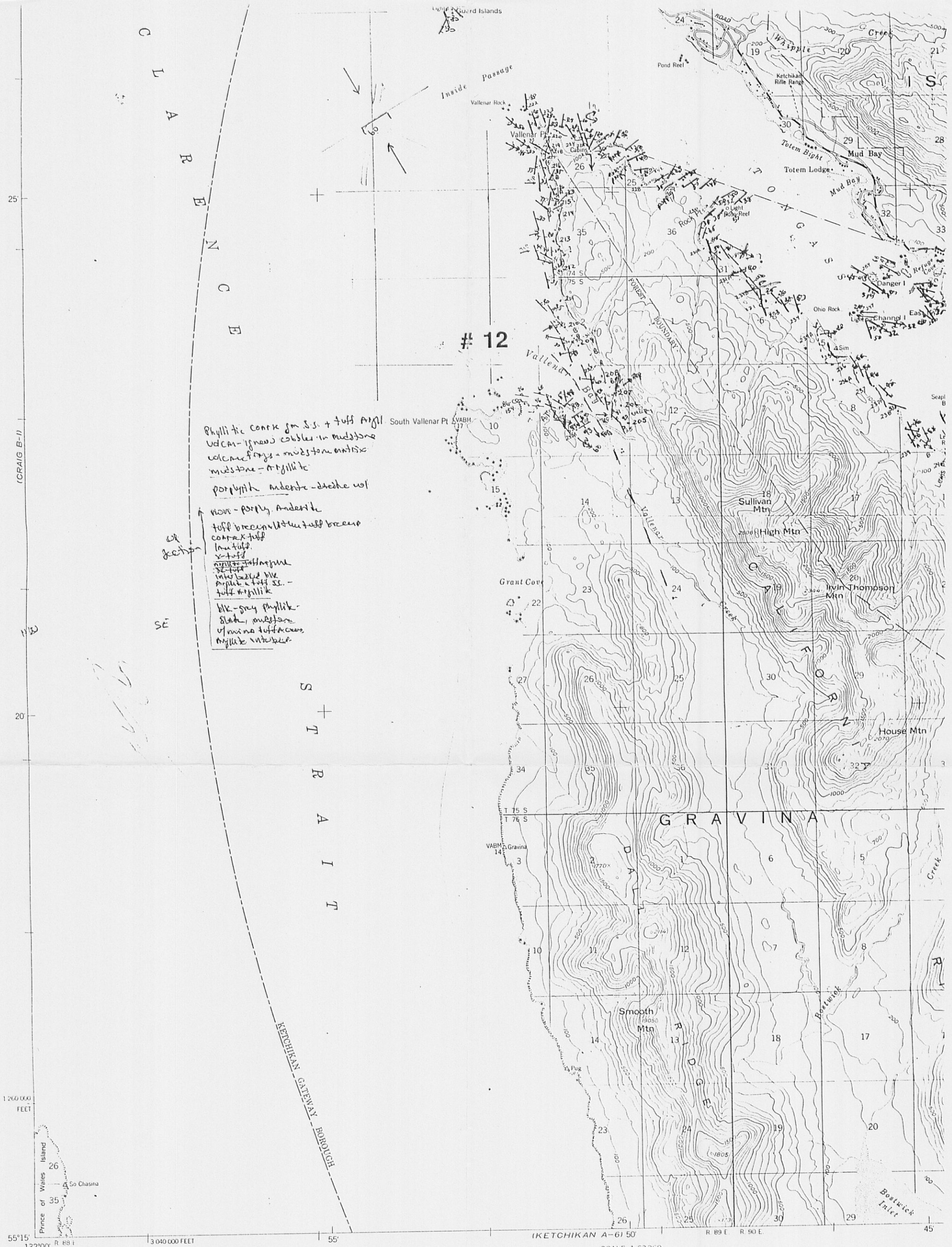
615300m.N
55°30'
131°20'





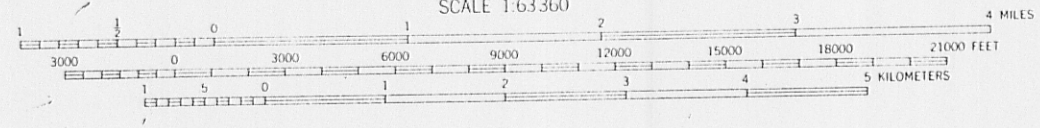




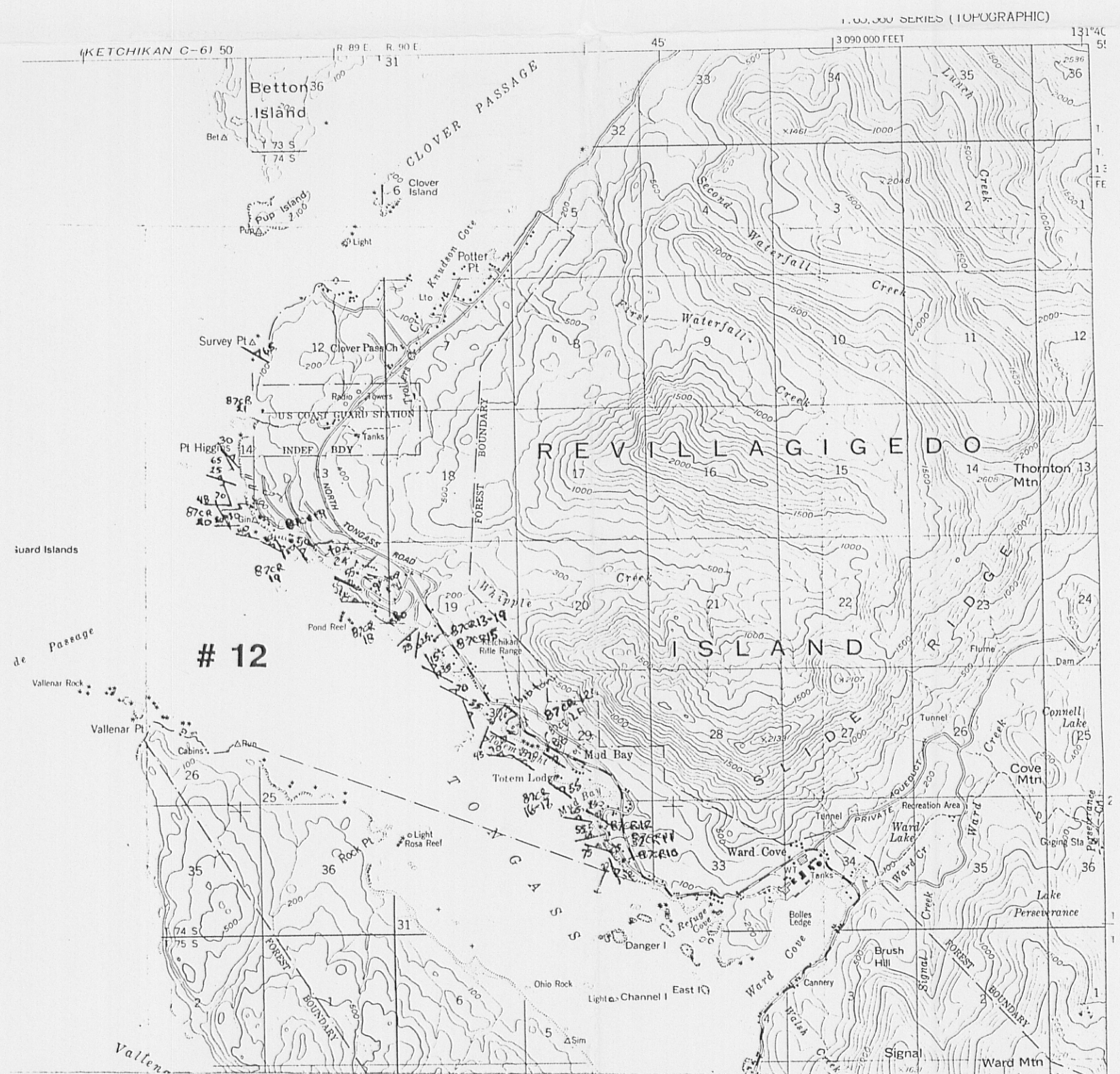


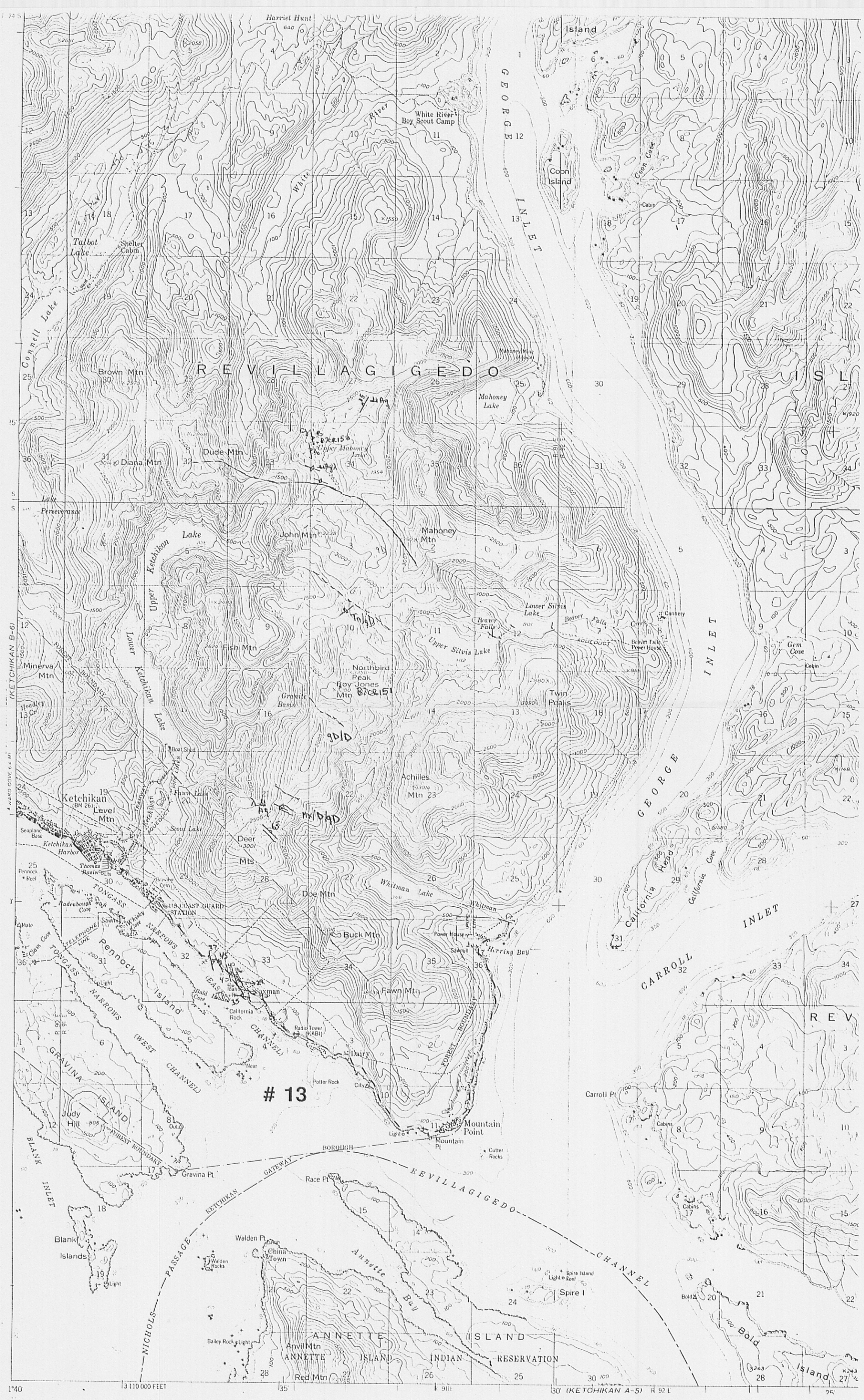
Phyllitic congl. fm. ss. + tuff argill.
 Volcanic - igneous cobbles in mudstone
 volcanic frags - mudstone matrix
 mudstone - argillitic
 porphyritic mudstone - andesite vol.
 none - porphy. Andesite
 tuff brecciated tuff breccia
 coarse tuff
 fine tuff
 mudstone
 interbedded blk.
 argillitic tuff ss. -
 tuff argillitic
 blk.-gray phyllitic
 slate, mudstone
 of minor tuffaceous
 argillitic interbeds

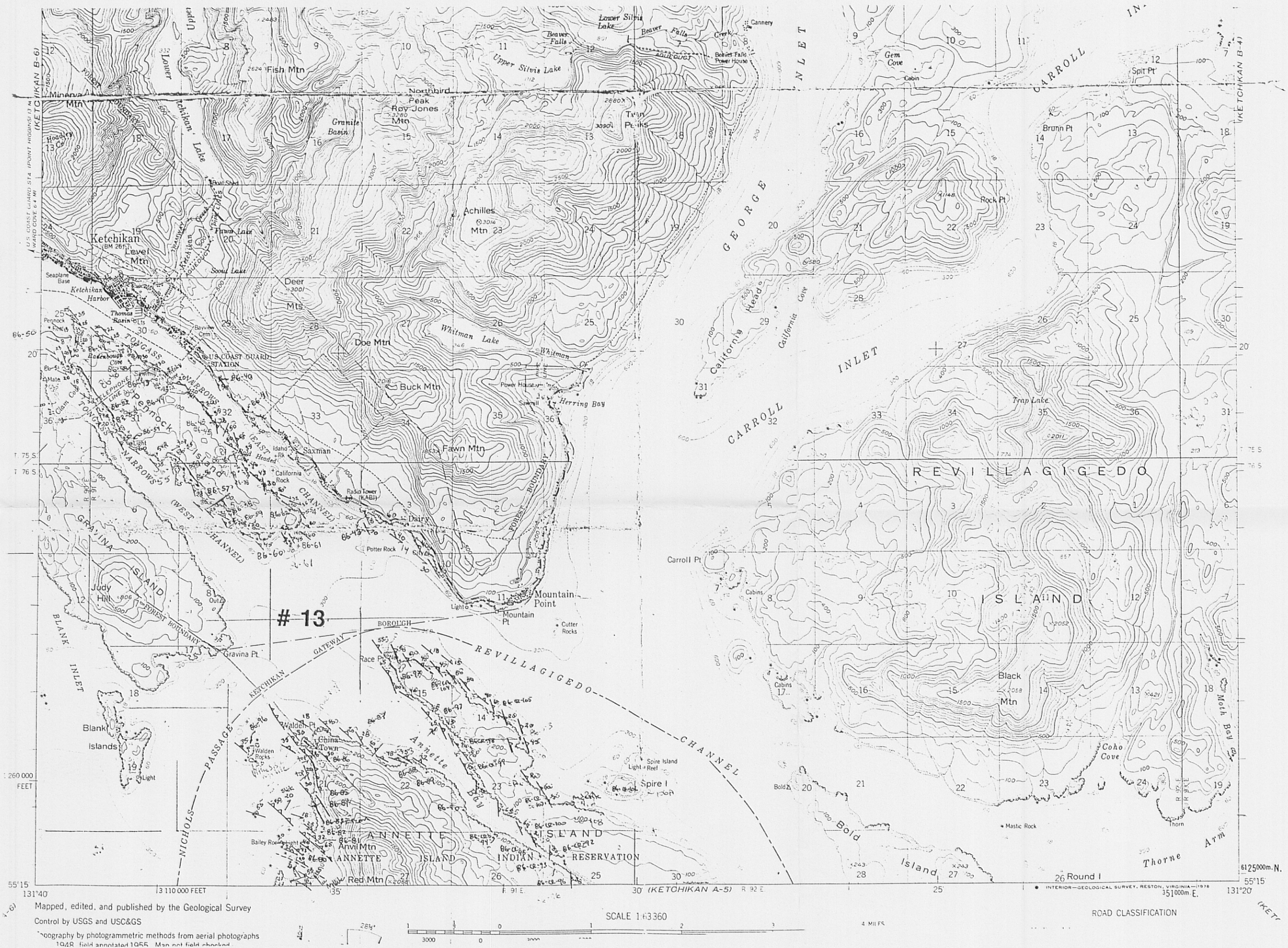
Mapped, edited, and published by the Geological Survey
 Control by USGS and USC&GS
 Topography by photogrammetric methods from aerial photographs
 taken 1948, field annotated 1954. Map not field checked











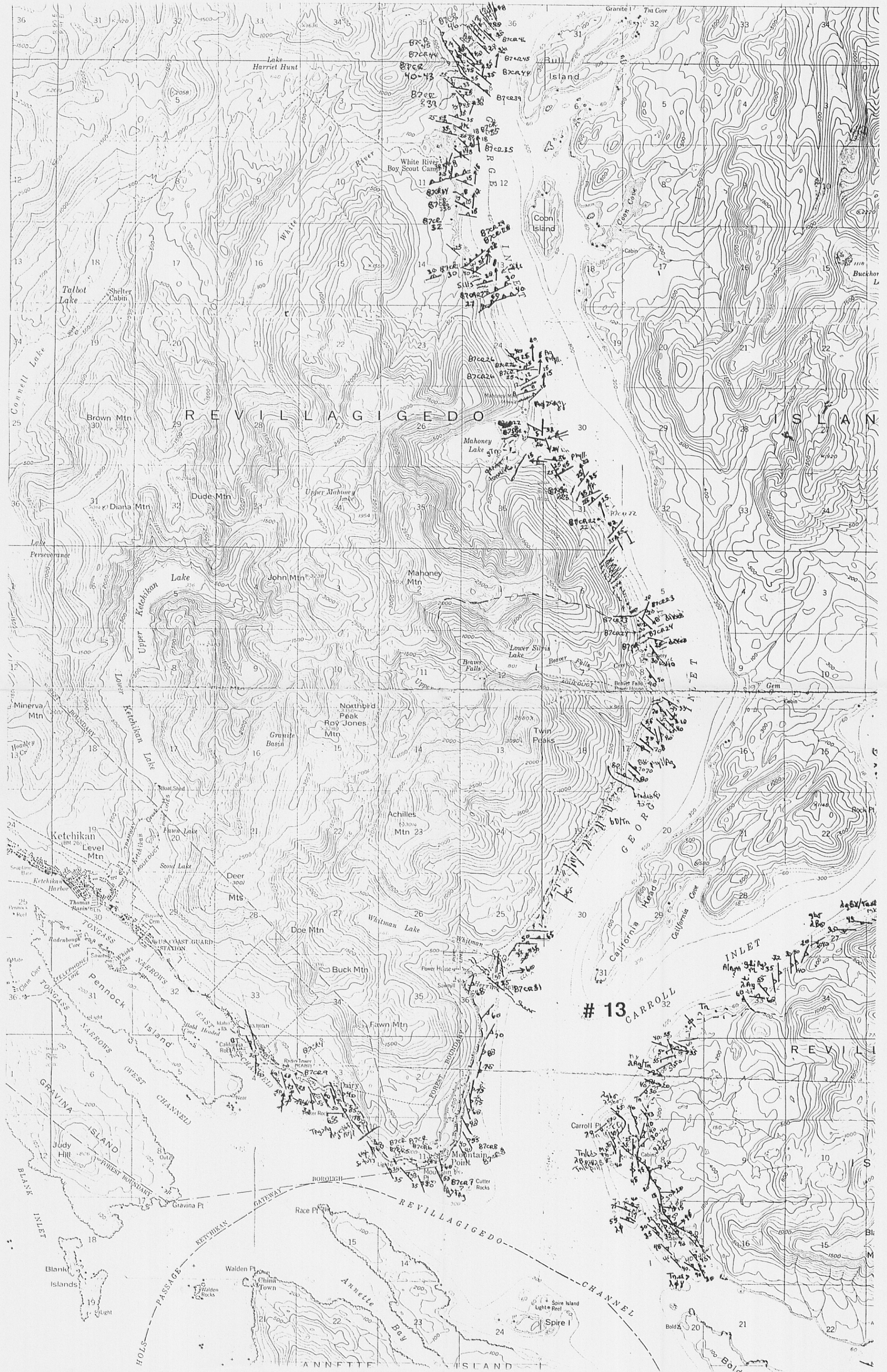
Mapped, edited, and published by the Geological Survey
Control by USGS and USC&GS

Topography by photogrammetric methods from aerial photographs
1948. field annotated 1955. Map not field checked.

SCALE 1:63360

4 MII FS

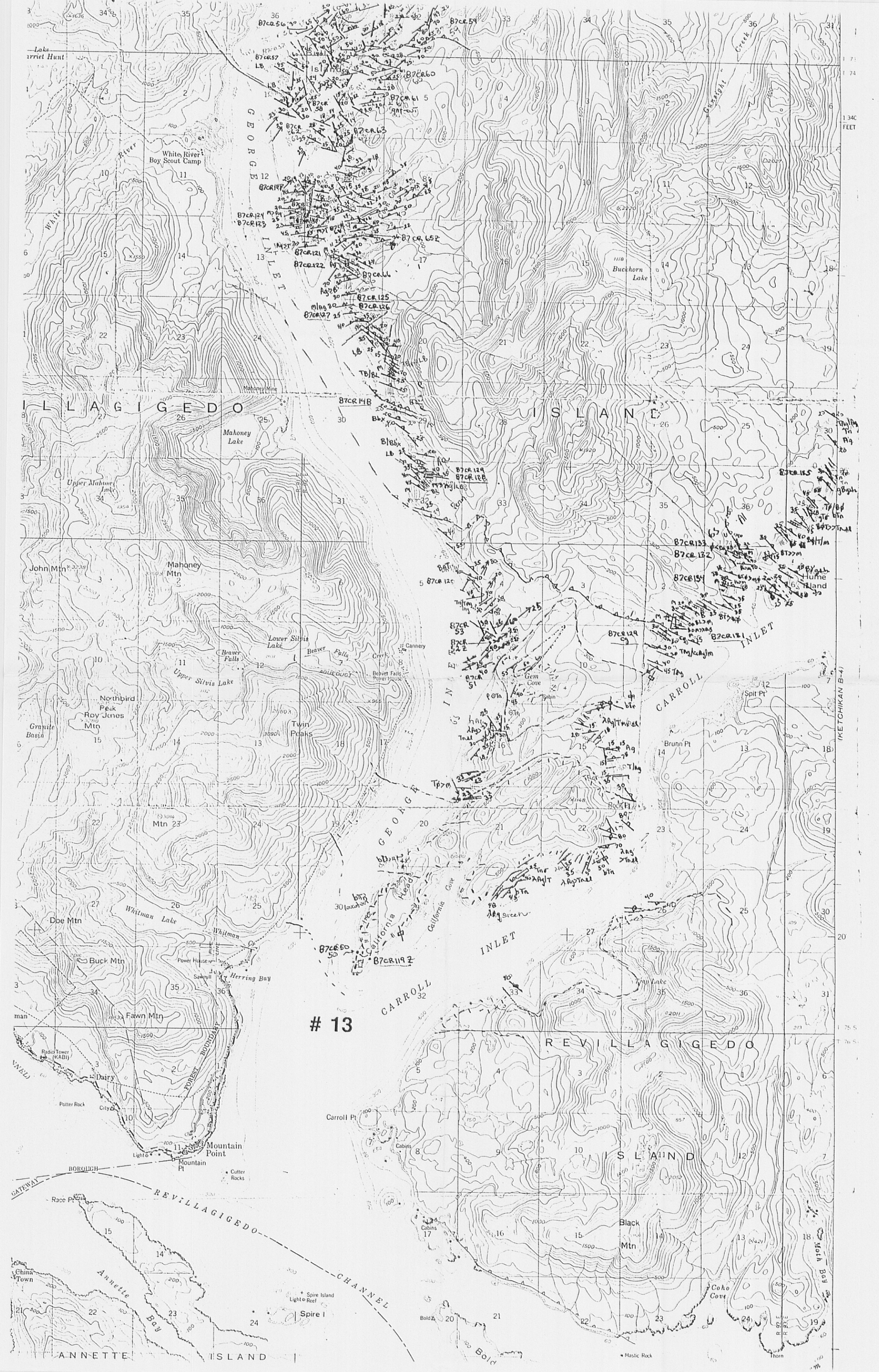
ROAD CLASSIFICATION

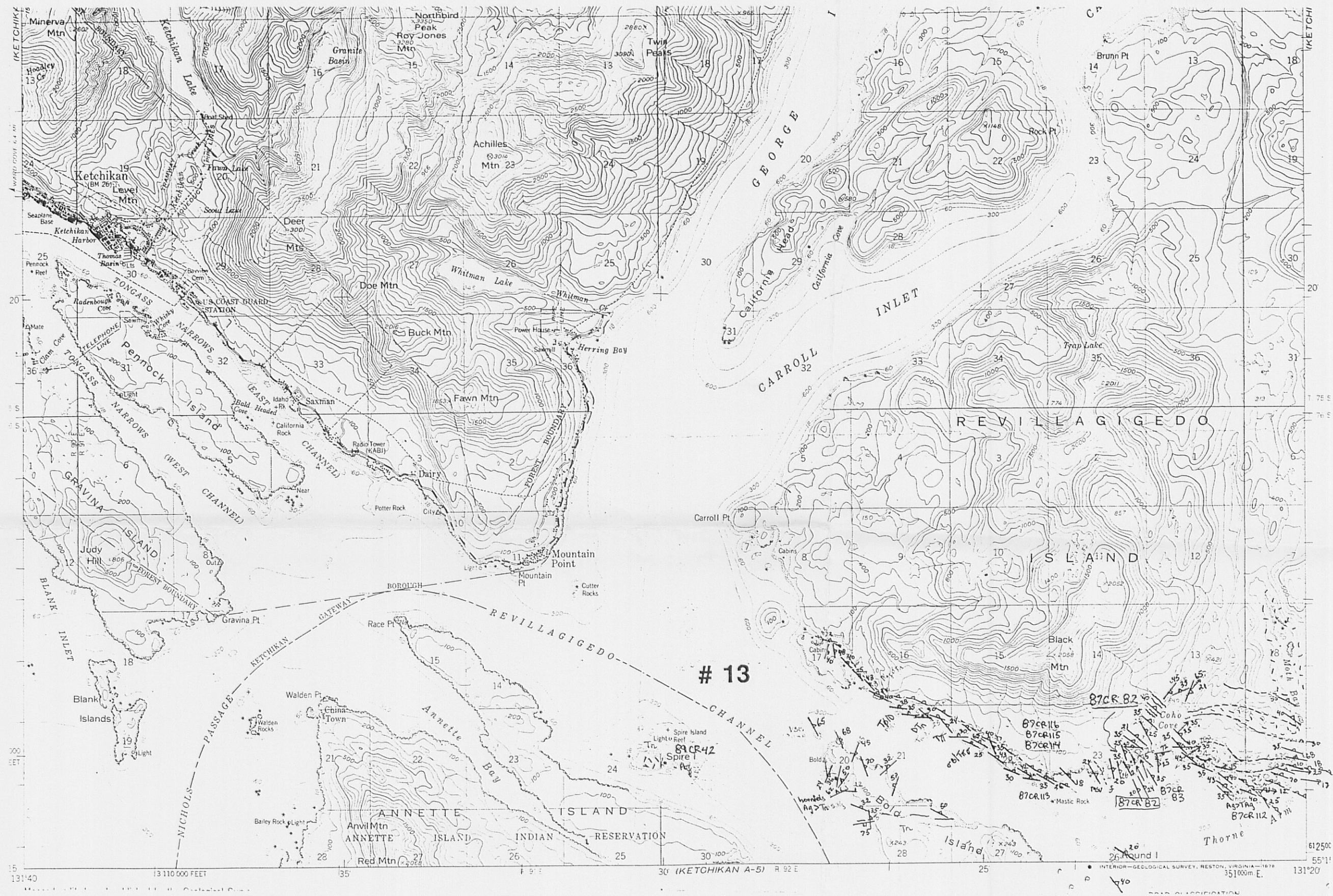




3 Mapped, edited, and published by the Geological Survey
Control by USGS and USC&GS
Topography by photogrammetric methods from aerial photographs
taken 1948, field annotated 1955. Map not field checked

ROAD CLASSIFICATION





13

87CR 82

87CR 116
87CR 115
87CR 114

87CR 113
87CR 112
87CR 111

87CR 110
87CR 109
87CR 108

87CR 107
87CR 106
87CR 105

87CR 104
87CR 103
87CR 102

87CR 101
87CR 100
87CR 99

87CR 98
87CR 97
87CR 96

87CR 95
87CR 94
87CR 93

87CR 92
87CR 91
87CR 90

87CR 89
87CR 88
87CR 87

87CR 86
87CR 85
87CR 84

87CR 83
87CR 82
87CR 81

87CR 80
87CR 79
87CR 78

87CR 77
87CR 76
87CR 75

87CR 74
87CR 73
87CR 72

87CR 71
87CR 70
87CR 69

87CR 68
87CR 67
87CR 66

87CR 65
87CR 64
87CR 63

87CR 62
87CR 61
87CR 60

87CR 59
87CR 58
87CR 57

87CR 56
87CR 55
87CR 54

87CR 53
87CR 52
87CR 51

87CR 50
87CR 49
87CR 48

87CR 47
87CR 46
87CR 45

87CR 44
87CR 43
87CR 42

87CR 41
87CR 40
87CR 39

87CR 38
87CR 37
87CR 36

87CR 35
87CR 34
87CR 33

87CR 32
87CR 31
87CR 30

87CR 29
87CR 28
87CR 27

87CR 26
87CR 25
87CR 24

87CR 23
87CR 22
87CR 21

87CR 20
87CR 19
87CR 18

87CR 17
87CR 16
87CR 15

87CR 14
87CR 13
87CR 12

87CR 11
87CR 10
87CR 9

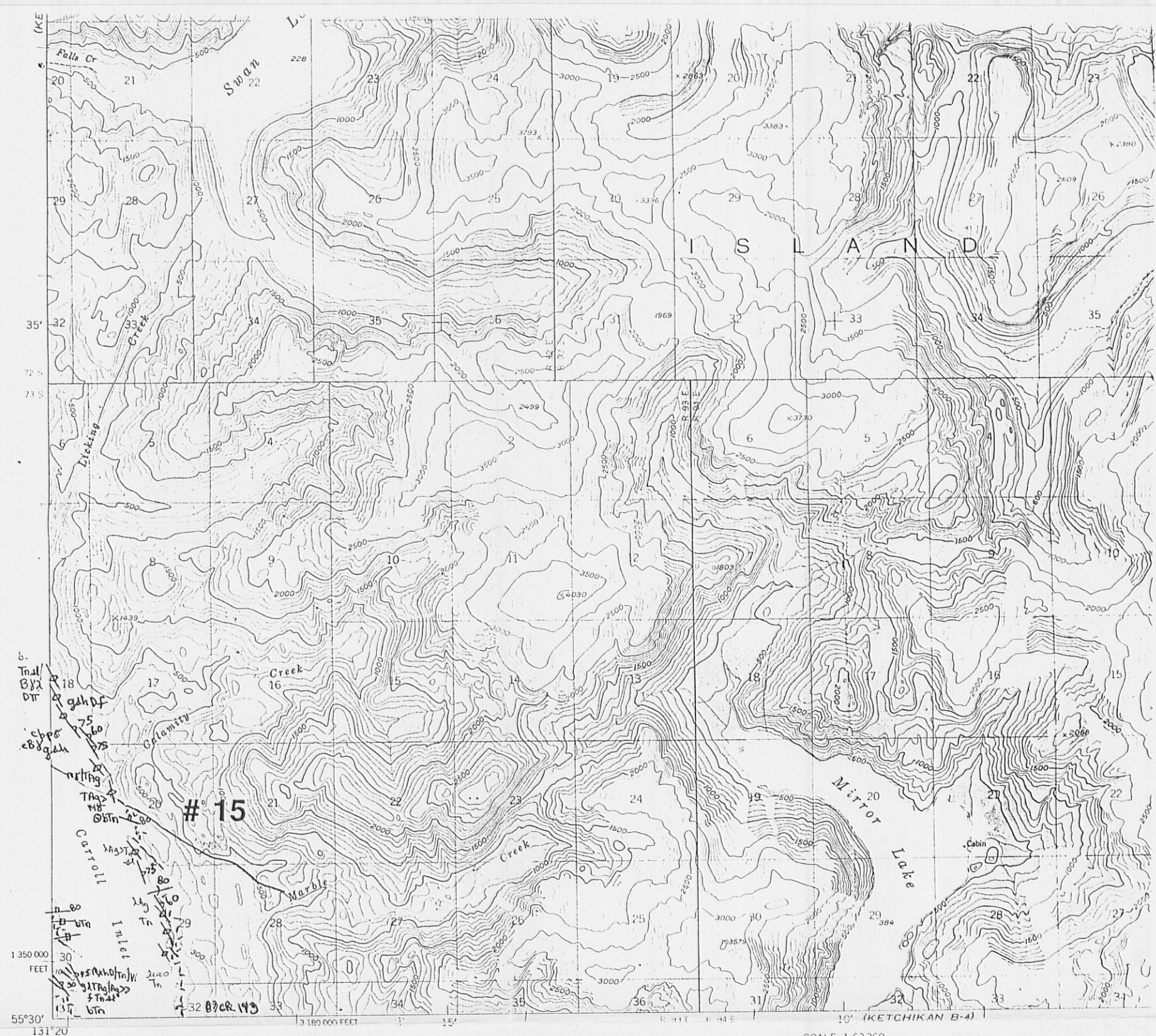
87CR 8
87CR 7
87CR 6

87CR 5
87CR 4
87CR 3

87CR 2
87CR 1
87CR 0

131°20' 353000m. E.





Mapped, edited, and published by the Geological Survey

SCALE 1 €3360

GEO

